Downstream Effectors of Cyclic Adenosine Monophosphate Signalling in *Trypanosoma brucei*

Daniel Nii Aryee Tagoe

Institute of Infection, Immunity and Inflammation

College of Medical, Veterinary and Life Sciences

This thesis is submitted for the degree of Doctor of Philosophy

Institute of Infection, Immunity and Inflammation of the

School of Life Sciences

University of Glasgow

September, 2015

Abstract

African trypanosomiasis is caused by a unicellular eukaryote that parasitizes multicellular organisms and causes medically and economically important diseases in humans (Human African Trypanosomiasis) and their domestic animals (African Animal Trypanosomiasis). Incidence is currently declining due to the application of present chemotherapy, although the drugs are old, toxic, difficult to administer and in some cases expensive, and of diminishing efficacy due to resistance. However, this trend needs to be sustained with the discovery of new compounds active against the resistant strains. These new treatment options must meet the current pharmacological requirements, must be parasite specific and must be relatively cheap to produce. Pharmacological manipulation of phosphodiesterases (PDEs), which hydrolyse cyclic Adenosine Monophosphate (cAMP), have been extensively studied in humans and found to have great therapeutic effect. Kinetoplastid genomes code for the same set of cyclic nucleotide-specific class 1-type phosphodiesterases, with catalytic domains similar to those of human PDEs. The locus of *Trypanosoma brucei* PDEB1/2 was found to be essential, by either genetic manipulation or the use of the pharmacological inhibitor CpdA, but therapeutic exploitation of TbPDEB1 has so far been hampered by its catalytic domain similarity to human PDEs. However, investigating the unique downstream cAMP signalling cascade, which includes the recently identified cAMP Response Proteins (CARPs), could reveal potentially new trypanosome-specific therapeutic targets.

In this study we show that single knockout (sKO) of the CARP genes causes a decreased susceptibility to CpdA, and that null mutants of CARP2-4 display significantly increased intracellular and extracellular cAMP levels. A double knockout (dKO) of CARP2 also shows a significant growth defect. Conversely, overexpression of CARP3 causes a growth delay in both WT s427 and CpdA resistant (R0.8) cells, when exposed to CpdA, and were more sensitive to CpdA compared to other CARP overexpressing cells as well as the WT s427 and R0.8 controls. These cells also have significantly higher intracellular and extracellular cAMP levels relative to the control lines and the other CARP overexpressors. In the cells overexpressing CARP3, whether WT s427 or R0.8, the cellular content

of both CARP3 messenger Ribonucleic Acid (mRNA) and protein decreases extensively within 6 h of CpdA exposure.

The CARP3 protein has domains that are indicative of a role in protein-protein interaction, signalling, regulation and degradation and probably undergo acylation. Some experimental confirmation of these traits was obtained, using Co-immunoprecipitation (Co-IP) and Mass Spectrometry (MS), with the identification of Adenylyl cyclase (AC) GRESAG4s (also found through RNA-interference Target Sequencing (RITseq) and confirmed by quantitative Reverse Transcription PCR), and proteasome regulatory proteins (PRNs) in addition to membrane and flagellar binding proteins, as potential interactors. Preliminary Immunofluorescence (IF) microscopy showed that CARP3 localizes to plasma membrane ad the flagellum, CARP2 to specific bodies/organelles in the cytosol and CARP1 in the cytosol. RNA sequencing of overexpressing CARP3 reveals differentially expressed proteins involved in cell cycle and cytokinesis as well as transport proteins with several transmembrane domains, consistent with the proposed acylated membrane localisation, and with interaction of CARP3 with membrane proteins and ACs (GRESAG4 isoforms).Thus CARP3 has the domains, interactions and localization consistent with a regulatory role in cAMP metabolism.

Thus the CARPs and especially CARP3 are interesting biological molecules providing key new insights into signalling and the cell biology of the trypanosome.

Table of Contents

List of Figures

List of Tables

Acknowledgements

Firstly, I thank God Almighty Maker of Heaven and Earth for life and grace to undertake this period of study. For what do we have that we did not receive?

I thank my supervisor, Prof Harry de Koning, who did not just supervised this work but also mentored me and made me a better individual. Finishing the PhD is about the least l have learnt from him. What he has impacted will stay with me as l traverse this tortuous life as a career academician.

To the de Koning group, Gordon Campbell, Barrett group, and people in the Wellcome Trust Centre for Molecular Parasitology, Glasgow, thank you.

Many thanks go to Prof Darren Monckton (Director) and Dr Olwyn Byron (Deputy Director), University of Glasgow, Wellcome Trust 4-yr PhD for their support and encouragement over the period.

I thank the Wellcome Trust, of London, UK, and the University of Glasgow, Glasgow, UK, for sponsoring my PhD. I also thank the University of Cape Coast, Cape Coast, Ghana, for additional support.

To family and friends in Ghana and Lighthouse churches, Royston, Dennistoun and Edinburgh, God bless you.

Additional thanks go to my daughter and son; Daphne Naa Ayeley Tagoe and David Nii Boye Tagoe, for their understanding in all the times without their dad, the late nights in the lab as well as weekends.

Special thanks also go to my wife Mrs Ruby Naa Ayeley Tagoe, for her understanding and support without which l might not have even started this PhD to consider finishing it. She has been the rock behind me through this period of training.

Finally, I dedicate this book to my mother Mrs Theresa Amelor Tagoe. God gave you the grace to bring a fine young man into this world. God bless you.

Author's Declaration

I declare that the results presented in this thesis are my own work and that, to the best of my knowledge, it contains no material previously substantially overlapping with material submitted for the award of any other degree at any institution, except where due acknowledgment is made in the text.

Daniel Nii Aryee Tagoe

Abbreviations

AC	Adenylyl Cyclase
AMP	Adenosine monophosphate
ATP	Adenosine triphosphate
cAMP	Cyclic adenosine monophosphate
cGMP	Cyclic guanosine monophosphate
Co-IP	Co-immunoprecipitation
cN	Cyclic Nucleotide
CSF	Cerebro-spinal fluid
DAPI	4,6-diamidino-2-phenylindole
DFMO	DL-alpha-difluoromthylornithine
dKO	Double Knockout
DMSO	Dimethyl sulphoxide
DNA	Deoxyribonucleic acid
EC_{50}	Effective concentration inhibiting 50% cell proliferation
EF1-α	Elongation factor 1-α
ELISA	Enzyme-linked immunosorbant assay
ERK	mitogen-activated extracellular signal-regulated kinase
ESAG	Expression-site associated gene

EPAC	Exchange Protein Activated by cAMP
F	Flagellum
FAZ	Flagellar attachment zone
FBS/FCS	Foetal Bovine Serum/Foetal Calf Serum
FP	Flagellar Pocket
GAF-domain	Allosteric binding domain named after cGMP-specific and binding phosphodiesterases, adenylyl cyclase of *Anabaena* and FhlA of *E. coli*
GC	Guanylyl cyclase
GFP	Green Flouresence Protein
GPCR	G-Protein Coupled Recepetors
GPI	Glycophosphatidylinositol
GRESAG	Gene related to expression-site associated gene
GTP	Guanosine triphosphate
HAT	Human African trypanosomiasis
IBMX	Isobutylmethylxanthine
IC_{50}	50% inhibitory concentration
IFA	Immunoflouresence assay
K	Kinetoplast

K_i	Inhibition Constant
K_m	Michaelis-Menten constant
LBP	Leucine-binding protein
LdPDE	*Leishmania donovani* phosphodiesterase enzyme
LmjPDEB	*Leishmania major* phosphodiesterase enzyme B
LRRP	Leucine rich repeat protein
MMS	Methyl methane sulphonate
mRNA	Messenger-ribonucleic acid
MS	Mass Spectrometry
N	Nucleus
NTDs	Neglected Tropical Diseases
o.e	Overexpression
ORF	Open reading frame
PBS	Phosphate-buffered saline
PCR	Polymerase chain reaction
PDE	Phosphodiesterase enzyme
PFR	Paraflagellar rod
PK	Protein kinase
PKA	Cyclic adenosine monophosphate-specific protein kinase

PKA-C	Catalytic subunit of PKA
PKA-R	Regulatory subunit of PKA
PKC	Calcium/calmodulin-specific protein kinase
PKG	Cyclic guanosine monophosphate-specific protein kinase
PKI	Specific peptide inhibitor of PKA
RNAi	RNA interference
RPNs	Regulatory Protein Networks
QRT-PCR	Quantitative Reverse Transcription PCR
RHS	Retrotransposon hot spot
SIF	Stumpy induction factor
sKO	Single knockout
Tb427	*Trypanosoma brucei* strain 427
TbAT	*Trypanosoma brucei* adenosine transporter
TbrPDEB	*Trypanosoma brucei* phosphodiesterase enzyme B
TcrPDEB	*Trypanosoma cruzi* phosphodiesterase enzyme B
TPR	Tetratricopeptide Repeats
TM	Trans-membrane
UTRs	Untranslated regions
VSG	Variant surface glycoprotein

WHO	World Health Organization
+/-	Single knockout
-/-	Double knockout

Chapter 1

General Introduction

1.1 Trypanosomiasis and Human African Trypanosomiasis (HAT)

1.1.1 Definition and classification

Human African trypanosomiasis (HAT) also known as African sleeping sickness is a vector-borne parasitic disease caused by the protozoan pathogen *Trypanosoma brucei* (WHO, 2011) and transmitted by several *Glossina* species, commonly called tsetse flies (Stich et al., 2002). There are three sub-species of *Trypanosoma brucei* that infect mammals: *T. b. brucei, T. b. gambiense* and *T. b. rhodesiense*. However, only *T. b. gambiense* and *T. b. rhodesiense* infect and cause clinical disease in humans.

T. b. rhodesiense causes the acute form of HAT in which the patient's condition deteriorates rapidly as the parasite moves from the blood and lymphatic systems (early stage infection) into the central nervous system (CNS). The process starts with a tsetse bite and an immunological response (inflammation) which leads to the development of a chancre at the site of the infection (Moore et al., 2002). Parasites then move to the lymph nodes and are distributed in the circulation, multiplying in the blood and lymph. Inflammation of brain tissues (meningo-encephalitis) follows parasite invasion of the CNS as well as infiltration of spinal nerve tissue and inflammation of the meninges. This results in severe neurological symptoms followed by coma (Brun et al., 2010; Moore et al., 2002). In the absence of treatment, death usually occurs in 6-8 months. However, recent evidence implicates geographical variation in the speed at which *T. b. rhodesiense* infections progress to the late stage (MacLean et al., 2004).

T. b. gambiense is usually described as the chronic form of HAT, often with a long pauci-symptomatic stage of some years, and a chronic meningo-encephalitic condition during the late stage (Fevre et al., 2006; Taelman et al., 1987).

Although either *T. b. gambiense* and *T. b. rhodesiense* infection is considered HAT, staggering differences in clinical features of the infections, the treatment protocols used, the geographical range of the parasites, the epidemiology and transmission and the control options available suggests that each form of HAT is

in effect a separate disease entity (Fevre et al., 2006). Although the important epidemiological distinction in the clinical conditions lies in the length of the clinical course and the degree of disability, these differences have profound impact on disease transmission and control policies.

1.1.2 Disease burden and distribution

HAT is considered one of the world's Neglected Tropical Diseases (NTDs). These are diseases that cause substantial morbidity among the world's poorest people but have historically not been targeted for intensive drug development because of limited financial incentives in the private sector (Hotez et al., 2007; Molyneux et al., 2005). It has been estimated that the core group of NTDs results in greater than 57 million disability-adjustable life years (DALY) lost which are greater than those for malaria and HIV (Hotez et al., 2006). The features of NTDs are the fact that they lead to poverty, that they can be eliminated using low-cost and highly cost-effective control approaches and that their control would have a simultaneous and sustainable effect on poverty reduction (Hotez et al., 2009).

Human African trypanosomiasis is endemic in many countries between latitudes 14^{o} north and 29^{o} south across many countries in sub-Saharan Africa with an estimated 60 million people in 38 nations at risk of infection (Brun et al., 2010; Kennedy, 2004; Simarro et al., 2011) (Figure 1.1).

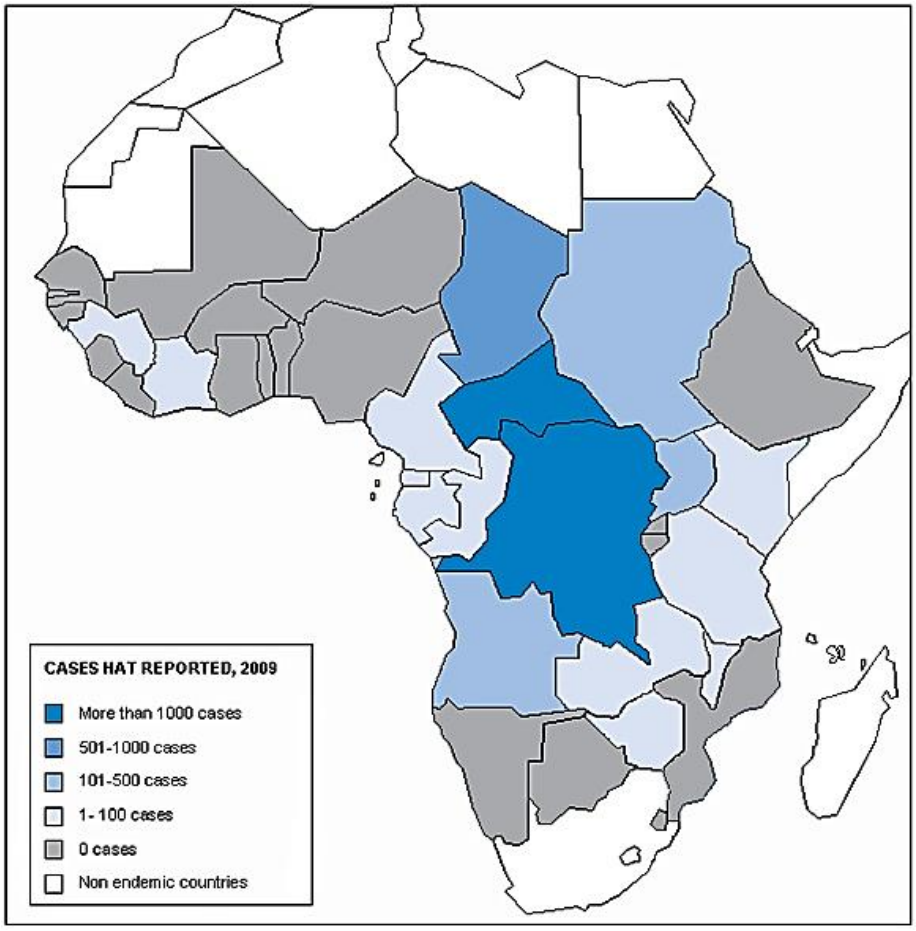

Figure 1.1: Disease distribution and burden of the Human African Trypanosomiasis. Reproduced from Simarro P.P et al. (2011).

It is estimated that approximately 98% of reported HAT infections leading to sleeping sickness is caused by *T. b. gambiense* which results in the chronic form of the disease, while *T. b. rhodesiense* represents fewer than 2% of the reported cases and causes an acute infection (Brun et al., 2010; Kennedy, 2004). However, *T. b. rhodesiense* have been shown to be a potential hazard in travellers from Europe and the USA returning from visits to east Africa game parks, where the parasite exists as a zoonotic infection in wild animals (Blum et al., 2012; Simarro et al., 2012b) (Figure 1.2).

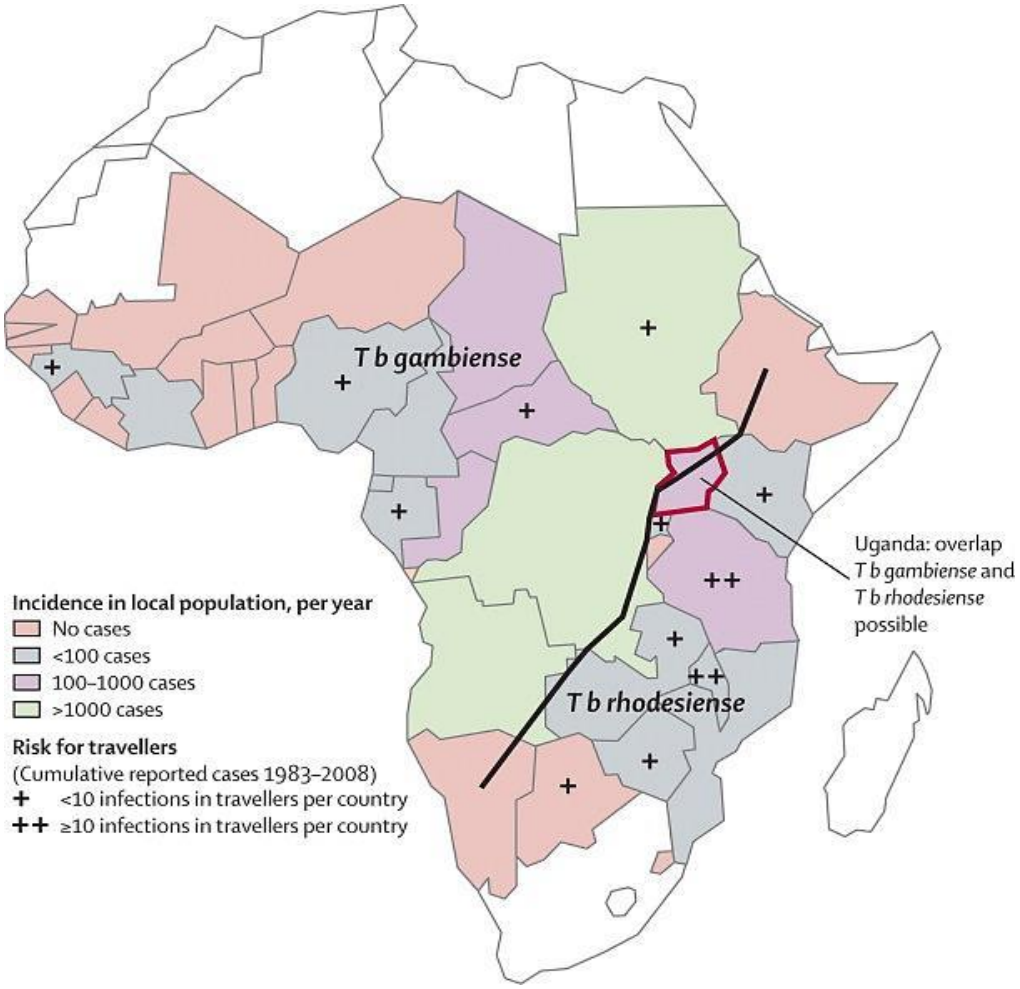

Figure 1.2: Distribution of human African trypanosomiasis with incidences and risk for travelers. The black line divides the areas in which *Trypanosoma brucei gambiense* prevails and those in which *Trypanosoma brucei rhodesiense* predominates. Reproduced from Blum J et al, 2010

The two human-infective species of African trypanosomes are also distinguished by ecology, animal reservoir and geographical differences. *T. b. rhodesiense* is transmitted by the vector *G. morsitans* which are found in woodlands and dry bush environments and it infects wild animals like antelope (Gooding and Robinson, 2004). *T. b. rhodesiense* also infects domestic animals which usually serve as reservoirs. Epidemiological studies have shown that cattle are important reservoirs (Fevre et al., 2001; Welburn et al., 2001). *T. b. rhodesiense* is primarily a zoonosis (Stich et al., 2002).Transmission of the disease is by contact with infected vectors through activities such as safaris, which bring humans into contact with infected vectors; only little human-fly-human transmission occurs.

The *Glossina palpalis* group are involved in the transmission of *T. b. gambiense*. These vectors are found along lakes and are often in close proximities to human

habitation (Gooding and Krasfur, 2004). *T. b. gambiense* appears to be almost exclusively transmitted via a human-fly-human transmission cycle. Although it can be found (with some difficulty) in wild and domestic animals the epidemiological role of this is uncertain since humans are the main reservoir (Welburn et al., 2001). The clinical features of HAT also vary relative to geographical location in Africa, both in different countries and different regions in the same country. There have been cases of differences in neurological symptoms and signs in *T. b. rhodesiense* HAT in Tanzania and Uganda, whilst within Uganda itself, variations have been observed in the speed and severity of disease progression in different foci (Kuepfer et al., 2011; MacLean et al., 2010).

Major international efforts by the World Health Organization (WHO), partner agencies and governments in infected regions have resulted in a dramatic improvement in both human case detection and treatment as well as vector control, leading to a sharp decline in the number of reported cases to levels below 10,000 for the first time in decades (Simarro et al., 2011). However, there are fears of possible unreported and under-reported cases to the WHO such as occurred in Uganda and the Democratic Republic of Congo in 2005 and 2007 respectively (Mumba et al., 2011; Odiit et al., 2005). These fears are exacerbated by the possibility of co-infection due to the existence of both HAT forms in Uganda (Picozzi et al., 2005) as well as documented incidence of HAT in Europe and the USA from travellers (Blum et al., 2012).

1.1.3 Lifecycle of the trypanosome

African trypanosomes have their life cycle in their invertebrate host and their mammalian host. The tsetse fly takes a bloodmeal by piercing the skin of the mammalian host. An infective vector transfers the parasite into the host during feeding. The infective stage for the human host is the metacyclic trypomastigote which is introduced with the saliva of the tsetse during feeding. Inside the host, they transform into bloodstream trypomastigotes, are carried to other sites throughout the body, reach other blood fluids (e.g., lymph, spinal fluid), and continue the replication by binary fission. The entire life cycle of African trypanosomes is represented by extracellular stages. Metacyclic and bloodstream forms are covered with a surface coat. When the tsetse fly feed off the blood of

an infected human, it picks up the bloodstream form and this differentiates into a procyclic trypomastigote and replicates in the gut of the vector before migrating to the salivary glands and converting to an epimastigote form. The epimastigotes convert to metacyclic trypomastigotes to complete the life cycle (Wiser, 2011). The cycle in the fly takes approximately 3 weeks. A schematic representation of this is shown in figure 1.3.

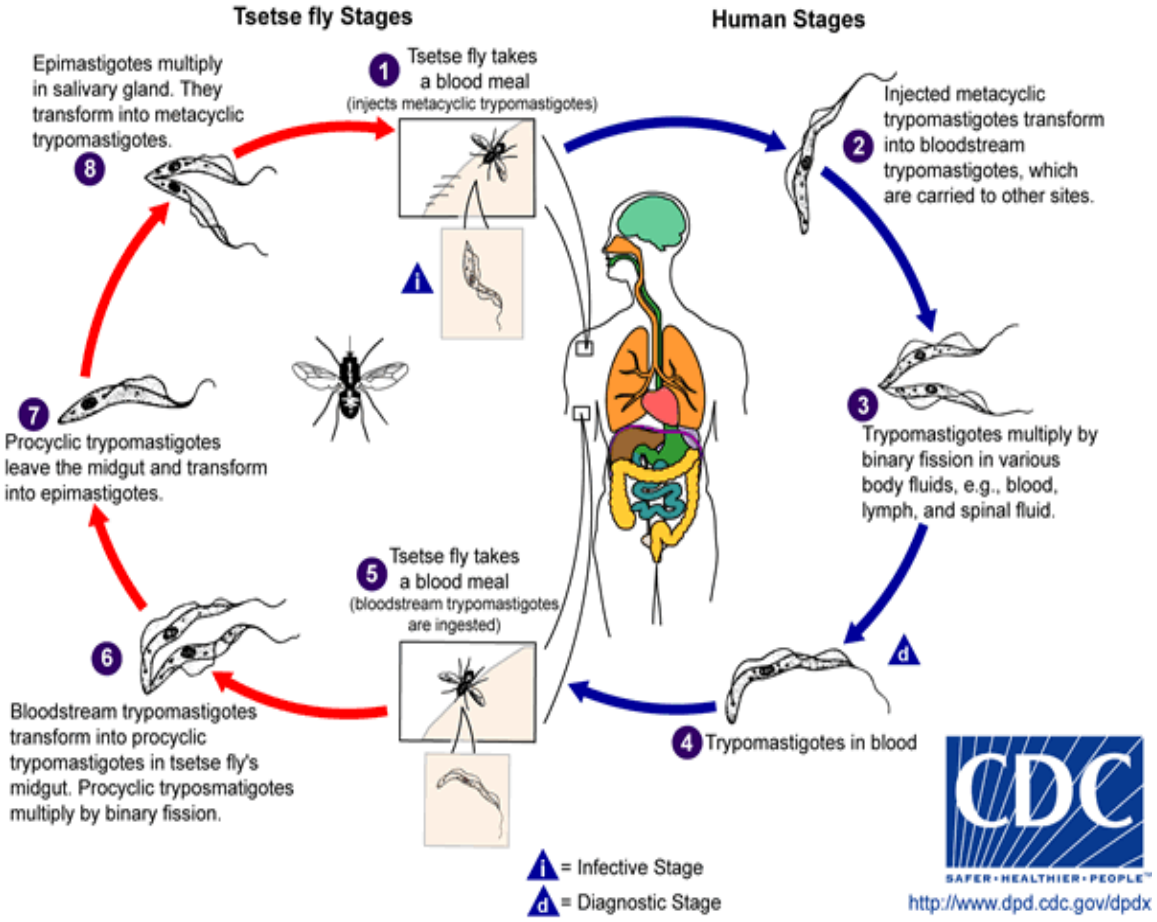

Figure 1.3: The life cycle of *Trypanosoma brucei.* Reproduced from the CDC website: http://www.dpd.cdc.gov/dpdx/HTML/TrypanosomiasisAfrican.htm

1.1.4 Diagnosis

The direct detection of parasites in HAT remains essential as a result of the grim outcome of the natural disease and the toxicity of the drugs used for its treatment. Although time spent in a HAT-endemic region as well as suggestive clinical presentation will point to the possibility of infection, several alternative diagnoses or coexisting diseases must be investigated and excluded (Kennedy, 2008a).

Microscopical detection of parasites is the 'gold standard'. This is especially the case in *T. b. rhodesiense* HAT, where due to the typically high level of parasitaemia trypanosomes can easily be identified on a thin or thick smear of the peripheral blood (Kennedy, 2006). The cyclical nature of parasitaemia in *T. b. gambiense* makes parasite detection difficult although it is still mandatory to identify parasites in the peripheral blood or lymph node aspirate using methods of concentrations (Brun et al., 2010).

The Card Agglutination Test for Trypanosomiasis (CATT) is a serological test designed especially for the detection of *T. b. gambiense*, and it has been heavily relied upon since its development in 1978 (Magnus et al., 1978). This is a simple and quick test which is particularly effective in population screening with a high sensitivity and specificity (Truc et al., 2002). There are however, issues with the high frequency of equivocal results due to differences in titre values that make the decision whether to treat or not difficult (Chappuis et al., 2005). Another serological test, the Latex/IgM can be used to detect elevated IgM in the CNS of second stage patients as a result of inflammatory response to *T. b. gambiense* invasion of the CNS and could have similar application in *T. b. rhodesiense* where similar changes in antibody levels have been observed (Lejon et al., 1998; Lejon et al., 2002).

DNA amplification techniques such as Polymerase Chain Reaction (PCR) has been shown to improve diagnosis substantially due to its high sensitivity and specificity (Mugasa et al., 2012) The loop-mediated isothermal amplification of DNA has been developed for rapid detection of both *T. b. rhodesiense* and *T. b. gambiense* with a high potential for diagnosis of HAT in endemic countries (Kuboki et al., 2003; Njiru, 2012) coupled with its improved sensitivity as a result of the inclusion of detergents in the reaction mix (Grab et al., 2011).

Besides the need for positive diagnosis, there is also the critical need for accurate staging of the disease as a result of the potential risks associated with the pharmacological treatment of CNS. The currently used WHO staging methods for diagnosing late-stage HAT implicates the presence of trypanosomes in the lumbar puncture (Kennedy, 2008b) of Cerebrospinal fluid (CSF) or a white blood cell count of more than 5 cells/µl or both (WHO, 1998). However, controversy rages as to the accuracy of this diagnostic measure primarily due to the need to

weigh the potential good of therapeutic treatment to the harm of drug toxicity. Several diagnostic staging techniques are being pursued as an adjunct or separate detection technique, including the determination of CSF IgM concentrations (Lejon et al., 2002; Lejon et al., 2003), the loop-mediated isothermal amplification assays, chemokine assays (CXCL10 and CXCL8) (Hainard et al., 2009) and the identification of biomarkers (neopterin) (Tiberti et al., 2012). Clearly, the need for a reliable and validated non-invasive staging technique would be of great benefit in the fight against HAT. In the meantime a good microscope and a trained microscopist at a health centre especially in *T. b. rhodesiense* affected areas should improve the level of detection of HAT and reduce the disease burden suffered by patients.

1.1.5 Treatment of HAT

The differences in the epidemiological characteristics and clinical course of *T. b. rhodesiense* and *T. b. gambiense* HAT infections necessitate that drugs used to treat them differ. However, common to drugs used in treating either disease is the fact that they are unavailable orally, often toxic, and sometimes ineffective (Fairlamb, 2003).

Pentamidine administered intramuscularly or intravenously has been used as a first-line treatment for early-stage *T. b. gambiense* since the 1940s with good clinical outcomes whilst early stage. However, pentamidine treatment has the potential of complications of hyperglycaemia or hypoglycaemia, prolongation of the QT interval on electrocardiogram, hypotension, and gastrointestinal features in *T. b. gambiense* and potential complications such as renal failure, skin lesions, anaphylactic shock, bone marrow toxicity, and neurological complications such as peripheral neuropathy (Barrett, 2010; Brun et al., 2010; Burri, 2010; Jacobs et al., 2011a). *T. b. rhodesiense* HAT is treated usually effectively especially in the early stages of the disease with intravenous suramin which was first used in the early 1920s. Just as pentamidine, suramin is also saddled with adverse clinical outcomes including neuropathy, rash, fatigue, anaemia, hyperglycaemia, hypocalcaemia, coagulopathies, neutropaenia, renal insufficiency and transaminitis (Barrett et al., 2007; Brun et al., 2011).

Treatment of the late stage is usually more problematic due to the fact that the available drugs are more toxic. Historically, melarsoprol (a highly toxic arsenic compound) is the only drug that is effective in treating late-stage *T. b. rhodesiense* by acting on trypanothione, a kinetoplastid-specific thiol that maintains an intracellular reducing environment (Fairlamb et al., 1989). Melarsoprol is usually effective, despite its painful route of administration and toxicity. It produces a post-treatment reactive encephalopathy in 10% of patients, half of whom die, leading to an overall mortality from treatment of about 5% and treatment failures due to drug resistance are major drawbacks (Kennedy, 2008a, 2012; Pepin and Milord, 1994).

Eflornithine, also called difluoromethylornithine (DFMO), is an ornithine carboxylase inhibitor and an effective anti-trypanocidal drug that was initially developed as an anti-cancer agent; it is effective against late-stage *T. b. gambiense* HAT (Burri and Brun, 2003; Wickware, 2002). However, there arose concerns of development of resistance to eflornithine due to the fact that it is trypanostatic and has a short half-life in the body. Eflornithine is also difficult to administer and requires huge doses, raising serious issues of drug compliance (Simarro et al., 2012a) – a potential risk factor for resistance development. Additionally, eflornithine resistance was easily selected in the laboratory (Vincent et al., 2010). Thus nifurtimox, which was used mainly for *Chagas* disease (caused by *Trypanosoma cruzi*) but displayed some reported efficacy in second-stage HAT (Pepin et al., 1992) was added to eflornithine as a nifurtimox-eflornithine combination therapy (NECT) and this has now become the standard first-line treatment for CNS-stage *T. b. gambiense* HAT, with intravenous melarsoprol now being used as second line treatment for this disease form (Simarro et al., 2011; Simarro et al., 2012a). NECT has a mortality rate of 0.7% compared with 2.1% for eflornithine monotherapy and 5% for melarsoprol leading to a substantial switch to combination therapy for late-stage *T. b. gambiense* HAT (Simarro et al., 2011). However, like all current treatment of HAT, NECT has some drawbacks: it is ineffective against *T. b. rhodesiense* HAT; the eflornithine component still has to be given intravenously; it can have many side-effects, such as bone marrow toxicity, alopecia, seizures, and gastrointestinal symptoms and there is the potential for drug resistance to occur in the affected areas in Africa through loss of the putative amino acid

transporter *Tb*AAT6, as has been shown in vitro (Burri and Brun, 2003; Kennedy, 2004; Vincent et al., 2010).

The prospect of more effective and less toxic drugs in trypanosomiasis is looking more promising over the past decade and into the future. This is mainly due to concerted and impressive efforts, primarily by WHO and various non-governmental organisations, but aided by partnerships between governments, universities, and the pharmaceutical industry. These have resulted in more effective drug regimens and also the development of several promising oral drug candidates (Barrett, 2010; Brun et al., 2011; Simarro et al., 2011). Two of these promising candidates are fexinidazole (Torreele et al., 2010) and the oxaboroles of which the orally available SCYX-7158 (AN5568) is the lead candidate (Jacobs et al., 2011b). Fexinidazole, is an oral treatment with good clinical outcomes against both *T. b. gambiense* and *T. b. rhodesiense* HATs with the ability to cross the blood-brain and also effective against both drug sensitive and resistant trypanosomes (Kaiser et al., 2011). It is a prodrug that is rapidly metabolized in vivo into two metabolites, sulfoxide and sulfone through the cytochrome P450 and flavin containing monooxygenase. It is presently in a phase II/III randomised clinical trial having met clinical requirements in a phase I trial (Eperon et al., 2014; Torreele et al., 2010). SCYX-7158 (AN5568) is also an oral drug with good bioavailability, blood-brain barrier penetration and is quick acting with a low IC_{50} (Jacobs et al., 2011b). Having passed all preclinical studies, SCYX-7158 (AN5568) is presently in phase I clinical trials.

1.1.6 Cell biology of the trypanosome

The trypanosome's elongated cell shape is defined by the highly polarized microtubule cytoskeleton that remains intact and elongated throughout the cell cycle and is semi conservatively inherited by daughter cells (Sherwin and Gull, 1989). The microtubules show a uniform polarity: minus ends are anterior and plus ends are posterior (Robinson et al., 1995b). The single-copy organelles in the trypanosome cell (i.e. the flagellar pocket, flagellum, kinetoplast, mitochondrion and nucleus) are precisely positioned within the cytoskeletal corset and are concentrated between the posterior end and the centre of the cell. The flagellum exits at the most posterior point, the mouth of the flagellar

pocket is tethered along the exterior length of the parasite and is the only site of endo- and exocytosis (Overath and Engstler, 2004). The flagellar pocket and its associated endo- and exocytosis is essential in the ability of the parasite to evade the host immune system through Variable Surface Glycoprotein (VSG) switching to protect against the alternative pathway of complement activation and to shield common antigenic determinants from immune recognition (Engstler et al., 2004; Grunfelder et al., 2002). The motility of the trypanosome is dependent upon its single flagellum (a semi-rigid structure found in the kinetoplastids and Euglenoids), which has a conventional axonemal structure plus an associated paraflagellar rod (Vaughan and Gull, 2003). The trypanosome flagellum originates in a basal body that is, in turn, linked through the mitochondrial membrane to the mitochondrial genome, which comprises a mass of catenated DNA termed the kinetoplast. In *T. brucei* only the distal tip of the flagellum is free with the rest laterally connected to the cell body along its entire length. This lateral attachment is both important in cell motility and cell division. It also tends to divide the cell into several discrete membrane subdomains (Gadelha et al., 2009; Langousis and Hill, 2014). The kinetoplast and basal body are linked by a tripartite attachment complex that must traverse both the cell and the mitochondrial membranes (Ogbadoyi et al., 2003). This comprises a series of filaments providing guide ropes through which mitochondrial genome segregation is linked to replication and segregation of the basal body and flagellum. The kinetoplast is linked to the microtubule cytoskeleton, such that drugs that disrupt the cytoskeleton prevent both basal body and kinetoplast segregation (Gull, 2003). The mitochondrion itself is a single elongated structure that runs from the posterior to the anterior of the cell with varying requirements dependent on the growth cycle stage of the trypanosome (Matthews, 2005)(Figure 1.4).

Trypanosome regulation of cell cycle and other processes is highly dependent on the degree of structural organization such as the fact that the mitochondrial genome has a discrete periodic S phase and G2 phase that is coordinated with nuclear genome replication and segregation. The first example is the strict regulation of organelle positioning during division. Thus, the kinetoplast nuclear, and kinetoplast-posterior dimensions are fixed during the cell cycle of the procyclic form, cell growth at the posterior end occurring between the

segregating basal bodies and being maintained throughout S, G2 and M phase (Robinson et al., 1995a). The second is the observation that cytokinesis is not dependent upon the completion of nuclear mitosis: disruption of the mitotic spindle by drugs or genetic perturbation of trypanosome cyclin-dependent kinases (CDKs) generates cytoplasts that have a mitochondrial genome but no nucleus (these are termed zoids) (Hammarton et al., 2003; Li and Wang, 2003). The most obvious morphological difference between the different life cycle stages of the trypanosome is the position of the kinetoplast relative to the posterior end of the cell. In bloodstream forms, the kinetoplast lies close to the posterior end of the cell, and each daughter kinetoplast remains in this region throughout the cell cycle until cytokinesis. By contrast, the kinetoplast lies midway between the cell nucleus and posterior in procyclic forms; in epimastigote forms (in the tsetse salivary gland), the kinetoplast is anterior to the central nucleus. The reasons for these shape changes during the life cycle are completely unknown, although they are clearly required to establish the cell architecture necessary for cell division of each life cycle stage. Perhaps an increased length of attached flagellum along the cell body assists motility in bloodstream forms, whereas the longer anterior flagellum aids substrate attachment of the epimastigote stage (Matthews, 2005).

The trypanosome cell structure and the changes in the cell biology of the parasite as it traverses from the mammalian bloodstream to the tsetse fly and back again must be highly regulated and interconnected. The present available armoury of genetic tools, molecular markers and tractable biology makes these organisms an excellent model in their own right for addressing fundamental questions of broad interest and applicability as well as the importance of tackling the disease itself.

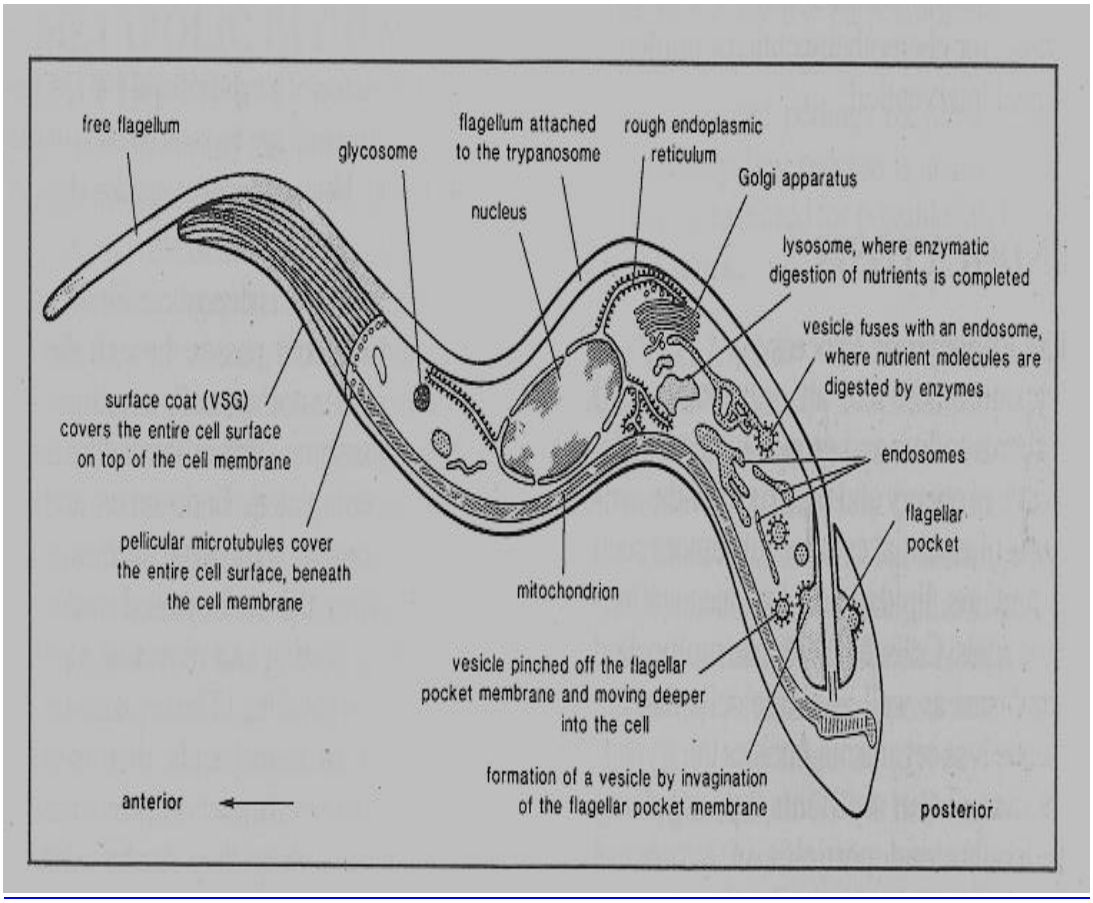

Figure 1.4: Schematic diagram of a trypanosome of the *Trypanosoma brucei* group in its intermediate bloodstream form. The arrow shows the direction of travel of the parasite. Reproduced from http://ilri.org/InfoServ/Webpub/fulldocs/ILRADre1989v7n1/endocytosis.html

1.2 Signal transduction

1.2.1 Introduction to signal transduction

Signal transduction pathways in mammalian cells are known to be of supreme importance in cellular function and indeed in the pharmacology of human and veterinary disease by converting extracellular stimuli into specific cellular responses (Maurice et al., 2014). Signal cascades frequently results in the amplification of a small signal into a large response leading to significant cell changes such as expression of DNA or activity of enzymes (Campbell and Reece, 2004). Signal transduction usually occurs with the binding and activation of a cell surface receptor by an extracellular molecule (ligand). This combination of a

messenger with a receptor causes a change in the conformation of the receptor, a process known as receptor activation and often triggers changes in (the concentration of) intracellular molecules. All this ultimately results in changes in the cell, either in the expression of the DNA in the nucleus or in the activity of enzymes in the cytoplasm. Through either process a single molecule can cause signal amplification and result in several cellular responses (Rodbell, 1980). Unicellular organisms such as slime moulds and yeast have been shown to respond to environmental stimuli either to aggregate or to locate and participate in mating respectively (Hanna et al., 1984; Sprague, 1991). Several environmental stimuli are able to initiate signal transmission processes in multicellular organisms and numerous signal transduction processes are required for coordinating the behaviour of individual cells to support the function of the organism as a whole (Campbell and Reece, 2004). Many disease processes, such as diabetes, heart disease, autoimmunity and cancer, arise from defects in signal transduction pathways further highlighting the critical importance of signal transduction to biology as well as the development of medicine (Huang et al., 2010). Receptors involved in signal transduction are divided into two main classes: extracellular and intracellular receptors.

1.2.1.1 Extracellular receptors

Extracellular receptors are integral transmembrane proteins that span the plasma membrane of the cell, with one part of the receptor on the outside of the cell and the other on the inside and make up most receptors. Signal transduction occurs as a result of a ligand binding to the outside without the molecule passing through the membrane. This binding stimulates a series of events inside the cell with different types of receptor stimulating different responses, whilst receptors typically only respond to the binding of a specific ligand. Upon binding, the ligand induces a change in the conformation of the inside part of the receptor (Rubenstein et al., 2006). This results in either the activation of an enzyme activity that is part of the receptor (e.g. adenylate cyclase) or the exposure of a binding site for other intracellular signalling proteins (e.g. G-proteins) within the cell, eventually propagating the signal through the cytoplasm.

In eukaryotic cells, most intracellular proteins activated by a ligand/receptor interaction possess an enzymatic activity; examples include tyrosine kinase and phosphatases. Some of them create second messengers such as cyclic AMP and inositol trisphosphate (IP_3), the latter controlling the release of intracellular calcium stores into the cytoplasm. Other activated proteins interact with adaptor proteins that facilitate signalling protein interactions and coordination of signalling complexes necessary to respond to a particular stimulus. Enzymes and adaptor proteins are both responsive to various second messenger molecules. Many adaptor proteins and enzymes activated as part of signal transduction possess specialized protein domains that bind to specific secondary messenger molecules. For example, calcium ions bind to the helix-loop-helix structural domain (EF hand domains) of calmodulin, allowing it to bind and activate calmodulin-dependent kinase. Phosphatidylinositol 4,5-bisphosphate (PIP_3) and other phosphoinositides do the same thing to the Pleckstrin homology domains of proteins such as Protein Kinase B (PKB), also known as AKT.

The G protein-coupled receptors (GPCRs) constitute the largest protein family of external receptors that sense molecules and activate intracellular signal transduction pathways and, ultimately, cellular responses. Others are Receptor tyrosine kinases (RTKs) which are transmembrane proteins with an intracellular kinase domain and an extracellular domain that binds ligands; examples include growth factor receptors such as the insulin receptor (Li and Hristova, 2006). Toll-like receptors (TLRs) which are involved in the innate immune response, take up adaptor molecules involved in signalling into the cytoplasm. Integrins and Ligand-gated ion channel are also involved in signalling.

1.2.1.2 Intracellular receptors

The main intracellular receptors are nuclear receptors and cytoplasmic receptors made up of soluble proteins localized within their respective areas. Nuclear receptors have the ability to directly bind to DNA and regulate the expression of adjacent genes, hence these receptors are classified as transcription factors (Olefsky, 2001). Nuclear receptors have two subclasses: Steroid hormone receptors found on the plasma membrane, in the cytosol and

also in the nucleus of target cells, and the retinoic acid receptor (RAR) a type of nuclear receptor which can also act as a transcription factor (Germain et al., 2006). The cytoplasm is involved in the regulation of the movement of calcium ions in and out of the cell and this is considered to be a signalling activity for metabolic processes since calcium is one of the key secondary messengers. Certain intracellular receptors of the immune system are cytoplasmic receptors. This includes the recently identified NOD-like receptors (NLRs) that reside in the cytoplasm of some eukaryotic cells and interact with ligands using a leucine-rich repeat (LRR) motif similar to TLRs. Some of these molecules like NOD2 interact with Receptor-interacting serine/threonine-protein kinase 2 (RIP2 kinase) that activates NF-κB signalling, whereas others like NALP3 interact with inflammatory caspases and initiate processing of particular cytokines like interleukin-1ß (Delbridge and O'Riordan, 2007).

Many intracellular receptors bind secondary messengers and the cascade effect brings about changes in the cell such as gene regulation and metabolism. Some secondary messengers include calcium, lipophilic second messenger molecules (diacylglycerol and ceramide), Nitric oxide (NO) and redox signalling (superoxide, hydrogen peroxide, carbon monoxide, and hydrogen sulphide) (Forman, 2009). One of the major signalling pathways is the cAMP dependent pathway.

1.2.2 G-Proteins, Adenylate cyclases and Protein Kinase A (PKA) in mammalian cells

Cyclic adenosine 3′,5′-monophosphate (cAMP) is an evolutionary conserved and important second messenger that plays fundamental roles in cellular responses to many hormones and neurotransmitters. Cyclic AMP is both produced and regulated by Adenylyl cyclases through the mediation of G-protein-coupled receptors (GPCRs) and catabolised from cAMP to AMP by cAMP phosphodiesterases (PDEs) (Conti and Beavo, 2007). Protein Kinase A (PKA) is one of the most important targets of cAMP and further regulates cAMP through the existence of a feedback loop involving PKA, both in yeast (Nikawa et al., 1987) and in mammals (Jin et al., 1998).

GPCRs are important regulators of several cellular functions through the activation of intracellular signals in response to a wide variety of agonists or stimulants. Recent estimates put drugs that exert therapeutic influence to GPCRs to be between 30-40% (Garland, 2013). G-proteins which are distinct are able to form heterodimer complexes through direct physical interaction resulting in an integrated physiological response. A recent review by Luttrell et al, discussed the regulatory role and complexity of GPCRs as a result of the ability of several G-proteins to couple with different G-protein families, that structural differences in ligands causes differential stimulations as well as the ability to signal through either G-protein and non G-protein effectors (Luttrell et al., 2015). The most important regulatory function of G-proteins is the mediated production of cAMP through the stimulation of ACs which are also directly stimulated by G-proteins.

Mammalian cells have two AC, transmembrane ACs (tmACs) regulated by GPCRs and Soluble ACs (sACs) regulated by bicarbonates and Calcium with structural similarity to tmACs but without transmembrane domains as well as discrete localization in different part of the cell (Schmid et al., 2014). Due to its location on the surface of the cell, the tmACs are considered the target where the majority of hormone sensitive cAMP stimulation occurs. ACs, together with other components of the cAMP signalling pathway, tend to be compartmentalized in lipid rafts. This compartmentalization helps to explain the nature of the discrete foci and tight spatial control of cAMP signalling and the resultant formation of microdomains. The formation of these large complexes and how they achieve this spatial regulation of cAMP is reviewed by (Dessauer, 2009). PKA is one of the key targets for cAMP produced from activation of ACs.

Cyclic AMP-dependent PKA is ubiquitous in mammalian cells where it exists in two forms made up of the inactive tetrameric holoenzyme and the active dissociated catalytic subunit (C-subunit) (Das et al., 2007). It has been shown to be an important down regulator of cAMP accumulation through several mechanisms so as to prevent the overstimulation of the cAMP signalling pathway. This includes the inhibition of cAMP synthesis, stimulating its hydrolysis, enhancing its excretion or a combination of these processes (Vandamme et al., 2012). Recently it is been shown that PKA is able to reset the mammalian cAMP signalling by forming an active site coupling in a PDE and PKA regulatory subunit

complex (Krishnamurthy et al., 2014). Several nuclear and cytosolic proteins act as substrate for PKA. One of the important means of regulation by PKA is through phosphorylation, such as phosphorylation of several metabolic enzymes, and transcriptional regulation by direct phosphorylation of transcriptional factors. PKA also regulates other signalling pathways such as the activation of MAPK, decreases the activities of Raf and Rho and modulates ion channel permeability as well as regulates the expression and activity of various ACs and PDEs (Sassone-Corsi, 2012) (Figure1.5).

Alternative and independent to PKA activation, cAMP are able to stimulate Exchange Proteins Activated by cAMP (EPACs). These are specific guanine nucleotide exchange factors (GEFs) for the Ras GTPase homologues, Rap1 and Rap2 (de Rooij et al., 2000). Mammals have two EPAC isoforms EPAC1 and EPAC2 which varies both in distribution as well as structure with EPAC2 having an additional Cyclic Nucleotide Binding (CNB) domain. Several researchers have shown the importance of EPAC proteins in mediating and regulatory of several and important actions of cAMP in humans. A previous review by Borland and colleagues, revealed the myriad effect of stimulation of EPAC by cAMP resulting in promotion and inhibition of cell division, promotion of cell differentiation, hyperthrophy, inflammation among others in several human cells (Borland et al., 2009). Recently, Parnell et al, discussed strategies being developed in the design of pharmacophores and their therapeutic potential (Parnell et al., 2015). Thus the selective modulations of EPACs offer additional sources of therapeutic targets in the general cAMP-PDE-PKA pharmacology.

It should however be noted that although cAMP signalling has been detected in all organisms except plants, there are varied differences in the components that make up the pathway in all these organisms. The underlying commonality which is also the only absolutely conserved signalling molecule is cyclic adenosine 3′,5′-monophosphate (cAMP).

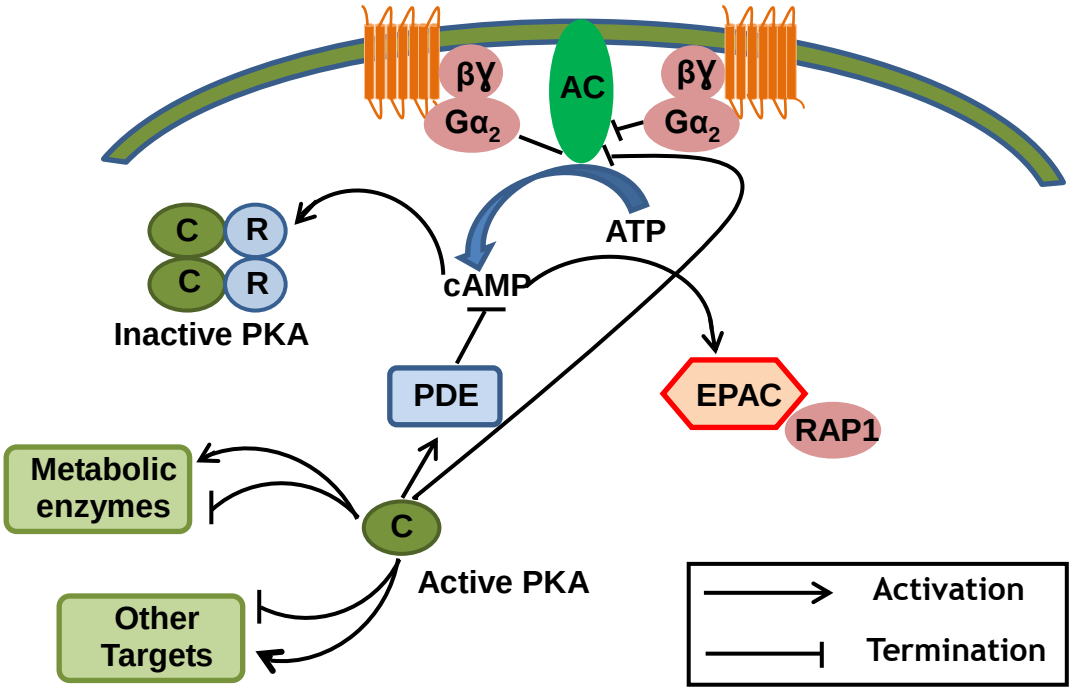

Figure 1.5: Components of cAMP signalling pathway showing adenylate cyclases and G-proteins in humans. Adapted from Sassone-Corsi P, 2012

1.2.3 Cyclic Nucleotide Phosphodiesterases

1.2.3.1 PDE family and diversity

Cyclic nucleotide phosphodiesterases class 1 (PDE-1) are a family of related phosphohydrolases that selectively catalyse the hydrolysis of the 3' cyclic phosphate bonds of adenosine and/or guanosine 3',5'- cyclic monophosphate. Increasing chemical and molecular biology techniques have revealed and continue to reveal the large diversity and complexity of PDEs.

PDEs have been grouped into three classes based on their different catalytic domains. Class I PDEs are found in all eukaryotes and they are the only forms of PDEs in higher eukaryotes (Beavo, 1995). Class I PDEs are the only enzymes which are capable of efficiently hydrolysing cyclic nucleotides. The genome of known kinetoplastids encodes four different class I PDEs (PDE-A to PDE-D) and does not contain members of the other PDE classes (Beavo, 1995) just as is the case in the human genome (Seebeck et al., 2011). At least one copy of each of the four PDE genes is present in the genome database of *T. brucei*, *T. cruzi* and *L. major* (Vij et al., 2014). Class II PDEs are found in certain prokaryotes (e.g.

Vibrio fischeri) or fungi (e.g. *Saccharomyces*, *Candida*) and in many lower eukaryotes (e.g. *Dictyostelium discoideum*) (Figure 1.6).

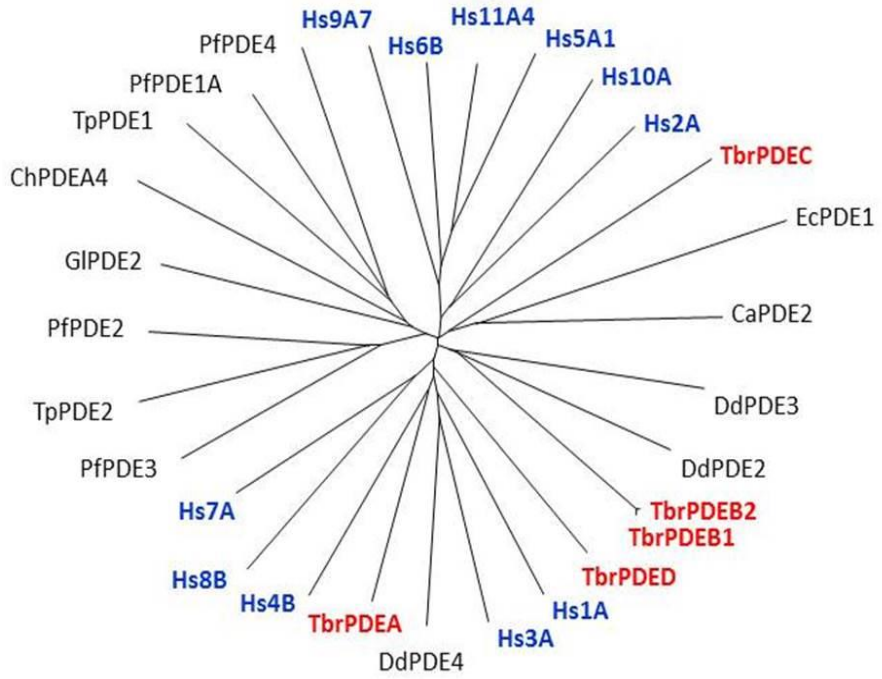

Figure 1.6: Non-rooted tree of Class I protozoan and human PDEs. The catalytic domains of many protozoan PDEs, including *T. brucei* (in red), are as closely related to the human PDEs (in blue) as these are among themselves. Hs, *Homo sapiens*; Pf, *Plasmodium falciparum*; Ca, *Candida albicans*; Tp, *Theileria parva*; Gl, *Giardia lamblia*; Ch, *Chilomastix hominis*; Ec, *Encephalitozoon cuniculi*; Dd, *Dictyostelium discoideum*. Figure courtesy of Professor T. Seebeck, University of Bern, Switzerland.

The PDE superfamily of enzymes is classified into 11 families (PDE1-PDE11) in mammals based on amino acid sequence, substrate specificity, regulatory properties, pharmacological properties and tissue distribution (Keravis and Lugnier, 2010). The 11 PDE families code for 21 genes (Conti and Beavo, 2007), although variations exist such that some families are coded for by one gene whilst others are a product of multiple genes. This extensive variations is further enhanced by multiple, differentially regulated promoters that influence expression of the PDE mRNA transcripts (Omori and Kotera, 2007b), as well as by extensive alternative splicing of the mRNAs resulting in a vast array of protein products, estimated to be close to 100 different protein products of these genes. These are distinguished by having different regulatory features, catalytic characteristics, tissue distributions, subcellular localizations, targeting to

signalling complexes and sensitivities to PDE inhibitors (Bender and Beavo, 2006; Francis et al., 2011b).

This complexity of the cyclic nucleotide PDE system has forced increasingly more sophisticated and complex approaches to be adopted to understand the roles of PDEs in regulation of cAMP and cGMP in the cell. It is now very clear that any single cell type can express several different PDEs and also that the nature and localization of these PDEs is likely to be a major regulator of the local concentration of cAMP or cGMP in the cell. PDEs are regulated not only at the genetic level but also by diverse biochemical mechanisms including phosphorylation/dephosphorylation (Ang and Antoni, 2002; Pozuelo Rubio et al., 2005), allosteric binding of cGMP or cAMP, binding of Ca^{+2}/calmodulin, and various protein-protein interactions (Bender and Beavo, 2006; Omori and Kotera, 2007a). Additional concepts of PDE regulations are being proposed. These include the concept that one of the major roles for PDEs is to modulate the three-dimensional shape, the amplitude, and the temporal duration of "clouds" of cyclic nucleotide in the cell as well as the possibility that some PDEs act as scaffolding proteins or use allosteric changes induced by binding of cyclic nucleotides to alter protein-protein interactions (Bender and Beavo, 2006; Conti and Beavo, 2007).

1.2.4 Therapeutic potential of PDEs

Although the therapeutic potential of PDEs was realised quite early, the first PDE inhibitors lacked specificity and thus had a very narrow therapeutic index. This has changed with the identification and classification of the different types of PDEs (Conti and Beavo, 2007). One important general reason that PDEs have been pursued as therapeutic targets is related to the basic pharmacological principle that regulation or degradation of any ligand or second messenger can often make a more rapid and larger percentage change in concentration than comparable regulation of the rates of synthesis (Pierre et al., 2009; Potter, 2011). This is true for either pharmacokinetic changes in drug levels or changes in amounts of an endogenous cellular regulatory molecule or metabolite. It has been recognized long ago that the complexity of the cAMP signalling pathway

and the several effectors involved implies that several of these effectors can be simultaneously affected in response to either cAMP or cGMP. This together would result in an integrated, fine-tuned and possibly multiple cellular signalling response (Maurice et al., 2014).

Additionally, it is clear that an extraordinary large diversity of PDE family is expressed in mammalian tissues. This diversity is present in the unique architecture at the active site (Conti and Beavo, 2007; Francis et al., 2011c; Keravis and Lugnier, 2012). And although some of these properties challenge the development of drugs that target individual enzymes, nevertheless, many of the characteristics of PDEs are also viewed as unique opportunities to increase specificity and selectivity when designing novel compounds for certain therapeutic indications. Moreover, there is increasing evidence that many of these PDEs are tightly connected to different physiological functions in the body and by inference also to different pathological conditions. This provides the platform to develop isoform-selective inhibitors that can target specific functions and pathological conditions without a high likelihood of causing nonspecific side effects (Bender and Beavo, 2006; Francis et al., 2011c). It has also been shown that functional features of closely related PDEs can differ substantially and that there is differential expression of the various PDE families (Francis et al., 2011a). Even PDEs within the same families, with catalytic domain similarities >50%, have been shown to have extensively different selectivity for cAMP and cGMP (Omori and Kotera, 2007b). This has resulted in the discovery of several PDE inhibitors such as Sildenafil (used to treat erectile dysfunction) as well as several newly identified PDE inhibitors in a variety of diseases (Dorsey et al., 2010; Galie et al., 2010; Ghofrani et al., 2006; Jaski et al., 1985).

Bender and Beavo discussed why PDEs are likely to be good drug targets, arguing that the concentrations of cAMP and cGMP (typically <1 – 10 μM) in most cells means that a competitive inhibitor would not need to compete with very high levels of endogenous substrate to be effective, unlike most protein kinase inhibitors that require a high enough affinity to displace millimolar concentrations of ATP (Bender and Beavo, 2006).

One of the reasons for this is the fact that the myriad forms of PDEs that serve as cellular targets of cyclic nucleotides (cN) and as major determinants of cyclic nucleotide action exceeds those of other targets, such as that of cN-dependent protein kinases, the cN-gated (CNG) channels and exchange-proteins activated by cAMP (EPACs). All PDEs contain a conserved catalytic site that interacts with cNs and hydrolyses them to respective 5'-nucleotides, with specificity for cAMP (4, 7, and 8), cGMP (5, 6, and 9) or both (1, 2, 3, 10, and 11) (Francis et al., 2011a). Differences have been observed in selective inhibition in families with highly similar amino acid sequences (~42%) (Zhang et al., 2005) and even among catalytic sites of PDE isoforms in the same family with greater than ~75% sequence homology (Bender and Beavo, 2006). These data suggest that subtle differences in the topography and chemical characteristics of the active site can have profound effects on substrate preference, catalytic efficiency, and inhibitor potencies (Francis et al., 2011c). The structural subtleties that provide for these differences in such closely related enzymes are typically not fully understood but they could relate to differences in the catalytic site pocket, reflect the influence of interactions of the inhibitors with regions outside the catalytic pocket, or of interaction with protein binding partners and posttranslational modification (Burgin et al., 2010; Houslay et al., 2007).

PDEs such as 2, 5, 10, and 11 contain cN-binding sites (Gross-Langenhoff et al., 2006; Handa et al., 2008; Martinez et al., 2008; Zoraghi et al., 2004) that comprise of ~120 amino acids known as GAFs [an acronym derived from the proteins in which these domains were originally identified, i.e., cGMP-binding PDEs, Anabaena adenylyl cyclases, and Escherichia coli transcription factor FhlA (Aravind and Ponting, 1997)] within their respective regulatory domains. GAF domains are found in many different proteins in nearly all phyla, including histidine kinases, phosphotransferases, ATPases, cyclases, and PDEs. They are thought to function as regulatory elements that bind nucleotides or other small molecules. These GAFs are also structurally and evolutionary distinct from PDE catalytic sites cN-binding sites in the cN-dependent protein kinases, cN-regulated channels, the bacterial catabolite-gene activator protein (CAP), and EPACs (Bos, 2006; Zoraghi et al., 2004). The regulatory nature of the GAF domains in binding both cAMP and cGMP in varied PDEs provides the basis for the functional activities of these PDEs as well as potential as targets for therapeutic

interventions. GAFs A and B are thought to be involved in dimerization of the PDE which in itself can regulate the functions of the PDEs. A specific example of the importance of GAF domains and cGMP allosteric interactions in the PDEs is illustrated by the H258D mutation in the GAF A domain of human PDE6B, which causes the autosomal dominant congenital stationary night blindness (Farber and Danciger, 1997).

Thus PDEs provides the numbers, the structures, the functions, the diversity and the locations that make them great pharmacological targets. These advantages have been and are still being exploited by many different companies that are developing small molecules with substantially different affinities for most of the different PDE families.

1.2.5 Cyclic AMP signalling of kinetoplastids

The order of the *kinetoplastida* in the group of the *Discicristates* covers a vast empire of unicellular eukaryotes (Baldauf, 2003), many of whom have adopted a parasitic lifestyle. They are characterized by an elongated cell body of 10–20 μM in length that is propelled by a single flagellum. Besides the cell nucleus, the kinetoplastids contain the name-giving kinetoplast, a specialized compartment of the mitochondrion that contains a mass of concatenated DNA circles, amounting to up to 10 percent of the total cellular DNA mass. Kinetoplastids causes several diseases in men and animals, the majority of which are fatal if untreated, and is compounded by lack of vaccines and poor therapeutic options - almost all of which are under threat due to the development of resistance. Thus the need to understand cell signalling, which is one of the greatest sources of drug targets in human pharmacology, and the opportunities it offers in therapeutic interventions.

The presence of cAMP in trypanosomes and its variation during the course of infection were recognized early on (Strickler and Patton, 1975). The completion of various kinetoplastid genome projects recently has, however, demonstrated that cAMP signalling in the kinetoplastids is starkly different from the pathways extensively studied in mammals. Some important differences include the fact that kinetoplastid genomes do not code for G-protein-coupled receptors, or for

heterotrimeric G proteins or protein kinase G; the adenylyl cyclases are structurally different from their mammalian counterparts although the basic catalytic mechanism seems to be conserved between them and may have assumed the role of receptors; few genes for cAMP effectors have been identified in these organisms; and the stringent need for regulation of cAMP in the small kinetoplastid cell to prevent flooding of the cell (Seebeck et al., 2001; Tagoe et al., 2015). The majority of what we know about cAMP signalling in kinetoplastids is derived from studies in trypanosomes.

1.2.5.1 Adenylyl cyclases of kinetoplastids

cAMP in most eukaryotes including kinetoplastids is produced by stimulated or constitutively active Adenylyl Cyclases (ACs), whilst cyclic nucleotide PDEs degrade the phosphodiester bond in cAMP thus abrogating signal transduction (Dorsey et al., 2010).

A putative kinetoplastid AC gene was first identified in *T. brucei* when the gene expression site of an active VSG was sequenced, revealing that there were multiple genes in the site that were co-expressed with VSG. These genes were termed expression site-associated genes (ESAGs), and one of them, ESAG4, showed homology with an AC from yeast (Pays et al., 1989). These paved the way for restriction mapping of the clones into two categories, with the largest from each further characterized and named GRESAG4.1 and GRESAG4.2 (genes related to ESAG4) (Gould and de Koning, 2011). Related genes were also found in *T. gambiense*, *Trypanosoma congolense*, *Trypanosoma mega* and *Trypanosoma vivax*. Through yeast complementation studies the *Trypanosoma equiperdum* AC genes were proven to actually code for AC enzymes as ESAG and GRESAG4.1 complement AC-deficient yeast mutants in *S. cerevisiae*, (Paindavoine et al., 1992; Ross et al., 1991). Further studies were undertaken on the differential expression of ESAG and GRESAG in bloodstream and stumpy forms (Rolin et al., 1996). Trypanosomal ACs are either transiently expressed in the BSFs like the ESAGs or are expressed constitutively in all the life form stages like the GRESAGs (Bieger and Essen, 2001). Since then similar multigene families with high homology to ESAG4 and GRESAG4.1 have also been identified in *Leishmania donovani* and *T. cruzi* that share the same predicted protein architecture (Sanchez et al., 1995). *T. brucei* encodes for approximately 65 GRESAG4

proteins, which are localized along the flagellum in both BSFs and procyclic (fly midgut-stage) cells. Their similarity and tandem arrangements results in cross-reactivity to some antibodies raised against ESAG4 (Oberholzer et al., 2011; Paindavoine et al., 1992). Whereas knocking out ESAG4 from the expression site does not affect parasite proliferation, a knockdown of all the AC family that includes ESAG4 and two *ESAG4*-like *GRESAG4* (*ESAG4L*) genes led to a total decrease in AC activity resulting in a phenotype that is defective in cytokinesis (Salmon et al., 2012a).

The genomes of all kinetoplastids contain multiple copies of genes for adenylyl cyclases. Interestingly, the genomes of African trypanosomes (*T. brucei, T. congolense*, and *T. vivax*; each about 35 Mbp) contain more than 50 different cyclase genes, while the similarly sized genomes of *T. cruzi* and the Leishmanias (*L. major*, *L. infantum*, and *L. braziliensis*) only contain 5 or 6 such genes. For instance the *T. brucei* genome encodes for more than 80 ACs, many of which are detected on the cell surface (Salmon et al., 2012a). The reason for the extensive numbers of ACs in trypanosomes is attributed to the size of the trypanosome and the need to tightly regulate cAMP levels. An additional reason for a greater number of ACs in *T. brucei* compared with other *Trypanosoma* and *Leishmania* species may be due to the need to evade the host immune system by continuously switching VSGs leading to a duplication of ESAGs. In fact it has been shown that ACs influence host-parasite interactions through the modulation of Tumour Necrosis Factor-alpha (TNF-α) and that AC activity of lysed trypanosomes favours early host colonization by parasites (Salmon et al., 2012b). This suggests that diversity in ACs provides an adaptive advantage to the extracellular *T. brucei* enabling host immune modulation and thus survival. All kinetoplastid cyclases exhibit a large, extracellular N-terminal domain, followed by a single transmembrane helix and a highly conserved class 3 catalytic domain (Naula and Seebeck, 2000; Schaap, 2005) which is different from mammalian ACs that contain several transmembrane domains and are regulated by G-protein-coupled receptors. Structurally *T. brucei* ACs differ from mammalian Class I ACs as a result of the insertion of a 36-amino acid region into the catalytic domain, forming two extra helices and termed the D-subdomain. In Class I ACs, this region, without the kinetoplastid insert, is involved in the interaction with G-protein subunits. The fact that trypanosomal ACs have such a variation at that

particular point in the structure suggests that the D-subdomain may play a regulatory role and provides a structural reason for interaction with kinetoplastid ACs. This is due to the fact that unlike in mammalian cells, trypanosomes have no GPCRs nor heterotrimeric G-proteins in their genome (Berriman et al., 2005). Thus the N-terminal domains of trypanosomal ACs may function as receptors akin to the mammalian receptor-type guanylyl cyclases. Although the catalytic domain is structurally very similar to those of mammalian adenylyl cyclases, it is not activated by forskolin, and may form homodimers (Bieger and Essen, 2001; Garbers et al., 2006; Gould and de Koning, 2011; Naula et al., 2001). The structural differences and the cellular localization of the ACs of kinetoplastids are also consistent with them acting as receptors. The result is the strong speculation of the possibility of the N-terminal extracellular domain of ACs acting as a receptor akin to GPCRs for signalling in the kinetoplastid (Laxman and Beavo, 2007; Seebeck et al., 2004). ESAG4 was shown to be present on the cell surface along the flagellum (Paindavoine et al., 1992) and the localization of ACs in BSFs was apparently identical to that in procyclics. Similarly, in *T. cruzi* epimastigotes, the calcium-stimulatable AC was found to be associated with the flagellum (D'Angelo et al., 2002). An *Escherichia coli* L-leucine-binding protein (LBP) and a similar LBP in *Pseudomonas aeruginosa* have been shown to stimulate trypanosomal ACs (Emes and Yang, 2008; O'Hara et al., 2000). Additionally, some extracts from *T. cruzi* and *T. brucei* insect vectors have been shown to activate ACs whilst a low-molecular-weight molecule, Stumpy Induction Factor (SIF), probably secreted by the trypanosome itself, was inferred to trigger the differentiation of long-slender bloodstream *T. brucei* to the non-replicating stumpy form via the cAMP signalling cascade (Garcia et al., 1995; van den Abbeele et al., 1995; Vassella et al., 1997).

Recently, ACs have been implicated in the conversion of epimastigotes of *T. cruzi* in the insect midgut and later hindgut into human infectious non-proliferative metacyclic trypomastigotes, a process known as metacyclogenesis akin to cellular differentiation of BSF *T. brucei* to procyclic forms (Paindavoine et al., 1992). Here, both AC expression and intracellular cAMP levels in *T. cruzi* increase significantly in a two-step process from point of stimulation (nutrient deprivation) through a 6-48 h period (Hamedi et al., 2015). This may suggests that variation of intracellular cAMP in response to nutritional stress potentially

regulates differential gene expression resulting in cellular and life cycle changes in the parasite.

Proteomic analysis of bloodstream *T. brucei* trypanosomes revealed receptor and transport-like proteins that likely play important roles in signalling as well as acting as potential effectors (Oberholzer et al., 2011). Recently, several receptor-type flagellar ACs have been shown to be specifically upregulated, are procyclic stage specific, glycosylated, surface–exposed and possess catalytic activity. Additionally, they are either distributed along the flagellum or localized to the flagellum tip (Saada et al., 2014). These observations suggest that ACs have specific subdomain localization and thus possibly a microdomain flagellar cyclic AMP signalling in *T. brucei*. These possibilities were further strengthened by the findings that one of these insect stage specific cyclases, AC6 (Adenylate Cyclase 6), is responsible for social motility and mutation and that knocking it down results in a hypersocial phenotype (Lopez et al., 2015). All these together coupled with the fact that cAMP levels are significantly increased *in vitro* during the differentiation of BSFs to procyclic forms suggests a probable role of cAMP involvement in parasite differentiation through ACs.

1.2.5.2 Cyclic nucleotide-specific phosphodiesterases of kinetoplastids

The kinetoplastid genomes all code for the same set of cyclic nucleotide-specific phosphodiesterases enzymes of the class 1 type of PDEs (Figure 1.7) with catalytic domains similar to those of the human PDEs (Beavo, 1995; Kunz et al., 2006).

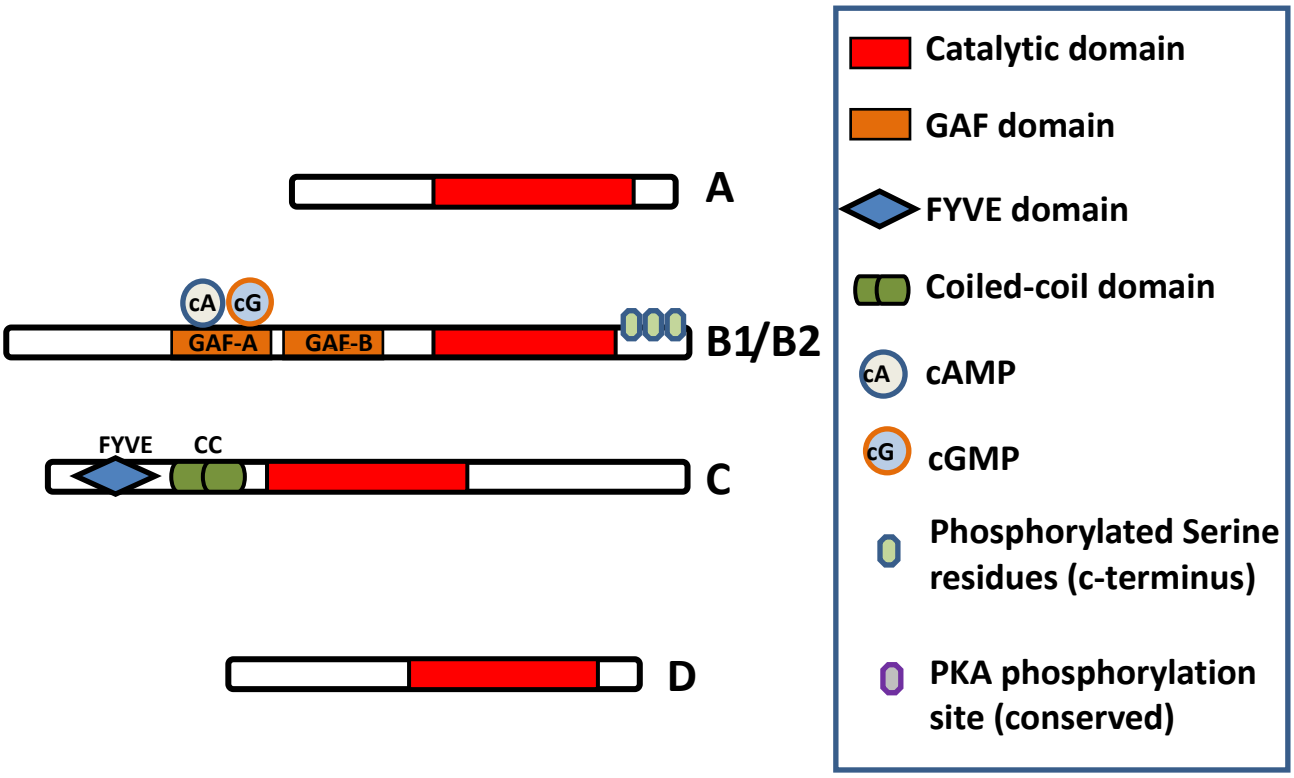

Figure 1.7: The conserved catalytic domain is the main functional domain of the PDEs and binds to cAMP. The GAF-A domains of PDEB1 and B2 binds cAMP and cGMP and regulate the function of the catalytic domain (Laxman et al., 2005). FYVE finger has been shown to bind two Zn^{2+} ions. Coiled-coil domains are important in stabilizing protein structure and thus for protein function. Phosphorylation of serine residue of PDEB1 has been observed in *T. brucei* phosphoproteome (Nett et al., 2009) whilst a probably functionally conserved PKA phosphorylation site is predicted in PDEB1/B2 (Shakur et al., 2011).

1.2.5.2.1 PDEA

PDEA is a high-*K*m (>200 µM), cAMP-specific PDE of about 620 amino acids. The polypeptide contains no discernible structural elements other than the PDE catalytic domain, which is located in the C-terminal part of the polypeptide. *PDEA* is a single copy gene (Kunz et al., 2006). It is a cAMP-specific PDE as it is neither inhibited nor activated by cGMP. In *T. brucei*, the enzyme is constitutively expressed. Genetic deletion experiments, both in cell culture and *in vivo*, have demonstrated that it is not essential. Homologues of *T. brucei* PDEA (TbrPDEA) have been identified with both similar sequence and experimentally functional characteristics in *L. major* and *T. cruzi* (Alonso et al., 2007; Bhattacharya et al., 2009; Gong et al., 2001).

1.2.5.2.2 PDEB

The two PDEB isoforms B1 and B2 are low-*K*m, cAMP-specific PDEs that are very similar to PDEA in their catalytic domain but differ in their N-terminal parts, which contain two GAF domains. The two closely related genes are tandemly arranged. The open reading frames predict proteins of 930 amino acids in length which contain the canonical Class 1 PDE signature motif in the catalytic region. The first and the second gene of the cluster are designated as B1 and B2, respectively. Characterization of these enzyme in *T. brucei* (Rascon et al., 2002), *T. cruzi* (Diaz-Benjumea et al., 2006), and *L. major* (Johner et al., 2006), revealed a cAMP-specific binding with *Km* values in the 1 - 5 µM range. The GAF domains of TbrPDEB1 and TbrPDEB2 (Laxman et al., 2005) bind cAMP with high affinity. In TbrPDEB2, binding of cAMP to the GAF-A domain decreases the K_m of the holoenzyme for cAMP as a substrate, suggesting an allosteric regulatory role of cAMP. The intracellular localization of TbrPDEB1 is exclusively along the paraflagellar rod complex of the flagellum, with which it remains tightly associated upon cell lysis. TbrPDEB2 is distributed between the paraflagellar rod structure and the cytoplasm (Oberholzer et al., 2007). In *T. cruzi*, the analysis of TcrPDEB2 has provided very similar results (D'Angelo et al., 2004). Early attempts to delete the PDEB genes in *T. brucei* showed no phenotype in procyclics (Zoraghi and Seebeck, 2002). However, later experiments using inducible RNAi confirmed that ablation of both TbrPDEB1 and TbrPDEB2 in either BSFs or procyclics led to a dramatic reduction in mRNA of both genes and was completely lethal for the BSF parasites, both in culture and in the mouse model. The resulting BSF phenotype is multinuclear, multikinetoplastic and multiflagellated with normal proliferation being completely disrupted leading to cell death approximately 50 h after induction (Oberholzer et al., 2007). There is about a 100-fold increase in intracellular cAMP in BSFs compared with 10-30-fold increase in procyclics as a result of the knockdown of both TbrPDEB1 and TbrPDEB2 and this correlates strongly with the observed phenotypes in BSFs and procyclics as well as experimental evidence of higher sensitivity of BSFs to membrane-permeable cAMP analogues (Oberholzer et al., 2007; Zoraghi and Seebeck, 2002). These findings show that kinetoplastid PDEBs represent interesting drug targets. The crystal structure of the catalytic domain of LmjPDEB1 has been solved, confirming the structural similarity of the kineto-

plastid PDEs with their human counterparts (Wang et al., 2007), facilitating inhibitor design. More recently, a tetrahydrophthalazinone compound A (CpdA) has been pharmacologically validated in *T. brucei* and was found to be a very potent PDE inhibitor (de Koning et al., 2012). This was discovered from more than 400,000 compounds screened by scintillation proximity assay (SPA), which determines [^{3}H]-cAMP hydrolyzing PDE activity. CpdA was identified to be the most potent inhibitor of TbrPDEB1 (IC_{50}, ~10 nM) with similar activity on TbrPDEB2 with the resultant suppression of trypanosome proliferation. It has previously been shown to be a potent inhibitor of human PDE4 (Van der Mey et al., 2001a; Van der Mey et al., 2001b). Validation of the pharmacological importance of TbPDEB1 was further confirmed when homology modelling and docking studies was used to guide fragments of Catechol Pyrazolinones into the parasite pocket (P-pocket) of TbPDEB1 resulting in a low nanomolar inhibition (Orrling et al., 2012). The presence of the P-pocket is very important since it allows for the development of kinetoplastid specific PDE inhibitors with minimal or no cross reactivity with mammalian PDEs.

1.2.5.2.3 PDEC

PDEC is an intermediate-*K*m, dual-specificity PDE of 900–1000 amino acids. The PDE catalytic region is located in the middle of the polypeptide chain whilst the N-terminal contains a FYVE variant domain followed by two coiled-coil domains (Hayakawa et al., 2007) which have been found not to be essential for catalytic activity. However, this coiled region may serve to form homodimers of the enzyme (Kunz et al., 2005), which may facilitate the interaction of the FYVE domain with the target membranes. It has been shown that TcrPDEC hydrolyses cAMP with a K_m value in the 20 - 30 µM ranges, and it can complement PDE-deficient yeast strains (Alonso et al., 2006). It has been reported that TcrPDEC also hydrolyses cGMP with a K_m of about 80 µM. The enzyme is sensitive to several PDE inhibitors (trequinsin, etazolate and dipyridamole) in the low micro-molar range (Kunz et al., 2005). PDEC has also been identified in the genomes of *T. brucei* and *L. major* with the possibility of the *L. major* version hydrolysing cGMP (Johner et al., 2006).

1.2.5.2.4 PDED

This is a predicted PDE of about 700 amino acids containing the PDE catalytic domain in the C-terminal part of the polypeptide. No other functional domains are predicted (Kunz et al., 2006). PDED has not been characterised yet in any of the kinetoplastid species, and it is not yet known whether it might be essential in any of the life cycle forms.

1.2.6 Protein Kinase A

The cAMP-dependent protein kinase family or protein kinase A (PKA) is a collection of serine/threonine kinases whose activity is dependent on levels of cAMP in the cell and is one of the most studied and best known members of the protein kinase (PK) family (Huang, 2011).

The kinetoplastid genomes contain reasonably well-conserved genes for catalytic and regulatory domains of protein kinase A (Huang et al., 2006). In *T. brucei*, a 499-amino acid protein with high homology to eukaryotic regulatory subunits of PKA was identified and named *T. brucei* Regulatory Subunit (TbRSU). This led to the first actual measurement of the cyclic nucleotide-dependent kinase activity in *T. brucei*. The protein has the usual two cyclic nucleotide-binding domains, which are predicted to retain all the conserved residues necessary for function, as well as a pseudo-inhibitor site, which interacts with the catalytic subunit (Shalaby et al., 2001). However, further research on the presumed catalytic subunit co-immunoprecipitated with TbRSU showed that although it displays phosphorylation activity and is also inhibited by the peptide inhibitor (PKI) both characteristics of PKA, it is not stimulated by cAMP but instead stimulated by cGMP (Shalaby et al., 2001) proving that *T. brucei* expresses a PKG activity – albeit with the caveat that there are few indications that trypanosomes produce or contain cGMP (Tagoe et al., 2015).

The finding that cAMP signalling mediates *T. cruzi* differentiation (Flawia et al., 1997), and the fact that PKAs are the major cAMP-dependent effectors in most eukaryotic cells, led to the need to identify PKA activity in *T. cruzi*. A cAMP-stimulatable protein kinase fraction with a half-maximal effect at approximately

1 nM cAMP and activity not affected by cGMP, and phosphate-acceptor as expected for a cAMP-dependent protein kinase, was identified (Ulloa et al., 1988). The subunits (catalytic and regulatory) were purified and it was predicted that they form a tetrameric conformation similar to mammalian PKA (Ochatt et al., 1993). Expression of both the *T. cruzi* PKA catalytic unit (TcPKAc) and *T. cruzi* PKA regulatory unit (TcPKAr) appeared to be coordinated, indicating that the two subunits may be associated *in vivo*, as also shown by immunoprecipitation of the holoenzyme (Huang, 2011; Huang et al., 2002). TcPKAc activity was inhibited by the PKA-specific inhibitor PKI and both TcPKAc and TcPKAr localized to the plasma membrane and the flagellar region (Bao et al., 2010; Huang et al., 2006; Huang et al., 2002). TcPKAr was found to interact with several P-type ATPases, which suggests that these P-type ATPases may play a role in anchoring PKA to the plasma membrane (Bao et al., 2009) as reported for some mammalian P-type ATPases (Xie and Cai, 2003).

The functional importance of the TcPKAc in *T. cruzi* was examined by introducing into epimastigotes a gene encoding a PKI containing a specific PKA pseudo-substrate, R-R-N-A. Expression of PKI has a lethal effect in this parasite. Similarly, a pharmacological inhibitor, H89, killed epimastigotes at a concentration of 10 μM proving that PKA enzymatic activity is essential for the survival of the parasites (Bao et al., 2008). A yeast-two hybrid screen for the substrates of PKA identified 38 candidate proteins that interact with TcPKAc including 18 hypothetical proteins with unknown functions. Eight of the identified genes have potential regulatory functions with respect to environmental adaptation and differentiation, and are presumably important in regulating *T. cruzi* growth, adaptation and differentiation. These included a type III PI3 kinase (Vps34), a putative PI3 kinase, a MAPK, a cAMP-specific phosphodiesterase (PDEC2), a hexokinase, a putative ATPase, a DNA excision repair protein and an aquaporin. PKA phosphorylated the recombinant proteins of these genes (Bao et al., 2008). Additional findings also suggest that TcPKAc may play a role in invading cells by mediating protein trafficking that enables parasite adhesion to cells, enabling the invasion thereof, as trans-sialidases were found to be substrates of TcPKA (Bao et al., 2010). As discussed by Huang (2011), there seems to be co-incidence of cAMP production, PKA activity and trans-sialidase expression enabling the differentiation from late stage

epimastigotes to invasive trypomastigotes – all consistent with a role for cAMP signalling in differentiation and invasion by *T. cruzi*.

A Leishmania catalytic subunit of PKA (LdPKA) was first isolated and characterized from *L. donovani* promastigotes by column chromatography and found to be similarly inhibited by PKI activity as in *T. brucei* and *T. cruzi*, indicating that the kinetoplastid enzymes are likely to be structurally related and topologically similar to mammalian PKA (Banerjee and Sarkar, 1992). Indeed researchers went further to clone an *L. major* gene encoding a protein with high homology to other PKA genes (LMPKA-C1). This protein was shown to have important features involved in ATP and phosphatase-acceptor binding. However, some structural and functional differences were observed with other PKA-C subunits, such as a unique 8-residue C-terminal extension (Siman-Tov et al., 1996; Siman-Tov et al., 2002). Expression of LmPKA-C1 was developmentally regulated with expression barely detectable in intracellular amastigotes, in contrast to a high expression level in insect-stage promastigotes (Duncan et al., 2001; Siman-Tov et al., 1996). The role of cyclic nucleotide-regulated protein kinase activities in promastigote proliferation and infectivity was confirmed in *Leishmania amazonensis*, with PKA activity particularly high in metacyclic promastigotes, which are primed for macrophage invasion (Genestra et al., 2004). PKA inhibitors PKI and H89 affected both replication and macrophage infection. Smaller effects were observed with the PDE inhibitors dipyridamole, rollipram and isobutyl-methyl-xanthine (IBMX) but to date there is no clear confirmation that these effects were mediated by one of the leishmanial PDEs, or which one. These effects were temporary and did not affect intra-macrophage growth (Malki-Feldman and Jaffe, 2009).

1.3 Cyclic AMP and cell cycle regulation in kinetoplastids

The need for parasite survival implicates the need for developmental responses to adapt to different environments encountered within the mammalian host and the arthropod vector. This is especially so during preparation for transmission, where specialized developmental forms are often generated to promote survival in anticipation of a host change (Baker, 2010; MacGregor et al., 2012). The result is a dynamic balance of transmissible and proliferative stages within a

host ensuring that the population can maximize its longevity within the host but also optimize its capacity for spread to new hosts (Mony et al., 2014). The morphotypes that characterize a certain genus are cell shape, dimensions and the positions of the complex kinetoplast-flagellar pocket relative to the nucleus (Svobodova et al., 2007). The complex morphological and biochemical changes during cell differentiation in trypanosomatids are most importantly environmentally driven through different ligands and or stimulatory molecules present in these environments. Although some differences in ligands of kinetoplastids and mammals have been shown and some stimulatory molecules are yet to be identified, the few receptors and signalling molecules that have been described have much structural and functional similarity to that of mammals. These signalling molecules display a wide range of activities including induction or inhibition of target cell survival, proliferation and differentiation which are similar to activities that occurs in mammals (Parsons and Ruben, 2000).

The report of AC activity in *Trypanosoma gambiense* in 1974 (Walter et al., 1974) implicated the possible role of cAMP signalling in the cell biology and virulence of kinetoplastids triggering the study of cAMP levels in the different life cycle stages of *Trypanosoma lewisi* (Strickler and Patton, 1975), *T. brucei* (Mancini and Patton, 1981), and *L. donovani* (Walter et al., 1978). Trypanosomes living in the bloodstream proliferate as morphologically ‘slender’ forms that evade host immunity by antigenic variation, generating characteristic waves of infection. As each wave of parasitaemia ascends, slender forms stop proliferating and undergo morphological and molecular transformation to stumpy forms, the parasite’s transmission stage (Vickerman, 1985). Earlier cAMP measurements showed increased cAMP levels in long slender bloodstream forms (BSF) during the cyclical wave of proliferation of this forms, and relatively low cellular cAMP concentrations when the abundance of stumpy forms increases (Mancini and Patton, 1981). This increase in cAMP in long slender blood stream forms however, may be metabolically induced due to their proliferative nature in comparison to stumpy form parasites. However, differentiation of longer slender forms to short stumpy forms have been shown to be density dependent (Vassella et al., 1997) with resemblance to quorum-sensing systems found in microbial communities (Waters and Bassler, 2005). The response to this density

dependent differentiation is triggered by a yet to be identified low molecular weight molecule called “stumpy induction factor” (SIF). Although the exact nature of SIF is yet to be identified, it has been shown to have some signalling characteristics that may implicate cAMP. Additionally, trypanosomes incubated with a conditioned medium containing SIF displayed a 2-3-fold increase in the intracellular concentration of cAMP compared with cells grown in a non-conditioned medium (Breidbach et al., 2002; Vassella et al., 1997). For example, cAMP analogue 8-(4-chlorophenylthio)-cAMP was demonstrated to have the same differentiation-inducing effect as SIF. Differentiation of BSF to procyclic forms correlates with the shedding of VSG (Barry and McCulloch, 2001). Although much similarities have been observed in VSG shedding and AC stimulation, monitoring of AC activity and VSG shedding after triggering differentiation to procyclic forms showed that AC stimulation was not responsible for the release of VSG (Rolin et al., 1993) and that cAMP was not required for this differentiation to occur (Mancini and Patton, 1981; Strickler and Patton, 1975). An analogue of cAMP, 8-pCPT-cAMP was able to induce a slender-to-stumpy differentiation in the pleomorphic bloodstream form (Vassella et al., 1997) although this did not correlated with the subsequent release of VSG either. High concentrations of extracellular cAMP, 5’-AMP or adenosine did not significantly affect the proliferation of *T. brucei*, suggesting that the antiproliferative effect caused by the nucleotide analogues was mediated by an intracellular “receptor”. And although 8-pCPT-cAMP did induce differentiation into stumpy-like non-proliferative forms, a hydrolysis-resistant analogue did not, whereas the hydrolysis products of 8-pCPT-cAMP (i.e. the equivalent AMP and adenosine analogues) had a more potent effect than 8-pCPT-cAMP itself. The clear conclusions of this study were that (1) cAMP is not the primary effector of the differentiation signal and (2) the hydrolysis products of 8-pCPT-cAMP trigger a differentiation-like transformation in *T. brucei* long-slender bloodstream forms (Laxman et al., 2006). Additionally, 8-Br-cGMP but not 8-Br-cAMP was found to significantly increase infection in the midgut of *Glossina m. morsitans* tsetse flies by *T. brucei* (MacLeod et al., 2008). It is however not yet established whether the effect of cGMP is on the trypanosome or the tsetse flies. Recently, a genome-wide Ion Torrent based RNAi target sequencing was used to identify signalling components driving stumpy formation by exposing and selecting proliferative monomorphic cell lines unresponsive to 8-(4-chlorophenylthio)-

cAMP (pCPT-cAMP) or 8-pCPT-2′-*O*-methyl-5′-AMP driven stumpy formation. This led to the identification of cohorts of genes implicated in each step of the signalling pathway, from purine metabolism, through signal transducers (kinases, phosphatases) to gene expression regulators a few of which may be involved in cAMP/AMP-analogue processing (Mony et al., 2014). Identified genes at each step of the signalling pathway were independently validated in cells naturally capable of stumpy formation, confirming their role in density sensing *in vivo*. The putative RNA-binding protein, RBP7, was required for normal quorum sensing and promoted cell-cycle arrest and transmission competence when overexpressed. This study reveals that quorum sensing signalling in trypanosomes shares similarities to fundamental quiescence pathways in eukaryotic cells, its components providing targets for quorum-sensing interference-based therapeutics (Mony et al., 2014).

Whilst the role of cAMP in cellular differentiation is not conclusive, the role and importance of cAMP in flagellar motility and signalling is increasingly being dissected with interesting findings. For example it is commonly believed that the flagellum, as an important host-parasite interface, has many essential sensory functions (Rotureau et al., 2009; Tetley and Vickerman, 1985). An example occurs in *C. reinhardtii*, where triggering of zygote formation is initiated by cAMP signalling response as a result of flagellum adhesion in gametes (Pan and Snell, 2000). Recently, it has been shown that cAMP regulates social motility in *T. brucei* either by increasing cAMP through the inhibiting of TbPDEB1 or using CpdA (Oberholzer et al., 2015). This is similar to social motility observation in *Dictyostelium discoideum* where cAMP signalling is critical for surface motility (Firtel and Meili, 2000).

Several mammalian cells and tissue types (erythrocytes, fibroblasts, hepatocytes, cardiomyocytes, adrenocortical cells etc.) are known to extrude cAMP which is unidirectional and could be inhibited by agents such as metabolic inhibitors (oligomycin and cyanide), inhibitors of membrane transport (probenecid and verapamil) and other compounds (papaverine and prostaglandins) (Sager and Ravna, 2009). When stimulated by ACs, the time-course for intracellular level cAMP shows a rapid rise to peak levels in a relatively short period of time whilst extracellular levels increased linearly for a

much longer time before plateauing which might be due to the enormously large volume of the extracellular medium verses the cell volume. There are considerable differences in the ability of cell types to extrude and it is believed that export and extrusion of cAMP plays a minor role in the control of intracellular cAMP levels in some cells (Ahlstrom and Lamberg-Allardt, 1999; Hamet et al., 1989; Sager and Ravna, 2009). Cellular unidirectional energy-dependent cGMP efflux has also been observed in cells (pancreatic, liver glioma, etc.) and could be inhibited with probenecid. Stimulation of guanylate cyclase and inhibition of cyclic nucleotide phosphodiesterase in human platelet cells results in a 5-fold increase in intracellular cGMP levels but an almost 20-fold increase in extracellular cGMP levels (Hamet et al., 1989; Radziszewski et al., 1995; Sager and Ravna, 2009).

The above statements suggests that either cAMP, maybe cGMP or SIF alone, or a combination thereof, tends to drive differentiation of long slender bloodstream forms into stumpy forms through a quorum sensing mechanism where cells that have started differentiating releases these factors that drive other cells in their environment to also differentiate.

1.4 Drug discovery for Neglected Tropical Diseases (NTDs)

Current drugs used in kinetoplastid treatments are old, toxic, and extremely difficult to apply as well as facing a serious threat of redundancy as a result of increasing parasitic resistance. However, about 73 million people are estimated to be at risk of infections caused by HAT, leishmaniasis and Chagas' disease globally, whilst the disability-adjusted life-years (DALYs) lost due to these diseases are estimated to be 5.6 million (WHO, 2013). A drive from the WHO with partner support has led to an increased interest and commitment to develop new drugs for these diseases, leading to several new therapies becoming available whilst other compounds are in clinical trials (Chatelain and Ioset, 2011). This drive needs to be sustained to overcome problems associated with the high attrition rate in drug development and to maintain a sustained effort to achieve landmark goals of eliminating HAT in Africa and visceral leishmaniasis (VL) in India, as well as to bring Chagas disease and the many forms of

leishmaniasis under control by 2020 (Barrett and Croft, 2012). To achieve that, strategies must be developed to make drug discovery easier and cheaper and target purposed for this NTDs considering that pharmaceutical companies will not even recoup expenditure to consider making profits in discovery of drugs for NTDs.

1.4.1 Potential of PDE inhibitors in kinetoplastids

The discovery of PDEs and cAMP activity in the kinetoplastids led to the logical question as to whether these PDEs can be targeted with inhibitors to bring about a therapeutic outcome. This question was legitimized when RNA interference (RNAi) against TbrPDEB1 and TbrPDEB2 found them to be essential for parasite survival both *in vivo* and *in vitro*.

Based on these findings, a library of compounds was screened at Altana Pharma and Nycomed for inhibition of TbrPDEB1. This revealed a few compounds with IC_{50} values in the nanomolar range. The lead compound BYK54826, later renamed CpdA, displayed a trypanocidal activity at EC_{50} 80 ± 10 nM as well as increases intracellular cAMP levels in cells within minutes (Shakur et al., 2011). 1 μM of CpdA raised cAMP levels by 50-fold (de Koning et al., 2012), similar to levels seen when RNAi is induced in TbrPDEB1 and B2 (Zoraghi and Seebeck, 2002). Although CpdA does not have an immediate effect on the viability of the cells except at very high concentrations (>50 μM), it rapidly halts cell division and growth, indicating that PDE inhibition leads to defects in cytokinesis during cell division resulting in multinucleated cells that were not ultimately viable (Shakur et al., 2011).

CpdA, a tetrahydrophthalazinone (Figure 1.8) has been pharmacologically validated in *T. brucei* and confirmed to be a very potent PDE inhibitor (de Koning et al., 2012). It is effective against the trypanosome because it displays similar activity against TbrPDEB1 and TbrPDEB2, with the resultant suppression of trypanosome proliferation. Its trypanocidal activity is similar to that of suramin and diminazene, and ≥10-fold better than nifurtimox (de Koning et al., 2012). It also showed similar potencies against wild-type and clinical and veterinary resistant cell lines. At 1 μM, CpdA causes a several fold (44) increase

in intracellular cAMP after 3 h incubation in contrast to low-potency PDE inhibitors such as dipyridamole (40 μM) and etazolate (100 μM) which did not significantly affect cAMP concentrations. This action is immediate and time and dose dependent although cell lysis and death only occurred after 15 h even at 3 μM concentration (de Koning et al., 2012).

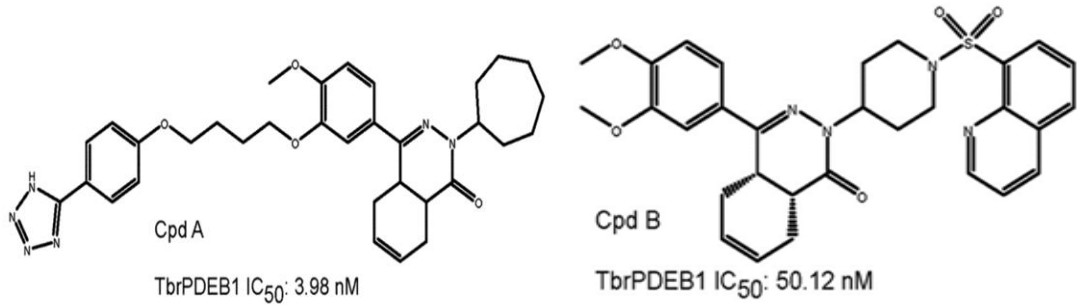

Figure 1:8: Structure of Cpd A and B showing their IC_{50} on TbrPDEB1. Reproduced from de Koning et al, 2012)

However, CpdA has previously been shown to be a potent inhibitor of human PDE4 (Van der Mey et al., 2001a; Van der Mey et al., 2001b). This was independently pharmacologically validated by Bland et al using the hPDE4 inhibitor piclamilast and a number of analogues (Bland et al., 2011). Thus it became clear that the TbrPDEB family is pharmacologically closest to this human PDE. In contrast, human PDE5 inhibitors including sildenafil and tadalafil analogues displayed only weak inhibition of TbrPDEB1 (Ochiana et al., 2012; Wang et al., 2012). This scenario presented a problem of designing trypanosomal PDE inhibitors with enough specificity and selectivity to prevent toxicity or at least reduce it to current pharmaceutical standards.

The resolution of the catalytic structure of *L. Major* PDEB1 in complex with the nonspecific inhibitor IBMX (Wang et al., 2007), the first for a kinetoplastid PDE confirmed the expected similarities with that of human PDEs especially in the catalytic domain (Ke and Wang, 2007). However, it also revealed subtle differences in key regions such as the active site and a unique pocket for inhibitor binding present in all members of the kinetoplastid PDEB family examined including TbrPDEB1 (Jansen et al., 2013), (Figure 1.9) as well as TcrPDEC (Wang et al., 2007). The question as to whether these subtle differences provide good enough basis to target PDEs in Kinetoplastids was tested when homology modelling and docking studies was used to guide

fragments of Catechol Pyrazolinones into the parasite pocket (P-pocket) of TbrPDEB1. The result was a discovery of a new series of compounds with nanomolar EC_{50} values against the enzyme while also displaying promising trypanocidal activity and stimulating cellular cAMP levels (Orrling et al., 2012).

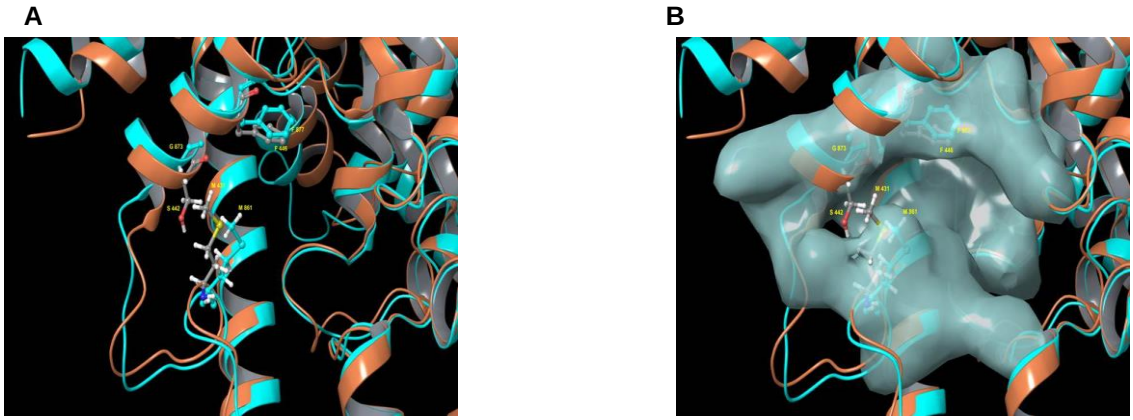

Figure 1.9: Model of the binding pocket of TbrPDEB1 and hPDE4. Model of the superimposed binding pockets of TbrPDEB1 (turquoise ribbons and carbon atoms) and hPDE4B (orange ribbons, grey carbon atoms). The figure depicts chain A from the published 4I15 PDEB1 structure and chain B of hPDEB structure 1XM4 (alignment RMSD 1.847 Angstrom). A. ribbon model of the cAMP binding pocket. B. Same view but with the molecular surface for TbrPDEB1 residues shown. Side chains for the conserved hydrophobic clamp phenylalanine residue in PDEB1 (Phe877, turquoise) and hPDE4B (Phe446, grey carbons) are shown to illustrate the orientation of the P pocket relative to this canonical binding site feature. Side chains for the pair of amino acid residues at the entrance to the P pocket in PDEB1 and hPDE4B are also shown - Met861 and Gly873 in PDEB1 (turquoise), and Met431 and Ser442 in hPDE4B (colored by element - carbon gray, hydrogen white, nitrogen blue, oxygen red, sulfur yellow). For TbrPDEB1 the P-pocket is clearly visible in Frame B, directly adjacent to the main ligand binding site and delineated by M861 and G873, where in hPDE4B this space is filled entirely by M431 and S442. The models were constructed by Dr R.K. Campbell of the Marine Biology Laboratory, Woods Hole, MA, USA, using Maestro software release 2015-2 (Schrodinger, Portland, OR, USA).

1.4.2 Potential effectors of PDE inhibition and cAMP signalling

Although cAMP has been noted to play important roles in cell differentiation in *T. b. brucei* and that inhibition of PDE results in increased cAMP, the effectors that mediate this differentiation are yet to be identified. These downstream effectors of cAMP signalling are important mediators of PDE inhibition effect in cells and will provide valuable information of drug action as well as offer additional potential therapeutic targets. Thus to study these downstream effectors, Gould et al, (2013) generated two CpdA resistance lines. The first method involved growing *T. b. brucei* in the mutagen Methyl methanesulfonate (MMS; Sigma), and the subsequent passage in incrementally sublethal concentrations of CpdA. The second method employed the use of a *T. b. brucei*

RNAi library approach (Alsford et al., 2012a; Alsford et al., 2012b; Alsford et al., 2011b; Baker et al., 2011) to select for resistance line under CpdA pressure. The RNAi library screen of resistance to the phosphodiesterase inhibitor CpdA revealed four distinct genes that were knocked down. These genes were designated cAMP Response Protein (CARP) (Gould et al., 2013).

One of the genes knocked down in the CpdA-resistant cultures was Tb427tmp.01.7890 (*CARP1*; Tb927.11.16210 in *T. brucei brucei* reference strain TREU 927), encoding a 705-amino-acid protein containing two apparently intact and one partial cyclic AMP binding-like domains that is conserved in synteny in each of the kinetoplastid genomes sequenced. No close orthologues were identified in other organisms, but cyclic nucleotide-dependent kinases and ion channels appear to be the most closely related proteins outside the Kinetoplastida. *CARP1* RNAi resulted in a slight growth phenotype (Gould et al., 2013). Mitochondrial RNA expression of CARP1 in pleomorphic cells at different time points in the lifecycle stages relative to a stably expressed gene (Tb10.389.0540) was performed using a whole-genome microarray analysis. The results showed that expression of CARP1 is relatively low in long slender forms and at 0 and 1 h with lower expression at 6 h in Stumpy form cells. However, expression level rose steadily and was highest at 18 h to coincide with procyclic cell proliferation (Kabani et al., 2009). Recently, the homologue of CARP1 in *T. cruzi* (TcCLB.508523.80) has been revealed to bind cyclic nucleotides using cAMP and cGMP displacement assays (Jäger et al., 2014), further validating the role of CARP1 as a downstream cAMP signalling effector.

CARP2 (Tb427tmp.52.0004; Tb927.11.12860 in TREU 927) codes for a hypothetical protein of 302 amino acids, but a downstream alternative start codon may produce a shorter protein of 235 amino acids (Siegel et al., 2010a). This corresponds to the ORF length of the majority of *CARP2* homologues that are well conserved across the Kinetoplastida (82% amino acid identity in all *Trypanosoma* spp. and 59% identity in *Leishmania* spp.) and many other species, including humans (47.7% identity). The apparent molecular mass of the C-terminally tagged *T. brucei brucei* protein (Broadhead et al., 2006) shows that the first ATG is in fact used and that the trypanosomal *CARP2* carries an N-terminal extension. There is no known function, and no recognizable functional

domains could be identified in any of the homologues. It has been detected in proteomes of the *T. brucei brucei* flagellum (Broadhead et al., 2006) and of cytoskeletal and plasma membrane fractions (Bridges et al., 2008), and its homologue was part of an *in silico* predicted proteome of the flagellar and basal body of *Chlamydomonas reinhardtii* (Li et al., 2004; Merchant et al., 2007). Similar mRNA analysis as performed in CARP1 showed that CARP2 is also not highly expressed in long slender forms and at the point of differentiation (0 h) into short stumpy forms. However, unlike CARP1, mRNA levels increased steadily from 1 h, plateauing at 18 h and continue through to 48 h (Kabani et al., 2009). This shows that CARP2 is steadily expressed in the differentiation into procyclics and continued throughout the insect stages of the trypanosome lifecycle.

CARP3 (Tb427.07.5340; Tb927.7.5340 in TREU 927) encodes a hypothetical protein of 498 amino acids with orthologues only in *Trypanosoma* spp. and strains. A BLASTP search identified the putative stibogluconate resistance gene family in *Leishmania* spp. as the closest homologue outside trypanosomes (*Leishmania braziliensis* LBRM_31_1110; 20.4% identity); amplification of this gene family in *Leishmania tarentolae* resulted in resistance to antimony-containing drugs (Haimeur and Ouellette, 1998). The protein was found in the plasma membrane-enriched fractions of bloodstream *T. brucei brucei* (Bridges et al., 2008) and in mitochondrial fractions of procyclic trypanosomes (Panigrahi et al., 2009) and is possibly palmitoylated (Emmer et al., 2011b). At the N-terminal end of the protein, a weak TPR-like domain (tetratricopeptide repeat) signature is detected. TPR domains can mediate protein-protein interactions such as dimerization and the assembly of multiprotein complexes (D'Andrea and Regan, 2003). Unlike CARP1 and CARP2, CARP3 levels are almost 3-fold higher in long slender forms than in stumpy forms. Although the level of expression in short stumpy forms are unchanged in CARP1 and CARP2 at 0 h, CARP3 levels increased rapidly to >1-fold at 1 h through to 6 h and reducing at 18 h to rise again (Kabani et al., 2009). This shows that CARP3 exhibit a cyclical expression level through the differential life stages which coincides with rapidly dividing prolific life forms of long slender forms, procyclic, and metacyclic forms.

The fourth ORF identified from the RNAi target fragments, *CARP4* (Tb927.3.1040/60), is a hypothetical gene that spans three automatically

annotated ORFs in release 5.0 of TriTrypDB (*T. brucei brucei* TREU 927 strain; the respective sequence segment of strain Lister 427 is annotated as incomplete). However, the middle ORF appears to be a sequence contaminant disrupting a single open reading frame encompassing Tb927.3.1040 and Tb927.3.1060. The middle ORF is absent from all RNA sequencing (RNAseq) data on the TriTrypDB website and has no homologues or orthologues in any of the other kinetoplastid genomes on the database. The full-length Tb927.3.1040/60 ORF, on the other hand, is conserved in synteny in all kinetoplastid genomes sequenced to date, with amino acid identity of 53.6% in *Leishmania major* and 96.3% in *T. brucei gambiense*. The combined Tb927.3.1040/60 ORF codes for a hypothetical protein of 779 amino acids and is predicted to have three DM10 domains and one EF-hand domain located at the C-terminal end. BLASTP and domain architecture (NCBI CDART) searches uncovered sequence assembling error and mis-annotation in that region of the reference TREU 927 genome sequence. Similar to CARP3, mRNA of CARP4 (Tb927.3.1060) is highly expressed compared with the stably expressed gene (Tb10.389.0540) in long slender forms and not expressed in short stumpy forms at 0 h. Significantly different from CARP3 however, its expression is relatively lower (-1.5-fold) at 1 h in short stumpy forms rising to that of control at 6 h and remaining relatively unchanged over the period of differentiation (Kabani et al., 2009). This expression profile showed that CARP4 is probably only abundantly expressed in bloodstream long slender forms.

1.4.2.1 CARPs affect CpdA sensitivity

All four CARP genes were targeted with RNAi constructs and transfected into *T. b. brucei* for tetracycline-inducible expression. RNAi induction for 24 h caused a substantial reduction of the specific tagged CARP protein as shown by Western blot; all were reduced by at least 2-3-fold, but CARP3 expression appeared to be down to approximately 5% (Gould et al., 2013). The RNAi-mediated knockdown resulted in significant resistance to CpdA. CARP1 showed the highest resistance of 117-fold followed by CARP2 (10.1-fold), CARP3 (7.9-fold) and CARP4 (5.4-fold) in that order. CARP1 knockdown also resulted in a 5.0- and 3.7-fold decrease in resistance to 8-bromo-cAMP and dibutyryl-cAMP, respectively, whilst knockdown of CARP2 showed 2.2- and 1.9-fold increases in EC_{50} to 8-bromo-cAMP and

dibutyryl-cAMP, respectively. CARP3 and CARP4 showed no significant sensitivity changes to these analogues. No cross-resistance was observed for several trypanocidal drugs in use such as pentamidine, suramin and DMFO (eflornithine) under RNAi induction. The discovery of the CARPs constituted a potential breakthrough in understanding a crucial cellular regulation pathway in kinetoplastids, especially as it begins to fill in some details of cAMP signalling in *T. brucei* of which there is paucity of knowledge compared with that in mammals (Figure 1.10).

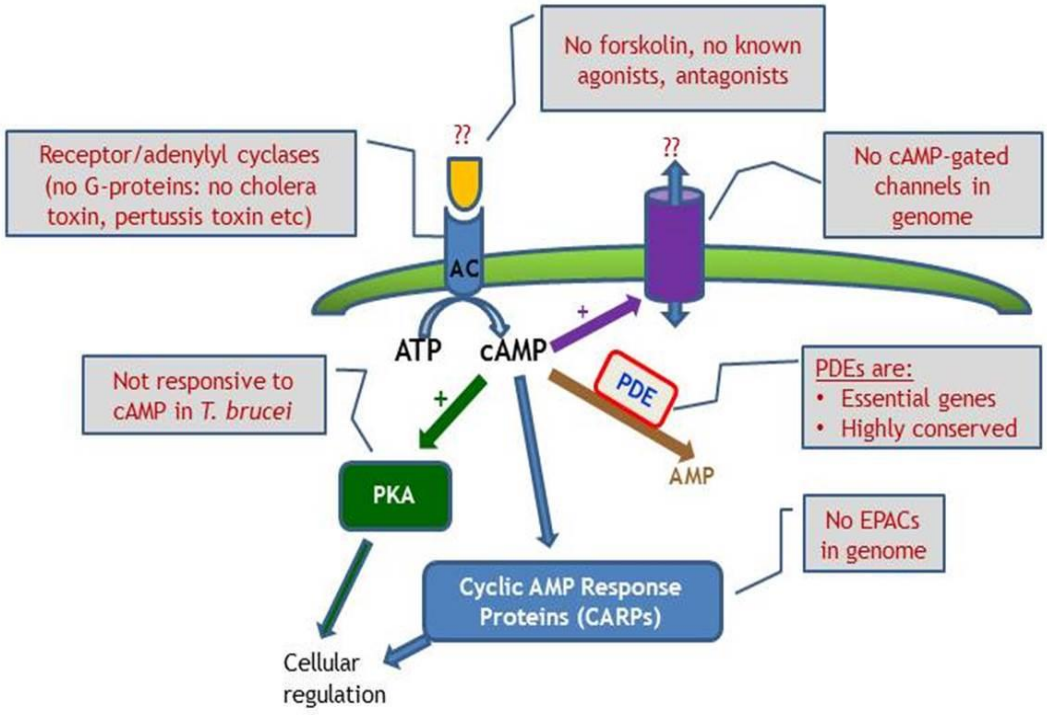

Figure 1.10: Schematic diagram of cyclic nucleotide signalling in *T. brucei*, emphasising the lack of investigative tools compared with the classical mammalian model, where manipulation of receptors, G-proteins and cyclases are all possible. EPAC, exchange protein directly activated by cAMP.

1.5 Hypothesis

We hypothesise that the trypanocidal effect of high cAMP levels is mediated by a pathway that includes the RNAi-identified CARP proteins. As these, in contrast to TbPDEB1/2, are mainly trypanosomatid-specific; their study will provide important new insights into unique parasite biology and into the mode of action of potential new trypanocides based on inhibition of PDEB. Whereas it is not proposed that the CARP proteins encoded by the genes under study are

necessarily drug targets, this study will greatly expand our understanding of cAMP-directed processes and cascades and is expected to identify additional genes involved in these pathways, beyond CARP1-4, some of which could be of therapeutic value as drug targets.

1.6 Aims

The primary goal of the project is to characterise the *T. brucei* CARP proteins as well as investigate some wider aspects of cAMP signalling in trypanosomes. Reverse genetics, genomics, proteomics and immunofluorescence microscopy will be used to elucidate potential pathways targeted by changes in cellular cAMP levels. These approaches together should investigate the trypanosomal processes regulated by cAMP.

Chapter 2

Material and Methods

2.1 Introduction

This chapter describes the materials and the methods used to probe the hypothesis and resolve the aims of the project. It includes molecular biological techniques (gene knockout and overexpression), biochemical assays (drug sensitivity assays, growth assays, Enzyme Linked Immunosorbant Assays (ELISA)), Immunofluorescence assays; Transcriptomics; Ribonucleic Acid Interference Sequencing (RIT-Seq), Ribonucleic Acid Sequencing (RNA-Seq) and Proteomic; Co-Immunoprecipitation (Co-IP) and Mass Spectrometry (MS).

2.2 Materials

Bloodstream forms of *T. b. brucei* MiTat 1.2 lines (WT s427) and BSF Lister 427 cells, clone 221a (2TI) were routinely cultured in HMI-9 medium (Invitrogen™), supplemented with 10% heat Inactivated Fetal Bovine Serum Gold (FBS with tetracycline; PAA Laboratories) in vented culture flasks (Corning, Sigma Aldrich), at 37 °C, in a 5% CO_2 atmosphere. A CpdA resistant line (R0.8) generated from WT s427 (Gould et al., 2013) was cultured similarly as WT s427 with occasional checks to ensure retention of CpdA resistance. To retain the tetracycline promoter, BSF Lister 427 cells clone 221a (2TI) cells were placed under phleomycin (0.5 µg/ml) and puromycin (0.2 µg/ml) antibiotic pressures. DNA was extracted from cell pellets using Nucleospin Tissue Kit (Machery and Nagel®) following manufacturers protocol. Concentration of DNA was checked on the Nanodrop (Thermo Scientific®). All primers were synthesized at Eurofins Genomics® (see primer table for list of primers). PCR amplification of UTRs were performed using Phusion High Fidelity Polymerase (New England Biolabs®), Gel and PCR products were cleaned using Nucleospin Gel and PCR clean kit (Machery and Nagel®), plasmids were extracted using Nucleospin plasmid extraction kit (Machery and Nagel®) and RNA was extracted using Nucleospin RNA extraction kit (Machery and Nagel®). All clean ups and extractions were performed following manufacturers protocols. CpdA was provided by Geert Jan Sterk of Mercachem, The Netherlands and Pentamidine (Sigma Aldrich®). Additional materials used are described with the required experiment.

2.3 Design and making of constructs for genetic manipulation of trypanosome

2.3.1 Making of CARP1-4 KO Plasmids

The homologous gene replacement method with antibiotics was used to generate knockout cells. Un-translated regions (UTRs) flanking the open reading frames (OFRs) of the genes of CARP1-4 were obtained from TriTrypDB based on *Trypanosoma brucei* TREU 927 (http://tritrypdb.org/tritrypdb/). Primers (forward and reverse) each were designed using CLC Genomic workbench version 7.0 for both the 5′ and 3′ UTRs of each gene adding the desired restriction sites (Appendix 1: Table 1.1) designed for Plasmid pMB G97 a kind donation of Prof Mike Barrett, (University of Glasgow, UK) (Figure 2.1).

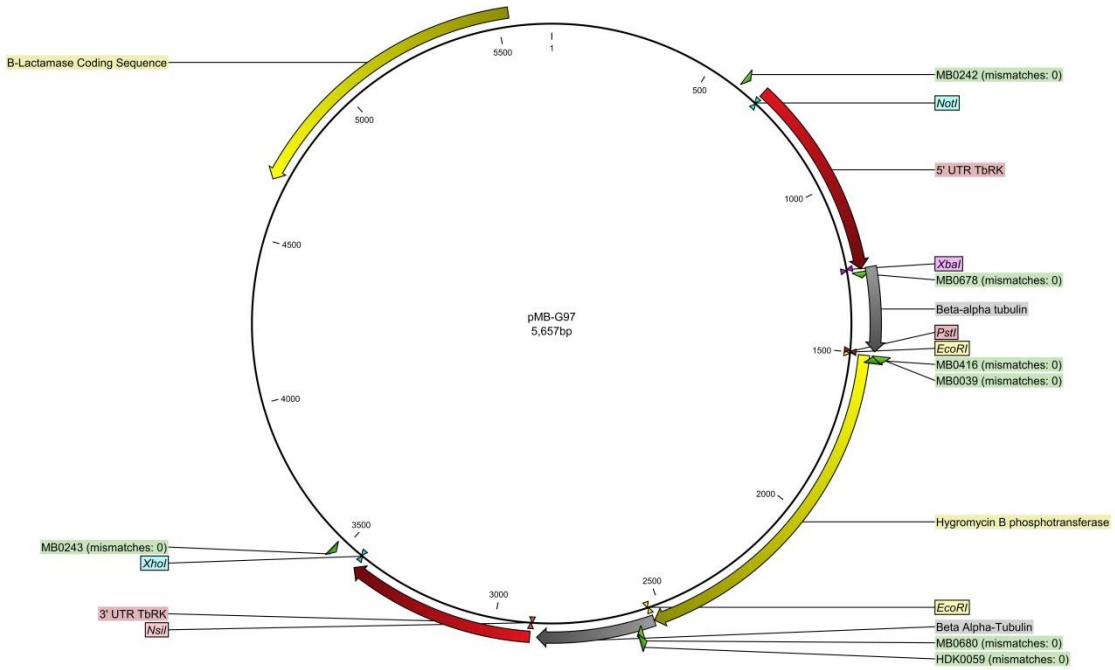

Figure 2.1: Plasmid map of pMB97 showing 5' and 3' UTRs and hygromycin antibiotic cassette.

A gradient PCR was performed to determine the best melting temperature (T_m) for each primer after which each UTR was amplified from200 ng of the isolated DNA with their respective primers. The PCR product was cleaned and concentration determined using the Nanodrop. The respective UTRs were restriction double digested using *NotI* and *XbaI* for 5′ UTRs and *NsiI* and *XhoI* for 3′ UTRs (Promega®) in a 50 µl total reaction volume of 2 µg PCR product, 5 µl 10X reaction buffer D, 5 µl 10X Bovine Sheep Albumin (BSA) and 2.5 µl enzyme each supplemented with double deionized H_2O (dd H_2O) with incubation at 37 °C for 1 h. The digested UTRs were PCR cleaned and the concentration determined. Plasmid DNA was extracted from pMB97 (hygromycin selectable cassette) from an overnight culture and the 5′ UTR region of pMB97 digested in a similar reaction as the CARPs 5′ UTRs using 5 µg of DNA and 5.5 µl of enzyme (*NotI* and *XbaI*), 10 µl 10X reaction buffer D and 10X BSA each in a 100 µl total reaction volume to allow for the ligation into the plasmid of the 5′ UTRs of each gene. The digest was run on a 1% agarose gel, the backbone cut with a sharp clean blade, gel extracted and concentration determined.

Each UTR was ligated to the backbone of pMB97 in a ligation reaction mix made up of 50 ng of 5′ UTR insert and 150 ng of pMB97 backbone, 1 µl 10X ligase buffer and 1 µl T4 ligase supplemented with ddH_2O to a total of 10 µl. This was incubated at room temperature for 3 h after which the ligation was ready for transformation.

Following ligation the plasmid was transformed into XL1 blue (Agilent Technologies®) competent *E. coli* cells as follows: 5 µl of ligation reaction was pipetted into a sterile 1.5 ml Eppendorf tube (Eppendorf®) and a 50 µl aliquot of XL1-blue cells defrosted on ice was then added; the mixture was incubated on ice for 30 minutes, heat-shocked for 45 s at 42°C and then incubated on ice for another 2 minutes. 200 µl of LB broth was added and incubated at 37°C for 1 hour with shaking. Finally, 50 µl of the transformation reaction was spread on a Luria agar supplemented with ampicillin (100 µg/ml Ampicillin (Sigma-Aldrich®) and incubated at 37°C overnight.

Colonies from the overnight transformation were PCR screened using primers that check for integration of the respective 5′ UTR of each CARP1-4 gene into pMB97. Screening was performed by picking a bacteria colony from each agar plate with a sterile 200 µl pipette tip, streaking on a fresh LB agar plate, numbering each streak and dipping each tip thereafter in the PCR tube bearing corresponding number. After colony plasmid amplification, correct integration was checked by electrophoresis on 1% agarose gel. The new agar plate was then incubated at 37°C overnight. Positive clones were identified as colonies that gave bands on the agarose gel corresponding to the desired molecular weight (~1.2 kb band) of which bacteria was inoculated into 10 mL Luria broth (LB) supplemented with 100 µg/ml Ampicillin overnight. Plasmid DNA was extracted from each positive overnight culture and sent for Sanger sequencing of the respective 5′ UTRs. One plasmid from each gene with the right 5′ UTR integration was selected for 3′ UTR integration which was performed exactly as that of 5′ UTR integration. However, the enzymes *NsiI* and *XhoI* were used to digest the 3′ UTR inset and the 5′ UTR-integrated plasmid of each of CARP1-4. The knockout constructs were then sent for Sanger sequencing of the 5′ UTR, 3′ UTR and the hygromycin selectable cassette.

The hygromycin cassette in pMB97 is flanked by two *EcoRI* restriction sites. To generate additional selectable marker constructs, primers were designed with *EcoRI* to amplify blasticidin and neomycin. DNA from plasmids with these markers were amplified, restriction digested and PCR cleaned. Each hygromycin selectable knockout construct of the CARPs was digested with EcoRI and treated with antartic phosphatase (New England Biolabs®) to prevent self-ligation due to the similar restriction sites on the ends of the cut region followed by electrophoresis on 1% agarose gel. The backbone (without the hygromycin gene) was gel cleaned. Each of blasticidin and Neomycin were ligated individually into the backbone of each of CARP1-4 genes with transformation, screening and overnight cultures performed as described above for the integration of 5′ UTR. Each generated construct was Sanger sequenced both to check for the presence of the UTRs as well as the correct sequence of the selectable cassettes to ensure appropriate gene expression and thus resistance selection. Constructs were ready for transfection (Figure 2.2).

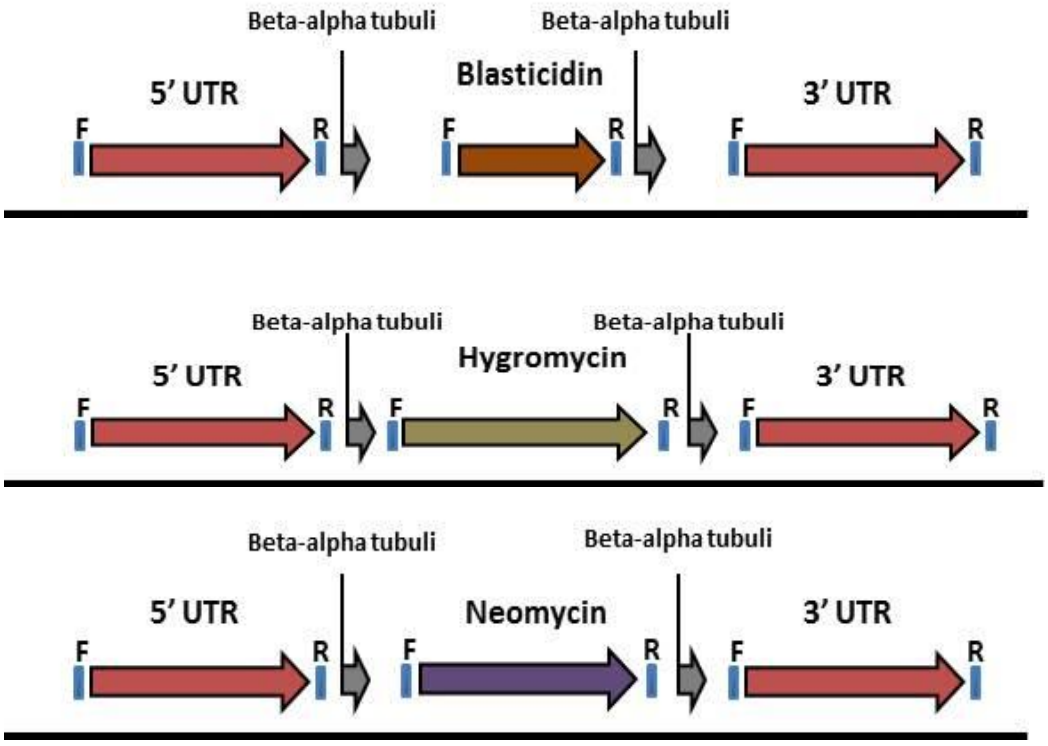

Figure 2.2: KO constructs designed with the various resistant cassettes to replace CARP1-4 genes. F-forward primer; R-reverse primer.

2.3.2 Making of CARP1-4, TbPDEB1 Overexpressing (O.E) and N-Terminal GFP tagged plasmids

Open Reading Frames (ORFs) of CARP1-4 and TbPDEB1 were obtained from TriTrypDB (http://tritrypdb.org/tritrypdb/). Primers (forward and reverse) each to the ORF of each gene were designed using CLC Genomic workbench version 7.0 adding the desired restriction sites for each gene (Appendix 1: Table 1.2-3). Two sets of knockin constructs were made using the vector pHD1336 (Biebinger et al., 1997; Munday et al., 2013; Munday et al., 2015) (Figure 2.3) and the pRPa^{GFP} (Figure 2.4) which has the Tet-promoter for tetracycline induction (Alsford et al., 2005). A gradient PCR was performed to determine the best melting temperature (T_m) for each primer after which each ORF was amplified using 200 ng of the isolated DNA with their respective primers. The PCR product was cleaned and concentration determined using the Nanodrop. The respective ORFs were restriction sequentially digested using *ApaI* and *BamHI* (Promega®) for pHD1336 or *XbaI* and *BamHI* for pRPa^{GFP} in a 50 µl total reaction volume of 2 µg PCR product, 5 µl 10X reaction buffer Multicore, 5 µl 10X Bovine Sheep

Albumin (BSA) and 2.5 µl enzyme each supplemented with double deionized H_2O (dd H_2O) with incubation at 25 °C for 1 h followed by 37 °C for another hour for pHD1336 and 37 °C for pRPa^{GFP}. The digested ORFs were PCR cleaned and the concentration determined. Plasmid DNA was extracted from pHD1336 from an overnight culture and the restriction region of *ApaI* and *BamHI* (pHD1336) or *XbaI* and *BamHI* (pRPa^{GFP}) digested in a similar reaction as the ORFs using 5 µg of DNA and 5.5 µl of *ApaI* and *BamHI* and *XbaI* and *BamHI*, 10 µl 10X reaction buffer D and 10X BSA each in a 100 µl total reaction volume to allow for the ligation into the plasmid of the ORFs of each overexpressing CARP construct. The digest was run on a 1% agarose gel, the backbone cut with a sharp clean blade, gel extracted and concentration determined. Ligation, transformation and colony screening was performed just as described for making of KO construct. After sequencing, pHD1336 CARP1-4 and TbPDEB1 (Figure 2.5), as well as pRPa^{GFP} CARP1-3 were ready for transfection (Figure 2.6).

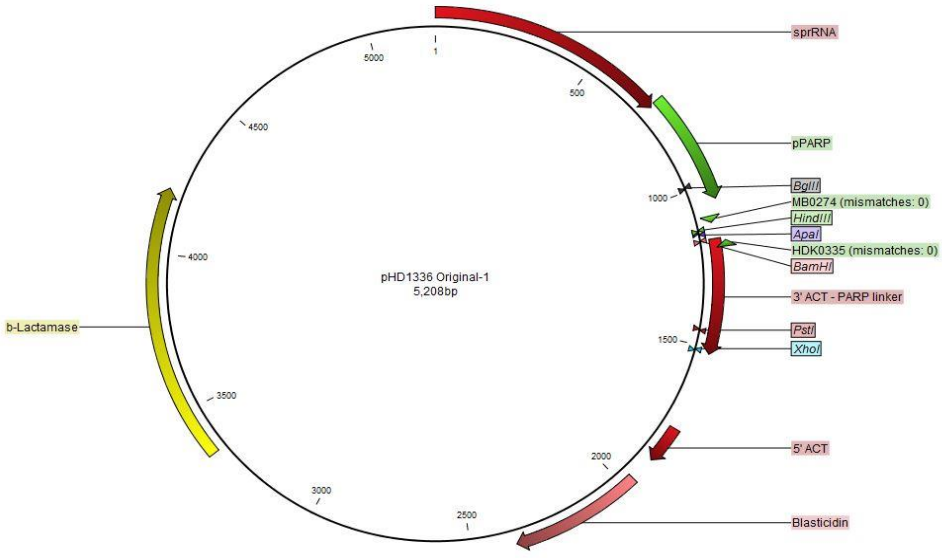

Figure 2.3: Plasmid map of pHD1336 showing the restriction sites and region for ORF integration.

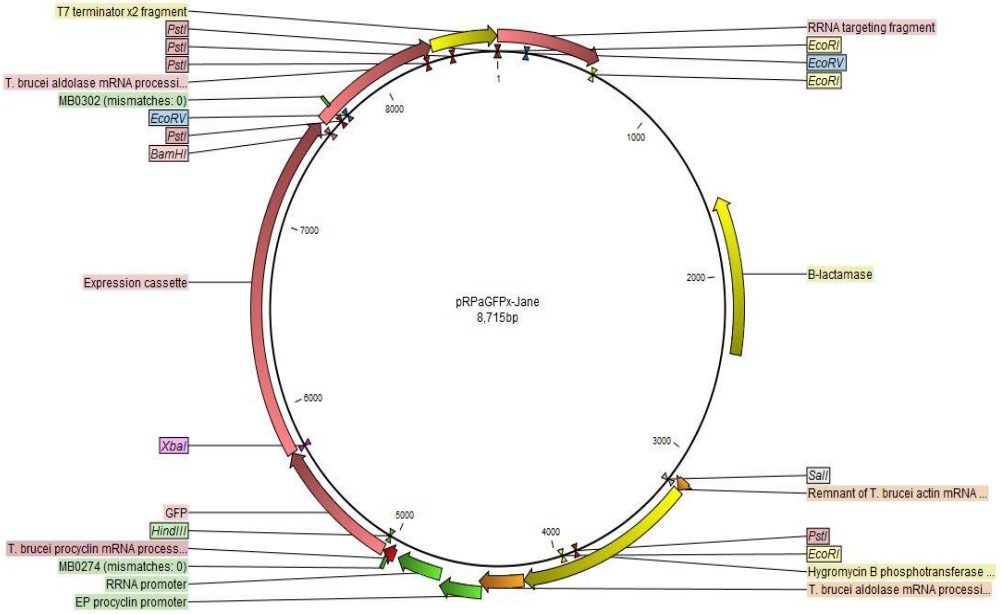

Figure 2.4: Plasmid map of pRPa^{GFP} showing the restriction sites, GFP and region for expression cassette. CARP1-3 replaces expression cassette.

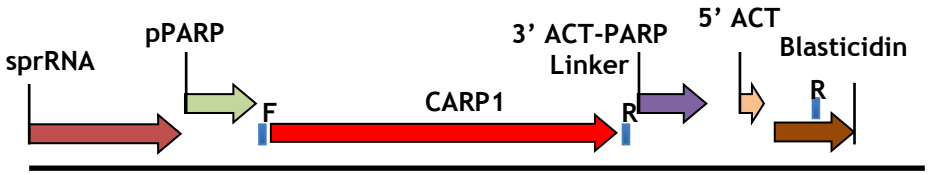

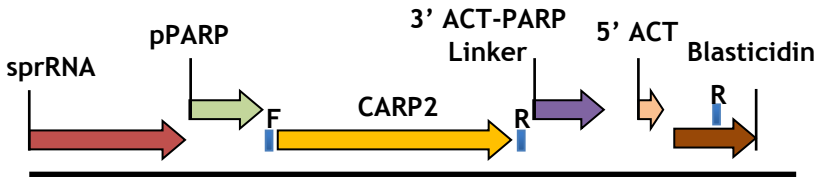

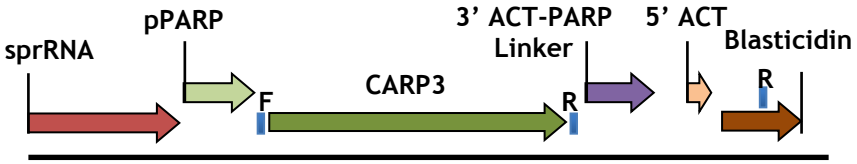

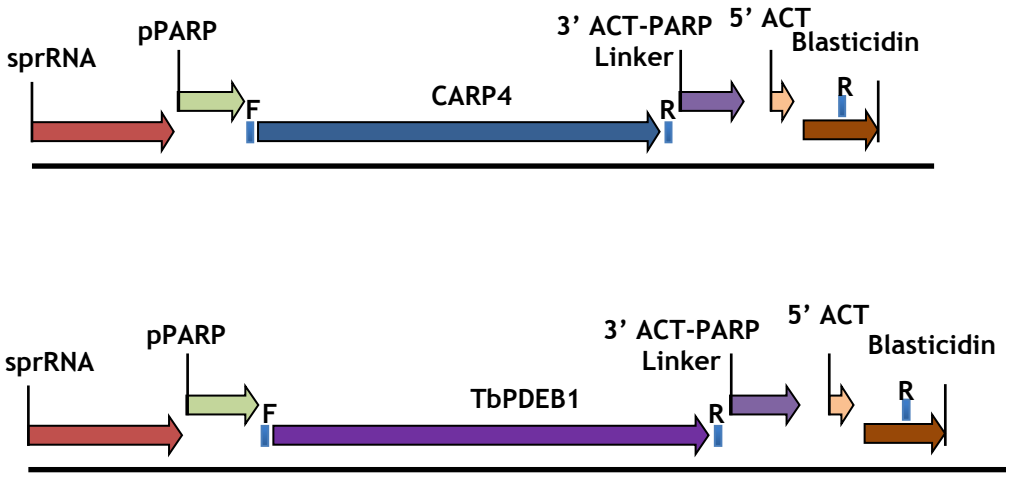

Figure 2.5: pHD1336 overexpression constructs with the CARPs and TbPDEB1. F-forward primer; R-reverse primer.

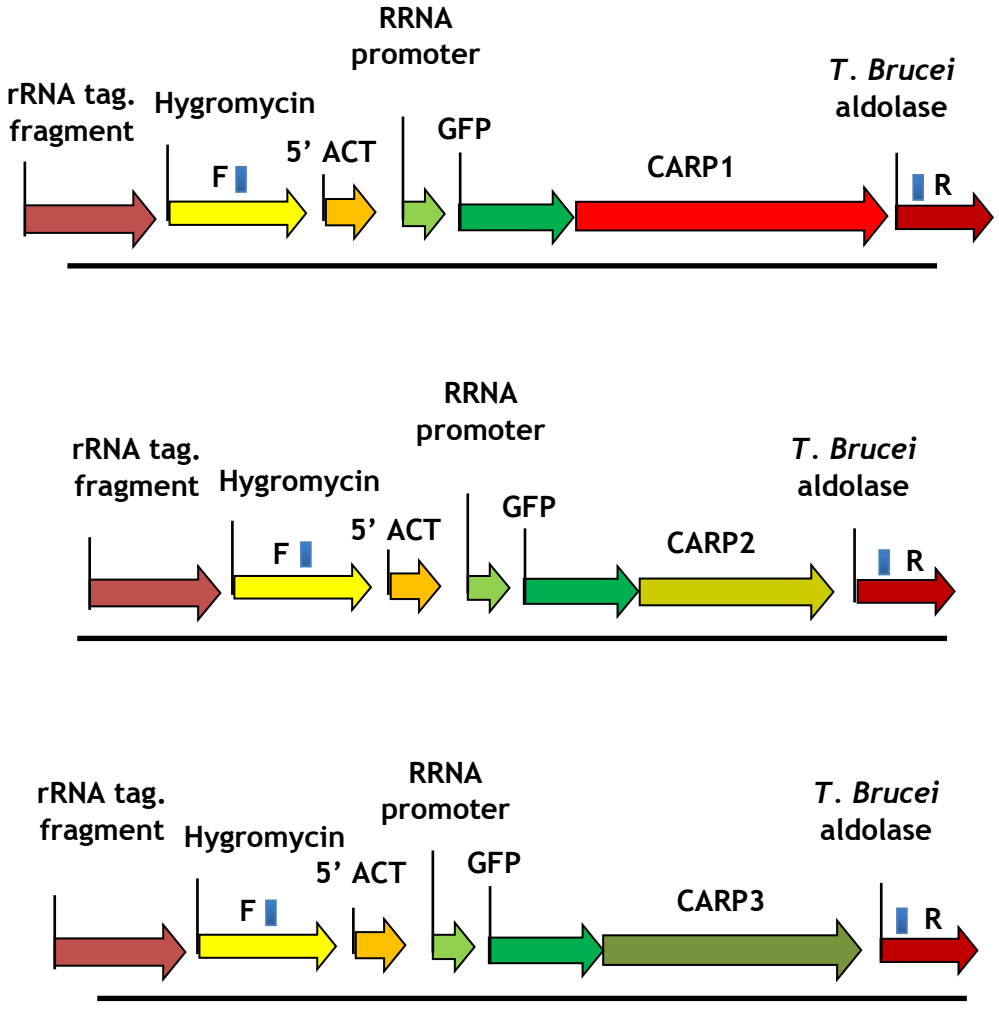

Figure 2.6: N-Terminal GFP tagged (pRPa^{GFP}) overexpression with CARP1-3. F-forward primer; R-reverse primer.

2.3.3 Transfection and selection of clonal CARP1-4 KO cells, CARP1-4 and TbPDEB1 overexpressing cells and N-terminal GFP tagged cells

The generated CARP1-4 KO constructs were digested using *NotI* and *XhoI* to create a vector that can integrate into the 5′ UTR and 3′ UTR flanking each CARP and replace each gene with the appropriate antibiotic cassette whilst CARP1-4^{oe} and TbPDEB1^{oe} were linearized with *NotI* to integrate as a vector into the ribosomal RNA locus. CARP1-3^{GFP} constructs were linearized with *AscI* and integrates to replace an in-house puromycin cassette allowing selection with hygromycin. 10 µg of each construct was digested in a 200 µl reaction volume using 11 µl each of their respective enzyme, 20 µl of 10X buffer D, 20 µl of BSA and ddH_2O with incubation at 37°C for 4 h. The digests were PCR cleaned and ethanol precipitated to concentrate the vectors for transfection. KO Vectors of CARP1-4 were transfected into WT s427 whilst CARP1-4^{oe}, TbPDEB1^{oe} were transfected into WT s427 and R0.8 cells (Gould et al., 2013). N-Terminal GFP-Tagged pRPa^{GFP} vectors were transfected into 2TI cells.

Bloodstream form *T. b. brucei* WT s427 strains, 2TI and R0.8 were cultured to a density of 1 x 10^6 cells/ml. 5 mL (5 x 10^6 cells) of culture for each transfection were transferred into a 15 mL centrifuge tube (Corning®) and centrifuged at 2600 rpm for 10 minutes at 22°C in a Heraeus Biofuge centrifuge. The supernatant was decanted off and the pellet washed into 100 µl Human T-Cell solution for transfection with 10 µg ethanol-precipitated vector DNA (10 µl) using an Amaxa Nucleofector™ II electroporator (Amaxa Biosystems) program X-001. The transfections were transferred into pre-warmed HMI-9 with 10% FBS medium and allowed to recover for 8 – 16 h at 37°C and 5% CO_2. Appropriate antibiotics corresponding to the selection marker of the vector used in transfection were added. Cells transfected with pHD1336 constructs were selected with blasticidin (5 µg/ml) whilst pRPa^{GFP} were selected with hygromycin (2 µg/ml) and respective antibiotic for KO vectors and neomycin (2 µg/ml) (Sigma-Aldrich®) before the cells were cloned. The cells were cloned out using limiting dilution into three 96 well plates (1/24 dilution for plate 1, 1/288 dilution for plate 2 and 1/576 for plate 3). Three clones were selected for each gene and the preference was for the lowest dilution to select for transfectants.

Two selectable markers (blasticidin and hygromycin) were initially used for transfection for KO lines. Thus two sets of heterozygote cell line of three clones each of CARP1-4 (CARP1-4$^{+/-}$ blasticidin) and (CARP1-4$^{+/-}$ hygromycin) were obtained from the first transfection. The generated sKO and overexpressing CARP cell lines were immediately analysed for correct heterozygosity, gene integration and overexpression and used for downstream experiments whilst attempts were made to generate dKO CARP cell lines.

To generate a homozygote allele deletion of each of CARP1-4 (CARP1-4$^{-/-}$), the antibiotics were swapped in a repeated transfection in an attempt to delete the second allele of both CARP1-4$^{+/-}$ blasticidin and CARP1-4$^{+/-}$ hygromycin using hygromycin and blasticidin respectively as well as neomycin selectable cassettes were performed. As a control, the neomycin selectable vector was used for a single allele deletion. All neomycin single allele deletion yielded clones. Several attempts were made in an attempt to obtained double gene deleted CARP cell lines. There were double deletions of CARP2$^{-/-}$, CARP3$^{-/-}$ and CARP4$^{-/-}$.There were however no viable clones for CARP1$^{-/-}$ double gene deletion after three attempts.

2.3.4 Confirmation of CARP1-4 single (sKO) and double KO (dKO), O.E and N-Terminal^{GFP} generated lines.

Successful gene deletion, correct antibiotic cassette integration and presence of expression vectors were confirmed with PCR, qRT-PCR and restriction digest Southern blotting.

2.3.4.1 PCR confirmation of antibiotic integration of sKO CARP1-4, dKO CARP2-3 and vector integration of pHD1336 and pRPa^{GFP}.

For KO confirmation, primers were designed to bind to a region pre 5′ UTRs and a post 3′ UTRs and normal PCR reaction performed with the reverse and forward primers of the integrated antibiotic cassette to the respective UTR primers (Appendix 1: Table 1.4). To confirm O.E in WT s427 and R0.8 and GFP-tagged in 2TI cells, primers were designed to bind to a region pre ORF and use in a normal

PCR reaction with the reverse primer of the integrated antibiotic cassette. In these reactions, Wild type s427, R0.8 and 2TI cells were used as controls for the respective experiments.

2.3.4.2 Quantitative Real Time-PCR (qRT-PCR) confirmation of reduction and increase in mRNA transcripts of sKO and O.E cells respectively.

Confirmation of sKO CARP1-4, CARP1-4^{oe} and TbPDEB1^{oe} using qRT-PCR was carried out as previously described (Ali *et al.,* 2013). Primers for qRT-PCR were designed using Primer3® (Appendix 1: Table 1.5). The constitutively expressed gene GPI8 was used as an endogenous control (Wilson et al., 2012). Primer efficiency was performed for each of the primers and the endogenous control (GPI8) (5′- TCTGAACCCGCGCACTTC-3′ and 5′-CCACTCACGGACTGCGTTT-3′) using the previously described method of Pfaffl (Pfaffl, 2001). Generated cell lines and their respective controls were grown to log phase densities in HMI-9 with 10% FBS medium. Cells were counted and 2 x 10^6 cells were spanned down at 2600 rpm for 10 min and the supernatant decanted. RNA was isolated from the pellets following manufacturer's protocols and quantified using a Nanodrop (Thermo Scientific). 200 ng of RNA from each generated cell and control was converted into complementary DNA (cDNA) using a Reverse-Transcriptase (RT) kit (Primerdesign®). The cDNA for each sample was subsequently diluted with RNase free water to 20 ng/µl for Real Time-PCR. Amplification of cDNA was performed in a 7500 Real Time PCR System (Applied Biosystems®). A dissociation curve was used to ensure the amplification of only one product; samples without RT or without cDNA were used as controls. The entire experiment was performed on three independent occasions, starting from cell culture and RNA isolation of the different cell lines. Fold change was calculated using the determined primer efficiency (Pfaffl, 2001).

2.3.4.3 Southern blot confirmation of CARP2-3 dKO lines

Double allele deletions of CARP2, CARP3 AND CARP4 were confirmed using Southern blot restriction digest of genomic DNA from knockout cell lines as previously described (Ali et al., 2013). 10 µg of DNA from each of the cell lines were digested overnight (O/N) with *EcoRI* and *SacII* (CARP2$^{-/-}$), *EcoRI* and *XhoI* (CARP3$^{-/-}$) and *EcoRV* and *XhoI* (CARP4$^{-/-}$). These were then run on a 0.8% gel for

24 h at 20 V. Thereafter, the DNA was blotted O/N onto Hybond Nylon membrane (Amersham®). The DNA was cross-linked onto the membrane using a UV cross-linker and then hybridized for 2 h at 42°C. Probes were prepared using 50 ng restriction digested DNA (ApaI and BamHI) of CARP2, CARP3 and CARP4, 10 µl random oligo primers (Prime-it II Radom Primer Labelling, Stratagene®) and ddH_2O to a volume of 37 µl. This was heated 95-100 °C for 5 mins. 10 µl 5x primer buffer, 2 µl α^{32} Phosphorous dATP and 1 µl Klenow (5U/µl) added after brief centrifugation. The probe was further incubated at 37-40 °C for 10 mins after which the reaction was stopped with 2 µl Stop mix. Finally, the reaction was purified with a resin column, heated to 95 °C for 5 min and immediately added to the hybridisation solution and membrane. This was incubated for more than 16 h. The filters were washed twice using standard high stringency solutions at 55 °C for 20 and 45 min in the rotisserie respectively after which they were heat sealed in a plastic film and exposed to Amersham Hyperfilm™ MP for an initial 3 h and O/N at -80 °C. The films were developed using the KODAK® RP X-omat developer.

2.3.4.4 Western blot confirmation of loss, decrease and increase in protein levels of CARP3$^{-/-}$, CARP3$^{+/-}$, s427 CARP3^{oe} and R0.8 CARP3^{oe}.

Peptide antigens were designed for CARP1 (N-DREKGKRRIKENSKAC-C), CARP2 (N-DYFHRRKRLTPRRTD-C) and CARP3 (N-QSNMSEESGGEGGDTN-C) and antibody raised against them in rabbits (by Eurogentec, Belgium). Out of these three anti-CARP antibodies, only CARP3 gives the right Molecular Weight (MW) and size for Western blotting. Thus to determine if gene deletion or overexpression of CARP3 results in a concomitant change of CARP3 protein, Western blotting was performed as previously described (Gould et al., 2013).

CARP3$^{-/-}$, CARP3$^{+/-}$, s427 CARP3^{oe}, R0.8 CARP3^{oe}, WT s427 and R0.8 cells were cultured in HMI-9 media to log phase. Two sets of 1 x 10^7 cells each were centrifuged at 2600 RPM for 10 mins at 4°C. The supernatant was discarded. 100 µl of protein sample buffer was added to the pellet and heated at 100°C for 5 min. 15 µl of the sample was run on a 8-12% Novex® NuPAGE® Bis-Tris gels (life Technologies, UK) at 80 V for 2 h. Gels were blotted for 3 h at 20 V onto Amersham® Hybond ECL, (GE Healthcare Life sciences, UK) using the Xcell

Surelock™ mini-cell electrophoresis system. Blots were blocked using 5% milk in PBS-Tween (0.01%) (Sigma-Aldrich®) for 1 h. Primary antibodies of Anti-CARP3 polyclonal antibody and control antibody of Elongation factor 1-α (EF1-α) were added in blocking solution of 5% milk in PBS-Tween (0.01%) to respective blots on a shaker O/N at 4 °C. Blots were washed and incubated in blocking solution containing secondary antibody of Horse-Radish anti-Rabbit IgG (Sigma-Aldrich®) for 1 h. After washing blots, Pierce™ ECL Western Blotting Substrate (Life Technologies) was added and the blots exposed to Amersham® Hyperfilm. Films were developed using KODAK® RP X-omat developer.

2.3.5 Effect of CpdA on transcript (mRNA) of CARP1-4^{oe} in s427 and R0.8 and CARP3 protein levels of sKO CARP3 and CARP3^{oe}

2.3.5.1 Determination of CpdA effect on mRNA levels of CARP1-4^{oe} and TbPDEB1^{oe}.

To determine the effect of CpdA on mRNA of the overexpressing CARP1-4 and TbPDEB1 genes in WT s427 and R0.8, the generated trypanosomes were seeded at 2 x 10^4/ml in 20 ml culture media and incubated at 37 °C, in a 5% CO_2 atmosphere. WT s427 and R0.8 were also similarly seeded as controls. 2 x 10^6 of the overexpressing cells in both WTs427 and R0.8 and their controls were pelleted for RNA extraction as 0 h samples. 100 nM of CpdA was added to s427 CARP1-4^{oe}, TbPDEB1^{oe} and WT s427 whilst 3 µM of CpdA was added to R0.8 CARP1-4^{oe}, TbPDEB1^{oe} and R0.8 respectively. At 6 h, 2 x 10^6 cells were pelleted and at 24 h and 48 h for RNA extraction. Pelleted cells for RNA extraction were frozen at -20 °C after each incubation period. RNA was extracted after 48 h incubation for all the samples. All the RNA samples were reverse transcribed into cDNA and qRT-PCR performed as previously described. This experiment was repeated independently on three different occasions.

2.3.5.2 Determination of CpdA effect on protein levels of CARP3$^{+/-}$, s427 CARP3^{oe} and R0.8 CARP3^{oe}

To investigate the effect of CpdA on protein expressions in CARP3$^{+/-}$, s427 CARP3^{oe} and R0.8 CARP3^{oe}, cells were grown without and in 100 nM and 3 µM CpdA over a period of 48 h. 5 x 10^6 cells were seeded in 50 ml culture media and incubated at 37 °C, in a 5% CO_2 atmosphere. 1 x 10^7 cells overexpressing CARP3 in both WT s427 and R0.8 and their controls were pelleted and 100 µl of protein loading buffer added and heated at 100 °C as 0 h samples. Subsequently, 100 nM CpdA was added to CARP3$^{+/-}$, s427 CARP1-3^{oe} and WT s427 whilst 3 µM of CpdA was added to R0.8 CARP3^{oe} and R0.8 respectively. At 6 h, 1 x 10^7 cells were pelleted and at 24 h and 48 h and prepared as above for protein gel electrophoresis and Western blotting. Ready loading protein samples were frozen at -20 °C after each incubation period. Western blotting was performed as previously described.

2.3.6 Drug sensitivity assays of sKO CARP1-4, dKO CARP2-3, s427 CARP1-4^{oe} and TbPDEB1^{oe}, R0.8 CARP1-4^{oe} and TbPDEB1^{oe} and controls.

Sensitivities of CARP1-4$^{+/-}$, CARP2-4$^{-/-,}$ s427 CARP1-4^{oe} and TbPDEB1^{oe}, R0.8 CARP1-4^{oe} and TbPDEB1^{oe} and controls cells to CpdA and pentamidine (Sigma-Aldrich®) were determined using the Alamar Blue assay (de Koning et al., 2012). Alamar blue dye was prepared by dissolving 12.5 mg of resazurin sodium salt (Sigma-Aldrich®) in 100 ml of PBS (Sigma-Aldrich®) at pH 7.4. The mixture was then filter-sterilized and stored at -20°C in foil-wrapped tubes to avoid exposure to light. Starting from a 5 mM stock solution in dimethyl sulfoxide (DMSO; Sigma-Aldrich®), CpdA was diluted to 200 µM in HMI-9 media for CARP1-4$^{+/-}$, CARP2-4$^{-/-,}$ s427 CARP1-4^{oe} and TbPDEB1^{oe} and WT s427 control and 1 µM for R0.8 CARP1-4^{oe} and TbPDEB1^{oe} and R0.8 control. Starting from a 20 mM stock solution in DMSO, pentamidine was diluted to 200 µM in HMI-9 media. 200 µl of CpdA solution was then added to the first well in a 96-well plate, while 100 µl of fresh medium was added to the remaining wells (24 wells for each compound). Doubling dilutions were done by pipetting 100 µl from the first well into the second well, mixing well by pipetting up and down several times then removing 100 µl from the

second well to the third, and so on. The last well was left drug free. 100 µl of 2×10^5 cells/ml were added to all the wells, giving a final drug concentration of either 100 µM (KO and s427 overexpressing cells) or 500 µM (R0.8 overexpressing cells) in the first well and $2x10^3$ cells in all wells. The plates were incubated at 37°C and 5% CO_2 for 48 hours. After 48 h, 20 µl of alamar blue dye was added to all wells and incubated for a further 24 hours at 37°C and 5% CO_2. The plates were read using the FLUOstar Optima (BMG Labtech) fluorimeter at 530 nm and 590 nm, excitation and emission respectively. EC_{50} values were subsequently determined using the GraphPad® Prism 5 software.

2.3.7 Growth curves of sKO CARP1-4, dKO CARP2-3, s427 CARP1-4^{oe}, R0.8 CARP1-4^{oe} and controls.

Growth of sKO CARP1-4, dKO CARP2-3, s427 CARP1-4^{oe}, and WT s427 control were assessed in HMI-9 only and in HMI-9 supplemented with 100 nM of CpdA whilst that of R0.8 CARP1-4^{oe} and R0.8 control were performed in 3 µM CpdA similar to (Ali et al., 2013). Bloodstream forms of each cell type were seeded at 2×10^4 cells ml^{-1} and for this purpose grown in 24-well plates, with each condition set up in 2 wells; incubation was at 37 °C and 5% CO_2. Cells were counted every 24 h using a haemocytometer. Cells in drug free medium and 100 nM or 3 µM of CpdA supplemented media were diluted every 48 h to concentrations of 2×10^4 or undiluted if density is lower than 1×10^6. Based on the results, an additional growth curve was performed for s427 CARP1^{oe} and CARP3^{oe} against WT s427 (100 nM) and R0.8 CARP1^{oe} and CARP3^{oe} against R0.8 (3 µM) without diluting cells over the period of the growth curve. The entire experiments were performed on three independent occasions. GraphPad® Prism 5 software was used to generate linear regression curves.

2.3.8 Immunofluorescence microscopy of CARP cellular localizations

To determine protein localization, IFA was performed by expressing the full ORF of CARP1-3 attached to an N-terminal GFP. Additionally, the availability of a peptide polyclonal anti-CARP3 antibody allowed for a direct IFA of CARP3^{oe}, WT

s427 and CARP3$^{-/-}$ cell lines. IFA was performed similar to previously described (Saada et al., 2014).

The N-terminally tagged GFP cells (pRPa^{GFP}) are tetracycline inducible. Thus to ensure maximal protein expression, cells were induced with 1 µg/ml tetracycline for 48 h.10 ml of 1 x 10^6/ml induced log phase cells were pelleted and washed twice with 1ml PBS. This was re-suspended in 200 ml of PBS and 50 µl spread on a clean labelled frosted slide. The slides were air fixed after which additional fixing was performed in 4 % paraformaldehyde/PBS solution for 10 min. The cells were washed twice with PBS and then permeabilized with 0.1% Triton x-100 (Sigma-Aldrich®) for 5 min. The Triton was washed off with PBS and 1% BSA/PBS used to block unspecific binding for 45 min. The cells were incubated with primary anti-GFP antibody (Sigma-Aldrich®) diluted (1:1000) in 1% BSA/PBS for O/N at 4 °C with gentle rocking. The primary antibody was washed with PBS after which the cells were incubated in a secondary antibody; HRP anti-Rabbit IgG coupled with FITC (1:500) dilutions at room temperature for 1 h. Cells were rinsed 3X with PBS. Coverslips were mounted in mounting medium with DAPI (4',6-diamidino-2-phenylindole) VectaShield® (Vector Laboratories Inc., USA). Similar protocol was used to prepare s427 CARP3^{oe}, WT s427 and CARP3$^{-/-}$ for imaging using anti-CARP3 antibody (1:125) instead of anti-GFP. Samples were imaged on a Zeiss® Axioskop II microscope (Zeiss, Inc) and DeltaVision Core (AppliedPrecision®). Images were processed using GIMP 2.8.10 (http://www.gimp.org/).

2.3.9. Cyclic AMP measurements in sKO, dKO and O.E cell lines

Cyclic AMP measurement was performed exactly as previously described (de Koning et al., 2012; Gould et al., 2013) with minor modifications.

For extracellular cAMP, log-phase Bloodstream form trypanosomes at 2 x 10^6 were inoculated into 20 ml of HMI-9 media and incubated at 37 ºC overnight. The cells were counted and then split into two. 300 nM of CpdA was added to one set of flasks (CpdA +) whilst the other was retained as a control (CpdA -). Both were further incubated for 3 h. After the 3 h incubation, a total of 5 x 10^6 cells were counted using a haemocytometer for both CpdA + and CpdA – and the

trypanosomes pelleted at 2600 RPM, 10 min at 4 ºC. 1 ml of the supernatant was carefully removed into labelled eppendorfs and kept at -80 °C for extracellular cAMP assay.

For intracellular cAMP, the rest of the supernatant was removed and the cell pellet resuspended in 100 µl 0.1 M HCl and left on ice for 20 minutes to complete cell lysis. The samples were centrifuged at 12,000 RPM, 10 min at 4 ºC and the supernatant transferred to new labelled eppendorf and stored in a freezer at -80 ºC. Cyclic AMP content was assessed exactly as per the Cyclic AMP ELISA Immunosorbent Assay (EIA) Kit (Cayman Chemical Company, Missouri, USA) instructions from the manufacturers. Briefly, assay specific buffers, standards and samples were prepared according to recommended protocols (intracellular samples were diluted 1 in 2 with EIA buffer). Non-acytelated cAMP assay was performed in 96 well plates pre-coated with mouse monoclonal cAMP-specific rabbit antiserum. Eight serially diluted standards (double wells), blanks, buffer, tracer and antiserum together with the samples were added to the 96 well plates. The plates were incubated for 18 h, washed and developed with Ellman's reagent for 2 h. The plates were read on Dynex® Technologies Revelation plate reader. Each sample was assayed in duplicate whilst the whole experiment from sample preparation to cAMP measurement was performed independently on at least three occasions.

2.4.0 Effect of extracellular cAMP on growth of overexpressing CARP1, CARP3 and WT s427 cells

Overexpressing CARP1, CARP3 and WT s427 cells at 2 x 10^6 were inoculated into 40 ml of HMI-9 media and incubated at 37 ºC overnight. The cells were counted and then split into two. 100 nM of CpdA was added to one set of flasks (induced) whilst the other was retained as a control (un-induced). Both were further incubated for 3 h. After the 3 h incubation, a total of 1 x 10^8 cells were counted using a haemocytometer for both induced and un–induced and the trypanosomes pelleted at 2600 RPM, 10 min at 4 ºC. The supernatant was carefully removed into labelled eppendorfs and kept at -80 °C for growth curve assays. CARP1, CARP3 and WT s427 cells were inoculated in either their respective induced or un-induced media as well as HMI-9 + 100 nM CpdA, HMI-9 + 100 nM CpdA + 1 uM

cAMP (Sigma-Aldrich®), HMI-9 + 100 nM CpdA + 10 uM AMP (Sigma-Aldrich®), HMI-9 only, HMI-9 + 5 uM cAMP and HMI-9 + 50 uM AMP. Cells were counted every 24 h using the haemocytometer. Each cell line and condition was double seeded from two different flasks each whilst the whole experiment was independently repeated at least twice. To confirm that 100 nM CpdA causes the release of cAMP into the media, induced and un-induced supernatants were both assayed for cAMP levels same as described previously.

2.4.1 Transcriptomics and Proteomic investigations of CARPs and their interactions

2.4.1.1 Ribonucleic Interference Sequencing (RIT-Seq)

RNAi interference knockdown approach was performed to discover downstream effectors of cAMP signalling. Here, blood stream forms *T. brucei* trypanosomes were transfected with the RNAi library and grown in HMI-9. After recovery from the transfection, the cells were grown under CpdA pressure with RNAi induction using tetracycline (Gould et al., 2013). DNA was extracted from surviving cells and separated on a 1% gel. Distinct bands were excised and sequenced revealing four distinct genes that were designated cAMP Response Proteins (CARPs). Characterization of these CARPs has been described in the previous chapters. However, to maximize the discovery of distinct genetically induced loss of function phenotype as well as survey the representation of genetically distinct cells in a complex population, RIT-seq was performed on some of the DNA extracted from the surviving cells from which the initial CARPs were discovered.

RNAi library screen that generated resistance clones for the RIT-Seq has been previously described (Baker et al., 2011; Gould et al., 2013). Firstly, a genome RNAi library of *T. brucei brucei* Lister s427 trypanosomes was induced with tetracycline under CpdA pressure to select for resistant clones. DNA was extracted from the surviving cells and the RNAi target DNA fragment amplified from the genomic DNA using primers Lib2 forward, 5'-TAGCCCCTCGAGGGCCAGT-3', and Lib2 Reverse, 5'-GGAATTCGATATCAAGCTTGGC-3' which are RNAi insert specific for amplifying RNAi inserts from genomic DNA. This was run on a gel and the specific bands excised and sequenced. The sequence was mapped to the

reference genome sequence. Some of this DNA was sent to the Glasgow Polyomics Centre for library preparation and illumina sequencing. Library preparation was performed using the TrueSeq® Stranded mRNA Sample Prep Kit (Illumina) similar to previously described (Alsford et al., 2012b; Alsford et al., 2011b; Baker et al., 2011). Briefly, DNA from the RNAi libraries were PCR amplified (19-22 cycles, 95 ◦C for 30 s, 57 ◦C for 30 s and 72 ◦C for 130 s; 0.5 µg of substrate DNA) using upstream primer (LIB2f 5'- TAGCCCCTCGAGGGCCAGT'-3) which includes RNAi vector tagged sequence and downstream primer (LIB2r 5'-GGAATTCGATATCAAGCTTGGC'-3). Band sizes of ~150-300 bp of both WT s427 and resistant clones were excised, shredded, DNA extracted and indexed together. WT s427 showed no PCR amplification due to the absence of vectors. Adapters were ligated to the ends of the libraries after which the libraries were amplified and quantified. Paired-end sequencing was performed on illumina Genome Analyzer II. Reads from the illumina sequencing were firstly trimmed of adapters and RNAi-vector junctions and then mapped to the *T. brucei* 927 genome (Berriman et al., 2005) obtained from TryTripDB (http://tritrypdb.org/tritrypdb/) using Bowtie (Langmead et al., 2009) to obtain coverage, uniqueness of plot, read counts and alignment score. This was followed by normalization of CDS using DEGseq R to the control. Data analysis was performed by Dr Jon Wilkes (Wellcome Trust Centre for Molecular Parasitology, University of Glasgow, UK).

2.4.1.2 Co-Immunoprecipitation (Co-IP) and Mass Spectrometry (MS)

Peptide antigens were designed for CARP1 (N-DREKGKRRIKENSKAC-C), CARP2 (N-DYFHRRKRLTPRRTD-C) and CARP3 (N-QSNMSEESGGEGGDTN-C) and antibody raised against them in rabbits (by Eurogentec, Belgium). Out of these three anti-CARP antibodies, only CARP3 gives the right Molecular Weight and size in Western blotting and thus was considered specific enough for pull-down studies with CARP3. However, anti-CARP1 and 2 were thus used in a tandem pull-down assay as controls instead of beads to provide a much stronger filter for CARP3 specific pull-down proteins.

A total of 2.5 X 10^8 log-phase of each of CARP1^{oe}, CARP2^{oe} and CARP3^{oe} and WT s427 *T. brucei* cells growing in HMI-9 were pelleted, washed with PBS and

immediately frozen at -80^{0}C until ready for Co-IP. Cells were resuspended in 500 µl ice cold IP Lysis/wash Buffer (0.025mL Tris, 0.15M NaCl, 0.001M EDTA, 1% NP-40, 5% glycerol; pH7.4) as previously described (Paterou et al., 2006) and incubated on ice for 5 min with periodic mixing. Supernatant was separated from cell debris at 13,000 x g for 10 min according to manufactures protocol (Pierce® Crosslink Immunoprecipitation Kit, Thermo Scientific, Illinois, USA). Protein concentrations were determined using the Nanodrop (Thermo Scientific®). CARP3 antibody as well as non-specific CARP1 and CARP2 (150 µg) were coupled to protein agarose resin and then crosslinked with disuccinimidyl suberate (DSS). Protein lysates were immunoprecipitated on the resin-bound and crosslinked CARP antibodies for 2 h at 4^{0}C followed by three steps of washing with IP Lysis/Wash buffer and elution of bond antigens. Eluates were quantified on nanodrop and prepared for MS. The FASP protein digestion kit (FASP™ Protein Digestion Kit; Expedeon, Cambridgeshire) was used to prepare samples following manufacturer's protocol for MS analysis. Briefly, gel free eluate was added to spin columns together with urea sample solution and centrifuge at 14000 x g 12 mins, repeated twice. This was followed by 10 X Iodoacetamide solutions with urea and 30 min incubation in the dark. The spin column is washed with Urea Sample Solution followed by 100 µl of 50 mM Bicarbonate solution. Trypsin digest was performed overnight at 37^{0}C after which samples were acidified with Triflouroacetic acid (TFA) followed by drying in 96 well plates in a vacuum chamber. Samples were sent to Glasgow Polyomics Centre were it was loaded into MS Instrument for amaZon speed ETD Ion Trap mass spectrometer with UltiMate™ 3000 RSLC nanoseparation system: <200ppm (external); <200ppm (internal): for High-sensitivity protein identification. Three independent co-immunoprecipitations and MS analysis were carried out for CARP3 and CARP1 and once for CARP2 overexpressing cells. MS/MS data were firstly converted into mgf file which were then searched against *T. brucei* predicted proteome (Trypan.Brucei_PEP 20070228 (10409 sequences; 5108677 residues)) data using the mascot search algorithm (Mascot Science). Fixed modification was set as carbamidomethyl (C), variable modifications of oxidation (M) as previously described (Adung'a et al., 2013). Missed cleavage was set at 1. Both Peptide Mass and Fragment Mass Tolerance were set at ±0.4 Da. Expectation value was set at 0.05 and used as a cut off.

One of the hits from RIT-seq and Co-IP, an adenylate cyclase (Tb927.4.4460; GRESAG4.4) was thought to be important and potentially involved in cAMP regulation through a feedback loop. To confirm that, already prepared cDNA from CARP3^{oe} and WT s427 in HMI-9 only, 0 h (no CpdA) and in CpdA (6 h) used in gene expression in CpdA and freshly prepared cDNA of CARP3$^{-/-}$ were used in a qRT-PCR assay using GRESAG4.4 primers and endogenous GPI8 primers as previously described. Gene expression was performed independently on at least three occasions.

2.4.2.3 Ribonucleic Acid Sequencing (RNA-Seq)

To compare gene expression of CARP3^{oe}, R0.8 and WT s427, 5 flasks each of the individual cell lines were inoculated from a single growing flask O/N. A total of 5 x 10^6 log-phase trypanosomes were pelleted from each flask, RNA extracted as previously described using RNeasy kit (Machery-Nagel®) and quantified on the nanodrop. Three out of the 5 RNA samples of each cell type was sent to the Glasgow Polyomics for RNA-Seq. Library preparation and further sample preparation was performed using the TrueSeq® Stranded mRNA Sample Prep Kit (Illumina) as previously described (Kolev et al., 2010; Siegel et al., 2010b). Briefly, mRNA samples were purified using poly-T oligo attached magnetic beads and fragmented in preparation for cDNA synthesis. Reverse transcription and random primers were used to synthesis first stranded cDNA. A double cDNA strand was generated through the synthesis of a second strand by removing the last RNA and replacing dUTP with dTTP followed by adenylation of the 3' end to prevent self-ligation. Adapters were added to the ends of the cDNA after which they were enriched through PCR amplification of only adaptor ligated cDNA. The library preps were validated, quantified and checked for quality using Agilent Technology 2100 Bioanalyzer (Life Technologies®). The preps were then paired-end sequenced on NextSeq™ 500 (2x150bp). The quality of paired-end reads from the sequencer were firstly checked with FastQC and then trimmed of library adaptors with Tophat followed by mapping to the trypanosome genome (http://tritrypdb.org/common/downloads/release-8.1/TbruceiTREU927/) using Bowtie (Archer et al., 2011; Kolev et al., 2010; Langmead et al., 2009). The mapped reads were then assembled into sets of transcripts and their relative abundance estimated using Cufflinks. Cuffdiff is then performed to determine

log_2-fold differential expression in the transcripts between the test sample (CARP3^{oe} and R0.8) against the control. RNAseq data analysis was performed by Graham Hamilton of the Glasgow Polyomics, University of Glasgow, Glasgow, UK. Significant log_2-fold expression was set at *P*-value 0.05. Of the significantly expressed genes, 0.5 and 0.75 log_2-fold difference were used as cut-offs for s427 CARP3^{oe} and WT s427 and R0.8 CARP3^{oe} and R0.8 respectively. TIBCO® Spotfire® Desktop 7.0.0 (Boston, MA) was used for visualization.

Chapter 3

Deletion of alleles of CARP1-4 and its effects on sensitivity, growth and cyclic AMP levels

3.0 Deletion of alleles of CARP1-4 and its effects on sensitivity, growth, cAMP and protein levels of CARP3

In order to investigate whether the CARP proteins are essential for *Trypanosoma brucei* bloodstream forms, knockout constructs with three antibiotic selectable cassettes (hygromycin, blasticidn and neomycin) were made for CARP1-4 and transfected for the generation of CARP1-4$^{+/-}$. Additional transfection with alternate antibiotics of the CARP1-4$^{+/-}$ yielded CARP2-4$^{-/-}$. Attempts were made to obtain a double gene deletion for CARP1 but no viable clones were obtained. Although three clones were selected for each selectable marker and gene, only one clone of one selectable maker was used for downstream experimental assays after confirmation of both single and double gene deletions.

3.1.0 Evidence of gene deletion of CARP1-4

After transfections and selection, gene deletion and antibiotic integration was confirmed using PCR, qRT-PCR and restriction digest Southern blotting. All of these techniques together ensure that the experiment was successful allowing for the study of downstream effect of the loss of these genes in trypanosomes.

3.1.1 PCR evidence of plasmid integration of sKO and dKO CARP cell lines

Primers that bind pre 5' UTR and reverse of antibiotic cassette and post 3' UTR and forward of antibiotic cassette were used to check for correct integration of the knockout vector (refer to Figure 2.2 for construct design and primer positions). The PCR product of CARP1-4$^{+/-}$, CARP2-3$^{-/-}$ and WT s427 were run on a 1% gel. Single and double gene deleted CARP cells showed bands of the right sizes indicative of correct vector integration for both 5′ UTR (F) and 3′ UTR (R) and presence of antibiotic cassettes compared with WT s427 (Figure 3.1). The bands visible for WT s427 PCR in Figure 3.1C, were a result of unspecific primer products and does not correspond to the expected sizes of ~1.5-1.8 kb for blasticidin and ~2.0-2.5 kb for neomycin integrations.

3.1.2 Reduced messenger RNA expression of single deleted *CARP1-4* genes in trypanosome cells

To further confirm *CARP1-4* single allele gene deletion, RNA was extracted from the generated cells and converted into cDNA using reverse transcriptase for qRT-PCR analysis of gene expression. All four genes showed significant reductions in gene expression compared with WT s427 cells. Expression of CARP1 was reduced by almost 50% whilst CARP2 expression only decreased by approximately 20% (Figure 3.2).

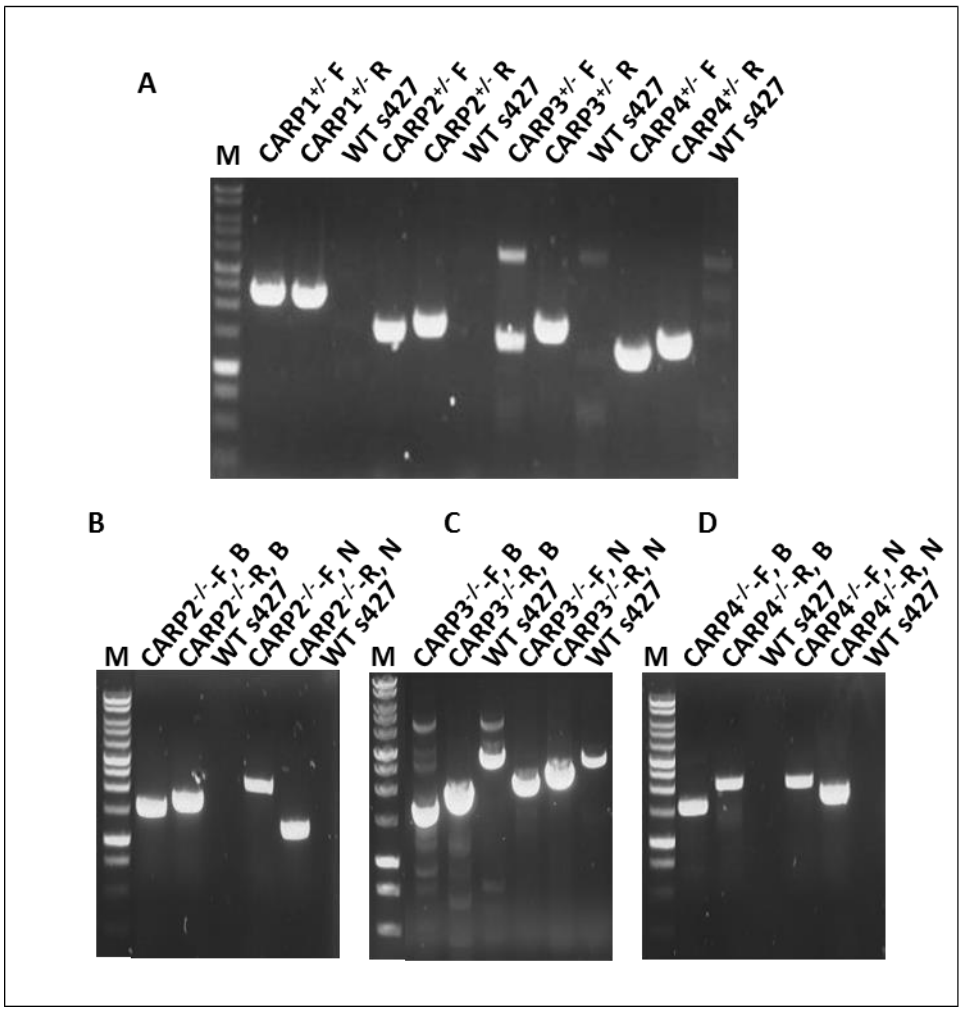

Figure 3.1: PCR evidence of plasmid integration and antibiotic gene replacement. A) Single gene deletion confirmation PCR using primers pre 5'UTR of each gene of CARP1-4 and reverse primer of antibiotic and post 3' UTR and forward of antibiotic cassette. B-D) Double gene deletion of CARP2-4 (CARP2$^{-/-}$, CARP3$^{-/-}$ and CARP4$^{-/-}$) using same primers as before and for both antibiotic integration as well as UTR's into antibiotics. F, forward primer; R, reverse primer, B, blasticidin; N, neomycin); M, maker (refer to Figure 2.2 for construct design and primer positions).

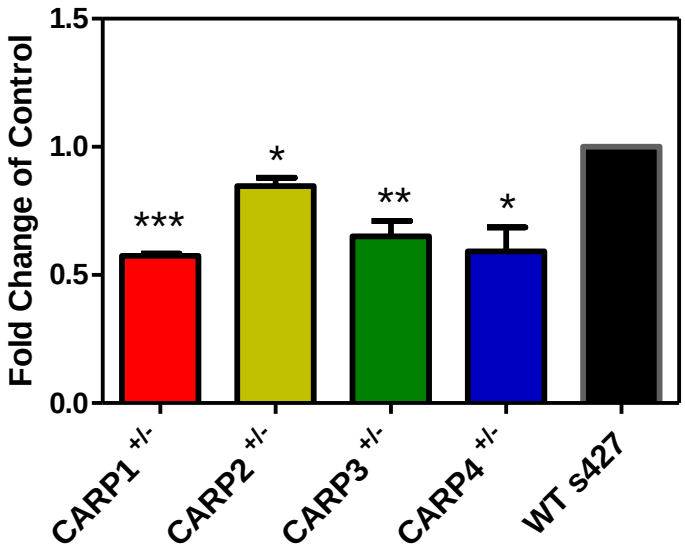

Figure 3.2: Quantitative Reverse Transcriptase PCR (qRT-PCR) of sKO CARP1-4 cells. RNA was extracted from each single gene deleted CARP cell line, reverse transcribed into cDNA and used for qRT-PCR. All single gene deleted cell lines showed significant fold reduction in transcript levels. Error bars show ± standard error. T-test single-tailed, unpaired (* p>0.05, ** p>0.01, *** p>0.001; n=3).

3.1.3 Southern Blot confirmation of double gene deletion

Double gene deletions of CARP2-4 (dKO) were confirmed using Restriction digest Southern blotting. DNA from CARP2-3$^{-/-}$ were digested using *EcoRI* and *SacII* and *XhoI* to yield specific size fragments. Genomic DNA of CARP4$^{-/-}$ was digested using *EcoRV* and *XhoI* restriction enzymes. These were then probed with restriction digest (*ApaI* and *BamHI*) excised open reading frames of CARP2-4. When ran on agarose gel, the digests produced a smear of DNA whilst the blots showed specific bands for WT s427 for CARP2-4, sKO CARP2 and CARP4. sKO CARP3 showed 2 bands which is due to the presence of additional *EcoRI* restriction sites in the resistant cassette present in the sKO cell line. sKO CARP4 showed a drop in band size due to the presence of an additional *XhoI* site in the sKO construct. There were no bands for CARP2$^{-/-}$, CARP3$^{-/-}$ and CARP4$^{-/-}$ confirming double gene deletion (Figure 3.3).

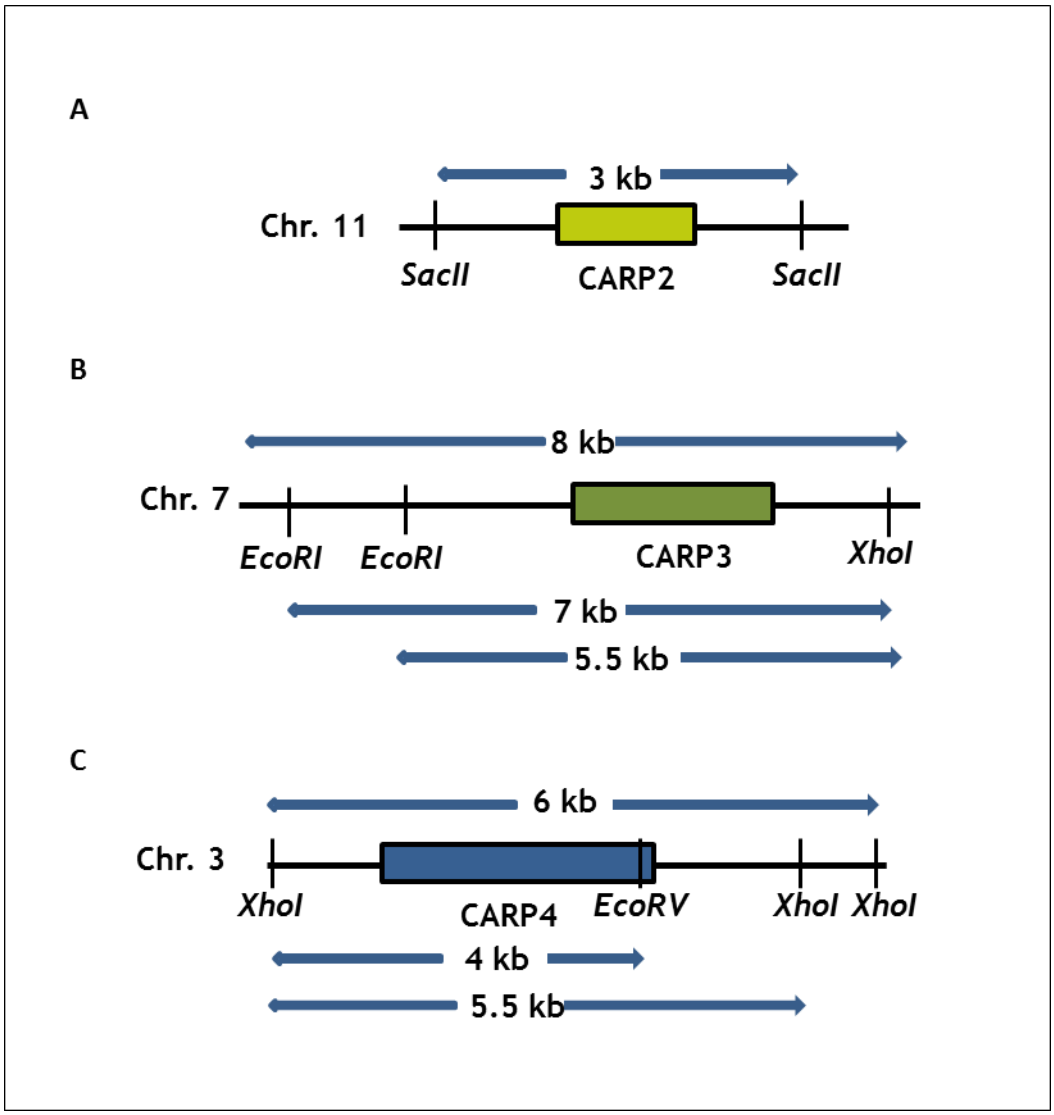
A
3 kb
Chr. 11
SacII
CARP2
SacII
B
8 kb
Chr. 7
EcoRI
EcoRI
CARP3
XhoI
7 kb
5.5 kb
C
6 kb
Chr. 3
XhoI
CARP4
EcoRV
XhoI
XhoI
4 kb
5.5 kb

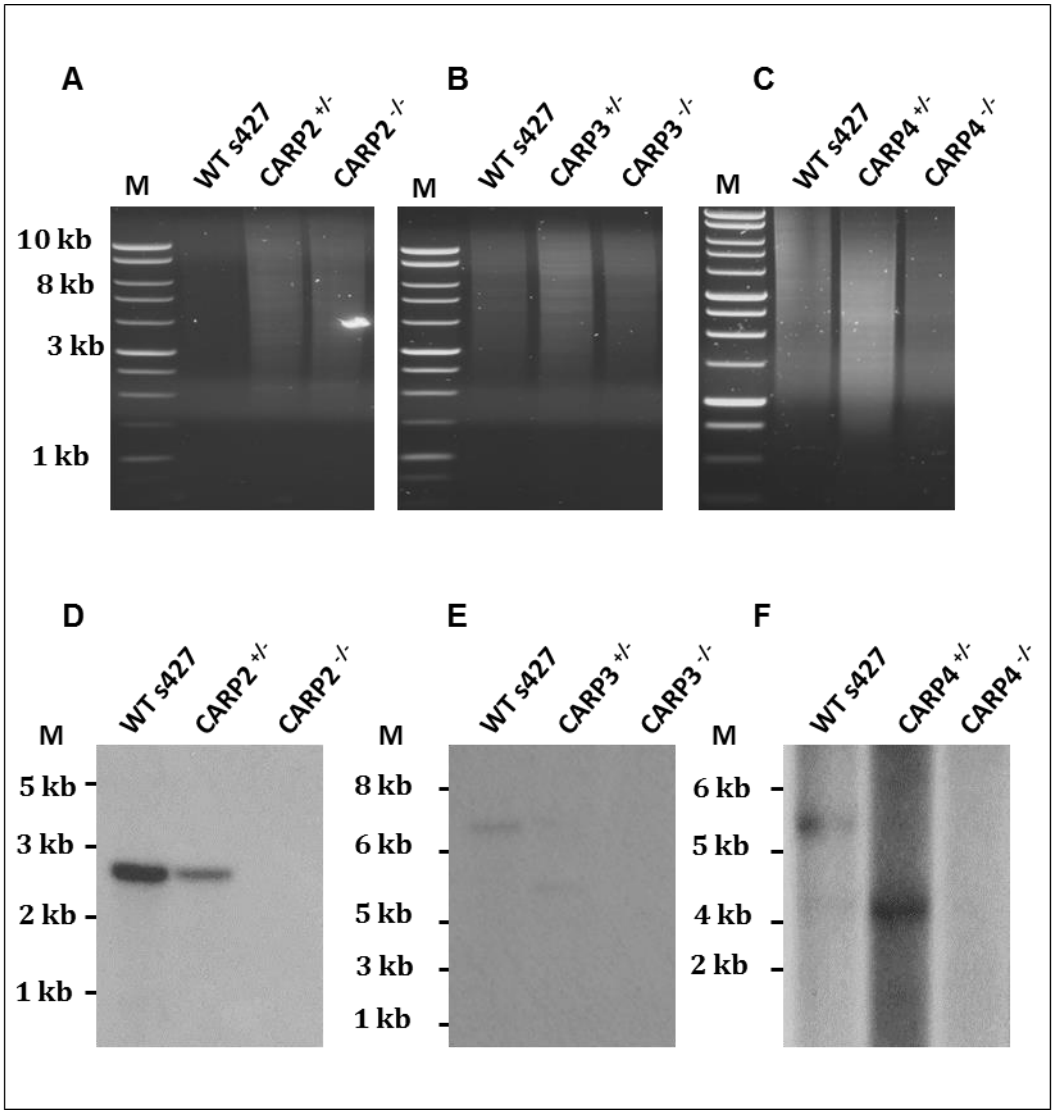

Figure 3.3: Restriction digest and Southern blot confirmation of dKO CARP2-4 cells. A) Restriction digest of CARP2 using *EcoRI* and *SacII* showing fragment binding size. B) Restriction digest of CARP3 using *EcoRI* and *XhoI* showing possible fragment sizes. C) Restriction digest of CARP4 using *EcoRV* and *XhoI* showing possible fragment sizes. D) Shows a band for WT s427, CARP2$^{+/-}$ (2.8 kb) and no band for CARP2$^{-/-}$. E) Shows a band for WT s427 (7 kb) dual bands for CARP3$^{+/-}$ (7 and 5.5) kb and no band for CARP3$^{-/-}$. F) Shows a band for WT s427 (5.5 kb), CARP4$^{+/-}$ (4) kb and no band for CARP4$^{-/-}$.

3.1.4.1 Effect of CARP3 gene deletions and CpdA on protein levels of CARP3$^{+/-}$

Western blotting was performed to confirm presence (WT s427), decrease (CARP3$^{+/-}$) and loss of protein (CARP3$^{-/-}$). The effect of CpdA on protein levels of CARP3$^{+/-}$ was investigated by keeping the cells under pressure with periodic sampling for protein analysis by Western blotting. There was a noticeable reduction in protein levels of CARP3$^{+/-}$ after 6 h and 24 h under CpdA pressure. At 48 h, protein levels have returned to pre-incubation level. WT s427 CARP3

protein levels remained significantly low over the period of incubation (Figure 3.4).

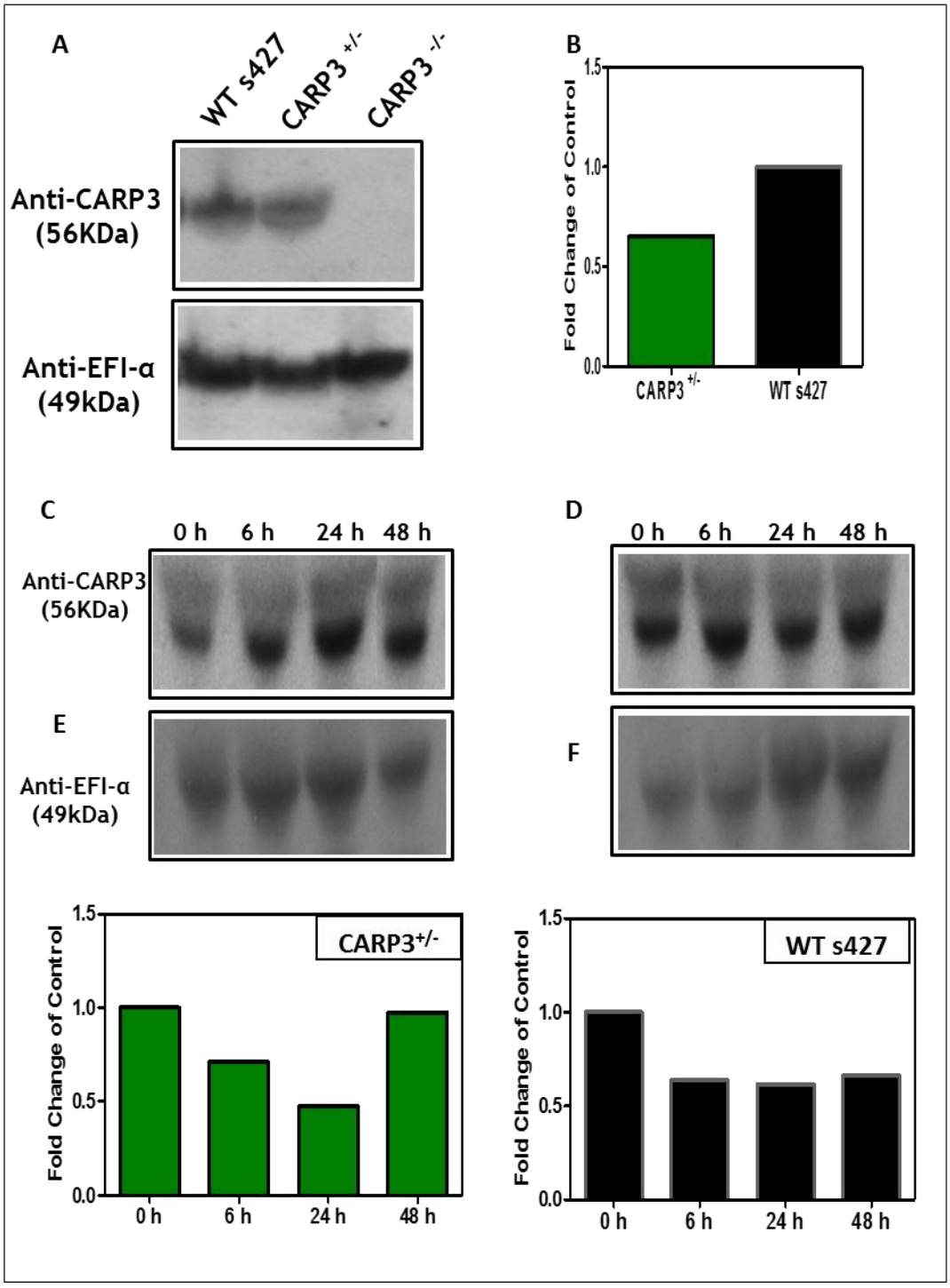

Figure 3.4: Western blot confirmation of CARP3 protein levels in genetically manipulated CARP3 cell lines. A-B) Western blot and image quantification of WT s427, CARP3$^{+/-}$ and CARP3$^{-/-}$. C) Protein levels of CARP3$^{+/-}$ over 48 h. D) CARP3 levels in WT s427 over 48 h. E. quantification of C. F, quantification of panel D. Quantification was normalized to constitutively expressed EFI-α.

3.3.0 Effect of CARP1-4 gene knockouts on CpdA sensitivity

The alamar blue drug sensitivity assay was used to determine the effect of a single CARP gene deletion on CpdA sensitivity. CARP1-4$^{+/-}$, CARP2-4$^{-/-}$ and control WT s427 cells were added to serially diluted wells of CpdA and pentamidine in a 96 well plate. Viable cells after 48 h will convert alamar blue dye to the fluorescent metabolite (convert resazurin to the fluorescent resorufin) which will be measured in a fluorimeter after 24 h incubation. A sigmoid curve of fluorescence intensities gives the EC_{50} value. All 4 single CARP gene deleted cells displayed significantly reduced susceptibility to CpdA. Double gene deleted CARP2-4$^{-/-}$ showed a further reduction in CpdA susceptibility ranging from ~3-fold reduction (CARP3$^{-/-}$ and 4$^{-/-}$) to approximately 17-fold (CARP2$^{-/-}$). Both sKO and dKO Cells of CARP2 and CARP3 also showed a significantly increased susceptibility to pentamidine (Figure 3.5).

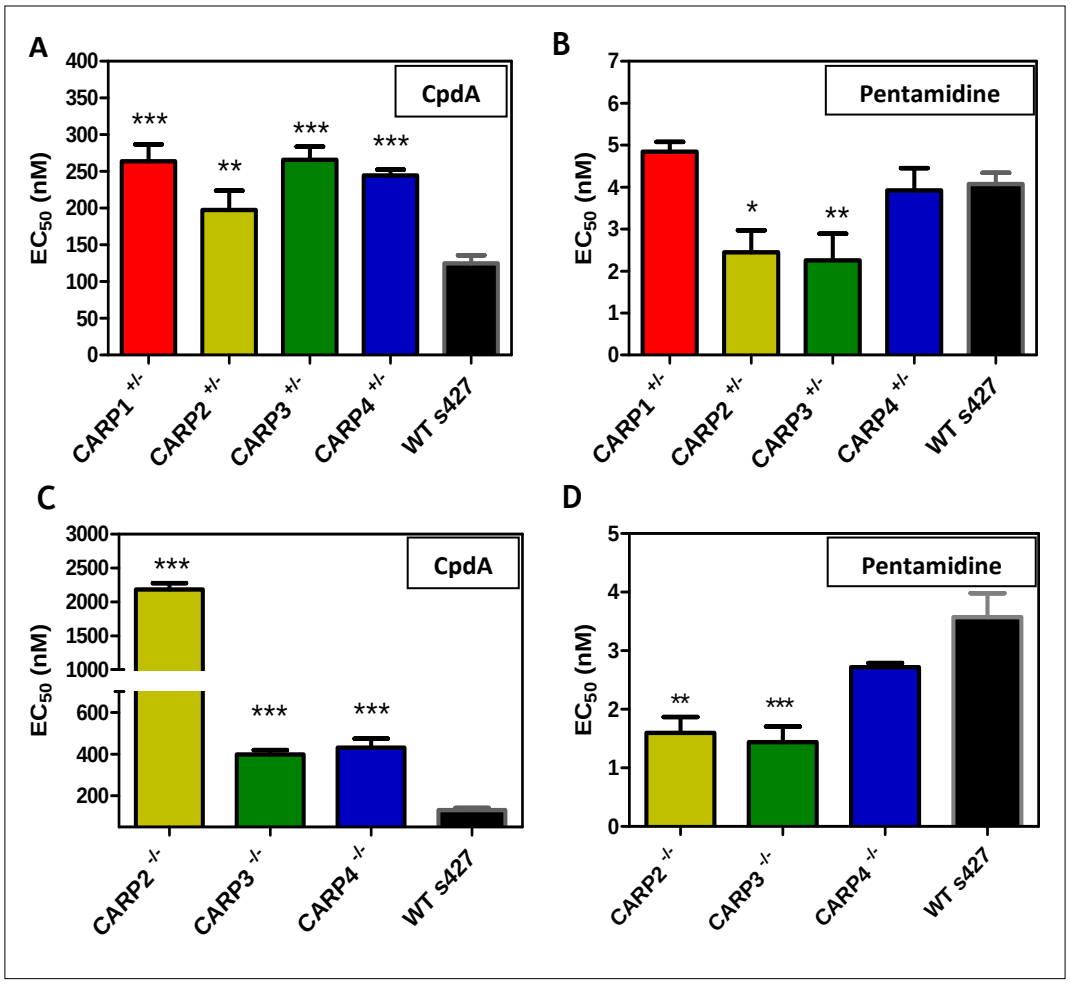

Figure 3.5: Alamar blue drug sensitivity assay of sKO CARP1-4 and dKO CARP2-4 using CpdA and Pentamidine. A) and C) CpdA. B) and D) Pentamidine. Error bars show ± standard error. T-test single-tailed, unpaired (* p>0.05, ** p>0.01, *** p>0.001; n>4).

3.4.0 Effect of CARP1-4 gene deletions on cell proliferation in the presence and absence of CpdA

A cell proliferation assay was used to determine the effect of gene deletion on cell growth compared with WT s427 in a cumulative log phase growth curve with cells continuously grown in the presence or absence of CpdA. Cells were passage back to starting concentrations into fresh media with and without CpdA every 48 h. There were no differences in growth rates of single CARP gene deleted cells compared with WT s427 cells without and with CpdA. Both slopes and intercept were not significantly different nor were the mean cell counts at individual time points. Strains with double gene deletions of CARP3$^{-/-}$ and CARP4$^{-/-}$ followed similar trends as single allele deleted cells with and without CpdA. However, CARP2$^{-/-}$ showed a significant growth delay ($p=0.0201$) resulting in differences in slope and intercept for growth without CpdA. However, growth rates were identical in the presence of CpdA (Figure 3.6).

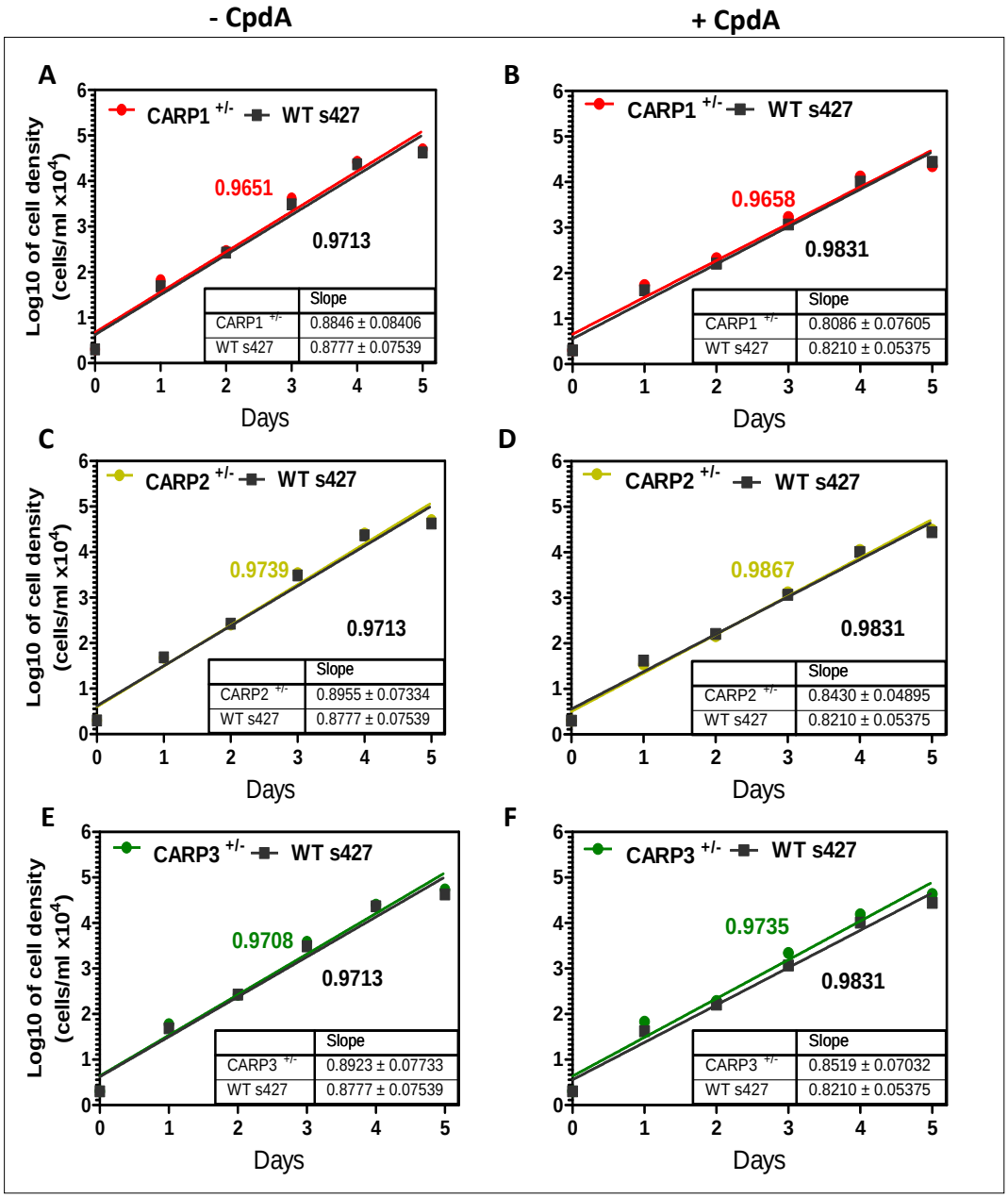
- CpdA
+ CpdA
A
CARP1 +/- WT s427
0.9651
0.9713
Slope
CARP1 +/- 0.8846 ± 0.08406
WT s427 0.8777 ± 0.07539
Log10 of cell density (cells/ml x10^4)
Days
B
CARP1 +/- WT s427
0.9658
0.9831
Slope
CARP1 +/- 0.8086 ± 0.07605
WT s427 0.8210 ± 0.05375
Days
C
CARP2 +/- WT s427
0.9739
0.9713
Slope
CARP2 +/- 0.8955 ± 0.07334
WT s427 0.8777 ± 0.07539
Log10 of cell density (cells/ml x10^4)
Days
D
CARP2 +/- WT s427
0.9867
0.9831
Slope
CARP2 +/- 0.8430 ± 0.04895
WT s427 0.8210 ± 0.05375
Days
E
CARP3 +/- WT s427
0.9708
0.9713
Slope
CARP3 +/- 0.8923 ± 0.07733
WT s427 0.8777 ± 0.07539
Log10 of cell density (cells/ml x10^4)
Days
F
CARP3 +/- WT s427
0.9735
0.9831
Slope
CARP3 +/- 0.8519 ± 0.07032
WT s427 0.8210 ± 0.05375
Days

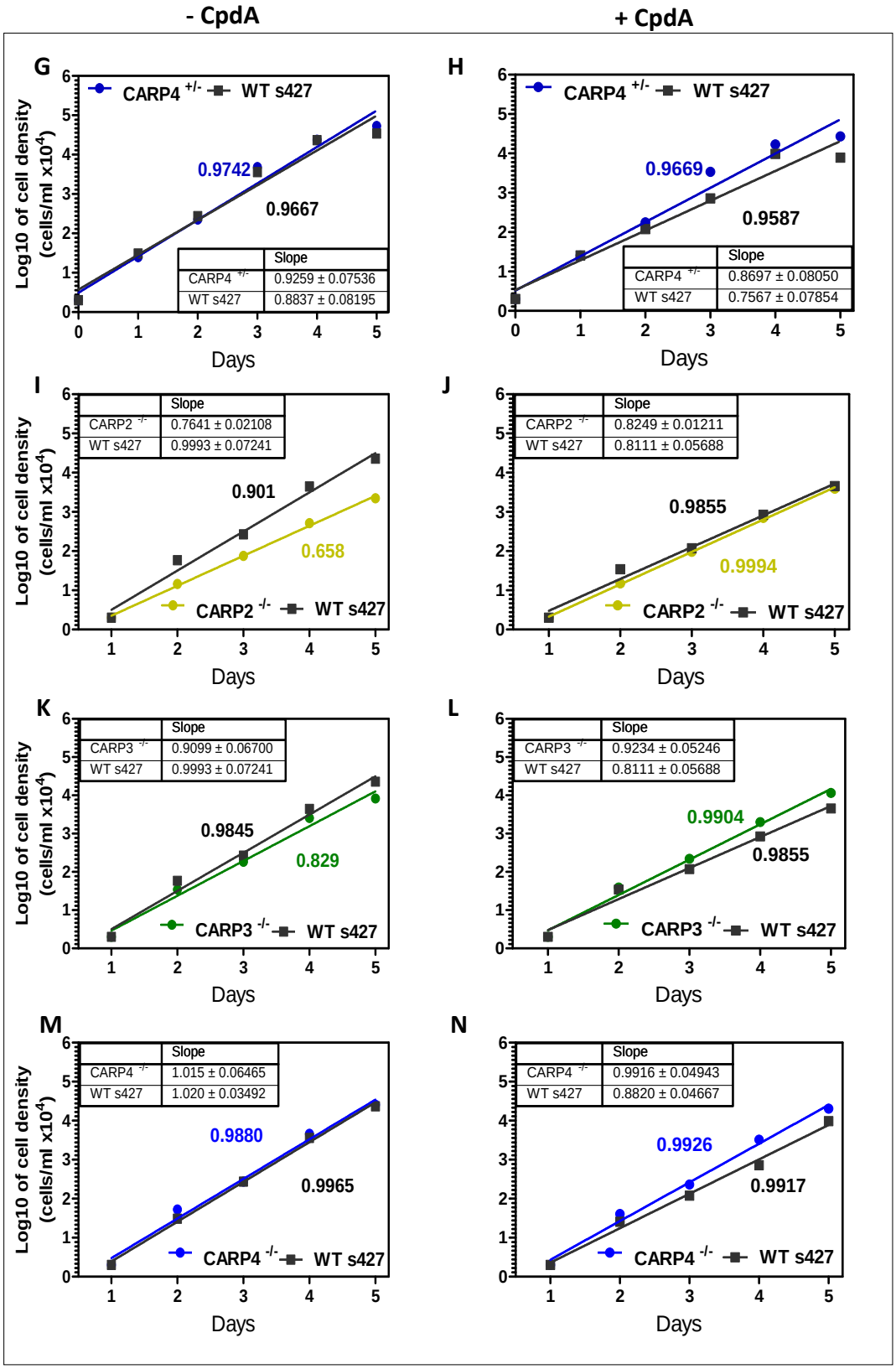

Figure 3.6: Cell proliferation assay of gene deleted CARP cells in the presence and absence of CpdA. Each generated cell and control were seeded (2 x10^4) in duplicates, counted every 24 h and passaged back to seeding concentration without or with same concentration of CpdA every 48 h. A), C), E), G) and K) show cumulative growth of the respective cells without CpdA whilst B), D), H), J) and L) show same cells grown in 100 nM CpdA. Growth curve was repeated independently on 3 occasions. Graph show cumulative average cell counts of all 3 experimental replicates.

3.5.0 Cyclic AMP levels in gene deleted CARP1-4 cells

The effect of gene deletion on cAMP was determined by incubating sKO and dKO CARP cells in 300 nM CpdA for 3 h. Both intracellular and extracellular cAMP levels were measured pre and post incubation in CpdA.

3.5.1 Intracellular cAMP levels in sKO and dKO CARP cells

Single CARP gene deletion did not significantly increase intracellular cAMP levels without and with CpdA compared with WT s427. However, as expected, CpdA inhibiting TbPDEB1 causes a general significant increase in intracellular cAMP levels in both the sKO and WT cells (Figure 3.7A). Double gene deletion in CARP2 however resulted in a significant increase in intracellular cAMP levels both in the absence (~3-fold) and presence of CpdA (~3-fold) in comparison with WT s427 cells. Cyclic AMP levels also significantly increased in dKO CARP3 cells without CpdA (~4-fold) and with CpdA (~2-fold). Cyclic AMP levels only increased slightly (~1.3-fold) in the addition of CpdA to dKO CARP4 cells (Figure 3.7B).

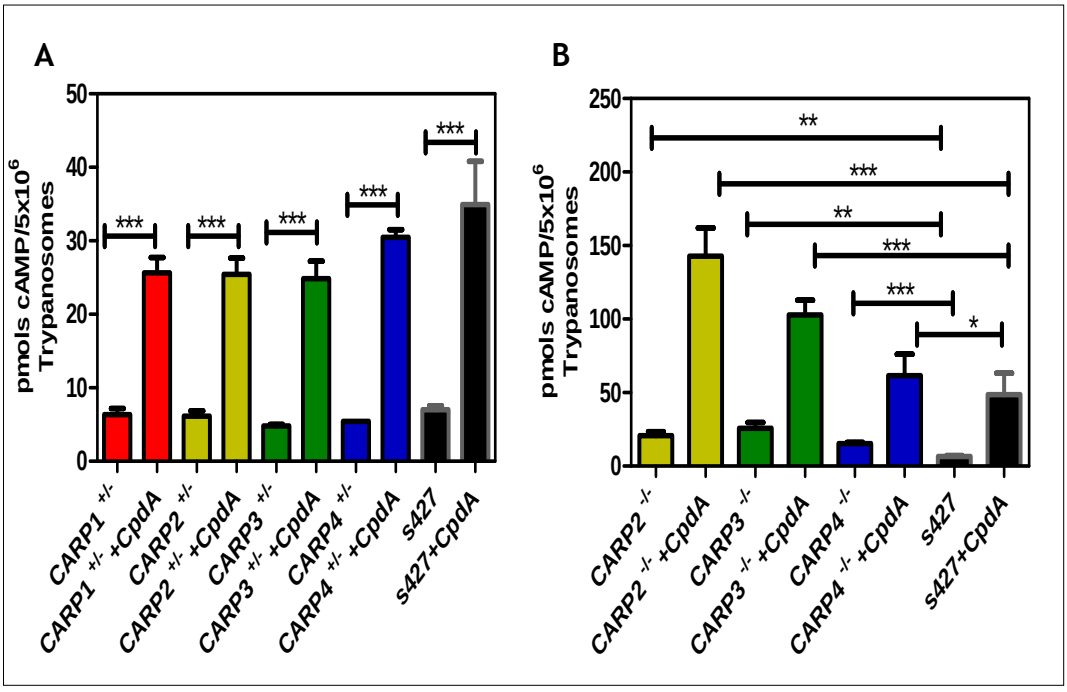

Figure 3.7: Intracellular Cyclic AMP measurements in sKO CARP1-4 and dKO CARP 2-3 cells. Each generated cell and control were divided into 2, either without or with 300 nM and incubated for 3 h. 5 x10^6 from each cell type and control were pelleted and processed for cAMP measurement (ELISA). A) cAMP levels in CARP1-4$^{+/-}$ cells in the absence and presence of CpdA was not different from WT s427. B) cAMP levels in CARP2-4$^{-/-}$ cells in the absence and presence of CpdA was significantly different from Wt s427. Error bars show ± standard error. T-test single-tailed, unpaired (* p>0.05, ** p>0.01, *** p>0.001; n=3-5)

3.5.2 Extracellular cAMP levels in sKO and dKO CARP cells

Extracellular cAMP levels in single gene deleted CARP1-4 cells were similar to WT s427 showing a similar trend as that of intracellular cAMP in the same cell lines. CpdA however increased extracellular cAMP within the same cell lines (Figure 3.8A). Double knockout CARP2-4 cells displayed significantly increased extracellular cAMP relative to the WT control both without (~2.5-fold) and with CpdA (~1.5-fold) (Figure 3.8B).

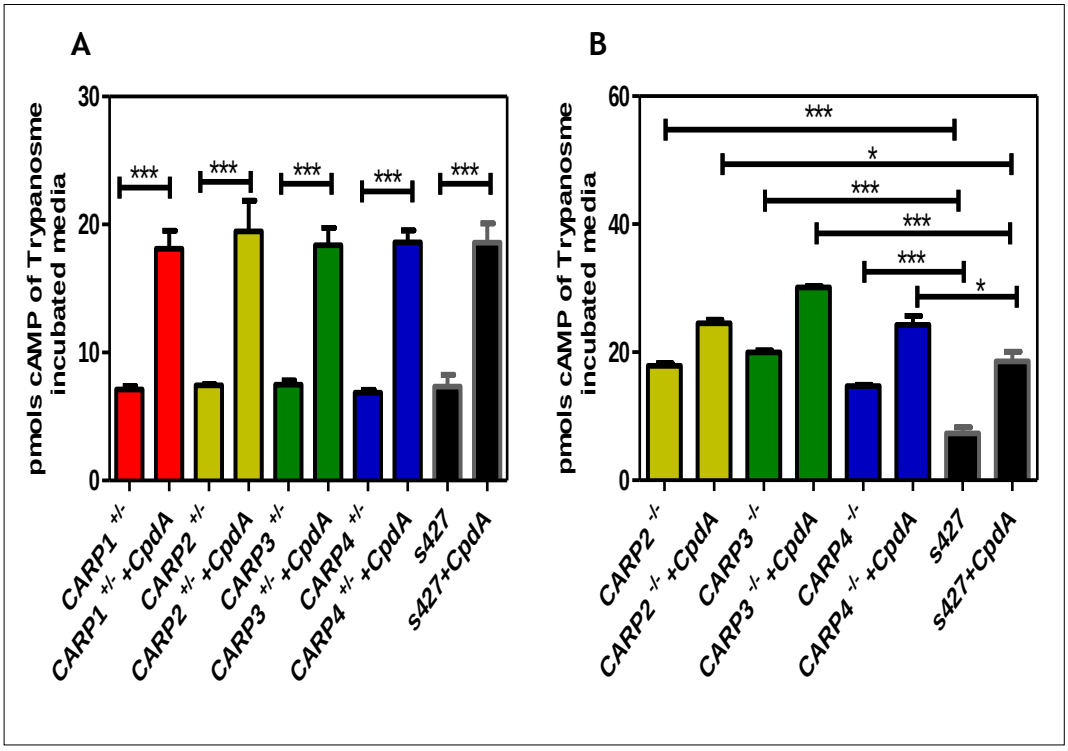

Figure 3.8: Extracellular Cyclic AMP measurements in sKO CARP1-4 and dKO CARP 2-3 cells. Each generated cell and control were divided into 2, either without or with 300 nM and incubated for 3 h. 5 x10^6 from each cell type and control were pelleted and the incubating media used for cAMP measurement (ELISA). A) Single gene deletion of CARP1-4 did not result in any significant differences in cAMP levels without and with CpdA compared with WT s427. CpdA significantly increased cAMP levels within the same cell line. B) Deletion of both allele of CARP2-4 causes significant increases in cAMP levels without and with CpdA when compared to WT s427. Error bars show ± standard error. T-test single-tailed, unpaired (* p>0.05, ** p>0.01, *** p>0.001; n=3-5)

3.6.0 Discussion

The phosphodiesterase inhibitor , CpdA has been reported to have trypanocidal activity in the range of 30-70 nM which is similar in activity to suramin and diminazene, and ≥10-fold more active than nifurtimox with similar potencies against clinical and veterinary resistant cell lines as against wild-type *T. brucei* cell lines (de Koning et al., 2012). CpdA (1 μM) causes a strong increase in intracellular cAMP after 3 h incubation compared with low-potency PDE inhibitors such as dipyridamole (40 μM) and etazolate (100 μM) which did not significantly affect cAMP concentrations. CpdA had an immediate and time and dose dependent effect on cellular cAMP levels although cell lysis and death only occurred after 15 h, even at a concentration of 3 μM (de Koning et al., 2012). Recently, a genome-scale RNAi library screen of resistance to CpdA revealed four distinct genes that were knocked down. These genes were designated cAMP Response Protein (CARP) 1-4. RNAi against CARP1-4 resulted in significant increases in resistance to CpdA but no cross resistance to other trypanocides (Gould et al., 2013). Thus CARP1-4 represents the first downstream effectors of cAMP signalling in *T. Brucei*. However, there was the further need to understand how these effectors act to bring about cellular regulation such as control of cAMP levels and the phenotype of cytokinesis inhibition. The question as to whether these effectors act individually or as a complex, and whether there is a "single" most important effector is very important in the understanding of the parasite's cell biology and the answers may provide trypanosome- specific cAMP-dependent therapeutic targets.

Results of drug sensitivity of CpdA on sKO CARP1-4 confirmed both the CARPs as well as the RNAi knockdown observed previously. RNAi knockdown and single gene deletion did not affect normal cell growth. The sequential increase in resistance to CpdA in the dKO CARP2-3 further showed the importance of these proteins as downstream effectors of cAMP signalling. The inability to delete both genes of CARP1 likely indicates that this protein is essential in bloodstream forms. CARP1 codes for a 705-amino-acid protein containing two apparently intact and one partial cyclic AMP binding domains that are conserved in synteny in each of the kinetoplastid genomes sequenced. Recently, it has been shown that the orthologue of CARP1 in *T. cruzi* TcCLB.508523.80 binds to cyclic

nucleotides, using cAMP and cGMP displacement assays (Jäger et al., 2014) further validating the role of CARP1 as a downstream cAMP signalling effector. Thus it is expected that cAMP produced from CpdA inhibition of TbPDEB1 will mostly likely firstly bind to CARP1 after which it will cascade down the signalling pathway. Thus the absence of CARP1 will results in an important break point in the signalling pathway and, judging by the inability to create a double knockout, seems to result in cell death.

The significant increase in both intracellular and extracellular basal and CpdA-induced cAMP levels of the dKO cells demonstrates the effect these proteins have on cAMP levels in the cells. The increase in cAMP shows that the proteins are important in direct regulation since their absence could result in increased accumulation of cAMP within the cell, compensating for the lack of effectors to transmit the cAMP signal. The cells similarly extrude more cAMP at a higher production level, to maintain physiological balance which is likely to be ATP-dependent similar to what occurs in mammals.

Single gene deletion of CARPs did not affect the growth rate of trypanosomes in standard culture. Similarly, cell proliferation of single KO CARP1-4 cells in continuous culture with CpdA 100 nM (2/3 EC_{50}) of WT s427 was unaffected. This was expected since gene knockout significantly increased resistance to CpdA in sKO cells compared with WT s427. However, dKO CARP2 showed a significant delay in growth in the absence of CpdA an observation similar to that seen in the CpdA-resistance cell line R0.8. Thus the growth phenotype might be linked to the significant increase in resistance to CpdA (17-fold). Additionally, CARP2 is annotated as a conserved protein detected in the flagellar proteome, implying a possible flagellar function. The flagellum has increasingly been shown to have important roles in determining cell shape, size as well as the fact that the regulation of its formation governs the morphological transitions that define *T. brucei* development (Langousis and Hill, 2014). Additionally, the role and importance of cAMP in flagellar motility and signalling is increasingly being dissected with interesting findings. For example it is commonly believed that the flagellum, as an important host-parasite interface, plays essential sensory functions (Rotureau et al., 2009; Tetley and Vickerman, 1985). For example in *C. reinhardtii*, triggering of zygote formation is initiated by a cAMP signalling

response, as a result of flagellum adhesion in gametes (Pan and Snell, 2000). Recently, it has been shown (either by increasing cAMP through the inhibiting TbPDEB1 or using CpdA) that cAMP regulates social motility in *T. brucei* (Oberholzer et al., 2015). This is similar to social motility observations in *Dictyostelium discoideum* where cAMP signalling is critical for surface motility (Firtel and Meili, 2000). Thus it is possible that CARP2 plays a very important role in regulating flagellar activity which in turn then affects cell survival hence the delayed defect in growth observed.

Double gene deleted CARP3 showed a minimal growth delay whilst dKO CARP4 also grew similar to WT s427. CARP3 and CARP4 dKO cell lines however, showed slightly better growth in CpdA whilst growth of dKO CARP2 was similar to WT s427. CpdA causes significant decrease in protein levels of CARP3$^{+/-}$ and in WT s427 cells. As significant reductions in mRNA levels of CARP3, using RNAi, has previously identified CARP3 as one of downstream effectors of cAMP (de Koning et al., 2012), it is not unexpected that WT s427 trypanosomes reduce the levels of this protein to minimise cAMP signal transmission in the presence of CpdA. We interpret the observations that CARP3 may directly influence cAMP production in trypanosomes, as well as mediate (part of) the signal transduction from cAMP to the ultimate cellular effect, as CARP3 having a regulatory role in modulating the (effects of) this signalling cascade. This is further explored in the chapters below.

Chapter 4

Over-expression of CARP1-4 and TbPDEB1 genes and its effects on CpdA sensitivity, cell proliferation, cAMP levels and localization

4.0 Over-expression of CARP1-4 and TbPDEB1 genes and its effects on CpdA sensitivity, cell proliferation, cAMP levels and localization.

RNAi Knockdown of the CARPs resulted in reduced susceptibility to CpdA (Gould et al., 2013) confirming their role as downstream effectors of cAMP. This raised the question of the possibility of a reverse effect when these proteins are overexpressed. This will allow a correlation of mRNA and/or protein levels to any observable phenotype seen when the overexpressing cells were challenged with CpdA in comparison with WT s427. Finally, to relate function to location, immunofluorescence was performed on tagged and untagged overexpressing CARP1-3 genes expressed in WT s427 *T. brucei* cells.

WT s427 and CpdA resistant (R0.8) cells were transfected with overexpressing constructs of CARP1-4 and TbPDEB1 to overexpress the desired genes. Three colonies each were selected after transfection, confirmed by PCR and assayed for mRNA expression. One out of the three was then selected for further downstream assays such as drug sensitivity, growth curves, mRNA and protein level expressions etc. Three of the proteins were N-terminally GFP-tagged and transfected into an inducible cell line for IFA. Anti-CARP3 antibody was also used for immuno-fluorescence of CARP3^{oe}.

4.1.1 PCR evidence of plasmid integration of CARP1-4 and TbPDEB1 in WT s427 and R0.8 cells

PCR was performed on both transfected clones of WT s427 and R0.8 using primers binding to a region on the plasmid pre-start MB0274 (5′-TTGAAGACTTCAATTACACC-3′) codon of the ORF of each gene and the middle of the blasticidin resistant gene HDK0035 (5′-ATGCAGATCGAGAAGCACCT-3′) in pHD1336. Similar PCR was performed for pRPa^{GFP} transfected lines using primers binding to the pre-start codon of the N-terminal GFP MB0274 (5′-TTGAAGACTTCAATTACACC-3′) and the middle of the *T. brucei* aldolase mRNA processing 3′, MB0302 (5′-TAACCAACCTGCAGGCG-3′). The results showed presence of plasmid (indicated by gene sizes plus additional bases into the

resistant gene) in transfected overexpressing and tagged cell lines which are not present in the control cell lines of WT s427 and R0.8 (Figure 4.1).

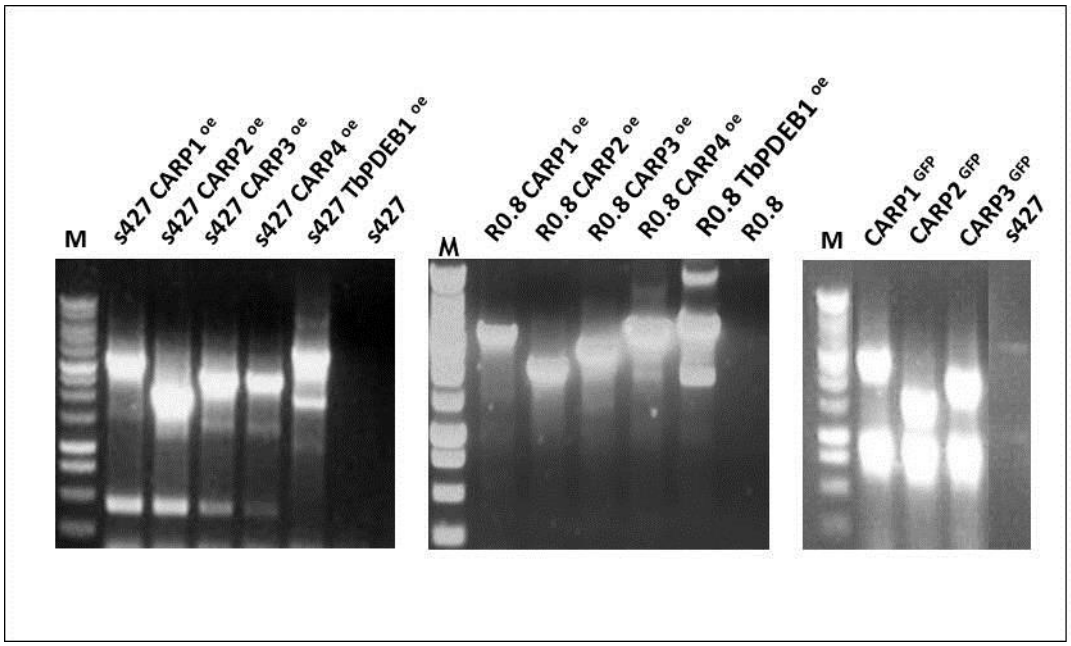

Figure 4.1: PCR confirmation of plasmid integration into genome of CARP1-4 and TbPDEB1 of WT s427 and CpdA resistant (R0.8) cells as well as N-terminal GFP tagged into 2TI cells. A-B) PCR was performed using plasmid primer flanking the start codon of the respective ORFs and the reverse of blasticidin antibiotic cassette for both WT s427 and R0.8. Band sizes correspond to sizes of the respective genes plus plasmid regions and indicative of plasmid (pHD1336) integration. None transfected WT s427 and R0.8 have no bands. C) PCR was performed as described in A and B but using reverse of hygromycin which is the resistant cassette in the pRPa plasmid. Upper band sizes correspond to respective gene sizes and lower bands are GFP amplification.

4.1.2 Increased Messenger RNA expression of CARP1-4 and TbPDEB1 in WT s427 and R0.8 cells

To verify that the CARPs and TbPDEB1 genes were being overexpressed above wild type levels (WT s427 and R0.8), primers were designed and qRT-PCR performed to determine expression levels normalized to the constitutively expressed internal control (GPI8). In both transfected WT s427 CARP1-4 and TbPDEB1 as well as R0.8 CARP1-4 and TbPDEB1, the genes showed significant fold increases in mRNA levels. In WT s427 cells overexpressing CARPs, CARP2 and CARP4 showed almost 2.5-fold increase expression above wild type levels. CARP3 was the highest expressed CARP in R0.8 (~4-fold) greater than base level expression. TbPDEB1 was ~3-fold and ~7-fold overexpressed above WT s427 and R0.8 levels (Figure 4.2).

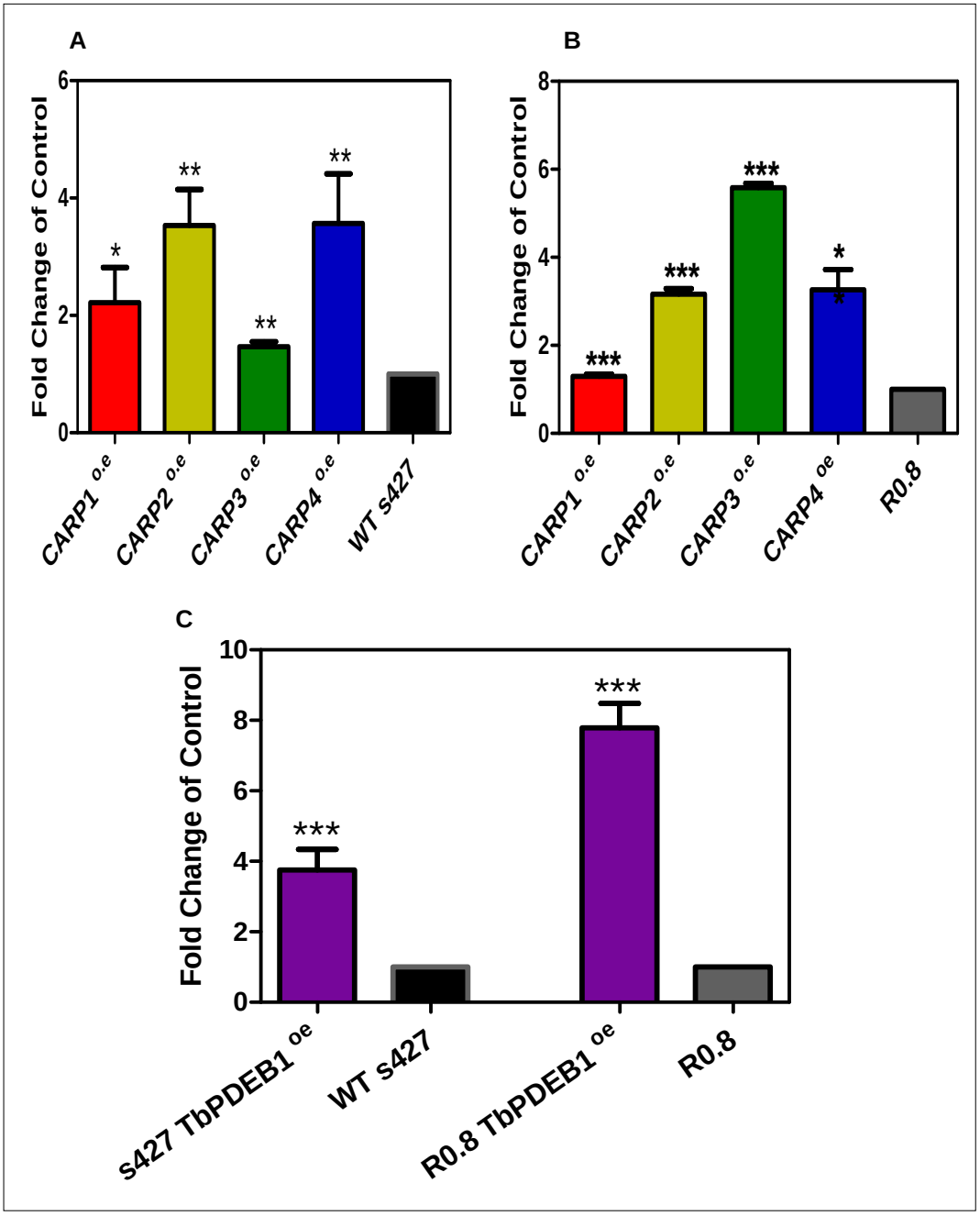

Figure 4.2: Quantitative RT-PCR confirmation of CARP1-4 and TbPDEB1 overexpression in WT s427 and R0.8 cells. RNA was extracted from log phase overexpressing CARP cells, reverse transcribed into cDNA and used for qRT-PCR. A) s427CARP1-4^{oe} against WT s427. B) R0.8 CARP1-4^{oe} against R0.8. C) WT s427 TbPDEB1^{oe} and R0.8 TbPDEB1^{oe} against WT s427 and R0.8 respectively. Expression levels of genes in both genetically manipulated cells and wild type/R0.8 strains were normalized to an internal control (GPI8). All CARPs and TbPDEB1 were overexpressed in both WT s427 and R0.8. Error bars show ± standard error. T-test single-tailed, unpaired (* p>0.05, ** p>0.01, *** p>0.001; n=3-6)

4.1.3 Increased level of CARP3 Protein in overexpressing cells in WT s427 and R0.8 cells

Western blotting was performed using the available anti-CARP3 antibody on CARP3^{oe} cells. Results (normalized to the loading control, EFI- α) showed a noticeable increase in CARP3 protein levels in both the WT s427 and the CpdA-resistant strain R0.8 overexpressing CARP3 compared with WT s427 and R0.8 controls confirming mRNA expression data as well as the effectiveness of pHD1336 as an overexpressing plasmid (Figure 4.3). However, it must be noted that the level of overexpression in the WT cells was relatively low, especially as this vector is known for a robust overexpression level (Biebinger et al., 1997). This appears to indicate that a much higher level of CARP3 is deleterious to the cell, and/or that CARP3 expression is under tight control. The protein overexpression levels in the WT and R0.8 strains appear to follow the observed mRNA levels (Figure 4.2) closely.

4.2.0 Effect of CpdA on transcript (mRNA) and protein levels of generated lines

To investigate how CpdA affects the increased levels of CARP genes and TbPDEB1, overexpressing cells were cultured in 100 nM and 3 μM CpdA for WT s427 and R0.8 respectively. Cells were separated for mRNA extraction, cDNA generation and qRT-PCR analysis at specific time points. For CARP3^{oe} cells, protein was extracted at the same time points for Western blotting analysis.

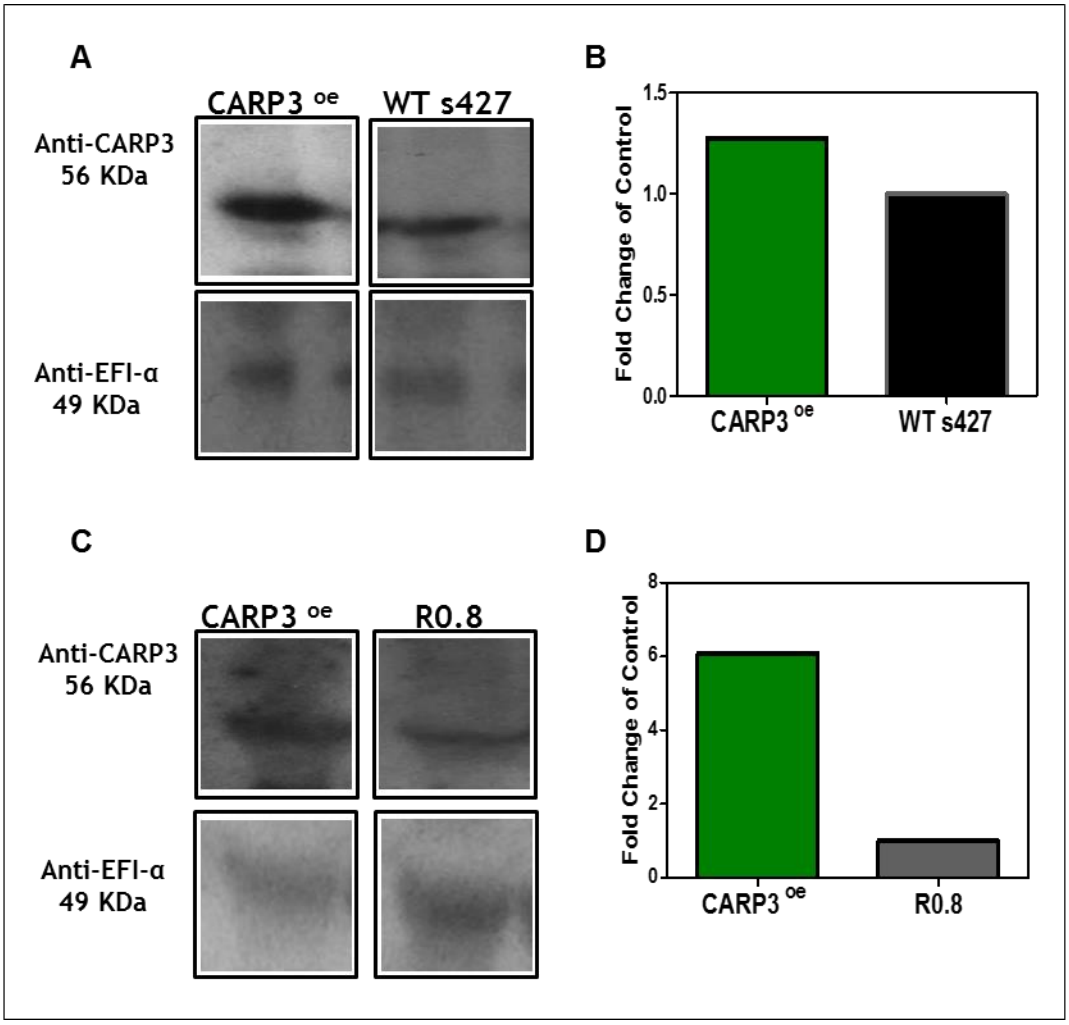

Figure 4.3: Western blotting and image quantification of CARP3 protein levels in WT s427 and R0.8 cells. Western blotting A) and image quantification B) of s427 CARP3^{oe} and WT s427. Western blotting C) and image quantification D) of R0.8 CARP3^{oe} and R0.8. Image quantification based on band intensity was performed with LiCOR software with images normalized to EFI- α (loading control). Band intensities indicate a noticeable difference in CARP3 protein expression in both WT s427 CARP3^{oe} and R0.8 CARP3^{oe} compared with WT s427 and R0.8 respectively.

4.2.1 CpdA effect on transcript levels of CARP1-4 and TbPDEB1 overexpressing cells in WT s427 and R0.8

The effect of CpdA on gene expression of CARP1-4 and TbPDEB1 was investigated using qRT-PCR of cDNA generated from cells incubated in CpdA for 6 h, 24 h and 48 h. 100 nM of CpdA was used for genes overexpressing in s427 whilst 3 μM of CpdA was used for genes in R0.8 cells. Expression levels were normalized to levels without CpdA incubation (0 h).

CpdA (100 nM) significantly reduced expression of genes of CARP1-4 in WT s427 cells overexpressing these genes after 6 h incubation and these levels remained significantly decreased at 48 h in the same concentration of CpdA and below WT s427 level. Variable changes occur when the same genes were assayed in just the WT s427 under the same condition: only CARP2 and CARP3 levels of mRNA in WT s427 decreased significantly below that seen before addition of CpdA over the period of incubation. There were no changes in mRNA levels in CARP4 whilst after an initial 6 h decrease in CARP1 the levels returned to that of pre-incubation with CpdA at 24 h and 48 h (Figure 4.4). The effect of CpdA on PDEB expression is depicted in Figure 4.6. It shows that the overexpression of TbPDEB1 in WT cells is also reversed by CpdA treatment, up to 48 h, whereas in the untransformed controls, expression was only reduced at the 6-h point.

In R0.8 CARP1-4 and TbPDEB1 overexpressing cell lines, the trend was reversed except in CARP3 and TbPDEB1. Overexpressing CARP1, CARP2 and CARP4 in R0.8, resulted in increases in their mRNA levels after incubation in 3 μM CpdA from 6-48 h. However, levels of CARP3 and TbPDEB1 decreased significantly after 6 h in CpdA and remained steadily below non-overexpressing R0.8 levels over the incubation period. Messenger RNA levels of CARP3 in non-overexpressing R0.8 cells remained unchanged in the presence of CpdA whereas that of CARP1, CARP2, CARP4 and TbPDEB1 increased significantly after 6 h in CpdA, remaining steadily high at 48 h except TbPDEB1 which dropped significantly after 48 h (Figure 4.5).

TbPDEB1 levels decreased significantly in both WT s427 and R0.8 overexpressing cells after 6 h in CpdA and remained at that level 48 h after incubation. Non-transfected WT s427 levels of TbPDEB1 dropped significant 6 h after incubation but returned to pre-incubation levels from 24-48 h in CpdA whilst TbPDBE1 in R0.8 cells increased significantly from 6 h and at 48 h remains at levels higher than pre-incubation in CpdA (Figure 4.6).

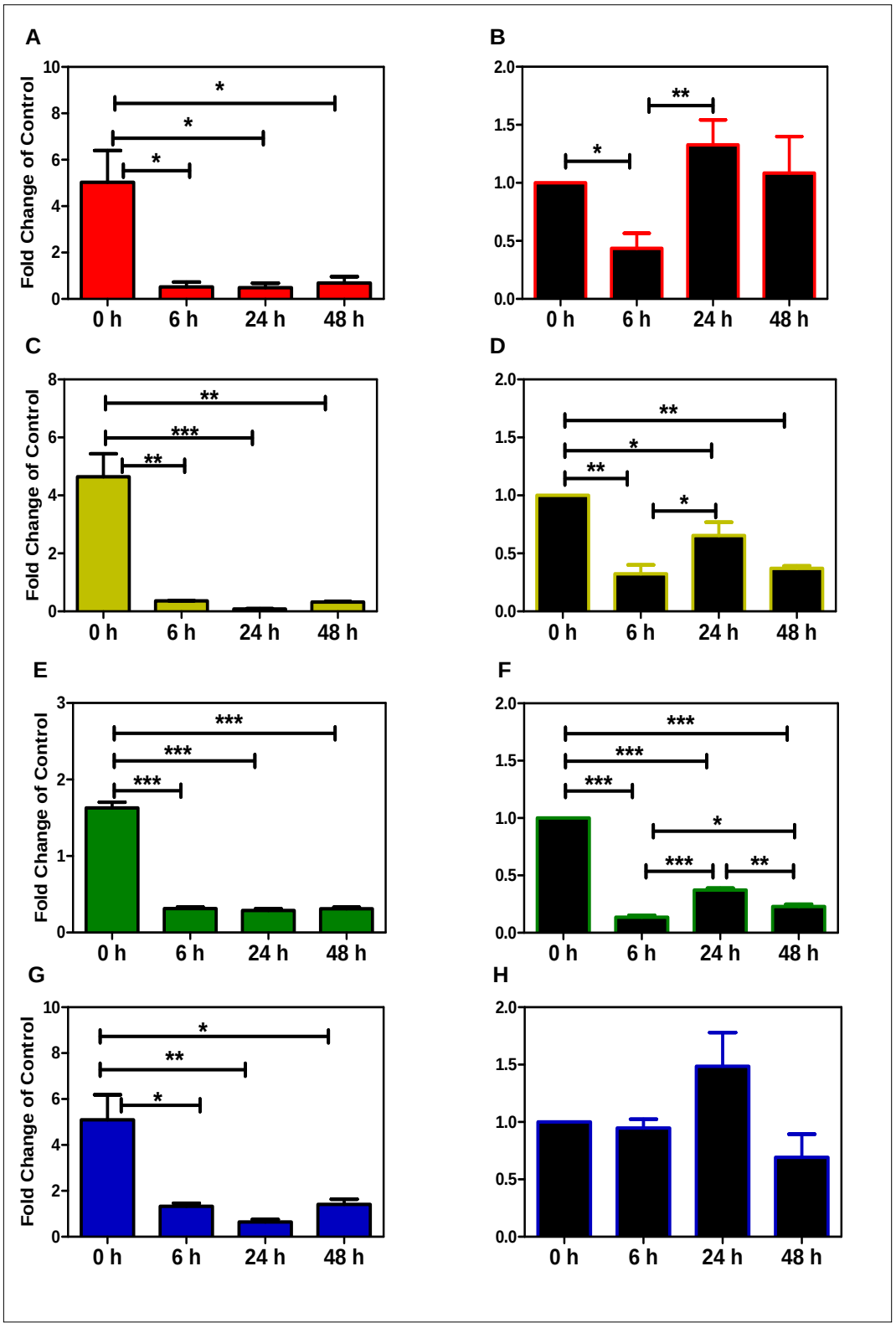

Figure 4.4: Quantitative RT-PCR of WT s427 overexpressing CARP1-4 and CARP1-4 expression in WT s427 in 100 nM CpdA at 0 h, 6-48 h of incubation. RNA was extracted from each single gene deleted CARP cell line under each condition, reverse transcribed into cDNA and used for qRT-PCR. CARP1-4^{oe} in WT s427 A), C), E) and G). Expression of CARP1-4: B), D) F) and H) in non-transfected WT s427. All overexpressed cell lines showed significant decrease in mRNA levels in CpdA from 6-48 h. Error bars show ± standard error. ANOVA, Tukey's Multiple Comparison Test, (* p>0.05, ** p>0.01, *** p>0.001; n=3).

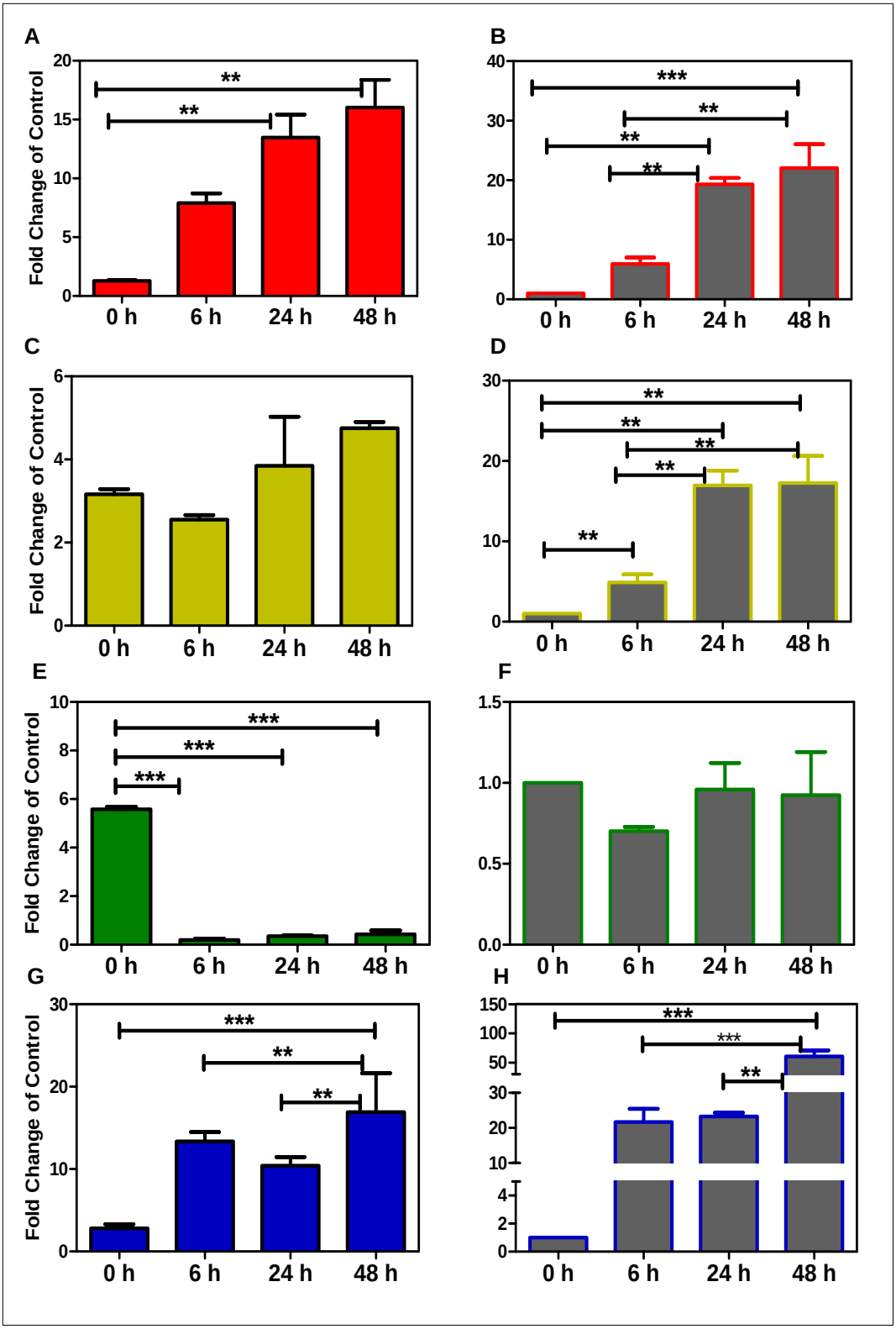

Figure 4.5: Quantitative RT-PCR of R0.8 overexpression CARP1-4 and CARP1-4 expression in R0.8 in 3 µM CpdA at 0 h, 6-48 h of incubation. RNA was extracted from each single gene deleted CARP cell line under each condition, reverse transcribed into cDNA and used for qRT-PCR. CARP1-4^{oe} in R0.8: A), C), E) and G). Expression of CARP1-4: B), D) F) and H) in non-transfected WT s427. Only cells overexpressing CARP3 showed decrease mRNA levels under CpdA pressure whilst CARP3 levels in untransfected R0.8 remains largely unchanged over incubation period. Error bars show ± standard error. ANOVA, Tukey's Multiple Comparison Test (* p>0.05, ** p>0.01, *** p>0.001; n=3).

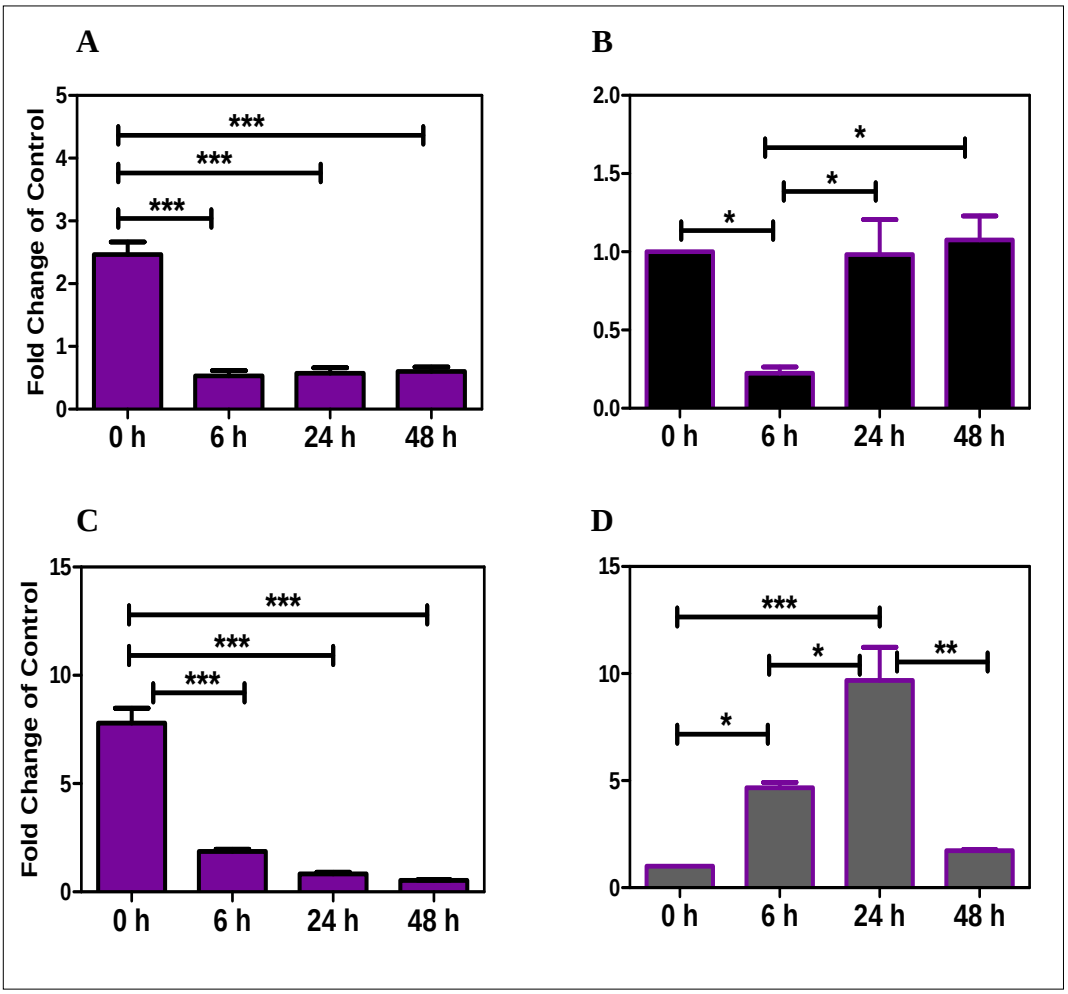

Figure 4.6: Quantitative RT-PCR of TbPDEB1 overexpression and TbPDEB1 expressions in WT s427 and R0.8 in 100 nM and 3 µM CpdA 0 h, 6-48 h of incubation. Overexpressing TbPDEB1 in WT s427 A), and TbPDEB1 expression in untransfected WT s427. B). Overexpressing TbPDEB1 C) in R0.8 and TbPDEB1 expression D) in untransfected R0.8. Error bars show ± standard error. Both WT s427 and R0.8 overexpressing TbPDEB1 showed decreased mRNA levels in CpdA. ANOVA, Tukey's Multiple Comparison Test (* p>0.05, ** p>0.01, *** p>0.001; n=3)

4.2.2 Effect of CpdA on Protein levels of CARP3^{oe} in WT s427 and R0.8.

Using the commercially manufactured antibody to CARP3, an attempt was made to correlate mRNA levels of CARP3 overexpression WT s427 and R0.8 to that of protein levels in the same cells under the same drug concentrations and incubation period. Cells were prepared as already described and proteins separated on a gel and Westerns performed using WT s427 and R0.8 as cell control cells and Elongation Factor 1-α (EF1-α) as loading control.

There was a noticeable decrease in protein levels of CARP3 when overexpressed in both WT s427 and R0.8 over the incubation period correlating directly with the observed decrease in mRNA levels observed from the qRT-PCR. The trend in the controls of WT s427 and R0.8 were also similar to that of the mRNA quantification showing a decrease in protein levels over the incubation period in WT s427 but a relatively unchanged protein level in R0.8 (Figure 4.7).

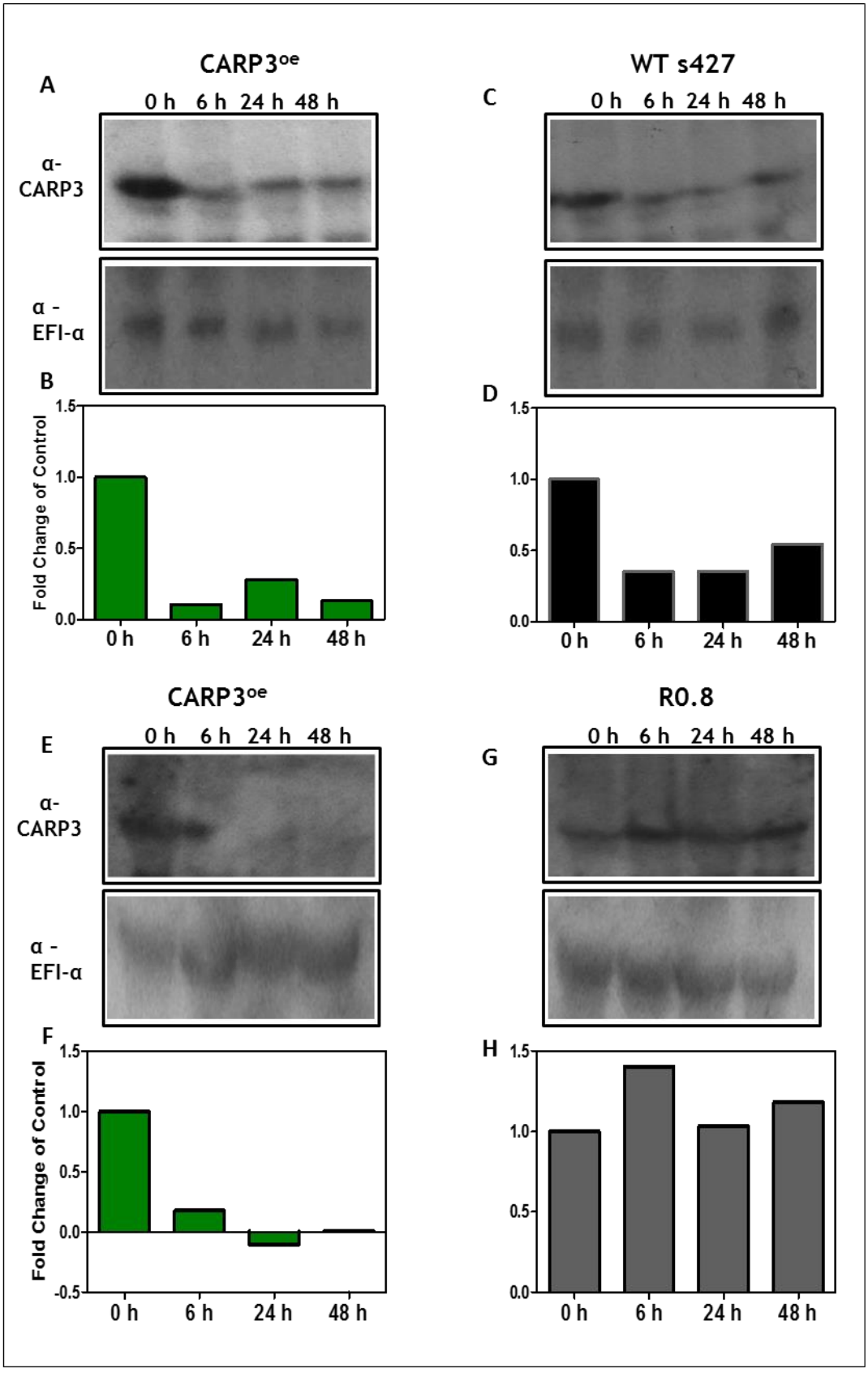

Figure 4.7: Western blotting and image quantification of CARP3 protein levels in WT s427 and R0.8 cells overexpressing CARP3 and non-transfected control WT s427 and R0.8 cells. A) Western blots and B) image quantification data of s427 CARP3^{oe}. C) Western blots and D) image quantification data of CARP3 in WT s427. E) Western blots and F) image quantification data of R0.8 CARP3^{oe}. G) Western blots and H) image quantification data of CARP3 in R0.8. CpdA causes a noticeable decrease in CARP3 levels in overexpressing both WT s427 and R0.8 cells

4.3.0 Effect of CARP1-4 and TbPDEB1 overexpression in WT s427 and R0.8 cells on CpdA sensitivity

The effect of increased gene expression of the CARPs and TbPDEB1 on CpdA sensitivity was analysed using the Alamar blue drug sensitivity assay with pentamidine as a control for s427 CARP1-4^{oe}, TbPDEB1^{oe} and WT s427 and R0.8 CARP1-4^{oe}, TbPDEB1^{oe} and R0.8 respectively. Results showed a significant increase in sensitivity of s427CARP3^{oe} to 100 nM CpdA compared with WT s427. A similar trend was observed when CARP3 was overexpressed in R0.8. There were no differences in sensitivity to pentamidine except in s427CARP4^{oe} which showed a slight but significant decrease in susceptibility to pentamidine (Figure 4.8).

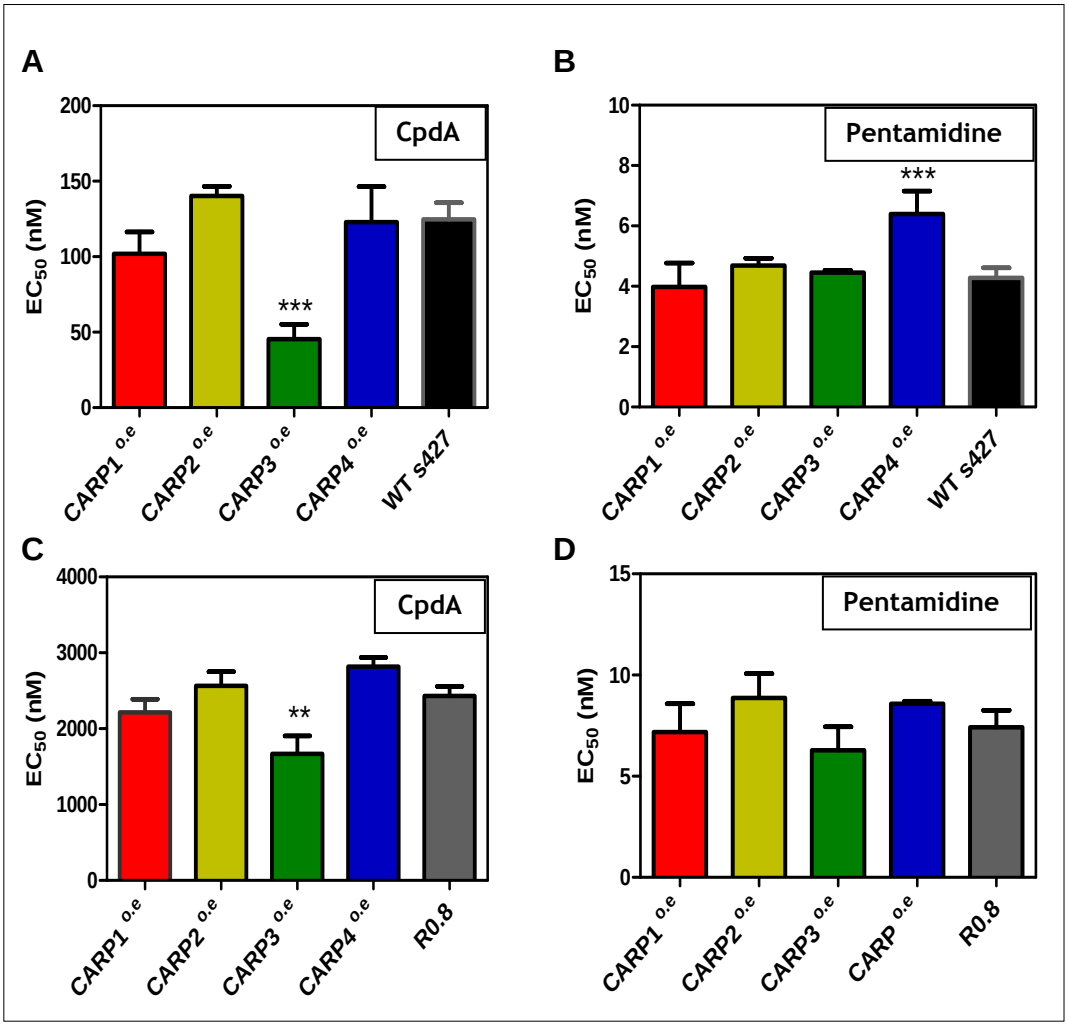

Figure 4.8 Alamar blue drug sensitivity assay of overexpressing CARP1-4 and TbPDEB1 in WT s427 and R0.8 cells. A) WT s427 CARP1-4^{oe} and WT s427 in CpdA. B) WT s427 CARP1-4^{oe} and WT s427 in Pentamidine. C) R0.8 CARP1-4^{oe} and R0.8 in CpdA. D) R0.8 CARP1-4^{oe} and R0.8 in Pentamidine. Overexpressing CARP3 sensitizes both WT s427 and R0.8 cells to CpdA. Error bars show ± standard error. T-test single-tailed, unpaired (* p>0.05, ** p>0.01, *** p>0.001; n>3).

As expected overexpressing TbPDEB1 leads to a significant decrease in sensitivity to CpdA in both WT s427 and R0.8. There were no significant differences in sensitivity to pentamidine (Figure 4.9).

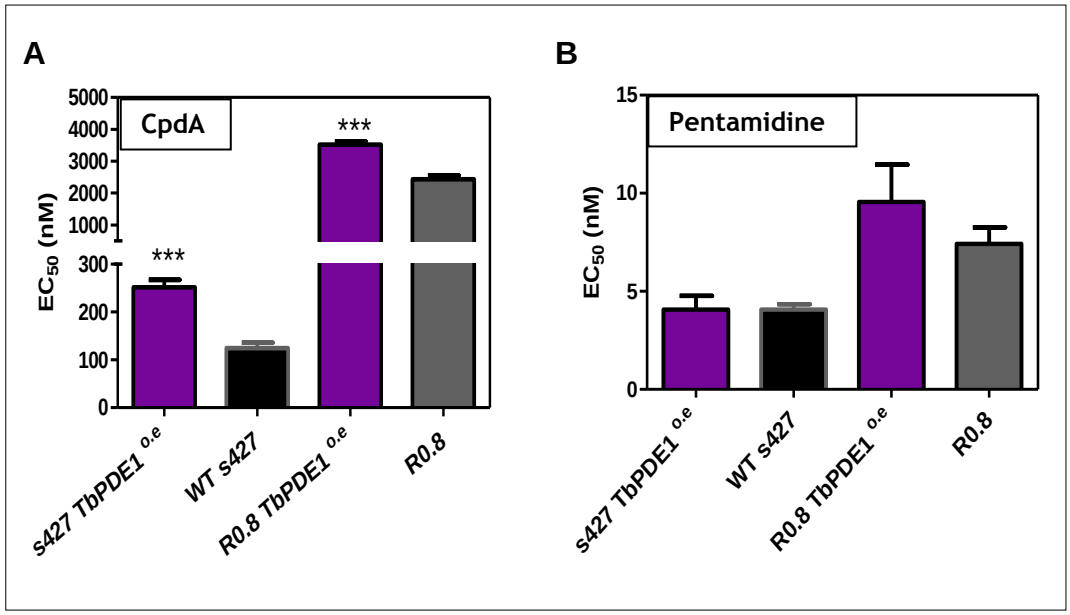

Figure 4.9: Alamar blue drug sensitivity assay of overexpressing TbPDEB1 in WT s427 and R0.8 cells. A) WT s427 TbPDEB1^{oe}, WT s427, R0.8 TbPDEB1^{oe} and R0.8 in CpdA. B) WT s427 TbPDEB1^{oe}, WT s427, R0.8 TbPDEB1^{oe} and R0.8 in Pentamidine. Overexpressing TbPDEB1 significantly leads to significant increase in resistance to CpdA in both WT s427 and R0.8. Error bars show ± standard error. T-test single-tailed, unpaired (* p>0.05, ** p>0.01, *** p>0.001; n>3).

4.4.0 Effect of CARP1-4 and TbPDEB1 overexpression in WT s427 and R0.8 cells on cell proliferation in the presence of CpdA.

The possibility of overexpression of CARP1-4 and TbPDEB1 genes in WT and R0.8 affecting the growth rate of *T. brucei* was determined using a growth curve in the presence and absence of CpdA. In a cumulative growth culture, cells were repeatedly passaged back to starting concentrations in order to allow growth over 6 days. Cells were seeded in duplicates and the experiment was repeated on three independent occasions.

In the absence of CpdA, overexpressing of CARP1-4 in WT s427 did not cause any growth phenotype when compared with the control strain over the period of the growth curve assay (Figure 4.10). Similarly, whereas 100 nM CpdA did not affect the growth of WT s427 cells overexpressing CARP1, 2 and 4 compared with growth of control under similar condition, number of cells overexpressing CARP3 in media with 100 nM CpdA was consistently lower than that of WT s427 cells over the growth period (Figure 4.10F). A similar growth pattern was observed when CARP1-4 was overexpressed in R0.8 (Figure 4.11). Here just as in WT s427, overexpressing of CARP3 only in the presence of CpdA (3 µM), caused a growth delay (Figure 4.11F) whereas none of the other CARPs showed any growth differences either in the absence of in the presence of (3 µM) CpdA.

To further verify the observed growth phenotype when CARP3 is overexpressed in both WT s427 and R0.8 strains, the experiment was repeated for CARP1 and CARP3 overexpressing cells in WT s427 and R0.8 with their respective controls. Only this time the cells were retained in a single growth media without passage into fresh media over the period of the growth curve.

Whereas none of the overexpressing cells showed any growth phenotypes in the absence of CpdA similar to the observation in the continuous growth culture previously described, growing s427 CARP3^{oe} in a single growth curve causes a much more pronounced growth delay (Figure 4.12F) compared with its control and growth in the continuous passaged culture (Figure 4.10F) in the presence of

100 nm CpdA. Overexpressed s427 CARP1 also showed a slightly delayed growth effect in 100 nM CpdA (Figure 4.12B) compared with growth in the continuous passaged culture (Figure 4.10B). The presence of 3 µM CpdA did not affect the growth of R0.8 cells overexpressing CARP1 and CARP3.

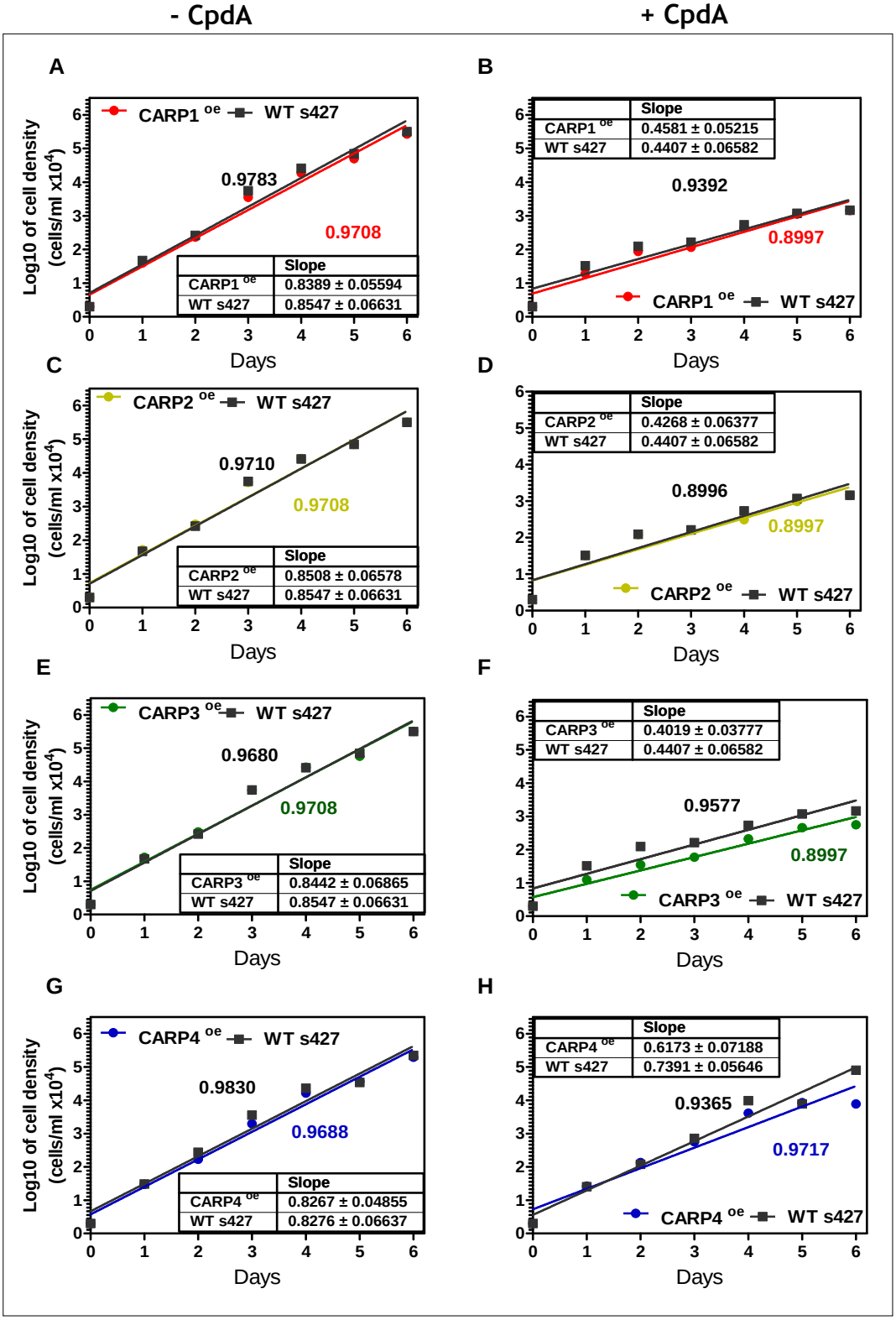

Figure 4.10: Cumulative cell proliferation assay of WT s427 cells overexpressing CARP1-4. A), C), E), and F) growth in the absence of CpdA. B), D), F) and H) growth in the presence of 100 nM CpdA. Cells were seeded in duplicates and the experiment repeated independently on 3 occasions. Graph show cumulative average cell counts of all 3 replicates. Overexpressing CARP3 in WT s427 cells leads to growth delay in CpdA.

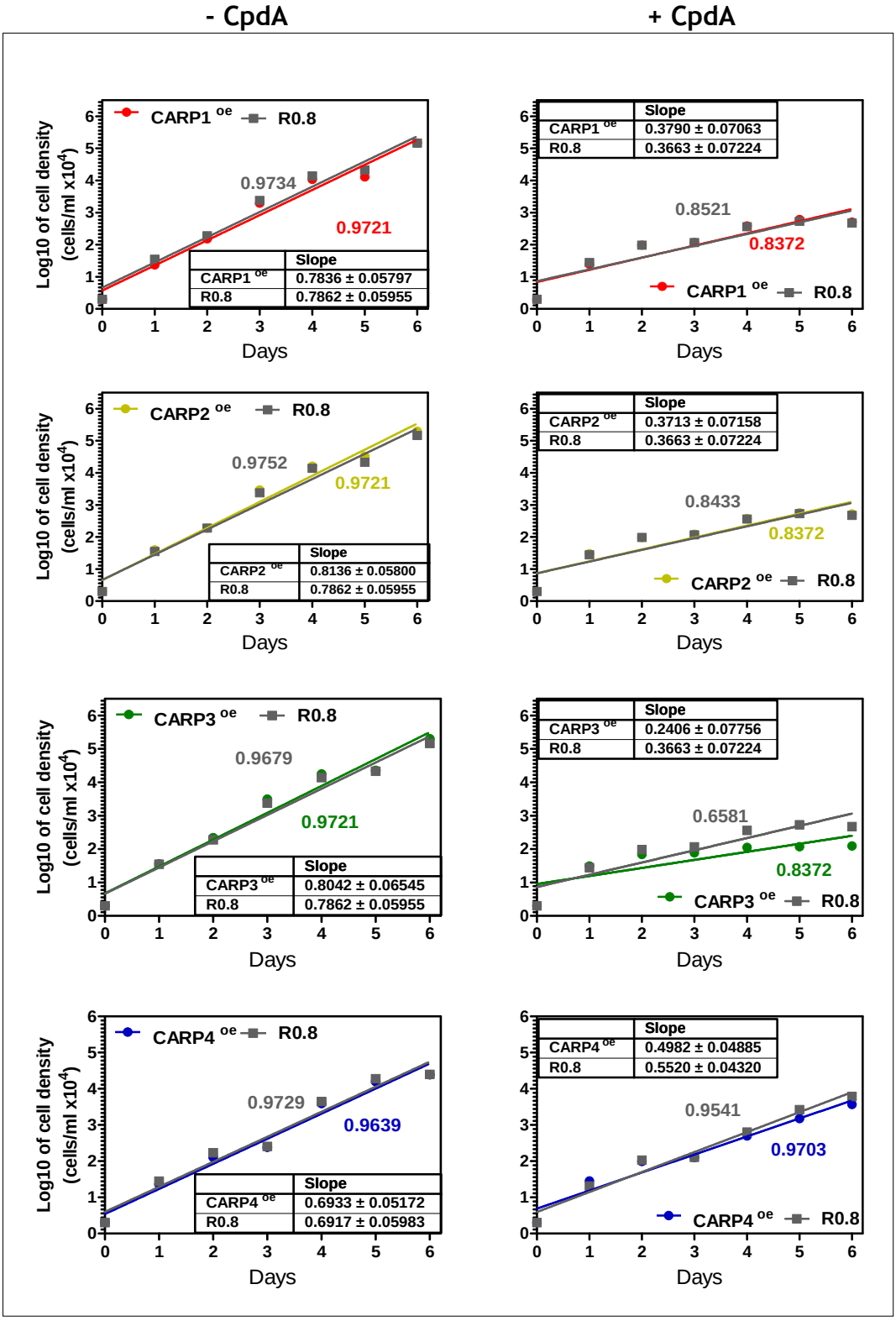

Figure 4.11: Cumulative cell proliferation assay of R0.8 cells overexpressing CARP1-4. A), C), E), and F) growth in the absence of CpdA. B), D), F) and H) growth in the presence of 100 nM CpdA. . Cells were seeded in duplicates and the experiment repeated independently on 3 occasions. Graph show cumulative average cell counts of all 3 replicates. Overexpressing CARP3 in R0.8 cells leads to a growth delay in CpdA.

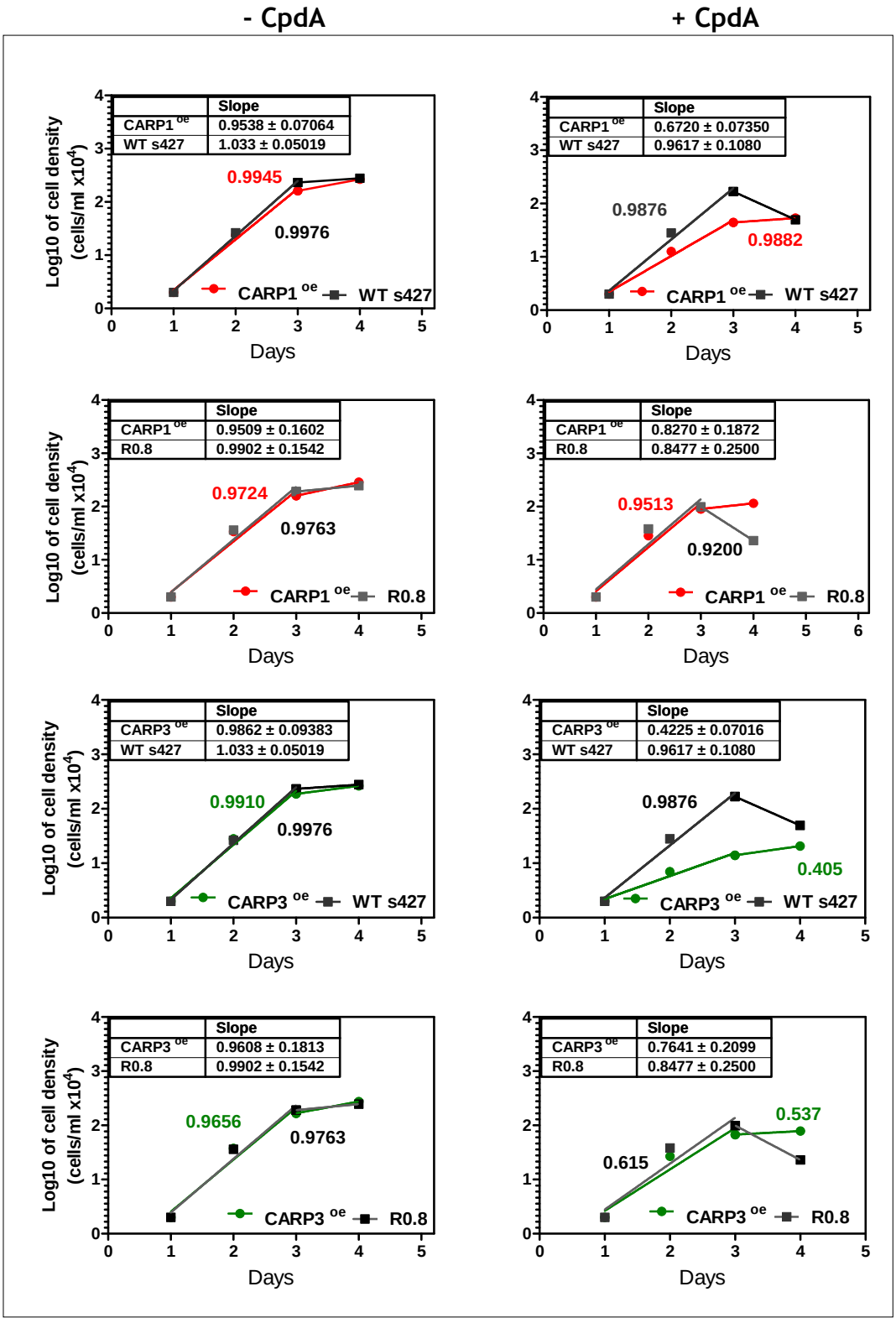

Figure 4.12: Single culture cell proliferation assays of WT s427 and R0.8 cells overexpressing CARP1 and CARP3. The experiment was repeated independently on three occasions. Cells were seeded in duplicates and the experiment repeated independently on 3 occasions. Graph show average cell counts of all 3 experimental replicates. Overexpressing CARP1 and CARP3 in WT s427 causes growth delays in CpdA.

4.5.0 Cyclic AMP levels in cells overexpressing CARP1-4 and TbPDEB1 in WT s427 and R0.8 cells

CpdA inhibits TbPDEB1, resulting in increased cAMP levels. The effect of increasing expression levels of CARP and TbPDEB1 on intracellular and extracellular cAMP levels in both WT s427 and R0.8 cells was studied by incubating overexpressing cells in 300 nM CpdA for 3 h. The possibility of cAMP entering into the cell, when experimentally added to the media, and thereby influencing the growth of cells in a similar way as CpdA inhibition does (i.e. by raising cellular cAMP above a threshold) was investigated and compared with similarly added AMP and with 'induced media' from cells, containing CpdA - induced cAMP extruded from the trypanosomes. Cyclic AMP release measured after a 100 nM CpdA, 3 h incubation.

4.5.1 Effect of overexpressing CARP1-4 genes on intracellular cAMP levels in WT s427 and R0.8

Overexpression of CARP3 led to a significant increase in both basal and CpdA-induced cAMP levels in WT s427. The cAMP concentration in the CpdA-resistant line was, however, only significantly increased when R0.8 CARP3^{oe} cells were incubated in CpdA for 3 h compared with just R0.8. There was no difference in cAMP levels, whether incubated with CpdA or not, in CARP1, 2 and 4 overexpressing cells compared with WT s427. There was also no difference in basal and stimulated cAMP levels in R0.8 CARP1, 2 and 4 overexpressing cells (Figure 4.13).

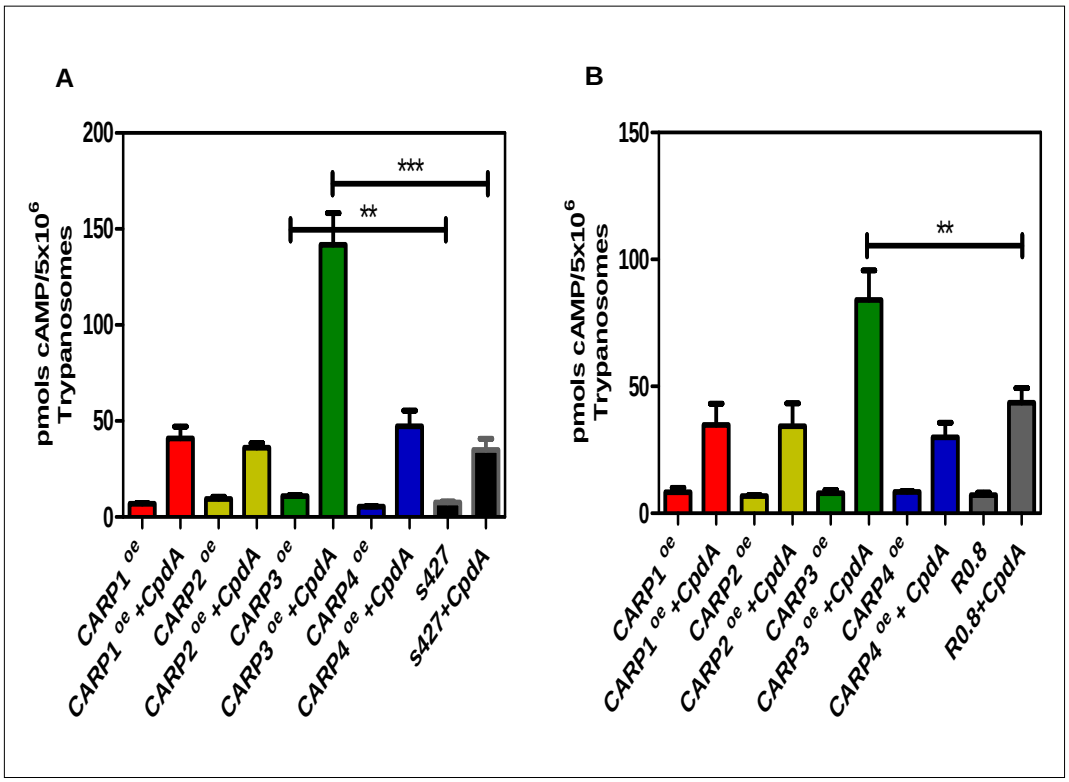

Figure 4.13: Measurement of intracellular cAMP in WT s427 and R0.8 cells overexpressing CARP1-4. A). CARP1-4 in WT s427 and control. B) CARP1-4 in R0.8 and control Error bars show ± standard error. Overexpressing CARP3 significantly raises both basal and CpdA induced intracellular cAMP levels in WT s427 CARP3^{oe} and CpdA induced cAMP in R0.8 CARP3^{oe}. T-test single-tailed, unpaired (* p>0.05, ** p>0.01, *** p>0.001; n>3).

4.5.2 Effect of overexpressing CARP1-4 genes on extracellular cAMP levels in WT s427 and R0.8

Extracellular cAMP levels were only increased in WT s427 cells overexpressing CARP3 and when pre-incubated with CpdA. Similarly overexpressing CARP3 in R0.8 increases both basal and CpdA induced extracellular cAMP levels. WT s427 CARP4^{oe} showed a significant decrease in basal cAMP level (Figure 4.14).

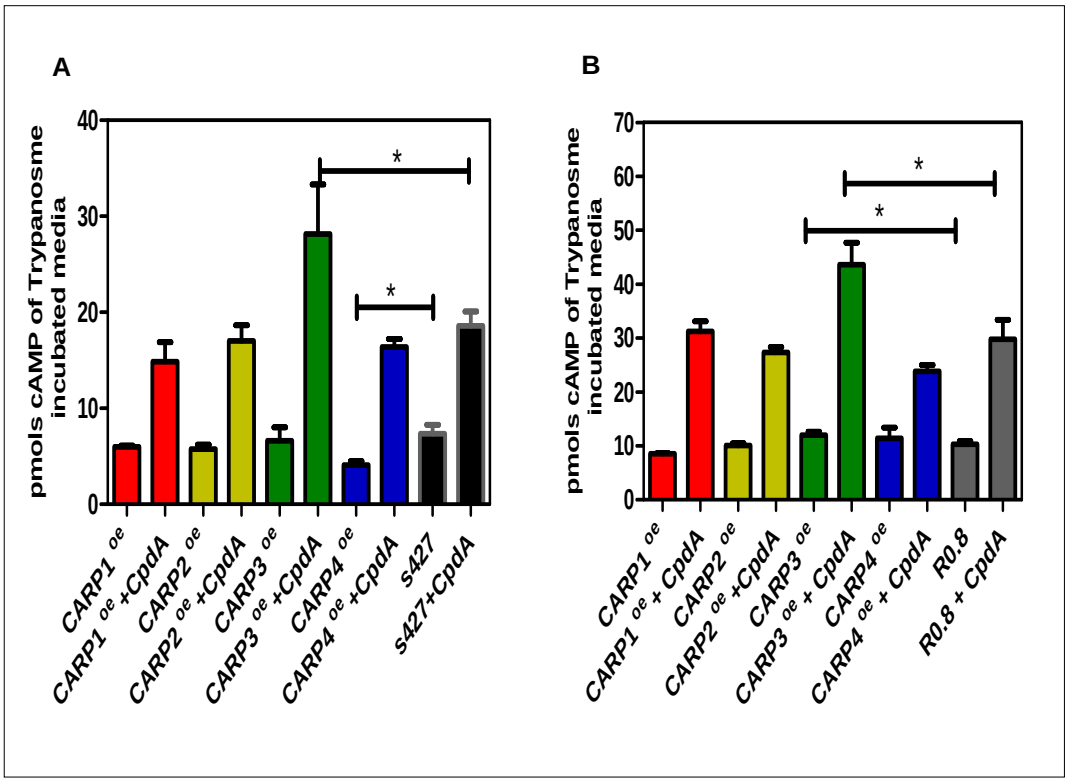

Figure 4.14: Extracellular cAMP measurements in WT s427 and R0.8 cells overexpressing CARP1-4.A). CARP1-4^{oe} in WT s427 and control. B) CARP1-4 in R0.8^{oe} and control. Overexpressing CARP3 significantly raises CpdA induced extracellular cAMP levels in WT s427 CARP3^{oe} and both basal and CpdA induced cAMP levels in R0.8 CARP3^{oe} Error bars show ± standard error. T-test single-tailed, unpaired (* p>0.05, ** p>0.01, *** p>0.001; n>3)

4.5.3 Effect of overexpressing TbPDEB1 genes on intracellular and extracellular cAMP levels in WT s427 and R0.8

Overexpressing TbPDEB1 in both WT s427 and R0.8 significantly increases basal intracellular cAMP levels but not in the presence of CpdA. There were no significant differences in both basal and CpdA induced extracellular cAMP levels in both WT s427 and R0.8 cells overexpressing TbPDEB1 cells (Figure 4.15).

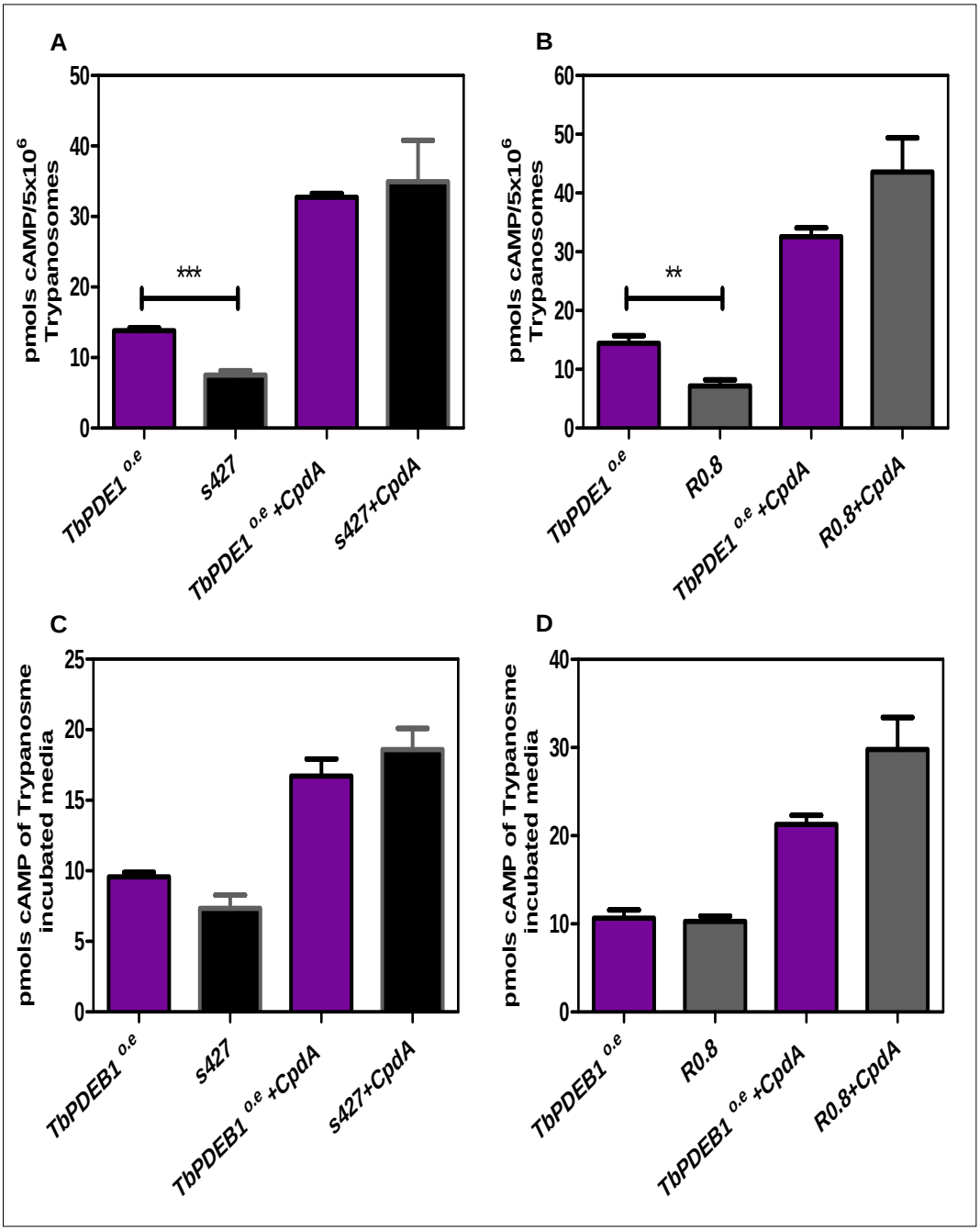

Figure 4.15: Cyclic AMP measurements in WT s427 and R0.8 cells overexpressing TbPDEB1. Intracellular cAMP levels in A) TbPDEB1^{oe} in WT s427 and B) TbPDEB1^{oe} in R0.8 and R0.8. Extracellular cAMP levels in C) TbPDEB1^{oe} in WT s427 and D) TbPDEB1^{oe} in R0.8 and R0.8. Overexpressing TbPDEB1 raises basal intracellular cAMP levels in both WT s427 and R0.8 cells. Error bars show ± standard error. T-test single-tailed, unpaired (* p>0.05, ** p>0.01, *** p>0.001; n>3)

4.5.4 Effect of extracellularly-added cAMP on cell proliferation of overexpressing CARP1, CARP3 and WT s427.

To study the effect of extracellular cAMP on the growth of trypanosomes, extracellular cAMP was measured in CARP1 and CARP3 overexpressing cells after incubation for 3 h in 100 nM CpdA. In CARP3 overexpressing cells, 300 nM CpdA significantly induces extracellular cAMP release compared with WT s427 and CARP1^{oe} (Figure 4.16). Growth of CARP1^{oe} and CARP3^{oe} in HMI-9 in which 5 µM cAMP had been added was not different from that of cells growing in HMI-9 only, without added cAMP, or from WT s427 growing in either media. Similarly, addition of 50 µM AMP did not affect growth of either overexpressing or WT s427 cells (Figure 4.17). However, CARP3^{oe} cells growing in media in which overexpressing CARP3 cells had previously been induced with 100 nM CpdA for 3 h during which cAMP had been extruded into the media (induced media) showed significant growth inhibition. Similarly, growth of the same cells in HMI-9 in which 100 nM CpdA + added cAMP (1 µM) also showed growth stagnation. CARP3^{oe} cells in HMI-9 + 100 nM CpdA only (no cAMP added) and same cells in HMI-9 + 100 nM CpdA + added AMP (5 µM) showed better growth compared with induced media and cAMP added media (Figure 4.17). Neither CARP1^{oe} nor WT s427 showed any growth inhibition in any of the media conditions comparatively nor CARP3^{oe} in media without CpdA (Figure 4.18).

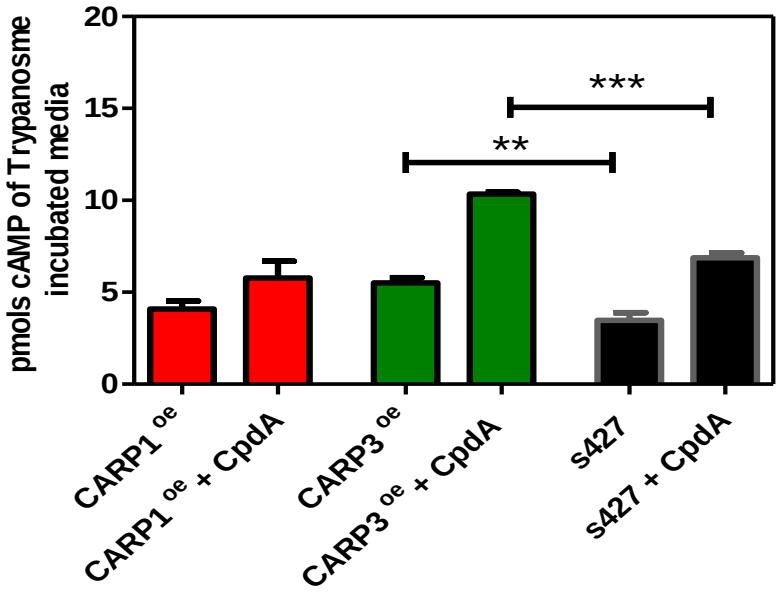

Figure 4.16: Cyclic AMP measurements in WT s427 overexpressing CARP1 and CARP3. Error bars show ± standard error. Overexpressing CARP3 causes significant increase in both basal and CpdA (100 M) induced extracellular cAMP levels. T-test single-tailed, unpaired (* p>0.05, ** p>0.01, *** p>0.001; n=3)

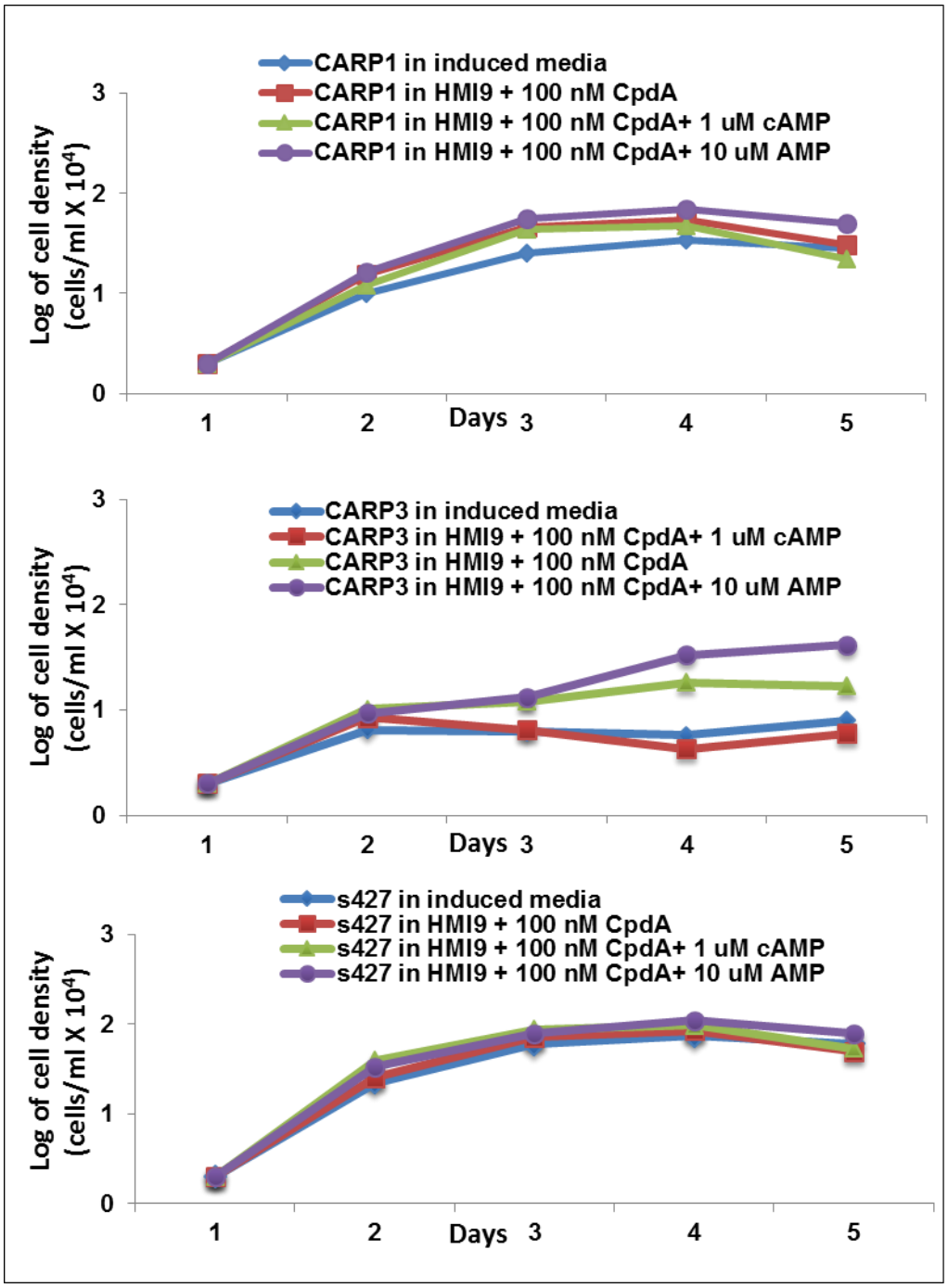

Figure 4.17: Growth of Overexpressing WT s427 CARP1, CARP3 and control WT s427 in CpdA cAMP induced media and commercially supplemented cAMP and AMP media. A) CARP1^{oe}, B) CARP3^{oe} and C) WT s427. Cells were seeded in duplicates and the experiment repeated independently on 2 occasions. Graph show average cell counts of all experimental. Overexpressing CARP3 leads to a noticeable delay in growth in CpdA induced media and un-induced media + HMI9 and cAMP.

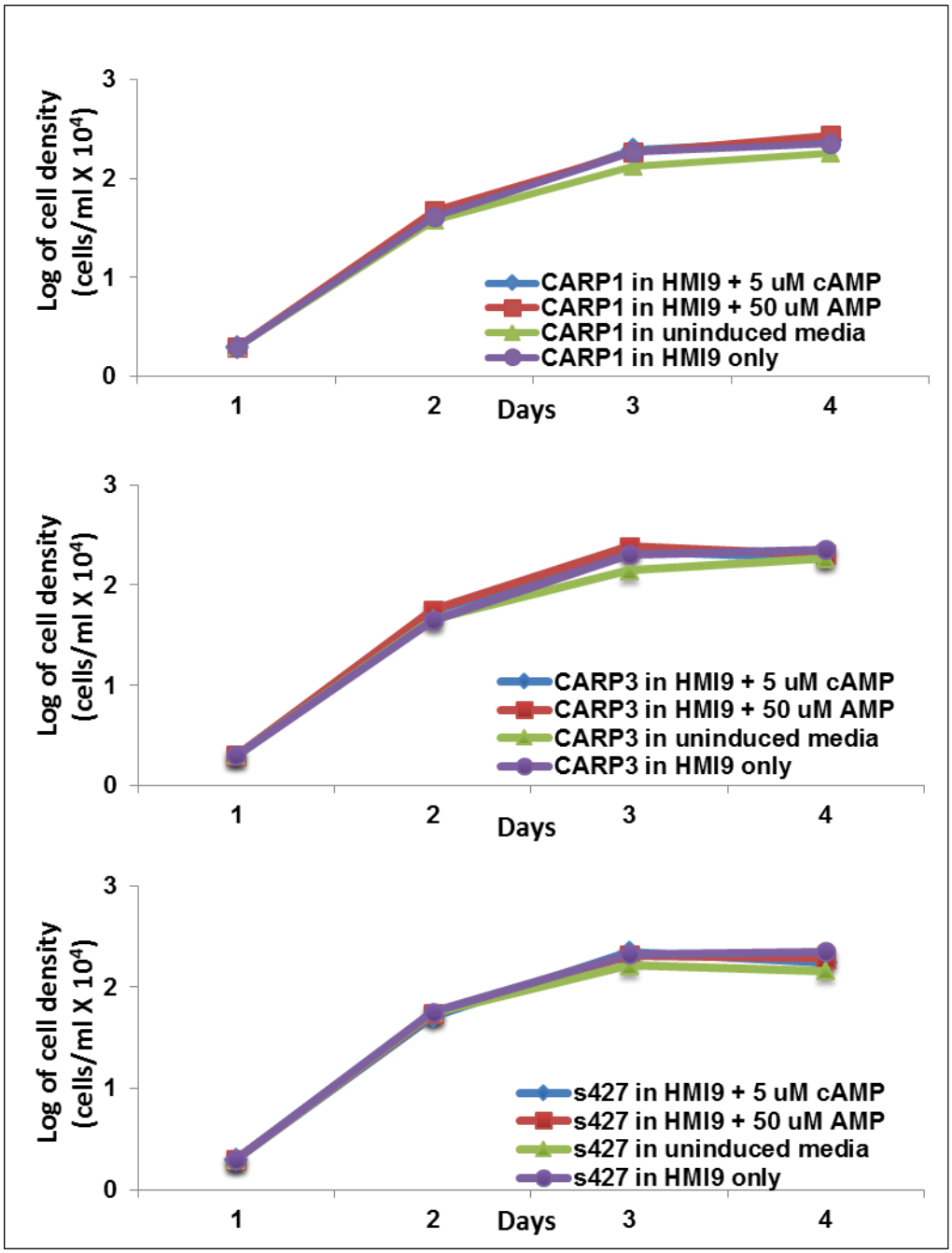

Figure 4.18: Growth of Overexpressing WT s427 CARP1^{oe}, CARP3^{oe} and control WT s427 in CpdA cAMP induced media and commercially supplemented cAMP and AMP media. A) CARP1^{oe}, B) CARP3^{oe} and C) WT s427. Cells were seeded in duplicates and the experiment repeated independently on 2 occasions. Graph show average cell counts of all experimental. Adding both cAMP and AMP alone does not lead to any growth effect in CARP1^{oe,} CARP3^{oe,} and WT s427.

4.6.0 Localization of CARP1-3 in trypanosomes

Locations of protein are usually associated with their function as structure is related to function. The CARPs have been annotated to perform certain functions in the cell and have been detected as protein fractions in various regions of the cell from proteomic pulldown analysis. However, none of the CARPs have been confirmed to be localized to these regions using microscopy. Thus, a preliminary localization was performed to determine the location of the CARPs in the cell and to relate these to functions.

4.6.1 Localization of CARP3 using anti-CARP3 antibody

Immuno-fluorescence using CARP3 antibody shows CARP3 localizes to the plasma membrane and flagellum of the trypanosome (Figure 4.19).

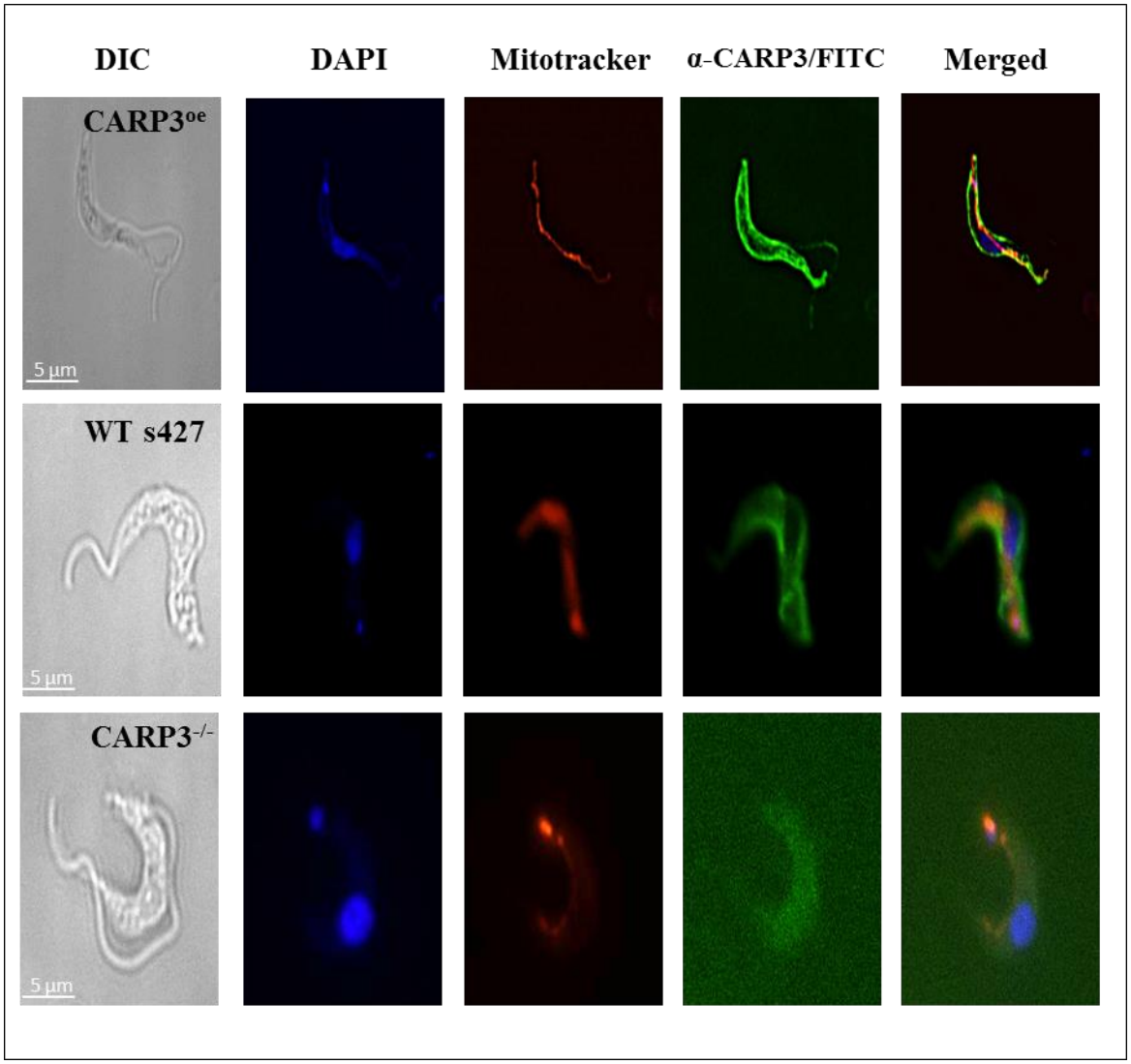

Figure 4.19: Immunofluorescence assay (IFA) of overexpressing CARP3 using peptide produced rabbit anti-CARP3 antibody. DIC, differential interference contrast; DAPI, 4',6-diamidino-2-phenylindole; FITC, Fluorescein isothiocyanate. CARP3 localizes strongly to the plasma membrane and flagellum when overexpressed. WTs427 shows similar localization whilst the CARP3$^{-/-}$ shows no localization.

4.6.2 Localization of N-Terminal GFP tagged CARP1-3

Genes of CARP1-3 were N-terminally tagged with GFP and overexpressed in 2TI cells. Preliminary Immunofluorescence assay (IFA) showed that CARP1 associated with specific regions or bodies within the cytosol with proximity to the basal body. CARP2 also seem to localize in discrete cellular compartments in the posterior region of the trypanosomes after the nucleus whilst CARP3 localizes to the pellicular plasma membrane (Figure 4.20).

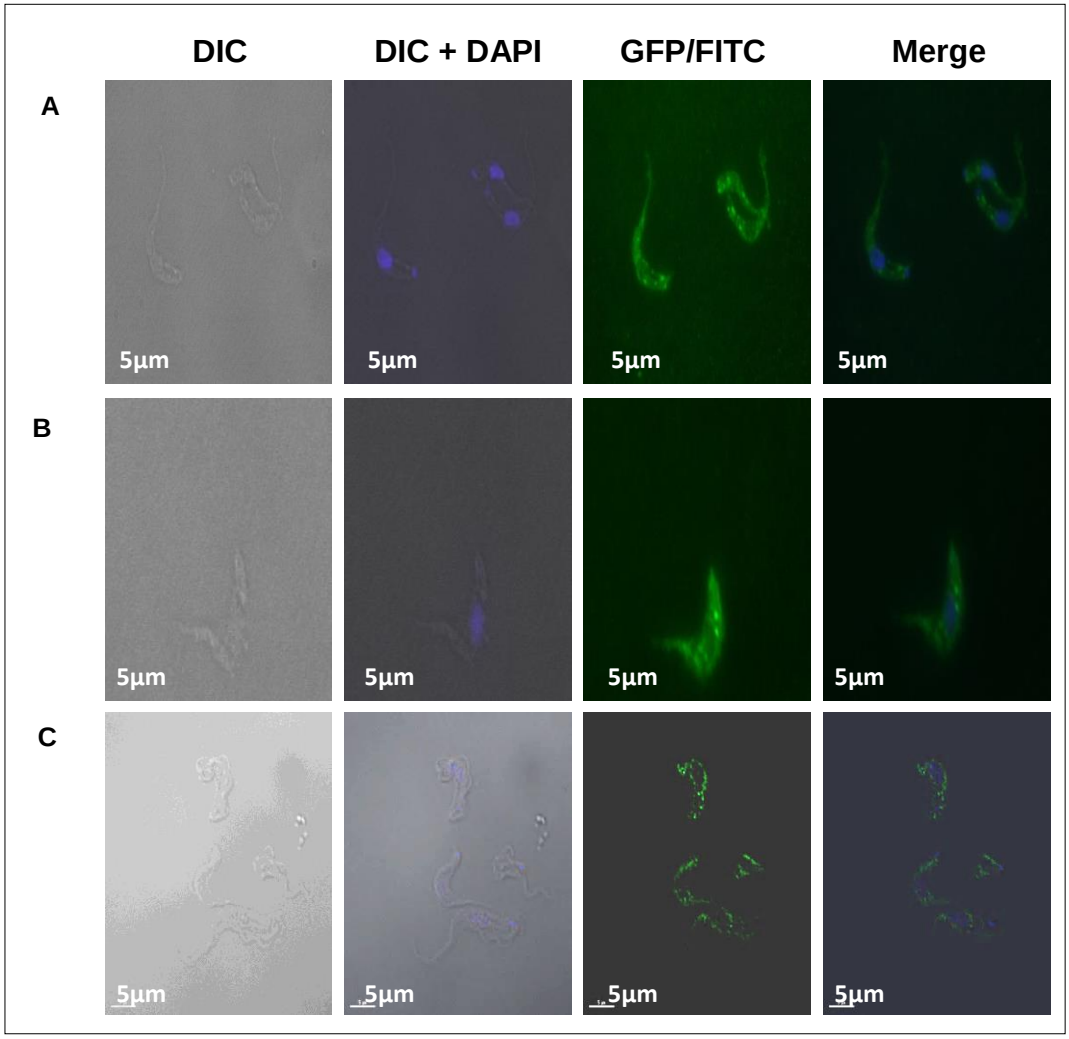

Figure 4.20: Immunofluorescence of N-terminal GFP tagged CARP1-3 using anti-GFP antibody and IgG coupled FITC for CARP3. A) CARP1^{GFP}. B) CARP2^{GFP}. C) CARP3^{GFP}. DIC, differential interference contrast; DAPI, 4',6-diamidino-2-phenylindole; FITC, Fluorescein isothiocyanate.

4.7.0 Discussion

Since RNAi and gene deletion of the CARPs led to decrease in susceptibility to CpdA, there was the need to study the concomitant effect of increasing the expression of the CARPs to study the effect on sensitivity, cell proliferation, cAMP, transcription and protein expression when CpdA is added to the cells. It is also important to know where these proteins localize in the trypanosome as a basis of relating location to function and appreciating the whole cell biology of the trypanosome in relation to downstream signalling of cAMP.

PCR confirmed the presence of the overexpression constructs whilst qRT-PCR showed the extent of the increased expression of the CARP and TbPDEB1 genes in the WT s427 and R0.8 cell lines. Increases in CARP3 transcripts were reflected in increased protein levels in both WT s427 and R0.8 validating the expression system and qRT-PCR results. Overexpression of TbPDEB1 in both the WT s427 and the CpdA resistant R0.8 resulted in a decreased susceptibility to CpdA. This is expected since CpdA inhibits TbPDEB1 and thus more CpdA is required to inhibit more TbPDEB1 to bring about cell death according to standard pharmacological theory. There was no significant difference in sensitivity to pentamidine when TbPDEB1 was overexpressed in either WT s427 or R0.8, in agreement with our understanding of the mechanism of action of pentamidine, which is unrelated to the cAMP system (Baker et al., 2013; Bray et al., 2003). This result further validates pHD1336 as a good expression construct. Overexpressing CARP3 in both WT s427 and R0.8 lines significantly sensitizes the cells to CpdA when compared with WT and that of the other overexpressing CARPs in both cell lines. There was no significant difference in sensitivity to pentamidine in the overexpressed cells except in WT s427 CARP4^{oe}. This implies that CARP3 plays a role in determining the final phenotype when CpdA is added to the cells that is parallel to that of TbPDEB1, as knockdown induces sensitivity and overexpression the reverse when overexpressed. Since CARP3 is downstream of TbPDEB1 in the cAMP signalling cascade, CARP3 might play an important role in the determination of the final growth phenotype which is impossible without the inhibition of TbPDEB1.

In both WT s427 and R0.8, overexpressing CARP3 significantly increases both intracellular and extracellular cAMP when CpdA is added, compared to the WT

un-transfected s427 and R0.8 lines and with the other overexpressing CARPs. This is likely to be due to the fact that CARP3 plays a very important role in cellular regulation which in TbPDEB1 inhibition results in cytokinesis defective trypanosomes (de Koning et al., 2012) of which cAMP is required to trigger or drive to completion. This is because whereas the double deletion of CARP3 genes resulted in significant increases in both basal innate and CpdA induced cAMP, this did not sensitize the cells to CpdA but rather decreased sensitivity just as in dKOs of CARP2 and CARP4. This clearly means that both an increase in cAMP and CARP3 proteins must be present for cAMP induced cellular phenotype (cytokinesis defects followed by cell death) to occur. CARP3 appears to be the key parameter and for that matter an increase in the levels of CARP3 significantly drove an increase in this cellular phenotype, as revealed by a shift in the CpdA IC_{50}, reflecting a higher sensitivity to an elevated cAMP concentration. However, CARP3 does not seem to be only a link in the cAMP response chain, as overexpression of CARP3 in WT s427 increased the basal intracellular cAMP levels as well as increased extracellular extrusion of cAMP in both WT s427 and R0.8. The fact that cAMP extrusion is similarly increased as the intracellular level shows that the intracellular level is not increased as a result of reduced efflux. Moreover, the observation that this difference was also seen in the presence of the PDE inhibitor CpdA means that the difference cannot be explained in terms of a difference in cAMP degradation rate either, and we conclude that CARP3 overexpression increased the activity of cAMP production by the *T. brucei* adenylyl cyclases, in a direct or indirect way.

Overexpressing TbPDEB1 in both cell lines caused a small but significant increase in basal intracellular cAMP levels. This must be the result of a feedback mechanism since an increase in TbPDEB1 protein is instead expected to increase breakdown of cAMP levels to that below normal cellular requirements. However, the increase was not pronounced and did not result in an increase release of cAMP from the cell. CpdA increased both intracellular and extracellular cAMP and although in both cases there was a reduction in cAMP levels as expected, in $TbPDEB1^{oe}$; however, this was not significant.

Increased sensitivity as a result of overexpression of CARP3 was further validated in growth phenotypes in WT s427 and R0.8. Both these overexpressed lines

showed delayed growth, in 100 nM and 3 µM CpdA, respectively, compared with media only incubations. None of the other overexpressed CARPs in either WT s427 and R0.8 showed any delayed growth phenotype either in normal media or media supplemented with CpdA. The delay in the growth of cells overexpressing CARP3 was further enhanced in WT s427 when the experiment was performed in single media and not in continuous passage into new media (every 48 h) with CpdA. The accumulation of cAMP in the media of the single growth experiment unlike the continuous growth were the media was refreshed every 48 h, cannot be interpreted as the creation of some sort of cAMP gradient in the media that works against the extrusion of further cAMP from the cells. This probably resulted in even higher intracellular cAMP levels in the single media growth curve and thus the increased growth delayed phenotype- although it can be excluded that other secreted factors contributed to the observed growth patterns. Although the effect of increased CARP3 transcript and protein was less pronounced on the growth rate of R0.8 CARP3^{oe}, it resulted in continued cell survival when the control R0.8 cell population was already declining. One mechanism by which R0.8 cells got adapted to CpdA was to upregulate the extrusion of cAMP into the surrounding media, when challenged by PDE inhibitors. This may provide an explanation as to why CARP3 overexpression in WT427 caused a significant growth delay, but not in R0.8 where, in fact, it seems to give a longer survival time at high cell densities. Importantly, this was observed only in ‘single culture’ growth curves, and not when medium was replaced on alternate days. The interpretation of these results is that R0.8 is less sensitive to an excreted factor, presumably cAMP, but only in the presence of a minimum expression level of CARP3.

The addition of 1 µM cAMP to the media inhibited growth of CARP3^{oe} when added together with CpdA. These conditions are similar to growth in CpdA-induced extracellular cAMP from CARP3^{oe} cells (in this case the conditioned medium also contains CpdA). The addition of AMP the breakdown product of cAMP, to the medium and under the same conditions did not cause growth stagnation thus confirming cAMP and not a metabolite was responsible for the observed growth inhibition, which was similar to that seen in the single growth curve of CARP3^{oe} in HMI9 + 100 nM CpdA. One interpretation is that a build-up of cAMP in the media prevented further extrusion of cAMP resulting in much higher intracellular

cAMP levels than observed in any other cell line tested in parallel (see figure 4.13); for instance, neither CARP1^{oe} nor WT s427 showed a similar phenotype. Clearly, the amount of CARP3 protein present in the cell is important to bring about this effect. This is further substantiated by the fact that 100 nM CpdA, 3 h incubation significantly increased cAMP in media of CARP3^{oe} and compared with either CARP1^{oe} or WT s427. The most straightforward explanation is that in CARP3$^{o.e}$ cells, the rate of cAMP production is substantially increased, although this is usually masked by the continued activity of the phosphodiesterases, keeping the cAMP homeostasis intact. However, in the presence of CpdA, the much higher cAMP production rate is revealed and leads to a much higher intracellular level and therefore efflux, which in turn leads to an accelerated cAMP build-up in the media, which (assuming the cAMP efflux is passive and thus equilibrative) in turn drives up the intracellular concentration even higher.

CpdA significantly decreases mRNA transcript levels of CARP1-4 and TbPDEB1-overexpressing WT s427 cells; the effect was highly significant within 6 h and maintained over the 48 h incubation period when normalized to pre-CpdA incubation. Messenger RNA levels of CARP2 and CARP3 were similarly significantly reduced in WT s427 over the same period, whereas levels of CARP4 remained steady, and mRNA of CARP1 and TbPDEB1 decreased significantly initially (6) h but returned to pre-incubation levels or higher for the rest of the 48 h period in WT s427. CpdA inhibits TbPDEB1 leading to increased cellular cAMP, which might be expected to require, if anything, an increased PDEB1 expression. Therefore, no direct explanation offers itself for the temporary reduction in TbPDEB1 mRNA levels at 6 h, similar to that of CARP2 and CARP3. A probable reason it could be that the presence of CpdA downregulates TbPDEB1, leading to a concomitant reduction in CARP2 and CARP3 expression thereby reducing the downstream effect of PDB1 inhibition in the initial 6 h period. It may be that this compensatory upregulation of PDEB1 after the initial 6 h reduction explains, in part, that the effects of CpdA with respect to cytokinesis are only observed after 24 h and even that at high concentrations of CpdA (1 μM) (de Koning et al., 2012) although there is a significant and immediate increase in cAMP, (de Koning et al., 2012). However, it is currently a matter of speculation whether the downregulation of CARPs 2 and 3 may not have a larger influence in protecting the cells that long against the elevated cAMP levels.

The need for the cellular response to immediately and significantly reduce transcript levels of CARPs in the presence of PDE inhibitors, which was especially prominent when the CARPs were overexpressed at the start of the incubation, CpdA confirms the importance of these proteins as downstream effectors of cAMP. The reduction in CARP3 transcript levels, after CpdA treatment, was directly correlated to a very similar reduction in protein levels confirming the overwhelming need of the cell to regulate both mRNA and protein levels of CARP3. The importance of CARP3 was further validated when expression of its transcript in R0.8 CARP3^{oe} and R0.8 showed a similar pattern to that in WT s427. At 6 h and by 24 h, there was almost no production of CARP3 mRNA in the cell; this coincided with a total depletion of CARP3 proteins at the same time. Importantly, this pattern was only observed in R0.8 cells overexpressing CARP3 and not in any of the other CARP over-expressors, as well as TbPDEB1^{oe}. CARP3 expression in un-transfected R0.8 was similar to levels pre incubation of CpdA. This is the reason for the observed CpdA sensitive phenotype observed in the drug sensitivity assay (only CARP3$^{o.e}$ was significantly sensitised to CpdA) and for the growth delay in the growth curve assays in R0.8 cells (only CARP3$^{o.e}$ were growth delayed in the presence of CpdA).

Although CARP3 is unique to trypanosomes and its crystal structure has not been resolved yet, protein prediction software predicts very important motifs with high confidence providing probable insightful explanations to the activity of the protein and its role in cAMP signalling. The SWISS-MODEL (Biasini et al., 2014) and the Protein Homology/analogY Recognition Engine V 2.0 (Phyre^2) (Kelley and Sternberg, 2009) predicted CARP3 proteins to have a tetratricopeptide repeat (TPR) and Protein database (PDB) annotations such as signalling protein, membrane protein, protein binding/transport protein, Peroxisome Targeting Signal 1 Receptor (PEX5), Regulatory Protein among others. It is also predicted to have a Nuclear Export Signal (NES) using the NetNES 1.1 Server (la Cour et al., 2003) that targets it for export from the nucleus to the cytoplasm as well as a domain typical of proteasome non-ATPase 26S subunit from the ROBETTA Full-chain Protein Structure Prediction Server (Bradley et al., 2005) and the proteasome regulatory particle subunit 6 (Rpn6) using the I-TASSER Protein Structure and Function predictions (Yang et al., 2015). The 26S proteasome is a protease with a core particle (CP) and a regulatory particle (RP) and is

responsible for the proteolytic breakdown of ubiquitinated proteins; a process which serves diverse and important cellular functions such as cell-cycle regulation, apoptosis, DNA repair, gene expression, transcription and signalling (Gu and Enenkel, 2014; Kaneko et al., 2009). The non-ATPase of the 26S proteasome is a regulatory particle that serves as receptor for poly-ubiquitined protein substrates (Gu and Enenkel, 2014). Ubiquitination prediction using UbPred: predictor of protein ubiquitination sites (Radivojac et al., 2010) revealed 9 ubiquitination sites on CARP3. Three of this prediction is of low confidence, 5 medium confidence and 1 high confidence. Thus it is probable that cAMP above a certain threshold will cause ubiquitination of CARP3, priming it for transport to the proteasome for degradation. CARP3 protein degradation in turn could signal a reduction in the production of CARP3 leading to a halt or down regulation of its transcription. This explains both the down regulation and CARP3 protein turn over within 6 h after the addition of CpdA. Proteins known to have TPR domains have been discovered to be involved in cell cycle regulation, transcription control, protein import and signalling (Cliff et al., 2005). Thus overall, CARP3 looks perfectly structured for a regulatory and signalling role that directly fits its importance as the main regulator of downstream cAMP signalling and the determinant of the cAMP-dependent phenotype.

CpdA decreases mRNA levels of TbPDEB1 overexpressing in R0.8, similar to overexpressing of same in WT s427. Overexpressing CARP1, 2 and 4 in R0.8 resulted in increased mRNA levels in the presence of CpdA and significantly so in R0.8 CARP1^{oe} and R0.8 CARP4^{oe}. Similarly, there were significant increases in mRNA of CARP1, 2, 4 and TbPDEB1 in R0.8 6 h after adding CpdA and up to 48 h above pre-incubation levels. However, the levels of CARP3 in untransfected R0.8 remain steady over 48 h. As of this moment, this is not well understood and especially since the basis for CpdA resistance in the R0.8 is yet to be clarified. It is expected that, further cellular and functional characterization of the CARPs and R0.8, will provide more information that will enable the interpretation of the present data.

Preliminary data on localization of the CARPs show localization in different places in the trypanosomes. CARP1 localized to discrete regions or organelles in the cytosol with some proximity to the basal body and flagellar pocket. CARP2

also seem to localize in discrete cellular compartments in the posterior cytosolic region of the trypanosomes. Proteomic data identified CARP2 peptides in both plasma membrane and cytoskeleton fractions of BSF (Bridges et al., 2008) and as part of the flagellar proteome in the PCF (Broadhead et al., 2006).

CARP3 localizes to the plasma membrane and the flagellum of *T. brucei*. This confirms previous finding of CARP3 peptide fragments in Plasma membrane of BSF (Bridges et al., 2008) and enriched in the flagellar proteome of PCF (Subota et al., 2014).

Additionally, CARP3 is predicted to undergo protein acylation (N-myristoylation and palmitoylation) which has been shown to be important in protein-membrane interactions by anchoring of proteins to membranes and stabilization, vesicle and protein targeting and cell signalling (Dunphy and Linder, 1998). Bioinformatics analysis using NMT algorithm (Maurer-Stroh et al., 2002) predicts with high confidence myristoylation on the glycine residue (G2) of the second position in the protein sequence (GGGSSVEDK RYSRLFQE). The cysteine residues on positions 162 and 256 were predicted as palmitoylation sites by PalmPred (Kumari et al., 2014) whilst CSS-Palm algorithm (Ren et al., 2008) predicted both sites as well as residue 386. Both myristoylation and palmitoylation together have been shown to cause proteins to localize to the flagellum (Emmer et al., 2011b; Liu et al., 2010). A specific example is protein Present in the Outer Membrane Proteome of mitochondrion (POMP39), a protein without the canonical mitochondrion membrane-spanning domain (Niemann et al., 2013), which undergoes both myristoylation and palmitoylation and localizes to the flagellum besides the mitochondrion (Albisetti et al., 2015). This is similar to another mitochondrion outer membrane protein (Tb927.9.4320) (Acestor et al., 2009) predicted to be palmitoylated (Emmer et al., 2011a; Emmer et al., 2011b) and detected in the flagellar proteome (Oberholzer et al., 2011).

IFA using antibody to the N-terminally fused GFP-CARP3 show localization to the pellicular plasma membrane confirming the α-CARP3 antibody localization.

A summary of biochemical characterization of the various genetically manipulated cell lines in both WT s427 and R0.8 strains is presented in Table 4.1.

Cell lines	Genetic line	Drug sensitivity		Growth Phenotype		cAMP measurements				mRNA Expression levels (qRT-PCR)				Protein Express.
		CpdA	Penta	nCpdA	+CpdA	Intra		Extra		nCpdA	+CpdA			
						nCpdA	+CpdA	nCpdA	+CpdA	0 h	6 h	24 h	48 h	-
	o.e	No	No	No	No	Norm	Norm	Norm	Norm	Inc.	Dec.	Dec.	Dec.	-
CARP1	+/-	Dec.	No	No	No	Norm	Norm	Norm	Norm	Dec.	-	-	-	
	-/-													
	o.e	No	No	No	No	No	Norm	No	Norm	Inc.	Dec.	Dec.	Dec.	-
CARP2	+/-	Dec.	Inc.	No	No	No	Norm	No	Norm	Dec.	-	-	-	-
	-/-	Dec.	Inc.	Yes	No	Inc.	Inc.	Inc.	Inc.	-	-	-	-	-
	o.e	Inc.	No	No	Yes	Inc.	Inc.	Norm	Inc.	Inc.	Dec.	Dec.	Dec.	Dec.
CARP3	+/-	Dec.	Inc.	No	No	No	Norm	No	Norm	Dec	Dec.	Dec.	Dec.	Dec.
	-/-	Dec.	Inc.	No	No	Inc.	Inc.	Inc.	Inc.	-	-	-	-	-
	o.e	No	Dec.	No	No	No	Norm	No	Norm	Inc.	Dec.	Dec.	Dec.	
CARP4	+/-	Dec.	No	No	No	No	Norm	No	Norm	Inc.	Dec.	Dec.	Dec.	
	-/-	Dec.	No	No	No	Inc.	Inc.	Inc.	Inc.	-	-	-	-	-
	o.e	Dec.	No	-	-	Inc.	No	No	No	Inc.	Dec.	Dec.	Dec.	
TbPDEB1	+/-	-	-	-	-	-	-	-	-	-	-	-	-	-
	-/-	-	-	-	-	-	-	-	-	-	-	-	-	-
						R0.8 Strain								
CARP1	o.e	No	No	No	No	Norm	Norm	Norm	Norm	Inc.	Inc.	Inc.	Inc.	-
CARP2	o.e	No	No	No	No	Norm	Norm	Norm	Norm	Inc.	Norm	Norm	Norm	-
CARP3	o.e	Inc.	No	No	Yes	No	Inc.	Inc.	Inc.	Inc.	Dec.	Dec.	Dec.	Dec.
CARP4	o.e	No	No	No	No	Norm	Norm	Norm	Norm	Inc.	Inc.	Inc.	Inc.	-
TbPDEB1	o.e	Dec.	No	-	-	Inc.	No	No	No	Inc.	Inc.	Inc.	Inc.	-

Table 4.1: Summary of biochemical characterization of the different genetically manipulated cells in WT s427 and R0.8 strains. o.e, over expression; +/-, single knockout; -/-, double knockout; Inc., increase; Dec., decrease; Norm, normal; -CpdA, No CpdA; +CpdA, addition of CpdA; Penta, Pentamidine; -, experiment not performed

Chapter 5

4 Proteomic, Genomic and Transcriptomic investigations of CARPs and their interactions

5.0 Proteomic, Genomic and Transcriptomic investigations of CARPs and their interactions

The “Omics” (genomics, transcriptomics and proteomics) approach makes a most powerful tool in understanding the most complex of biological phenomena. This is because they form both the basis and the final outcome of the activities that underpins these biological processes and interactions. The genes are transcribed into RNA of which transcription and regulation is essential for cell survival. RNA is then translated into proteins required for structural, enzymatic as well as regulatory functions, some with feedback on the transcription process. A combination of these proteomic and transcriptomic approaches is expected to together confirm the observations seen when the CARPs are genetically manipulated as well as provide further targets and interactors of the downstream signalling cascade of cAMP in *T. brucei*.

5.1.0 RNA Interference Target Sequencing (RIT-Seq)

The RNAi knockdown approach is a useful tool that allows for the study of gene effects in trypanosomes under selective pressure. This approach has been applied severally and successfully (Alsford et al., 2012b; Alsford et al., 2011b; Baker et al., 2011), and was also used in identifying the initial downstream effectors of cAMP signalling (CARP1-4) from PCR, gel excision and Sanger sequencing. This only revealed the very top hits from the knockdown but the technique used makes it probable that there could be further important proteins with perhaps lower representation in the recovered RNAi sample, which contributed to the final phenotype. Thus, in order to maximize the discovery of distinct genetically-induced loss of function phenotypes from the complex population of RNAi fragment-containing trypanosomes surviving CpdA challenge, RIT-Seq was performed on the library elements recovered from the screen.

A total of 51,600,585 reads were obtained from the sequencer. Out of this number 1,791,387 of 70 bases per read length were mapped to a coding sequence and the genome making a 100% un-paired mapping. The overall coding sequence alignment rate was 61.07% (1094006) which was made up of 60.54%

(1084575) exactly one time alignment and 0.53% (9431) more than one time alignment. About 38.93% (697381) showed no alignment. Whereas 20.35% (364474) did not align to the genome sequence, overall, 79.65% (1426913) aligned which is made up of 77.16% (1382226) single alignment and 2.49% (44687) greater than 1 alignment. About 0.65% (332907) reads mapped to the genome but not the coding sequence (Table 5.1).

Mappings	**Coding Sequence Mapping**		**Genome mappings**	
	Bases	**%**	**Bases**	**%**
Read length	70 bases		70 bases	
Total Reads	1791387		1791387	
un-paired	1791387	100	1791387	100%
0% alignment	697381	38.93	364474	20.35
aligned exactly 1 time	1084575	60.54	1382226	77.16
aligned >1 times	9431	0.53	44687	2.49
overall alignment rate	1094006	61.07	1426913	79.65

Table 5.1: Mapping and alignment in RIT-Seq. Majority of both CDS (60.54%) and genome (77.16%) mapped exactly once with overall alignment rate at 61.07% and 79.65% for CDS and genome mapping respectively.

Above 1190 genes had raw total counts of ≥1 compared with just tetracycline-induced cells without CpdA selective pressure. However, after normalized mapping, only about 45 genes show ≥0.05 mapping reads (Appendix 2). The top 20 percentage mapped reads included had CARP1-4 as expected, confirming the observation from the PCR and Sanger sequencing reported earlier (Gould et al., 2013). Although CARP1 remained the highest hit (75.01% of all reads), the next two hits Tb927.10.12390 (4.99%) and Tb927. 10.1740 (3.60%) were higher than CARP4 (3.26%), CARP3 (2.57%) and CARP2 (0.45%) (Figure 5.1). There were additional important hits associated with cAMP signalling such as receptor-type

adenylate cyclases, adenylyl cyclases, and protein phosphatases among others (Table 5.2).

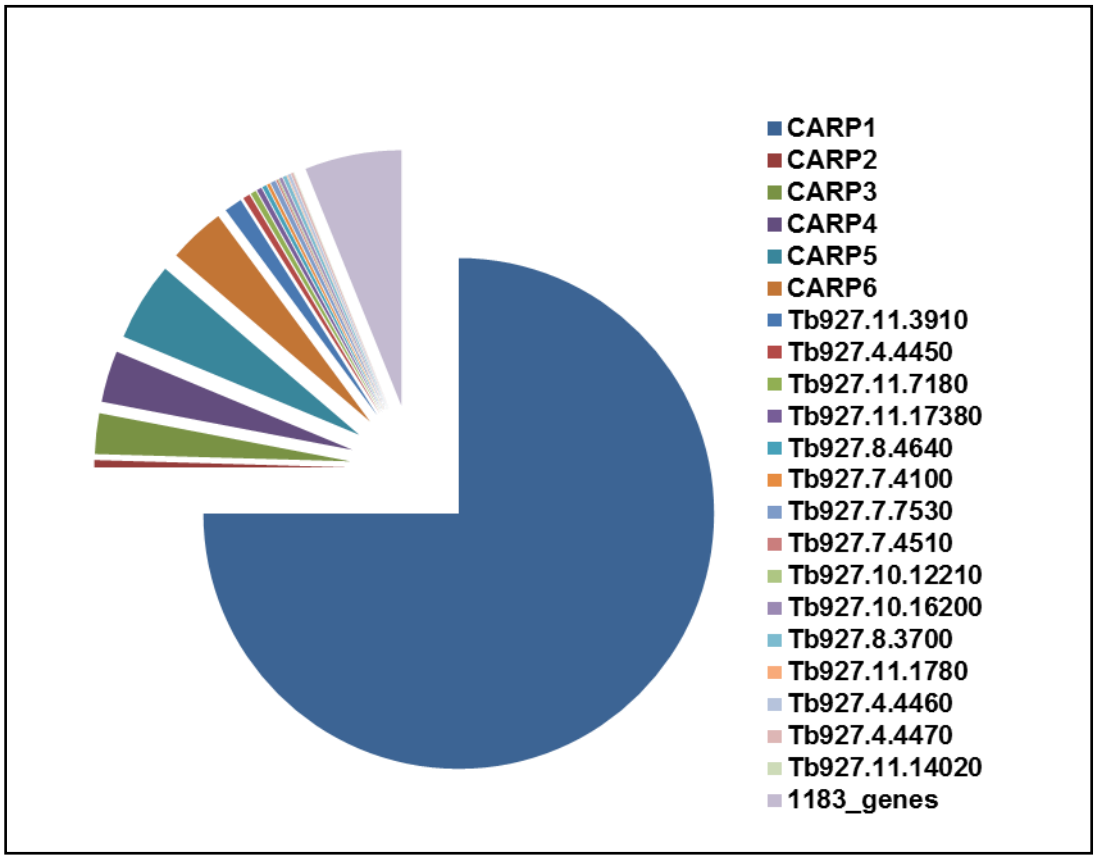

Figure 5.1: Distribution of percentage mapped reads among the various top hits in the RIT-Seq. CARP1 had the highest % Mapped reads (75%) and together with the other CARPs (2-6) makes up more than 85% of the reads. Tb927.10.12390 and Tb927. 10.1740 had 3.60% and 4.99% respectively which is higher than CARP2-4.

Gene ID	% mapped bases	Annotations
Tb927.11.16210	75.01	CARP1 - contains putative cyclic nucleotide binding domain; trypanosomatids only
Tb927.11.12860	0.45	CARP2 conserved hypothetical protein detected in flagellar proteome
Tb927.7.5340	2.57	CARP3 - tetratricopeptide repeat family, no orthologues outside Trypanosoma spp.; possible role in membrane fusion/division (cytokinesis/cell division?).
Tb927.3.1060	3.26	CARP4 conserved hypothetical protein with three DM10 and one EF-hand domains
Tb927.10.1740	3.60	Hypothetical protein unknown
Tb927.10.12390	4.99	Hypothetical protein unknown
Tb927.11.3910	1.13	Hypothetical protein unknown
Tb927.4.4450	0.44	adenylyl cyclase (inferred from sequence or structural similarity)
Tb927.11.7180	0.36	Hypothetical protein unknown
Tb927.11.17380	0.31	pseudogene?
Tb927.8.4640	0.27	flagellar protofilament ribbon protein, putative
Tb927.7.4100	0.20	Hypothetical protein unknown
Tb927.7.7530	0.32	receptor-type adenylate cyclase GRESAG 4, putative
Tb927.7.4510	0.10	Hypothetical protein unknown
Tb927.10.12210	0.06	ribulose-5-phosphate 3-epimerase, putative
Tb927.10.16200	0.20	Hypothetical protein unknown
Tb927.8.3700	0.23	Hypothetical protein unknown
Tb927.11.1780	0.05	protein phopsphatase
Tb927.4.4460	0.17	adenylyl cyclase (inferred from sequence or structural similarity)
Tb927.4.4470	0.14	adenylyl cyclase (inferred from sequence or structural similarity)
Tb927.11.14020	0.03	iron superoxide dismutase
1183_genes	**6.12**	1183_genes

Table 5.2: Annotation, % mapped reads and gene IDs of the top hits in the RIT-Seq. Four adenylyl cyclases, protein phosphatases, flagellar protein among others were among the top hits

5.2.0 Co-Immunoprecipitation (Co-IP) and Mass Spectrometry (MS)

Most biological processes involve the action of multiple protein complexes in one way or another. These complexes are either tightly regulated by a key protein or simply by forming complexes. A major goal of cell biology is to identify and characterize these protein complexes. The identification of these complexes has become more feasibly relevant with the advent and application of Mass Spectrometry (MS). Thus using Co-Immunoprecipitation (Co-IP), CARP3 and its interactors were pulled-down with α-CARP3 antibody, followed by MS proteomics for the identification of proteins that form complexes or tend to bind CARP3 and could be important in the observable phenotypes of CARP3 knockout and overexpression.

A total of about 200 proteins were pulled-down using anti-CARP3 antibody in the three replicates of Co-immunoprecipitation and MS/MS analysis. Cut off for significant expect-value was set at <0.05. The criteria of selection of interactors were in this order: (i) found in two or more independent experiments, (ii) highly significant identification from peptide, (iii) found in RIT-Seq hits (iv) orthology to proteins implicated in signalling and (v) presence of domains involved in signalling and/or protein-protein interactions. Additional filtering was performed by removing known contaminants of pulldowns as well as comparing proteins to those observed in pulldowns of CARP1 (3 replicates) and CARP2 (1 experiment) using antibodies designed for either CARPs but not binding to proteins with the right Molecular Weight (MW).

The majority (146) of the proteins detected in the Co-IP and MS were found in only one of the three replicated pull-down whilst the rest were found in more than one. Only five proteins were found in 2 or more replicates and exclusive to only CARP3 pulldown (Figure 5.2). These were made up of three adenylate cyclases (Tb927.4.4460, Tb927.4.4440, and Tb927.4.4410) with very high expect-values (3.7×10^{-5}) and protein score (75) and 2 hypothetical proteins (Tb927.10.1060 and Tb927.9.16060) with protein scores of 80 and 40 respectively (Table 5.3). There were 12 proteins in two or more CARP3 pulldowns with relatively high protein and peptide scores that were also found in

either CARP1 or CARP2 pulldowns (Appendix 3, Table 1). These include hypothetical proteins, variant surface glycoproteins (VSGs) and ribosomal proteins and are probably contaminants. Two of the annotated proteins in this group, Tb927.9.8740 (DRBD3 RNA-binding protein, putative; DRBD3) and Tb927.9.4680 (1L12.525 eukaryotic initiation factor 4a, putative) have been shown to drive abnormal phenotypes in RIT-Seq analysis in the different lifecycle stages (Alsford et al., 2011b). All the proteins found in all 3 replicates pulldowns of CARP3 (apart from CARP3 itself) were present in either CARP1 or CARP2 pulldowns and are mostly confirmed contaminants of pulldowns and MS proteomic data (Adung'a et al., 2013). Thirty-six proteins were pulled down with CARP3 in one replicate only out of which 11 were signalling mediated, ATP binding and proteasome regulatory proteins.

Two additional proteins Tb927.4.4470 and Tb927.8.7590 both putative receptor-type adenylate cyclases of the GRESAG 4 family, putative were also detected. Tb927.4.4470 had a very high protein (75) and peptide (58) score, and expect-value of (3.7×10^{-5}), the same as that found for Tb927.4.4460, Tb927.4.4440 and Tb927.4.4410 that were pulled down in 2 replicates. Tb927.8.7590 had a modest protein and peptide score of 30 each and expect-value of 0.032. Seven expression site associated gene 3 (ESAG3) and 2 other ESAGs were detected in both CARP3 and CARP1 pull downs but not in CARP2. A putative UBA1 ubiquitin-activating enzyme E1 (Tb927.8.2640) and putative PSA4 proteasome alpha 7 subunit (Tb927.11.7020) were both detected in just one replicate of both CARP3 and CARP2 only. There were additional hits that could be important interactors of cAMP signalling cascade that were also found in 1 replicate of CARP1 and CARP2 pulldowns (Table 5.4). Overall the identification of several adenylate cyclases, signalling mediated proteins, proteasome proteins and phosphatase binding proteins suggests a successful identification of important CARP3 interactors involved in cAMP signalling (Appendix 3: Table 2).

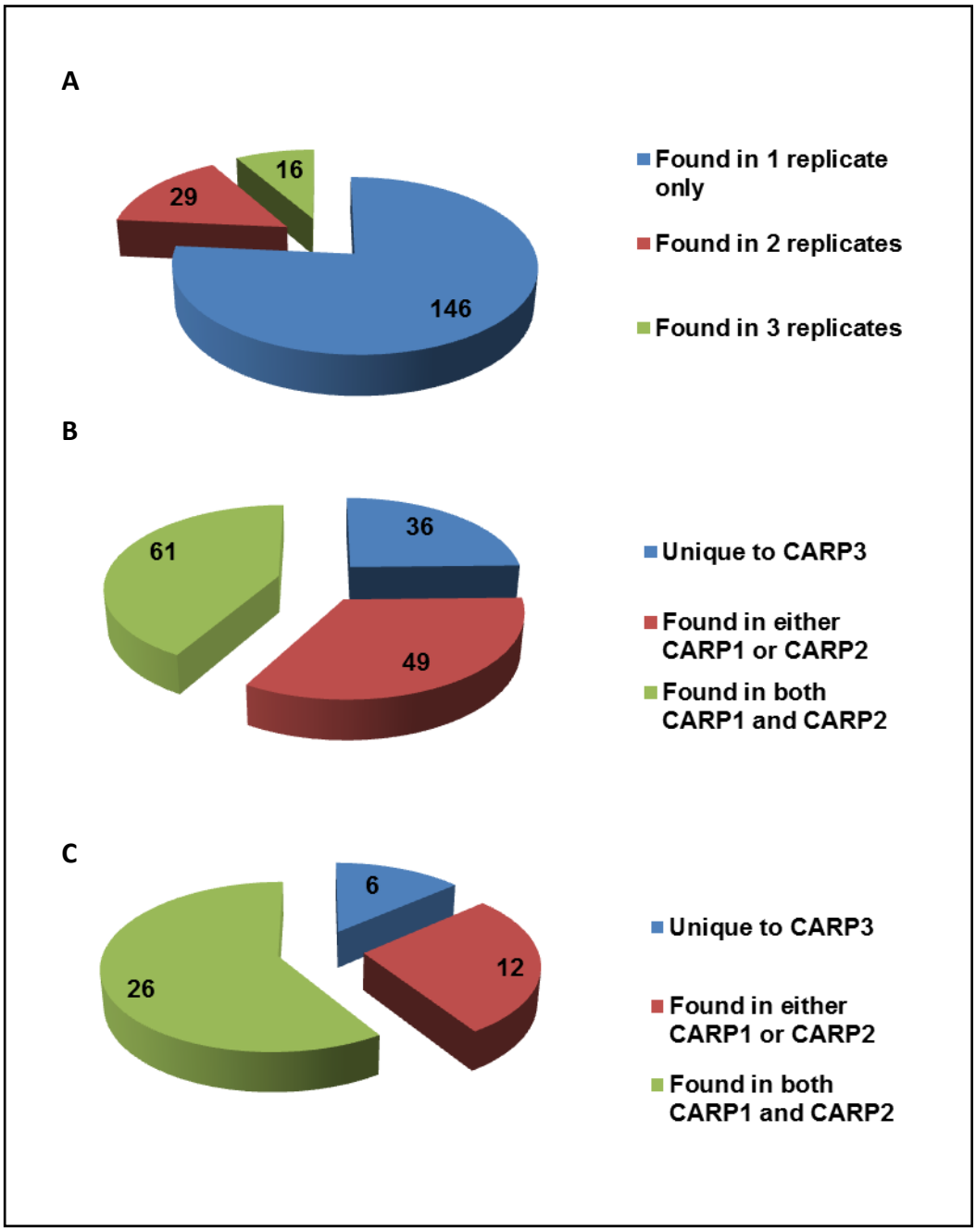

Figure 5.2: Distribution of hits from Co-IP and MS using CARP3 antibody and CARP1 and CARP2 antibodies as control. A) Majority of proteins (146) were found in just 1 pulled-down with CARP3 antibody. B) Of the 146 proteins found in the single pull-down of CARP3, 36 were unique to CARP3 whilst 61 were also present in CARP1 and CARP2. C) Of the proteins found in more than 1 replicate using CARP3 antibody, 6 were unique to CARP3 with the majority (26) found also in CARP1 and CARP2.

Gene ID	Annotation and Product	Size (kDa)	Protein Score	Peptide Score	Expect	Sequence Coverage (%)
Tb927.7.5340	CARP3	57	78	77.8	4.2×10^{-7}	13
Tb927.4.4460	GRESAG 4.4B receptor-type adenylate cyclase GRESAG 4, putative	144	75	58	3.7×10^{-5}	6
Tb927.4.4410	receptor-type adenylate cyclase GRESAG 4, putative	138	75	58	3.7×10^{-5}	3
Tb927.4.4440	receptor-type adenylate cyclase GRESAG 4, putative	138	75	58	3.7×10^{-5}	3
Tb927.10.2610	hypothetical protein, conserved	54	80	55	0.0001	5
Tb927.9.16060	hypothetical protein	11	40	40	0.0033	10

Table 5.3: Gene ID, annotations, protein and peptide scores and expect of the 6 unique hits found in more than 1 replicate of CARP3 pulldown. CARP3 as expected has the highest protein, peptide and expect scores. Three tandemly arranged GRESAG4s followed with high protein score and expect.

Gene ID	Annotation and Product	Found in	Size (kDa)	Protein score	Peptide score	Expect	Sequence Coverage (%)
Tb927.2.2440	RPN6 proteasome regulatory non-ATPase subunit 6	3 only	57	92	67	5.7×10^{-6}	5
Tb927.11.16030	RPN7 proteasome regulatory non-ATP-ase subunit 7	3 only	45	34	34	0.0093	3
Tb927.10.3030	RPN11 proteasome regulatory non-ATPase subunit 11; 19S proteasome regulatory subunit, Metallo-peptidase, Clan MP, Family M67	3 only	33	44	44	0.0013	3
Tb927.9.9670	TbPSA6 proteasome alpha 1 subunit, putative; 20S proteasome subunit alpha-6, putative	3 only	27	33	31	0.025	4
Tb927.4.4470	receptor-type adenylate cyclase GRESAG 4, putative	3 only	142	75	58	3.7×10^{-5}	6
Tb927.8.7590	receptor-type adenylate cyclase GRESAG 4, putative	3 only	139	30	30	0.032	4
Tb927.10.1060	TCP-1-delta t-complex protein 1, delta subunit, putative	3 only	58	88	88	4.8×10^{-8}	10
Tb927.5.3400	calcium-translocating P-type ATPase; calcium pump	3 only	41	53	53	0.00016	9
Tb927.7.6290	kinesin, putative	3 only	97	30	30	0.031	5
Tb927.10.2090	TEF1 elongation factor 1-alpha; EF-1-alpha	3 only	37	55	55	7.5×10^{-5}	10
Tb927.11.9530	14-3-3-like protein, putative	3 only	30	29	29	0.035	4
Tb927.8.2640	UBA1 ubiquitin-activating enzyme E1, putative	Also in 2	116	73	73	1.4×10^{-6}	9
Tb927.11.7020	PSA4 proteasome alpha 7 subunit, putative	Also in 2	27	46	46	0.00071	7

Table 5.4: Gene ID, annotations, protein and peptide scores and expect of important hits found in only 1 replicate of CARP3 pulldown. The presence of RPNs, TbPSA6 and PSA4 all predicted *in silico* confirms their role in CARP3 protein activity and regulation. Tb927.4.4470 (GRESAG4) was one of the hits from RIT-seq whilst CARP3 was predicted to be ubiquitinated.

An attempt was made to confirm one of the hits from both the RIT-seq and Co-IP an adenylate cyclase (Tb927.4.4460; GRESAG4.4). This was based on the hypothesis that it could be involved in a feedback loop through interaction with CARP3 which in turn regulates its expression. The hypothesis was tested by looking at the expression of GRESAG4.4 with and without CpdA (100 nM) added for 6 h. Expression of GRESAG4.4 was higher in CARP3^{oe} (2.3-fold) compared with WT s427 at 0 h. However, GRESAG4.4 mRNA levels drop significantly after 6 h incubation in 100 nM CpdA in CARP3^{oe} to a level similar to the level in WT s427. This trend was similar to the significant reduction observed in both transcript and protein levels of CARP3 in the same cells under same conditions. Levels of GRESAG4.4 in CARP3$^{-/-}$ cells remained virtually unchanged after 6 h incubation in CpdA and were not different from that of WT s427 in CpdA. In contrast the levels of GRESAG4.4 in WT s427 cells increased significantly 6 h in CpdA (Figure 5.3). This clearly shows that the presence and quantity of CARP3 directly affects the expression of GRESAG4.4 and that the manipulations of CARP3 reversibly affect the expression of GRESAG4.4.

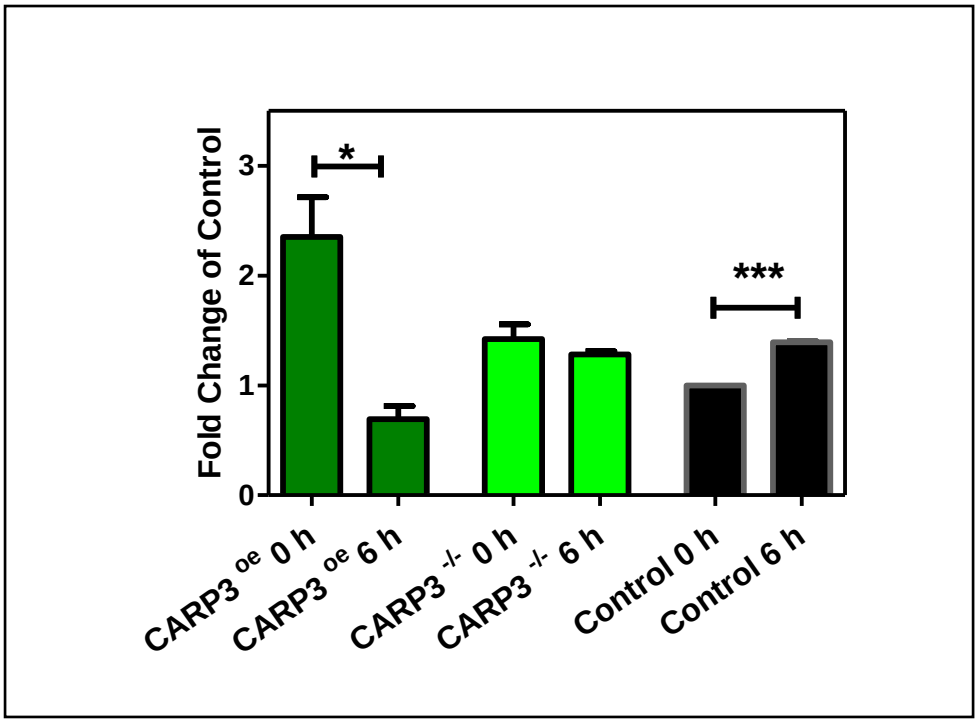

Figure 5.3: Expression of GRESAG4 (Tb927.4.4460) in CARP3^{oe} CARP3$^{-/-}$ cells without and with 100 nM CpdA for 6 h. Error bars show ± standard error. T-test single-tailed, unpaired (* p>0.05, ** p>0.01, *** p>0.001; n=3). CARP3^{oe} shows a significant increase (no CpdA) and decrease in expression of GRESAG4 (CpdA, 6 h).

5.3.0 Ribonucleic Acid Sequencing (RNA-Seq)

Important processes in the life of a parasite such as cell cycle progression, transition between cell types and developmental changes are usually synonymous with gene expression changes. However, the kinetoplastid lacks transcriptional regulation as a consequence of the unusual protein coding tandem genome arrangement that ensures polycistronic transcription (Clayton, 2002; Hall et al., 2003; Kramer, 2012). Yet, steady-state mRNA levels for specific genes can be very different in the different life stages, as well as in genetically manipulated cells due in part to mRNA stability (Kabani et al., 2009). It is this phenomenon, leading to different abundance of mRNA, that in *T. brucei* is referred to as 'differential expression'.

A total of 312 genes were significantly differentially expressed (Figure 5.4). Out of this total of differentially expressed genes, 18.3% (52) have a gene function annotation. Applying a cut-off of ±0.5 log_2-fold, lead to about 62 genes being upregulated whilst 7 genes were down-regulated when CARP3 was overexpressed compared with WT s427 (Appendix 4: Table 1 and 2). Of these upregulated genes, the majority were annotated genes (16), followed by hypothetical proteins and leucine-rich repeat protein (LRRP) (2) (Figure 5.5). Four annotated genes and 3 hypothetical proteins were down-regulated. The highest upregulated gene was an Expression Site Associated Gene 3 (ESAG3) Tb927.9.16700 (1.89) whilst putative 60S ribosomal protein L5 (Tb927.9.15110) most downregulated (-3.00). CARP3 had a log_2-fold of 1.58, consistent with the level of overexpression determined by qRT-PCR (Chapter 4). The majority of these changes have very high p-values (Figure 5.6). There were 3 tandemly arranged upregulated adenosine transporter proteins TbNT2 (Tb927.2.6150), TbNT4 (Tb927.2.6220) and TbNT6 (Tb927.2.6320) with high p-values (5×10^{-5}), 1 nucleoside transporter Tb927.9.15980 and 1 amino acid transporter Tb927.11.15960 with the same p-values. Tb927.11.15950, another amino transporter tandem to Tb927.11.15960 was down-regulated with the same p-value (5×10^{-5}).

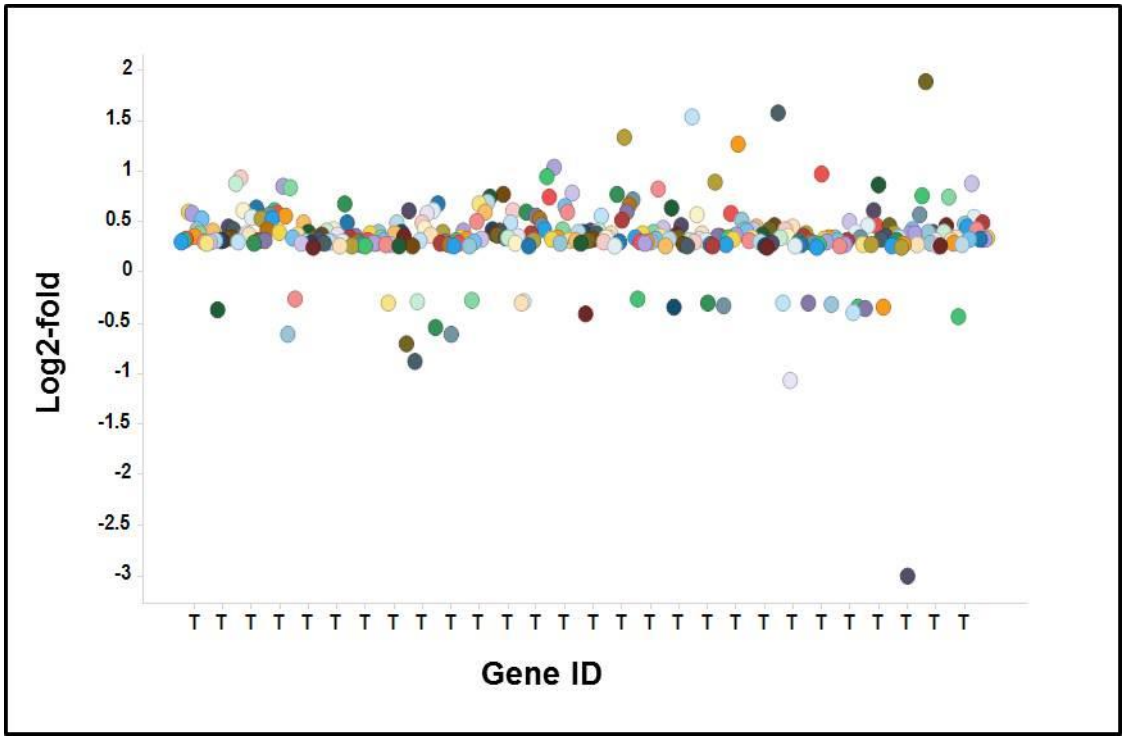

Figure 5.4: Scatterplot of log2-fold differential gene expression of overexpressing CARP3 against WT s427 cells. Majority of genes were about >±0.5 log2-fold expressed. T= Gene ID of each differentially expressed gene.

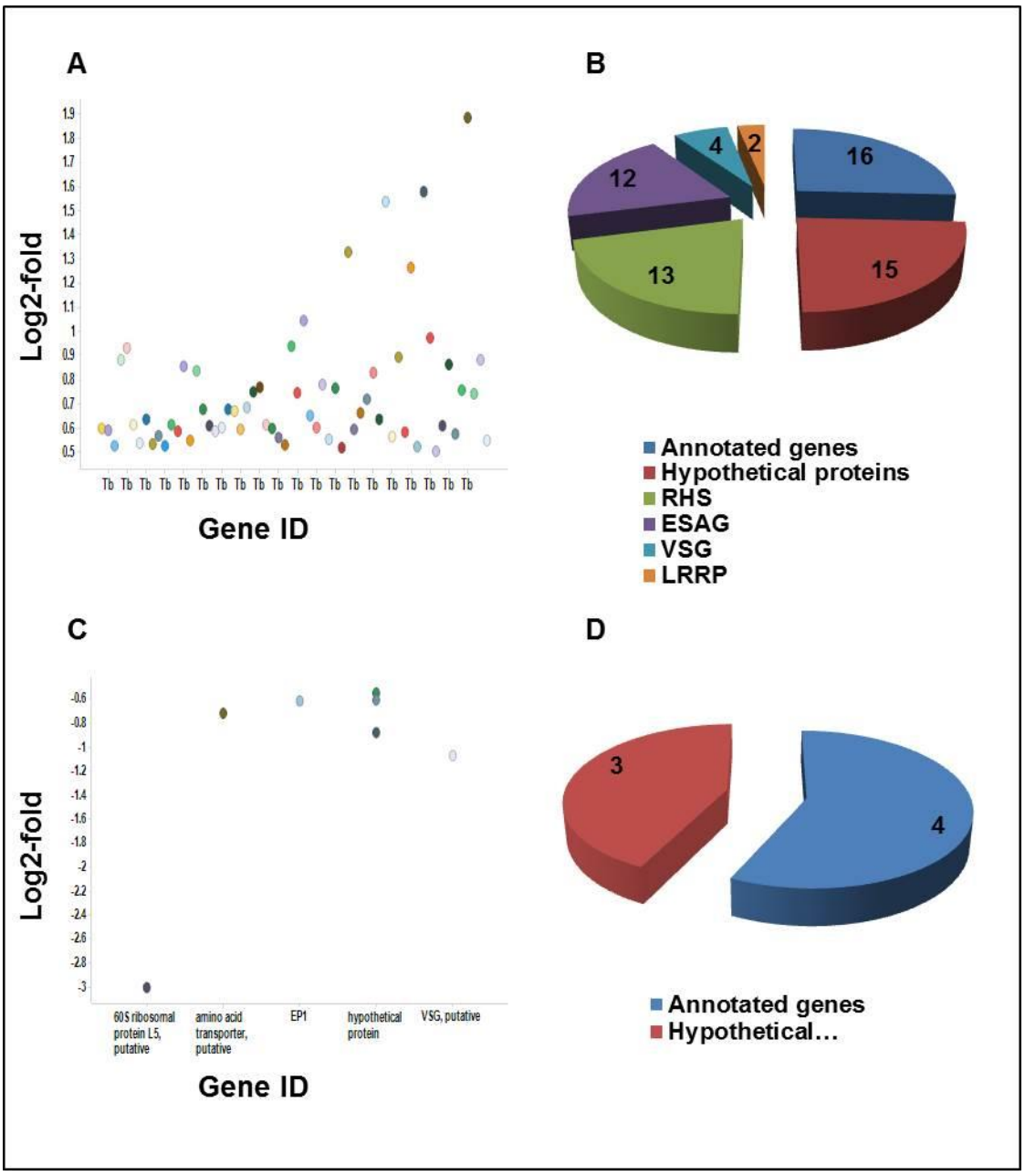

Figure 5.5: Scatterplot of log2-fold differential gene expression and distribution of genes showing >±0.5 log2-fold expression in overexpressing CARP3 against WT s427 cells. A) Majority of genes that were ≥0.5 log2-folds fell within 0.5-1 log2-fold increased expression. B) 16 of these genes have annotation and gene function, 15 were hypothetical proteins and 2 were leucine-rich repeat protein (LRRP). Only 7 genes were ≥0.5 log2-folds lower expressed than in the WT control cells (C). 4 were annotated proteins and 3 hypothetical proteins (D). RHS (retrotransposon hot spot), ESAG (expression site associated gene), VSG (variant surface glycoprotein)

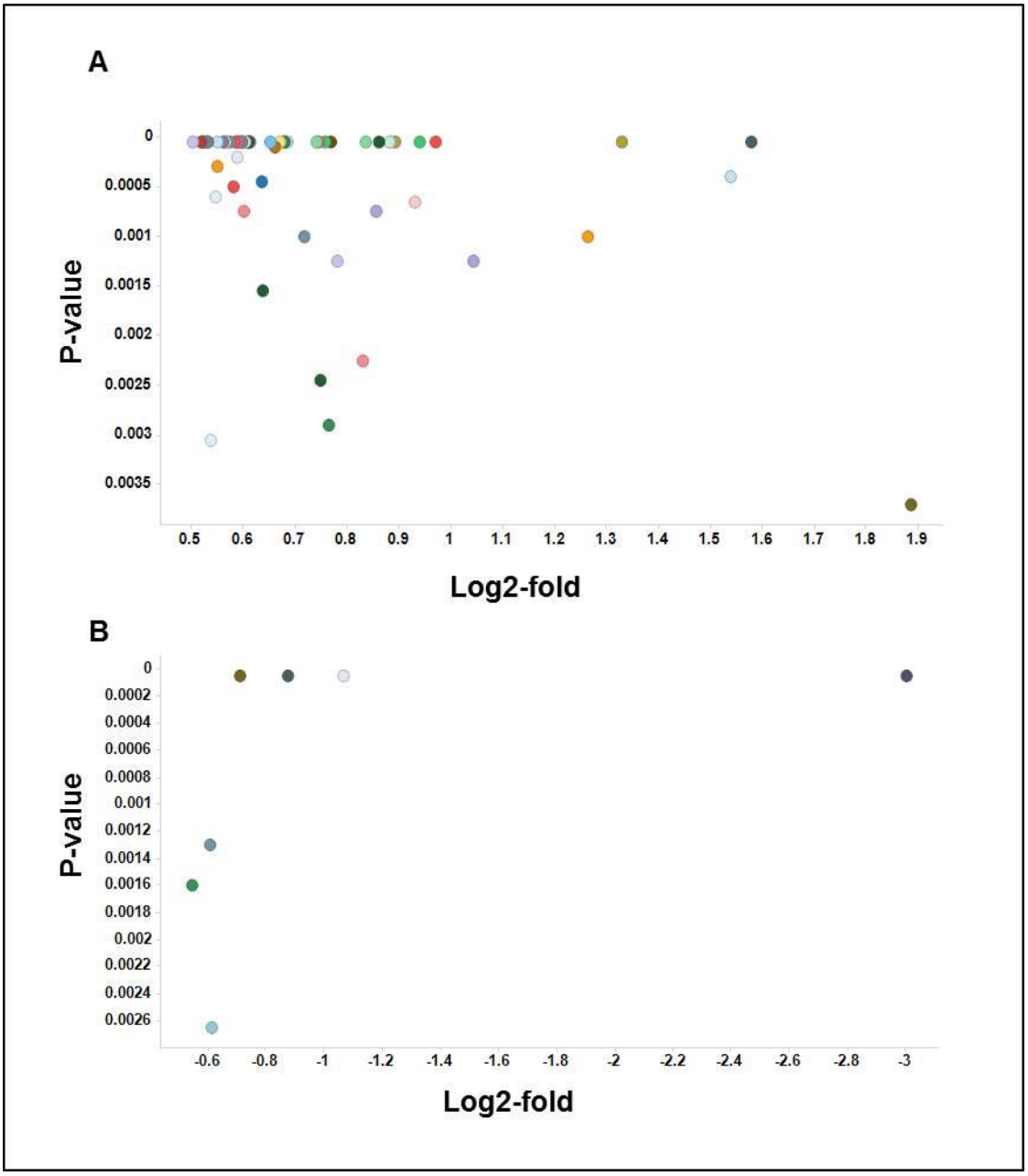

Figure 5.6: Scatterplot of p-value of genes >±0.5 log2-fold against log2-fold expression in CARP3 overexpressing and WT s427 cells. A-B) Majority of differentially expressed genes were highly significantly expressed having p-values of 5 x 10^{-5}.

Significantly more genes were differentially expressed in the R0.8 cells compared with those in CARP3^{oe} using WT s427 as a control. A total of 4103 genes were differentially expressed (Figure 5.7) with 10.4% (427) being functionally annotated. Of the differentially expressed genes, cut-off of ±0.5 log_2-fold shows 276 genes as being upregulated whilst 64 genes were down-regulated in R0.8 relative to WT s427 cells. Due to the large numbers of differentially expressed genes, a further filtering was performed using a cut-off

of ±0.75 log_2-fold. This resulted in 88 genes being upregulated, whilst 16 genes were downregulated (Appendix 5: Table 1 and 2). However, the categories of differential expressions were similar to that of CARP3^{oe} with majority of the highly expressed genes being hypothetical proteins (132), annotated genes (43) VSGs (29) and retrotransposon hot spot (RHS) protein, putative (26). Similarly, a majority of the down-regulated genes were hypothetical proteins (48) in addition to a number of annotated genes (14) (Figure 5.8). The majority of the genes were significantly expressed at p-value 5 x 10^{-5} (Figure 5.9). There were 12 receptor-type adenylate cyclase GRESAG4s that were highly expressed some of which were arranged in tandem on their chromosomes (Tb927.4.3860 and Tb927.4.3880), (Tb927.6.170, Tb927.6.310 and Tb927.6.3330) and others were not. The highest differentially expressed gene was a VSG (Tb927.9.1050) (5.02), whilst the lowest was a hypothetical protein (-2.15). The adenosine transporter TbNT6 (Tb927.2.6320) that was overexpressed in CARP3^{oe} was down-regulated in R0.8 with the same p-value (5 x 10^{-5}).

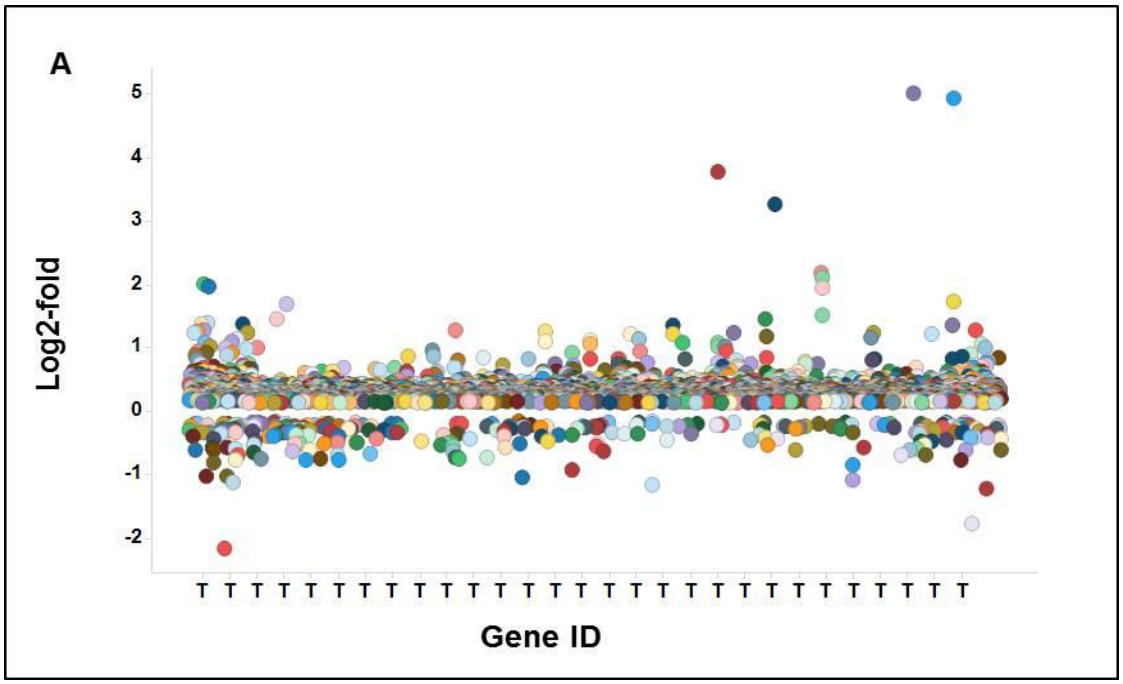

Figure 5.7: Scatterplot of log2-fold differential gene expression of CpdA resistant R0.8 against WT s427 cells. Majority of genes were about >±0.5 log2-fold expressed.

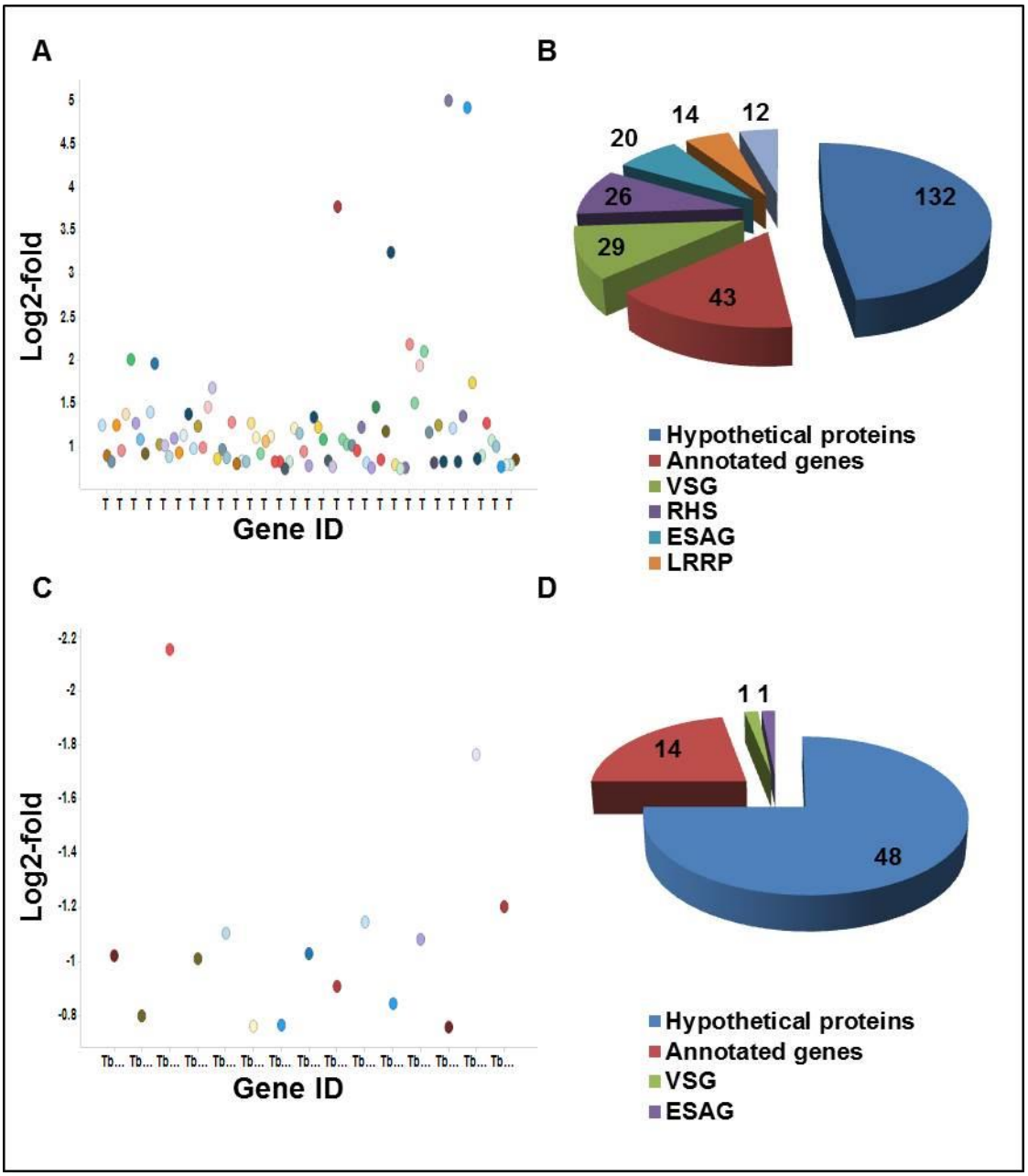

Figure 5.8: Scatterplot of log2-fold differential gene expression and distribution of genes showing >±0.5 and 0.75 log2-fold expression in R0.8 against WT s427 cells. A), C) Majority of genes were about 1 log2-fold differential expressed when ±0.75 log2-fold expression was used as the cut-off. B) 132 hypothetical genes, 43 annotated genes 20 ESAGS (expression site associated gene) and 12 GRESAGs (genes related to expression site associated genes) were all differentially expressed at a cut-off of >0.5 log2-fold expression. D) 48 hypothetical and 14 annotated genes were differentially expressed >-0.5 log2-fold expression. Leucine-rich repeat protein (LRRP), RHS (retrotransposon hot spot), ESAG and VSG (variant surface glycoprotein).

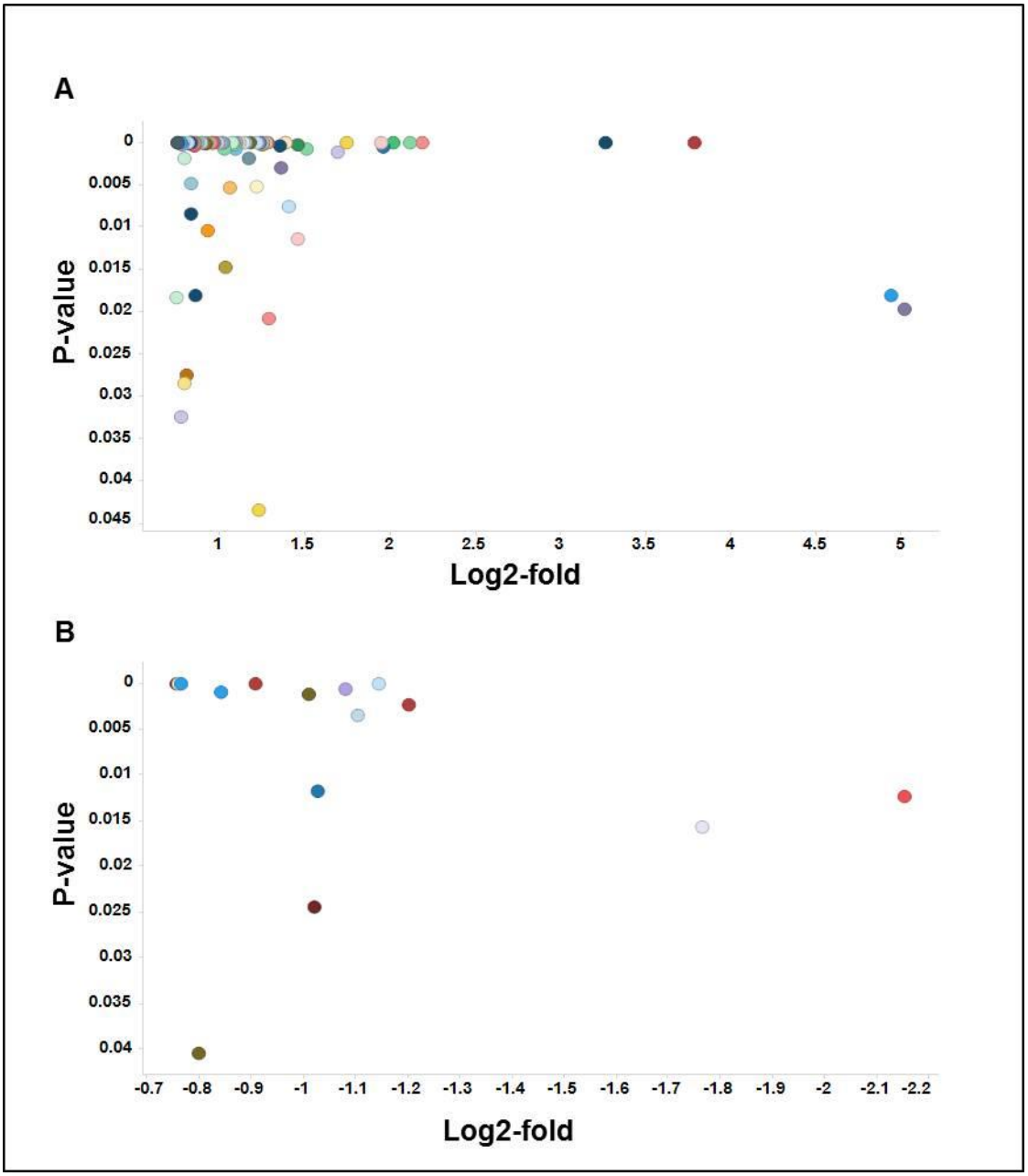

Figure 5.9: Scatterplot of p-value of genes >±0.75 log2-fold against log2-fold expression in R0.8 and WT s427 cells. A-B) Majority of differentially expressed genes were highly significantly expressed having p-values of 5 x 10^{-5}.

5.4 Discussion

The discovery of all the CARPs in the RIT-seq validates the genome-wide RNAi screen. It also confirms the assertion that there are more proteins involved in the downstream signalling of cAMP in *T. brucei*. The presence of adenylyl cyclases, (Tb927.4.4460 and Tb927.4.4470), a receptor-type adenylyl cyclase (Tb927.7.7530) and protein phosphatase (Tb927.11.1780) all important components of the known cAMP signalling cascade further cements the discovery of the role of CpdA in stimulating a cAMP release that triggers a downstream effector cascade. For example, Tb927.8.4640 was highly represented in the RIT-seq, indicating that its knockdown is associated with survival of high levels of cellular cAMP. This gene product has been annotated as a putative flagellar protofilament ribbon protein, which shares a high sequence identity to that of *T. cruzi* believed to be important in the formation and stabilization of doublet and triplet microtubule as well as their organization in a three-dimensional structure in *C. reinhardtii* (Norrander et al., 2000). This is consistent with previous findings that cAMP plays important roles in flagellar motility and signalling and that too high cAMP concentration disrupt cytokinesis. Additionally, in *C. reinhardtii*, triggering of zygote formation is initiated by cAMP signalling response as a result of flagellum adhesion in gametes (Pan and Snell, 2000). This together with CARP3 could be important in the CpdA induced phenotype observed in bloodstream forms as well as flagella motility. Recently, it has been shown that cAMP regulates social motility in procyclic *T. brucei,* with social motility absent when TbrPDEB1 was inhibited by CpdA or knocked down with RNAi. The reduction in PDEB activity appeared to disrupt the generation of an extracellular signal necessary for the behaviour, as the social motility was completely restored in mixed TbrPDEB1 knockdown and wild-type cells (Oberholzer et al., 2015). This is similar to social motility observation in *Dictyostelium discoideum* where cAMP signalling is critical for surface motility (Firtel and Meili, 2000). It is believed that the social motility exhibited by the procyclic forms is essential for their migration from the tsetse midgut to the insect's salivary gland, which allows it to complete it life cycle. In bloodstream forms of *T. brucei*, the most unambiguous role of cAMP is in cytokinesis, as either the knockdown of adenylyl cyclases (Salmon et al., 2012a), knockdown of TbrPDEB1 and B2 (Oberholzer et al., 2007) or the pharmacological inhibition of

these PDEs (de Koning et al., 2012) all lead to severe defects in the cytokinesis phase of cell division, resulting in misshaped cells with multiple nuclei and kinetoplasts, that are ultimately non-viable. The roles of these new RIT-seq proteins are currently being validated.

Co-IP with the CARP3 polyclonal antiserum followed by MS in all three replicates pulled down CARP3 protein; CARP3 pull down was not present in pull downs with the anti-CARP1 and anti-CARP2 antisera, which incidentally displayed at best marginal selectivity for their target proteins. This clearly confirmed that the pull-down worked and the technique was sound. At least one peptide sequence from the trypsin digest of CARP3 from all three pulldown has either one predicted ubiquitination site or is directly flanked by a ubiquitination site consistent with the *in-silico* prediction of ubiquitination as well the potential role of ubiquitination in the regulation of CARP3 protein abundance. Additionally, three adenylyl cyclases (Tb927.4.4460, Tb927.4.4410 and Tb927.4.4440) were pulled-down more than once with CARP3. These have high protein score (75), peptide score (58) and expect values (3.7×10^{-5}). Interestingly, these were unique to CARP3 pulldown only and were not found in either CARP1 or CARP2 pulldown assays. Two additional proteins (Tb927.10.2610 formerly (Tb10.70.5060) and Tb927.9.16060 formerly (Tb09.244.1960) also appeared more than once in the pulldown. Domains found on Tb927.10.2610 (Tb10.70.5060) include 4x Domain of Unknown Function (DUF) which is also found in the cysteine protease (Calpain) and a small myristoylated protein. Calpains are ubiquitous calcium-dependent cysteine proteases that are thought to function in stimulating Ca^{2+} signalling resulting in a wide-range of cell regulation and differentiation processes (Liu et al., 2010). Ersfeld et al, classified all calpain-like proteins in the various kinetoplastids into families using data mining and sequence analysis with Tb10.70.5060 being classified in the class 1 domain of small kinetoplastid calpain-related protein (SKCRP) (Ersfeld et al., 2005). The presence of myristoylated protein and its acylation is usually know to result in membrane association (Resh, 1999) which was confirmed when related SKCRPs localized to flagellar membrane, flagellum and even the tip of flagellum (Liu et al., 2010). Thus Tb927.10.2610 could be a very important partner of CARP3 in the downstream regulation of cAMP. Tb927.9.16060 however is a small protein (11 kDa) with no annotated domains. Twelve proteins that

were pulled down more than once with CARP3 were also found in either CARP1 (10) or CARP2 (2) pulldowns. Five were conserved hypothetical proteins, 3 VSGs, 1 each of 60S and 40S ribosomal proteins. Two of the proteins Tb927.9.8740 (DRBD3 RNA-binding protein, putative; DRBD3) and Tb927.9.4680 (1L12.525 eukaryotic initiation factor 4a, putative) have been shown in an RNAi high through put phenotypic screening to cause abnormal cell proliferation in BSF (Alsford et al., 2011b).

Thirty-six proteins uniquely co- immunoprecipitated with CARP3. These include proteins of the proteasome complex such as Regulatory Protein Network (RPN6, RPN7 and RPN11) and TbPSA6 proteasome alpha 1 subunit, putative; 20S proteasome subunit alpha-6, putative. The presence of these proteins as apparent interactors is consistent with CARP3 domain annotations as well as the observed rapid downregulation of CARP3 protein under specific conditions. There were also two receptor-type adenylate cyclases Tb927.4.4470 and Tb927.8.7590. Tb927.4.4470 had similar protein (75), peptide (58) and expect score (3.7×10^{-5}) as those found in more than 1 pulldown. Additionally, it was one of the hits in the RIT-Seq similar to Tb927.4.4460. The interaction with multiple adenylate cyclases further confirms the regulatory role of CARP3 on ACs and hence on cAMP production and levels in the cell. Six additional uniquely associated CARP3 proteins have been shown to have abnormal phenotypes in RIT-seq analysis (Alsford et al., 2011b). Tb927.10.1060 (TCP-1-delta t-complex protein 1, delta subunit, putative) is detected in plasma membrane fractions of BSF and is indicated to be important in translation initiation in eukaryotes (Dhalia et al., 2005). Tb927.5.3400 (calcium-translocating P-type ATPase; calcium pump) is also enriched in BSF plasma membrane fractions is directly involved in ATP-dependent Calcium transport across the plasma membrane as well as ATP-biosynthesis. Tb927.7.6290 (kinesin, putative) has been shown to localized exclusively to the axoneme and very important in cilium-dependent cell movement (Demonchy et al., 2009). Knockdown of Tb927.7.6290 (TbKIF9A) although did not affect flagella structure and components resulted in defective cell motility (Demonchy et al., 2009). Increase in cAMP due to either knockdown of TbPDEB1 or pharmacological inhibition has been shown to significantly inhibit cell motility (Oberholzer et al., 2015). Overexpressing CARP3 results in significant increase in cAMP and its association with KIF9A could lead to reduced

motility. Translation elongation factor 1-alpha; TEF-1-alpha (Tb927.10.2090) detected in both BSF cytoskeleton and plasma membrane fractions has been shown to experimentally bind to Calmodulin and involved in calcium-mediated signalling (Kaur and Ruben, 1994). Tb927.11.7170 (seryl-tRNA synthetase, putative) localizes mostly to the cytosol with an aminoacylation site that differ from other species. RNAi ablation of this protein results in cell death which is indicative of the essentiality of the enzyme (Geslain et al., 2006). Tb927.11.9530 (14-3-3-1 like protein, putative) is of a class of highly conserved eukaryotic proteins that functions as molecular chaperones involved in important cellular processes such as cell survival and signalling through protein-protein interaction that inhibits other protein-protein interactions or by causing conformational changes (Dougherty and Morrison, 2004; Inoue et al., 2005). In trypanosomes the proteins are diffusely distributed and when knocked down resulted in cells with defective motility, significant growth rate reduction and morphological changes akin to inhibition of cytokinesis and cell cycle progression (Inoue et al., 2005). These features were similar to the phenotype observed when CARP3 was over expressed in the presence of CpdA. It has been shown that mammalian 14-3-3-1 proteins complex with Protein Phosphatase 1 (PP1) and 2A (Pozuelo Rubio et al., 2004) both of which play important roles in mammalian cell cycle and sperm motility (Huang et al., 2004). Inhibiting *T. brucei* and *T. cruzi* protein phosphatases results in multinucleated cells characteristic of cell cycle defects (Das et al., 1994; Orr et al., 2000). This suggests that protein phosphatases through de-phosphorylation regulate the activity of 14-3-3 proteins by disruption protein-protein interactions leading to aberrant cytokinesis and cell division. Importantly, CARP3 have a TPR which is believed to be involved in protein-protein interaction and important to its regulatory function. Interestingly, RIT-seq revealed a protein phosphatase 2 as one of the downstream effectors of cAMP signalling. Thus together, CARP3, 14-3-3-1 and PP2 could be involved in a complex regulatory mechanism that drives phenotype observed in the inhibition of TbPDEB1 with CpdA; this process is exacerbated when CARP3 is overexpressed due to its influence on cAMP levels through direct interaction with the cyclases, and the concomitant effect on its turnover and thus regulatory activity.

There were several hypothetical conserved proteins (9) and VSGs (7) that immuno-precipitated with CARP3 only were not found in CARP1 or CARP2 pull downs. Forty-nine proteins were found in either CARP1 or CARP2 pull-down whilst 61 were found in both pull downs. Further work is ongoing to confirm this, among other interactions, to help better define the downstream cAMP signalling cascade in *T. brucei*.

Most of the genes differentially overexpressed in CARP3^{oe} were annotated genes. Genes such as Gim5A (Tb927.9.11580) a glycosomal membrane protein and CFB1B (Tb927.1.4560) cyclin-like-F-box protein have been implicated in abnormal cell proliferation (Alsford et al., 2011a; Alsford et al., 2011b) and growth arrest due to inhibition in cytokinesis (Benz and Clayton, 2007). Tb-17, a flagellar calcium-binding protein is important in cilium or flagellum dependent cell motility through calcium ion transport and binding (Wu et al., 1994). The three nucleoside transporters TbNT2/927, TbNT4 and TbNT6 could be important components of the extrusion of cAMP from the cell. These transporters have the classical transmembrane domains and are involved in an ATP-dependent active uptake of purines (de Koning and Jarvis, 1999; Sanchez et al., 1999). They have also been linked with nifurtimox efficacy and potential resistance when knocked down using RNAi (Alsford et al., 2012b). Another upregulated transporter is the nucleoside transporter 1, (Tb927.9.15980) with 11 transmembrane domains and similar attributes to that of the other transporters. It has previously been designated as TbNT11.1 and shown to transport pentamidine in *Xenopus* oocytes (Ortiz et al., 2009). Two tandemly arranged amino acid transporters were found to be either overexpressed (Tb927.11.15960) or under expressed (Tb927.11.15950). Both genes were found to be curated in a RIT-Seq phenotype to have abnormal cell proliferation in bloodstream form trypomastigotes. Overexpressing CARP3 results in a significant extrusion of cAMP which results in significant increase in extracellular cAMP. Extrusion of cAMP is an ATP-dependent active process which could be undertaken by one of these transporters or possibly one of the hypothetical proteins.

Most of the differentially expressed genes in R0.8, relative to WT s427, displayed differences 0.75 log2 fold differential expression and are annotated as hypothetical proteins, VSGs, RHS (retrotransposon hot spot) proteins and LRRPs

(leucine-rich repeat protein). The few interesting genes include the GRESAG4s. These are important because R0.8 has a higher tolerance to cAMP and also secretes more extracellular cAMP than WT s427. Thus it is most likely that in the process of adapting to higher concentrations of CpdA, during the generation of this resistant line, these genes were upregulated. This is similar to the fact that besides CARP3 (with log_2-fold differential of 0.005) which was not differentially expressed, CARP1 (0.26), CARP2 (0.35) and CARP4 (0.21) were all significantly log2 differentially expressed although below both 0.5 and 0.75. Additionally, both TbPDEB1 (0.09) and TbPDEB2 (0.12) were not differentially expressed. This contrasts with the fact that knockout of these CARPs and overexpression of TbPDEB1 causes significant resistance to CpdA. It was also previously shown that none of the CARPs were mutated in R0.8 cells when the genes were extracted, cloned into *E. coli* and Sanger sequenced (Gould et al., 2013). Thus it is likely that resistance to CpdA will involve several protein components of which some will be hypothetical proteins, GRESAG4s, possibly ESAGs, CARPs and other annotated proteins. The fact that CARP3 and the TbPDEB1/2 were both not differentially expressed could be indicative of their importance in the manipulation and signalling of cAMP and hence will be under tighter regulation. Only a few genes were downregulated. Serine threonine-protein phosphatase PP1, putative (Tb927.4.3630) was differentially down regulated with a log2 fold of -1.14. It has been implicated in quorum sensing as a component of the stumpy induction factor (SIF) signalling pathway (Mony et al., 2014). This could be important in the reduced growth rate of R0.8 cells compared with WT s427 as it could decrease stumpy formation and thus cell death in *in vitro* assays. Interestingly, one of the nucleoside transporters TbNT6 was also down regulated as well as a few hypothetical proteins and ESAGs.

Chapter 6

General Discussions

6.0 General Discussion

A major collaborative effort from the WHO and its partners have resulted in a drastic decline in the deaths and levels of infection in trypanosomiasis (Simarro et al., 2011). This decline has been achieved using the present therapeutic options although they are old, toxic and difficult to administer (Barrett, 2010; Delespaux and de Koning, 2007; Jacobs et al., 2011a; Kennedy, 2008a).Yet the current increase in resistance to these drugs is very worrying (Baker et al., 2013; Simarro et al., 2012a; Vincent et al., 2010).Thus the possibility of failure of the current treatment options together with previous experiences with recurrent epidemics even after near-eradication, migration and the instability in many endemic regions calls for caution in relation to the current optimism about elimination of the disease (Blum et al., 2012; Mumba et al., 2011; Odiit et al., 2005; Picozzi et al., 2005). However, the above problems are compounded by the fact that almost all of the current drugs used for treatment do not meet present day pharmacological standards. This is mostly due to the toxic nature of these drugs to humans. Thus the pipeline of drug discovery needs to remain open and be filled with potential candidates to ensure that the drive for elimination is sustained. To do this, there is a need to understand the cell biology of the trypanosomes, so as to develop drugs that are trypanosome target specific and therapeutically beneficial. One recent approach was to apply drug repurposing which is a cheaper and more affordable way to fill the drug discovery pipeline (Pollastri and Campbell, 2011) especially for neglected tropical diseases (NTDs).

One of the more interesting and important candidates for repurposing in trypanosome diseases are PDE inhibitors. PDEs have long been recognised as very amenable druggable targets (Bender and Beavo, 2006). This is because their substrate cAMP and cGMP have been found in every tissue and that their degradation can often make a more rapid and larger percentage change in concentration than comparable regulation of the rates of synthesis (Bender and Beavo, 2006). They are usually large in numbers (11 genes in humans), each of which often have unique architecture and quite often physiological function, isoform specific and catalytically dependent activity within the same PDE as well as tissue or cell specific activity due to compartmentalization (Bender and Beavo, 2006; Dorsey et al., 2010; Francis et al., 2011c; Galie et al., 2010;

Ghofrani et al., 2006; Jaski et al., 1985; Johner et al., 2006; Maurice et al., 2014; Omori and Kotera, 2007b). Major efforts, and important successes, are ongoing in the pharmacological exploitation of human PDEs (Azam and Tripuraneni, 2014; Chen et al.; Fallah, 2015; Maurice et al., 2014). The kinetoplastid genomes all code for the same set of cyclic nucleotide-specific class 1 type phosphodiesterases with catalytic domains similar to those of the human PDEs (Beavo, 1995; Kunz et al., 2006). *Trypanosoma brucei* codes for 4-5 PDEs which are TbPDEA, TbPDEB1/B2, TbPDEBC and TbPDED; PDEB1 and B2 are almost identical. This, on the one hand makes them great targets for compounds or drugs that target human PDEs, whilst on the other, raises the issue of toxicity. However, this toxicity could be ameliorated by studying the structure activity relationships (SAR) of individual PDEs with the aim of making the PDE inhibitor more *Trypanosoma* PDE specific and reduce potential side effect. *Trypanosoma brucei* PDEB1/2 was previously shown to be essential for cell proliferation with both *in vitro* and *in vivo* inhibition using RNAi leading to severe cell cycle defects and cell death with an attendant several fold increase in cAMP (Oberholzer et al., 2007). CpdA, tetrahydrophthalazinone compound was shown to inhibit TbPDEB1 and TbPDEB2 at low nanomolar concentrations affecting trypanosome viability similar to the RNAi knockdown (de Koning et al., 2012). Similarly, CpdA raises cAMP levels several folds resulting in cytokinesis defect (de Koning et al., 2012).

Cyclic AMP has been implicated in several developmental and lifecycle effect in trypanosomes since it was first discovered. It has been associated together with stumpy induction factor “SIF” to be involve in driving differentiation of long slender BSF to short stumpy forms (Mancini and Patton, 1981) similar to quorum-sensing systems found in microbial communities (Waters and Bassler, 2005). Some hydrolysable cAMP analogues have been shown to drive differentiation of long slender BSF to short stumpy forms together with genes involved in purine metabolism and signal transduction (kinases, phosphatases) to gene expression regulators (Mony et al., 2014). Additionally, cAMP regulation through adenylate cyclases (ACs) have been implicated in defective cytokinesis and the manipulation of the immune response to trypanosome infection (Salmon et al., 2012b). Cyclic AMP through Protein Kinase A stimulation has been shown to drive differentiation in *T. cruzi* (Flawia et al., 1997), promastigote proliferation and

infectivity in *Leishmania amazonensis* (Genestra et al., 2004), and flagellar motility and signalling in *T. brucei* procyclics (Oberholzer et al., 2015; Rotureau et al., 2009; Tetley and Vickerman, 1985). Pharmacological inhibition of TbPDEB1 by CpdA has been shown to disrupt the generation of an extracellular signal necessary for social motility (Oberholzer et al., 2015) the behaviour confirming the importance of TbPDEB1 inhibition derived increase in cAMP in the cellular activity of the trypanosomes.

However, the TbPDEB family has been shown to be pharmacologically highly similar to the human PDEs, particularly hPDE4, such that piclamilast, a human PDE4 inhibitor and several of its analogues inhibited the TbPDEB isoforms (Bland et al., 2011). Furthermore, CpdA the most potent TbPDEB inhibitor discovered to date, was found to be an even more potent inhibitor of human PDE4 (Van der Mey et al., 2001a; Van der Mey et al., 2001b). The discovery of P-pocket in the crystal structure of the highly conserved catalytic domain of LmjPDEB1 (Wang et al., 2007), could theoretically allow for the development of kinetoplastid specific PDE inhibitors with minimal or no cross reactivity with mammalian PDEs. This provides some optimism that it is feasible, through a structure-driven QSAR approach, to develop selective inhibitors of some of the trypanosomatid PDEs that have been shown to be essential (Amata et al., 2015; Amata et al., 2014; Blazer et al., 2010; de Koning et al., 2012).

Alternatively, to overcome the lingering potential toxicity effect, proteins downstream of TbPDEB1 inhibition and cAMP signalling could offer new therapeutic targets that are unique to trypanosomes. Thus using CpdA, Gould et al., applied a genome-wide RNAi *T. b. brucei* RNA library (Alsford et al., 2012b; Alsford et al., 2011b; Baker et al., 2011) to select for genes driving resistance under CpdA pressure which were designated cAMP Response Proteins (CARPs) CARP1-4. Targeted RNAi knockdown of these CARPs confirmed a significant increase in resistance to CpdA and to elevated cellular cAMP levels, confirming that they are real downstream effectors of cAMP signalling. One of the genes knocked down in the CpdA-resistant cultures was Tb427tmp.01.7890 (*CARP1*; Tb927.11.16210 in *T. brucei brucei* reference strain TREU 927), encoding a 705-amino-acid protein containing two apparently intact and one partial cyclic AMP binding-like domains that is conserved in synteny in each of the kinetoplastid

genomes sequenced. Recently, the homolog of CARP1 in *T. cruzi* TcCLB.508523.80 has been revealed to bind cyclic nucleotides, using cAMP and cGMP displacement assays (Jäger et al., 2014) further validating the role of CARP1 as a downstream cAMP signalling effector. CARP2-4 are proteins of as yet unknown functions but some of them have probable flagellar localisation, consistent with a role in mediating or regulating a cAMP signal (Gould et al., 2013). CARP1 and CARP3 are kinetoplastid specific with CARP3 being trypanosome specific. CARP2 and CARP4 are well conserved among the kinetoplastida but found in other species too. However, it was still important to determine which of these CARPs or which combination if any drives the observed phenotypic response of cytokinesis defect. Thus the characterization of the CARPs could reveal unique kinetoplastid targets for drug discovery and dramatically increase our understanding of the downstream cAMP signalling cascades, and of the cell biology of the trypanosome.

Single gene deletion of any of the CARPs decreased the sensitivity of *T. brucei* bloodstream forms to CpdA as expected from the RNAi knockdown phenotypes (Gould et al., 2013) but not cell growth in standard medium. However, double gene deletion resulted in a significant loss of growth fitness in CARP2 null mutant cells. This was accompanied by a significant increase in intracellular cAMP in these cells compared with WT s427. Either the loss of gene function or the sharp increase in cAMP levels, or likely the combination of both, resulted in the growth phenotype as the loss of both CARP3 and CARP4 genes and increase in cAMP did not show the same phenotype. CpdA causing a cAMP increase in these cells restored growth to levels of WT s427 in similar condition and further drives cAMP increase in this cell confirming that loss of gene rather than increase in cAMP was responsible for the delay in growth in these CARP2 dKO. However, significant increase in cAMP in only the null mutants suggests that these proteins are important in the downstream dissemination of cAMP. Thus inhibition of CARP2 could results in a direct therapeutic intervention in trypanosomiasis although CARP2 dKO cells can, with difficulty, be generated. This is unsurprising since CARP2 has been detected in proteomes of *T. brucei brucei* flagellum (Broadhead et al., 2006) and of cytoskeletal and plasma membrane fractions (Bridges et al., 2008), as well as in an *in silico* predicted proteome of the flagellar and basal body of *Chlamydomonas reinhardtii* (Li et

al., 2004; Merchant et al., 2007). The flagellum is a very essential feature in flagellated organisms. For example it is commonly believed that the flagellum, as an important host-parasite interface, has essential sensory functions (Rotureau et al., 2009; Tetley and Vickerman, 1985). For example in *C. reinhardtii*, triggering of zygote formation is initiated by cAMP signalling response as a result of flagellum adhesion in gametes (Pan and Snell, 2000). However, there is no known function, and no recognizable functional domains identified in any of the homologues of CARP2. Thus it is annotated to have a Domain of Unknown Function (DUF) of which there are about 3600 (Punta et al., 2012) and about 1,500 in eukaryotes (Goodacre et al., 2014). Thus there would be a high potential of off target effect especially since there are similar homologues in other organisms.

Overexpressing of CARP1, 2 and 4 did not result in any differences in cAMP levels compared with WT s427. The cells were not sensitized to CpdA and their growth with or without CpdA were not significantly affected. However, their expression levels decreased significantly in WT s427 cells but increased significantly in R0.8 cells when CpdA was added to the medium. In contrast, overexpressing CARP3 results in a growth phenotype in the presence of CpdA, significant sensitivitization to CpdA, an increase in both the basal and CpdA-induced intracellular and extracellular concentrations of cAMP, and a significant decrease in mRNA and protein levels in CpdA in both WT s427 and R0.8 cells. The fact that both the sensitization to CpdA and growth are associated with dramatic increases in cAMP levels and decrease in CARP3 transcript and protein levels suggests that both factors are required for these observations to occur. This was further confirmed in both the WT s427 and R0.8 control cells which , in the presence of CpdA, both CARP3 transcript and protein levels decreasing (WT s427) or unchanged (R0.8) unlike the other CARPs in either WT s427 or R0.8.

In silico predictions of CARP3 motif and annotations shows the presence of tetratricopeptide repeat (TPR) and Protein database (PDB) annotations such as signalling protein, membrane protein, protein binding/transport protein, Peroxisome Targeting Signal 1 Receptor (PEX5), Regulatory Protein and ubiquitination sites among others (Biasini et al., 2014; Kelley and Sternberg, 2009; Radivojac et al., 2010; Yang et al., 2015). These predictions were

validated in the Co-IP and MS of CARP3 with the detection of several proteasome regulatory proteins (RPNs), PSA4 proteasome alpha 7 subunit, UBA1 ubiquitin-activating enzyme E1, putative, membrane and flagellar binding proteins, GRESAG4s and ESAGs and signalling proteins. Thus it is likely that cAMP above a certain threshold will cause ubiquitination of CARP3, priming it for transport to the proteasome for degradation. CARP3 protein degradation in turn could signal a reduction in the production of CARP3 through a reduced steady-state level of its mRNA. This would explain both the down regulation and CARP3 protein turn over after the addition of CpdA. Thus clearly, the presence of CARP3 and an increase in cAMP to a certain threshold level is required to cause the phenotype of cytokinesis defect which results in growth delays. Importantly, the GRESAG4s (Tb927.4.4460 and Tb927.4.4470) were also hits in the RIT-seq among several important signalling mediated proteins. The fact that these GRESAG4s were only found in the CARP3 pulldown and not in any of the CARPs pulldown validates the role of CARP3 as a protein involve in a protein-protein interaction as well as a regulator of cAMP levels through regulation of ACs. This explains why CARP3 was the only CARP that significantly increased cAMP when overexpressed. The regulation of GRESAG4 (Tb927.4.4460) was validated by showing that there is a direct relation of reduction in CARP3 mRNA and protein levels, and the abundance of GRESAG4 (Tb927.4.4460) transcript.

Preliminary IFA show CARP3 localizes to the plasma membrane confirming previous observations of CARP3 peptide detection in the plasma membrane and flagellar of both BSF and PCF (Bridges et al., 2008; Subota et al., 2014). Prediction analysis indicates the possibility of CARP3 undergoing both myristoylation and palmitoylation both of which could lead to dual localization as observed for POMP39 (Albisetti et al., 2015).

Overexpressing CARP3 led to significant overexpressing of Gim5A (Tb927.9.11580) a glycosomal membrane protein and CFB1B (Tb927.1.4560) cyclin-like-F-box protein among several hypothetical proteins and nucleoside and amino acid transporters. RNAi against Gim5A have been implicated in abnormal cell proliferation (Alsford et al., 2011b) whilst overexpression of CFB1B results in reduced cell proliferation and growth arrest due to inhibition in cytokinesis (Benz and Clayton, 2007) similar to CpdA effect. Tb-17, a flagellar calcium-

binding protein is important in cilium or flagellum dependent cell motility through calcium ion transport and binding (Wu et al., 1994). Both CARP3 (0.005) and TbPDEB1 (0.09) were not significantly differentially expressed in R0.8 cells probably indicative of their importance in cAMP manipulation and regulation.

6.1 Proposed model of the role of CARP3 in the regulation and downstream signalling of cAMP in Trypanosoma brucei

Based on the above findings, we proposed a role for CARP3 as an important and integral component of the downstream signalling of cAMP in *T. brucei*. The addition of CpdA inhibits TbPDEB1 which leads to an accumulation of cAMP. The accumulation of intracellularly cAMP subsequently causes an increase in extrusion of cAMP from the cell. The accumulation of cAMP above a certain threshold possibly causes CARP3 to be ubiquitinated leading to it being likely targeted to the proteasome to be degraded. This proposed degradation is thought to subsequently result in a significant reduction in mRNA of Tb927.4.4460 (GRESAG4.4B), although it is unclear at this moment by which mechanism. Reduction of (GRESAG4.4B mRNA) should in turn decrease the conversion of ATP into cAMP. Finally, degradation of CARP3 is conjectured to lead to disruption of CARP3-protein interactions which probably drives cellular regulation processes such as cytokinesis, cell motility and other important flagellum functions.

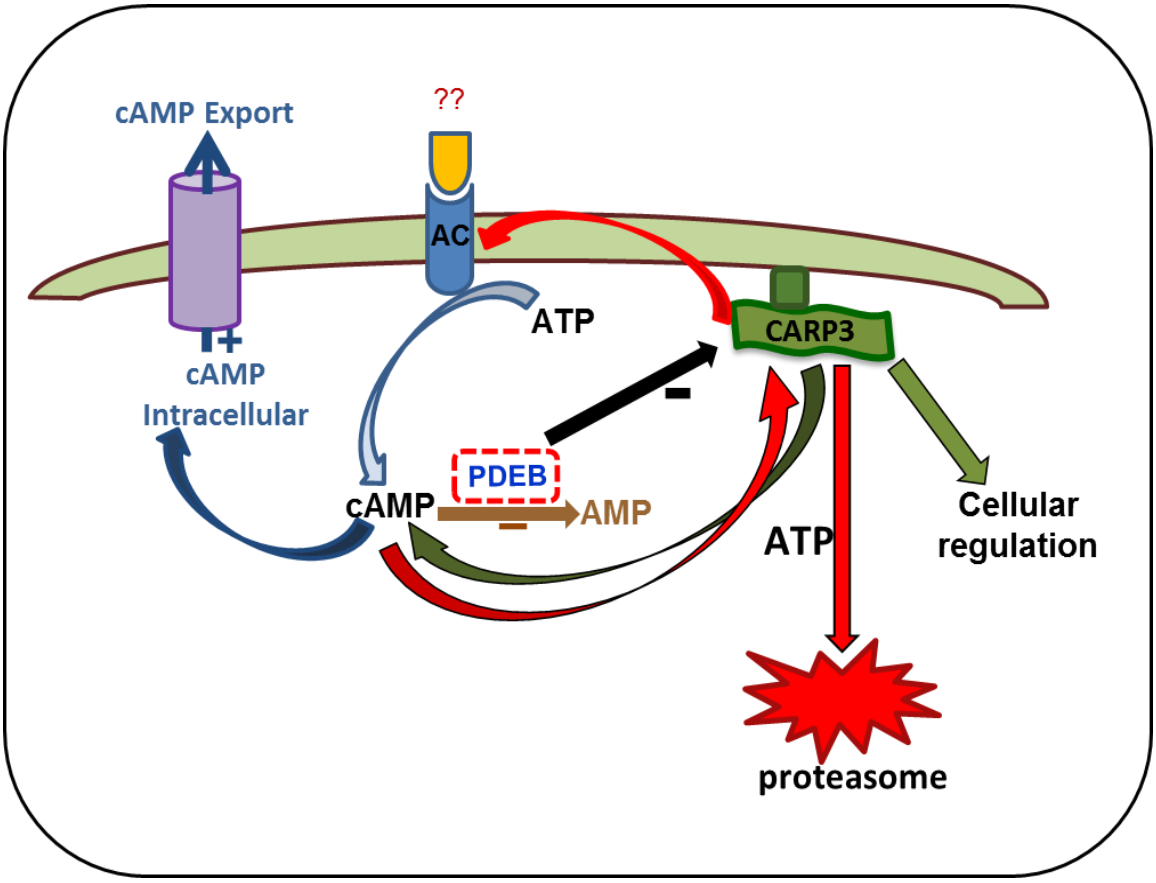

Figure 6.1: Proposed model of the role of CARP3 in the regulation and downstream signalling of cAMP in *Trypanosoma brucei*. The figure shows CARP3 interacting with the various components of the cAMP signalling and the role of CpdA in triggering this cascade that leads to cellular regulation.

The crystal structure of CARP3 is presently being determined in collaboration with **Dr David Brown of the University of Kent**. This will provide a structure of CARP3 and further confirm the various annotated regions determined from the *in silico* modelling as well as from the various hits from the Co-IP and MS. With the structure in place, potential experiments to validate certain components of the model will include,

1. Expressing a truncated version of CARP3 without the TPR to confirm its involvement in a protein-protein interaction, or alternatively, a mutated version with a disrupted TPR domain
2. Use of a proteasome inhibitor to confirm or otherwise proteasome mediated CARP3 degradation
3. Yeast-2-Hybrid analysis of CARP3 and some of the key proteins from both the Co-IP and RNA-seq.

Finally, the arrangement (positioning) of the various CARP proteins downstream of the signalling cascade (stream) will provide very interesting answers as to how

cAMP is signalled down after TbPDEB1 inhibition. The confirmation of interactions of CARP3 with if any of the other CARPs or, our investigation indicates, interaction with other proteins would provide valuable insights into the downstream cascade of cAMP of trypanosomes.

Appendix 1: Table of primers used in genetic manipulation of *T. brucei*.

Table 1.1: Primers for amplification of Untranslated Regions (UTRs) of the CARPs for the making of pMB homologous gene replacement of antibiotic constructs

Gene	Primer name	Position	Res. site	Sequence
CARP1	HDK369	5'Forward	NotI	5'- CGCGGCCGCGGCATGGAAGCAAACCA-3'
	HDK370	5'Reverse	XbaI	5'- CGTCTAGAGCCAACCACCAGTTGTGG-3'
	HDK371	3'Forward	NsiI	5'- GATGCATAGATGTGAAGCGGACACC-3'
	HDK372	3'Reverse	XhoI	5'- GCTCGAGACTGCCCATACATTGCGG-3',
CARP2	HDK372	5'Forward	NotI	5'- CGCGGCCGCAGGGGACCGCAGTTGCA-3''
	HDK374	5'Reverse	XbaI	5'- CGTCTAGAGGATACGGCACCACCGGG-3'
	HDK375	3'Forward	NsiI	5'- GATGCATCCCTAGCTTTTACCTTGG-3'
	HDK376	3'Reverse	XhoI	5'- GCTCGAGATTGTGTTGAGGGAGCCC-3'
CARP3	HDK377	5'Forward	NotI	5'- CGCGGCCGCGCCGCCGCATTATCACT-3'
	HDK378	5'Reverse	XbaI	5'- CGTCTAGACAAGCGTGACAATTGCAC-3'
	HDK379	3'Forward	NsiI	5'- GATGCATGGATGGGTGGATGTGAGA-3'
	HDK380	3'Reverse	XhoI	5'- GCTCGAGATATTTCCGCCCGCTCCT-3'
CARP4	HDK471	5'Forward	NotI	5'-GATCGCGGCCGCCTTGCCCCATATAAC-3'
	HDK472	5'Reverse	XbaI	5'-GATCTCTAGATGCAACTAATTAAAATC-3'
	HDK589	3'Forward	NsiI	5'-GCCTATGCATGGTGGATACACATCTTGTC-3'
	HDK590	3'Reverse	XhoI	5'-GATCCTCGAGTCAACGGATTTATACCA-3'

Table 1.2: Primers for amplification of Open Reading Frame (ORF) of the CARP genes, for making of pHD1336 over-expression constructs

Gene	Primer name	Position	Res. site	Sequence
CARP1	HDK361	Forward	ApaI	5'-GGGGCCCATGGGTAGTTATGAATACCC-3'
	HDK362	Reverse	BamHI	5'-GGGATCCTTACCTTTTCGCCATGAACT-3'
CARP2	HDK363	Forward	ApaI	5'-GGGGCCCATGCGAATACTTGCAGACTT-3'
	HDK364	Reverse	BamHI	5'-GGGATCCCTAGTTCTTACGGCGCGTAA-3'
CARP3	HDK365	Forward	ApaI	5'-GGGGCCCATGGGAGGAGGTTCATCCGT-3'
	HDK366	Reverse	BamHI	5'-GGGATCCTTAGTTCAATTGGTCATCAA-3'
CARP4	HDK475	Forward	ApaI	5'-GATCGGGCCCATGAAGAACAGTGTTGC-3'
	HDK591	Reverse	BamHI	5'-GATCGGATCCTTCGTTCTTCATGTAAC-3'
TbPDEB1	HDK367	Forward	ApaI	5'-GGGGCCCATGTTCATGAACAAGCCCTT-3'
	HDK368	Reverse	BamHI	5'-GGGATCCTCAACGAGTACTGCTGTTGT-3'

Table 1.3: Primers for making N-Terminal GFP-tagged construct in pRPa

Gene	Primer name	Position	Res. site	Sequence
CARP1	HDK421	Forward	XbaI	5′-GGTCTAGAATGGGTAGTTATGAATACCC-3′
	HDK362	Reverse	BamHI	5′-GGGATCCTTACCTTTTCGCCATGAACT-3′
CARP2	HDK422	Forward	XbaI	5′-GGTCTAGAATGCGAATACTTGCAGACTT-3′
	HDK364	Reverse	BamHI	5′-GGGATCCCTAGTTCTTACGGCGCGTAA-3′
CARP3	HDK423	Forward	XbaI	5′-GGTCTAGAATGGGAGGAGGTTCATCCGT-3′
	HDK366	Reverse	BamHI	5′-GGGATCCTTAGTTCAATTGGTCATCAA-3′

Table 1.4: Primers used to check for correct integration of KO UTRs and antibiotics in CARP KO cells

Gene	Primer name	Position	Sequence
CARP1	HDK0405	Forward	5′-GGGGCCGATTGCATCAAAA-3′
	HDK0408	Reverse	5′-TTGCCTTGAATAGACCATACG-3′
CARP2	HDK0409	Forward	5′-TTTCCCTCCCTCTTTCCCA-3′
	HDK0412	Reverse	5′-GCAAACAGACATACAAACG-3′
CARP3	HDK0413	Forward	5′-CTACCTGTCAGGTTGGACT-3′
	HDK0416	Reverse	5′-TCGCCCTCAACTTTGCCAA-3′
CARP4	HDK509	Forward	5′-CTTGGGCAGGAGGTCCTATTTC-3′
	HDK0655	Reverse	5′-ATGACGGCATTCACGTCAC-3′
Blasticidin	HDK0282	Forward	5′-ATGGCCAAGCCTTTGTCT-3′
	HDK0283	Reverse	5′-TATGTGTGGGAGGGC-3′
Neomycin	HDK0284	Forward	5′-CGAATTCATGATTGAACAAGATGGAT-3′
	HDK0285	Reverse	5′-CGAATTCTCAGAAGAACTCGTCAAGA-3′
Hygromycin	MB0416	Forward	5′-ATGAAAAAGCCTGAACTCAC-3′
	MB0415	Reverse	5′-CGTCCGAGGGCAAAGGAATA-3′

Table 1.5: Primers used for qRT-PCR after genetic manipulation of the CARPs

Gene	Primer name	Position	Sequence
CARP1	qCARP1F	Forward	5′-GTTTTTTGATGGATGGCCAAA-3′
	qCARP1R	Reverse	5′-ACGAGCCCTCCTTCAGATACAG-3′
CARP2	qCARP2F	Forward	5′-GGTGTCCGCCTACATCGATT-3′
	qCARP2R	Reverse	5′-CGGTGGAAGTAGTCGGAGAAGT-3′
CARP3	qCARP3F	Forward	5′-TCAGTTGCGCACCGACAT-3′
	qCARP3R	Reverse	5′-TGCTCGTGTGCCTCTTCGT-3′
CARP4	qCARP4F	Forward	5′-TGAGGAAGGTTTGCATTCGTT-3′
	qCARP4R	Reverse	5′-GCTTCGCCTCTTGCACAGAT-3′
TbPDEB1	qTbPDEB1F	Forward	5′-CAAAGCGGATTTACTCCAACAAG-3′
	qTbPDEB1R	Reverse	5′-TGCGTCATTGTGTGCTCCAT-3′

Appendix 2: Table showing hits from RIT-Seq with normalized reads ≥0.05

Gene ID	Gene Name	Raw-total counts	Transcript length	Normalised mapping
Tb927.11.16210	CARP1	74563689.000	2119	353.9897
Tb927.10.12390	Hypothetical protein unknown	4958603.000	778	64.1171
Tb927.10.1740	Hypothetical protein unknown	3574752.000	1150	31.2710
Tb927.7.5340	CARP3	2552287.000	1498	17.1400
Tb927.11.17380	Pseudogene?	310784.000	561	5.5730
Tb927.11.12860	CARP2	447275.000	910	4.9446
Tb927.11.3910	Hypothetical protein unknown	1127550.000	3328	3.4084
Tb927.3.1040/60	CARP4	3235998	2340	3.2603
Tb927.8.4640	Flagellar protofilament ribbon protein	263956.000	1159	2.2911
Tb927.11.7180	Hypothetical protein unknown	354258.000	1963	1.8155
Tb927.7.4100	Hypothetical protein unknown	196944.000	1504	1.3173
Tb927.4.4450	Adenylyl cyclase	439975.000	3733	1.1857
Tb927.7.7530	Receptor-type adenylate cyclase GRESAG 4	322614.000	3733	0.8694
Tb927.7.4510	Hypothetical protein unknown	97169.000	1225	0.7980
Tb927.10.12210	Ribulose-5-phosphate 3-epimerase	58772.000	742	0.7968
Tb927.10.16200	Hypothetical protein unknown	202451.000	3070	0.6634
Tb927.8.3700	Hypothetical protein unknown	225999.000	4462	0.5095
Tb927.11.1780	Protein phosphatase	46503.000	1006	0.4650
Tb927.4.4460	Adenylyl cyclase	168889.000	3868	0.4392
Tb927.4.4470	Adenylyl cyclase	143705.000	3817	0.3787
Tb927.11.14020	Iron superoxide dismutase	28601.000	841	0.3421
Tb927.7.5860	Hypothetical protein	18943.000	580	0.3286
Tb927.9.13300	Ring finger domain containing protein	50885.000	1582	0.3236
Tb927.10.1750	Hypothetical protein	21966.000	730	0.3027
Tb927.11.14010	Hypothetical protein	22112.000	760	0.2927

Gene ID		Raw-total counts	Transcript length	Normalised mapping
Tb927.10.16210	Hypothetical protein	25512.000	910	0.2820
Tb927.7.2320	Cyclic nucleotide-binding domain containing protein	48420.000	1819	0.2678
Tb927.11.10430	Hypothetical protein	31264.000	1708	0.1841
Tb927.2.2860	Hypothetical protein	19175.000	1108	0.1741
Tb927.7.4600	Calponin homology (CH) domain containing protein	47836.000	2833	0.1699
Tb927.10.14460	Leucine-rich repeat protein (LRRP)	40057.000	3040	0.1326
Tb927.3.1630	Casein kinase 1	15708.000	1204	0.1312
Tb927.9.12800	Hypothetical protein	35544.000	3181	0.1124
Tb927.11.3710	Hypothetical protein	13073.000	1549	0.0849
Tb927.3.5010	Hypothetical protein	4914.000	583	0.0848
Tb927.8.4660	Hypothetical protein	26676.000	3166	0.0848
Tb927.10.6910	Sterol methyltransferase	7983.000	1081	0.0743
Tb927.4.890	Small nuclear ribonucleoprotein SmD3	2377.000	349	0.0685
Tb927.10.13950	Tubulin-specific chaperone	4338.000	700	0.0623
Tb927.2.2950	Nop14-like family	17572.000	2869	0.0616
Tb927.7.2310	DNA primase small subunit	6952.000	1267	0.0552
Tb927.11.2700	Hypothetical protein	9586.000	1891	0.0510
Tb927.11.11410	Trans-sialidase	10355.000	2047	0.0509
Tb927.6.1890	Hypothetical protein	9034.000	1810	0.0502
Tb927.10.4150	Hypothetical protein	1738.000	391	0.0447

Appendix 3: Table showing hits from Co-IP AND MS of CARP3 with expect ≤0.05 compared with CARP1 and CARP2

Table 3.1: Hits found in more than 1 Co-IP and MS of CARP3 compared with CARP1 and CARP2

Gene ID	Annotation and Product	Found in	Size (kDa)	Protein Score	Peptide Score	Expect	Sequence Coverage (%)
Tb927.7.5340	CARP3	3 only	57	78	77.8	4.2×10^{-7}	13
Tb927.4.4460	GRESAG 4.4B receptor-type adenylate cyclase GRESAG 4, putative	3 only	144	75	58	3.7×10^{-5}	6
Tb927.4.4410	receptor-type adenylate cyclase GRESAG 4, putative	3 only	138	75	58	3.7×10^{-5}	3
Tb927.4.4440	receptor-type adenylate cyclase GRESAG 4, putative	3 only	138	75	58	3.7×10^{-5}	3
Tb927.10.2610	hypothetical protein, conserved	3 only	54	80	55	0.0001	5
Tb927.9.16060	hypothetical protein	3 only	11	40	40	0.0033	10
Tb927.9.8740	DRBD3 RNA-binding protein, putative; DRBD3	Also in 1	40	62	62	2.1×10^{-5}	7
Tb927.9.4680	1L12.525 eukaryotic initiation factor 4a, putative	Also in 1	45	36	36	0.0079	6
Tb927.2.2550	10C8.75 hypothetical protein, conserved	Also in 1	57	39	33	0.016	1
Tb927.10.3010	hypothetical protein, conserved	Also in 1	133	38	38	0.0046	3
Tb927.1.1330	hypothetical protein, conserved	Also in 1	46	36	36	0.0098	7
Tb927.10.14320	hypothetical protein, conserved	Also in 1	121	35	33	0.015	3
Tb927.10.4660	hypothetical protein, conserved	Also in 1	20	30	30	0.038	4
Tb927.11.17780	variant surface glycoprotein (VSG, pseudogene), putative	Also in 1	54	36	36	0.0076	7
Tb11.0640	variant surface glycoprotein (VSG, pseudogene), putative	Also in 1	53	31	33	0.016	5
Tb927.8.320	variant surface glycoprotein (VSG, pseudogene), putative	Also in 1	51	28	28	0.043	14
Tb927.3.5050	60S ribosomal protein L4	Also in 2	42	44	44	0.00081	7
Tb927.11.6140	40S ribosomal protein S15a, putative	Also in 2	14	28	28	0.037	10
Tb927.11.7460	glucose-regulated protein 78, putative; luminal binding protein 1 (BiP), putative	1 & 2	71	1427	113	1×10^{-10}	37
Tb927.9.12570	glk1 glycerol kinase, glycosomal	1 & 2	56	534	101	1.6×10^{-9}	23

Gene ID	Annotation and Product	Found in	Size (kDa)	Protein Score	Peptide Score	Expect	Sequence Coverage (%)
Tb927.3.3270	TbPFK ATP-dependent phosphofructokinase	1 & 2	53	225	58	6.5×10^{-5}	18
Tb927.10.14140	PYK1 pyruvate kinase 1	1 & 2	38	201	91	1.8×10^{-8}	16
Tb927.4.2530	hypothetical protein, conserved	1 & 2	16	161	68	5.2×10^{-6}	24
Tb927.11.11290	heat shock protein 70, putative	1 & 2	73	124	102	2×10^{-9}	8
Tb927.11.11680	2-oxoglutarate dehydrogenase, E2 component, dihydrolipoamide succinyltransferase, putative	1 & 2	41	95	69	8.9×10^{-6}	6
Tb927.1.700	PGKC phosphoglycerate kinase	1 & 2	47	77	49	0.00032	9
Tb927.5.1210	short-chain dehydrogenase, putative	1 & 2	33	56	40	0.0031	8
Tb927.2.5160	30J2.30 chaperone protein DnaJ, putative	1 & 2	44	43	43	0.0011	9

Table 3.2: Hits found in only 1 Co-IP and MS of CARP3 CARP1 and CARP2

Gene ID	Annotation and Product	Found in	Size (kDa)	Protein score	Peptide score	Expect	Sequence Coverage (%)
Tb927.2.2440	RPN6 proteasome regulatory non-ATPase subunit 6	3 only	57	92	67	5.7×10^{-6}	5
Tb927.11.16030	RPN7 proteasome regulatory non-ATP-ase subunit 7	3 only	45	34	34	0.0093	3
Tb927.10.3030	RPN11 proteasome regulatory non-ATPase subunit 11; 19S proteasome regulatory subunit, Metallo-peptidase, Clan MP, Family M67	3 only	33	44	44	0.0013	3
Tb927.9.9670	TbPSA6 proteasome alpha 1 subunit, putative; 20S proteasome subunit alpha-6, putative	3 only	27	33	31	0.025	4
Tb927.4.4470	receptor-type adenylate cyclase GRESAG 4, putative	3 only	142	75	58	3.7×10^{-5}	6
Tb927.8.7590	receptor-type adenylate cyclase GRESAG 4, putative	3 only	139	30	30	0.032	4
Tb927.10.1060	TCP-1-delta t-complex protein 1, delta subunit, putative	3 only	58	88	88	4.8×10^{-8}	10
Tb927.5.3400	calcium-translocating P-type ATPase; calcium pump	3 only	41	53	53	0.00016	9
Tb927.7.6290	kinesin, putative	3 only	97	30	30	0.031	5
Tb927.10.2090	TEF1 elongation factor 1-alpha; EF-1-alpha	3 only	37	55	55	7.5×10^{-5}	10
Tb927.11.9530	14-3-3-like protein, putative	3 only	30	29	29	0.035	4
Tb927.11.7170	seryl-tRNA synthetase, putative	3 only	53	27	27	0.039	3
Tb927.1.3300	zinc-binding phosphatase, putative	3 only	97	96	52	0.00021	10
Tb927.2.820	3B10.365 retrotransposon hot spot protein (RHS, pseudogene), putative	3 only	60	50	50	0.00024	10
Tb927.1.420	retrotransposon hot spot (RHS) protein, putative; retrotransposon hot spot protein 5 (RHS5), putative	3 only	76	33	33	0.014	8
Tb927.5.2570	translation initiation factor, putative	3 only	80	50	50	0.00025	11
Tb927.3.4500	fumarate hydratase, putative	3 only	62	27	27	0.033	5
Tb927.11.2990	KREPB4 RNA-editing complex protein; KREPB4	3 only	46	38	34	0.014	1
Tb927.10.1100	ribosomal protein L9, putative	3 only	21	30	30	0.027	7
Tb927.5.3810	orotidine-5-phosphate decarboxylase/orotate phosphoribosyltransferase, putative	3 only	50	33	33	0.019	9

Gene ID	Annotation and Product	Found in	Size (kDa)	Protein score	Peptide score	Expect	Sequence Coverage (%)
Tb927.11.16340	hypothetical protein, conserved	3 only	124	59	43	0.0023	2
Tb927.5.1220	hypothetical protein, conserved	3 only	21	33	33	0.018	4
Tb927.3.2190	hypothetical protein, conserved	3 only	29	30	30	0.031	10
Tb927.11.10550	hypothetical protein, conserved	3 only	90	33	33	0.015	2
Tb927.9.14190	hypothetical protein, conserved	3 only	146	29	29	0.036	3
Tb927.3.5250	hypothetical protein, conserved	3 only	61	28	29	0.042	14
Tb927.7.6560	hypothetical protein, conserved	3 only	25	40	33	0.02	15
Tb927.6.2930	hypothetical protein, conserved	3 only	50	32	32	0.02	13
Tb927.11.9320	hypothetical protein, conserved	3 only	60	30	30	0.034	12
Tb927.8.420	variant surface glycoprotein (VSG, pseudogene), putative	3 only	56	28	28	0.047	15
Tb927.11.4080	variant surface glycoprotein (VSG)-related, putative	3 only	41	52	52	0.00015	3
Tb927.8.440	variant surface glycoprotein (VSG, pseudogene), putative	3 only	54	33	30	0.029	4
Tb10.v4.0091	variant surface glycoprotein (VSG, pseudogene), putative	3 only	54	33	33	0.015	7
Tb927.4.5700	variant surface glycoprotein (VSG, atypical), putative	3 only	50	33	33	0.016	3
Tb927.6.5230	variant surface glycoprotein (VSG, pseudogene), putative	3 only	53	29	29	0.039	13
Tb927.6.5730	variant surface glycoprotein (VSG, pseudogene), putative	3 only	53	27	27	0.038	7
Tb927.9.6250	AK arginine kinase 14394319:14395431 forward MW:41597	Also in 1	41	324	79	1.4×10^{-7}	22
Tb927.8.5460	TB-44A flagellar calcium-binding protein TB-44A	Also in 1	45	198	88	3.5×10^{-8}	8
Tb927.11.9420	ATP synthase, putative	Also in 1	25	144	99	2.1×10^{-9}	31
Tb927.9.5150	NHP2 ribosomal protein S6, putative; NHP2/RS6-like protein	Also in 1	13	141	91	8.8×10^{-8}	12
Tb927.10.6510	HSP60 chaperonin Hsp60, mitochondrial precursor	Also in 1	59	117	48	0.00061	8
Tb927.1.720	PGKA phosphoglycerate kinase	Also in 1	56	77	49	0.00032	14
Tb927.10.200	vacuolar ATP synthase, putative	Also in 1	19	75	75	8.6×10^{-7}	21
Tb927.3.930	dynein heavy chain, putative	Also in 1	53	69	52	0.00022	6

Gene ID	Annotation and Product	Found in	Size (kDa)	Protein score	Peptide score	Expect	Sequence Coverage (%)
Tb927.1.2570	beta-coP coatomer beta subunit	Also in 1	46	36	36	0.0096	3
Tb927.10.3990	DHH1 ATP-dependent DEAD-box RNA helicase, putative; DHH1	Also in 1	46	81	63	1.5×10^{-5}	8
Tb927.11.10910	40S ribosomal protein SA, putative	Also in 1	31	46	47	0.00067	6
Tb927.9.2520	GB4 mitotubule-associated protein Gb4, putative; dynein heavy chain, cytosolic, putative; microtubule- associated protein	Also in 1	92	51	37	0.002	0
Tb927.11.740	eIF-5A eukaryotic translation initiation factor 5a, putative	Also in 1	17	39	28	0.03	27
Tb927.11.16140	minichromosome maintenance (MCM) complex subunit, putative	Also in 1	81	31	31	0.033	6
Tb10.v4.0147	variant surface glycoprotein (VSG, pseudogene), putative	Also in 1	33	46	46	0.00088	21
Tb09.v4.0115	expression site-associated gene (ESAG, pseudogene), putative; expression site-associated gene 3 (ESAG3), pseudogene	Also in 1	38	46	46	0.00088	17
Tb927.9.1220	expression site-associated gene 3 (ESAG3, pseudogene), putative	Also in 1	35	46	46	0.00088	26
Tb927.9.1220	expression site-associated gene (ESAG, pseudogene), putative; expression site-associated gene 3 (ESAG3), frameshifted and degenerate	Also in 1	39	46	46	0.00088	15
Tb11.0700	expression site-associated gene (ESAG, pseudogene), putative; expression site-associated gene 3 (ESAG3), degenerate	Also in 1	21	46	46	0.00088	11
Tb927.9.620	expression site-associated gene (ESAG, pseudogene), putative; expression site-associated gene 3 (ESAG3), pseudogene	Also in 1	32	46	46	0.00088	7
Tb927.11.19900	expression site-associated gene (ESAG, pseudogene), putative; expression site-associated gene 3 (ESAG3), degenerate and frameshifted	Also in 1	40	46	46	0.00088	26
Tb927.9.16260	expression site-associated gene 3 (ESAG3, pseudogene), putative	Also in 1	31	46	46	0.00088	10
Tb08.27P2.520	expression site-associated gene (ESAG, pseudogene), putative	Also in 1	38	46	46	0.00088	21
Tb08.27P2.160	expression site-associated gene (ESAG, pseudogene), putative	Also in 1	41	46	46	0.00088	11

Gene ID	Annotation and Product	Found in	Size (kDa)	Protein score	Peptide score	Expect	Sequence Coverage (%)
Tb927.7.3330	hypothetical protein, conserved	Also in 1	502	133	56	6.6×10^{-5}	3
Tb11.02.3760	hypothetical protein, conserved	Also in 1	11	127	92	1.3×10^{-8}	20
Tb927.4.2740	hypothetical protein, conserved	Also in 1	16	61	44	0.0012	37
Tb927.3.4080	hypothetical protein, conserved	Also in 1	62	39	39	0.001	10
Tb927.7.2570	hypothetical protein, conserved	Also in 1	52	30	30	0.033	4
Tb927.6.1220	hypothetical protein, conserved	Also in 1	65	28	28	0.039	3
Tb927.3.3580	LPG3 lipophosphoglycan biosynthetic protein, putative	Also in 2	88	136	85	8.7×10^{-8}	12
Tb927.7.4180	fatty acid elongase, putative	Also in 2	33	95	95	1.1×10^{-8}	8
Tb927.4.2070	antigenic protein, putative	Also in 2	511	80	47	0.00063	3
Tb927.10.3660	aspartate aminotransferase	Also in 2	45	76	52	0.00017	8
Tb927.2.5660	1F7.200 adenylate kinase, putative	Also in 2	29	73	49	0.0004	9
Tb927.8.2640	UBA1 ubiquitin-activating enzyme E1, putative	Also in 2	116	73	73	1.4×10^{-6}	9
Tb927.5.1300	vacuolar proton translocating ATPase subunit A, putative	Also in 2	89	66	44	0.00057	7
Tb927.10.1230	hypothetical protein, conserved	Also in 2	37	64	43	0.001	11
Tb927.9.15050	trypanin-related protein, putative	Also in 2	54	58	43	0.0014	7
Tb927.5.2960	PRS phosphoribosylpyrophosphate synthetase, putative	Also in 2	110	54	54	8.4×10^{-5}	4
Tb927.9.6070	RPS3 40S ribosomal protein S3, putative	Also in 2	30	49	49	0.00034	10
Tb927.4.1270	RuvB-like DNA helicase, putative	Also in 2	50	48	48	0.0004	10
Tb927.11.7020	PSA4 proteasome alpha 7 subunit, putative	Also in 2	27	46	46	0.00071	7
Tb927.7.4170	fatty acid elongase, putative	Also in 2	30	46	46	0.000585	11
Tb927.11.2670	hypothetical protein, conserved	Also in 2	58	44	44	0.0012	4
Tb927.4.3550	ribosomal protein L13a, putative	Also in 2	39	42	33	0.012	10
Tb927.11.4770	retrotransposon hot spot protein (RHS, pseudogene), putative; retrotransposon hot spot protein (RHS), degenerate	Also in 2	85	33	33	0.014	19
Tb927.2.1170	retrotransposon hot spot (RHS) protein, putative	Also in 2	76	33	33	0.014	11

Gene ID	Annotation and Product	Found in	Size (kDa)	Protein score	Peptide score	Expect	Sequence Coverage (%)
Tb927.2.1080	retrotransposon hot spot (RHS) protein, putative	Also in 2	76	33	33	0.014	6
Tb927.8.4430	nucleoside phosphorylase, putative	Also in 2	36	26	26	0.026	13
Tb927.10.2110	TEF1 elongation factor 1-alpha	Also in 2	49	42	42	0.0014	11
Tb927.10.4570	elongation factor 2	1 & 2	94	445	80	2.3×10^{-7}	29
Tb927.11.5520	TIM triosephosphate isomerase 22070477:22071229 forward MW:26819	1 & 2	26	317	71	2.0×10^{-6}	21
Tb927.6.3840	reticulon domain protein	1 & 2	21	264	123	7.3×10^{-12}	25
Tb927.7.710	HSP70 heat shock 70 kDa protein, putative	1 & 2	70	223	75	7.4×10^{-7}	15
Tb927.7.3440	I/6 autoantigen	1 & 2	27	211	108	3.1×10^{-10}	23
Tb927.10.8230	BS2 protein disulfide isomerase; bloodstream- specific protein 2 precursor	1 & 2	55	208	67	3.6×10^{-6}	25
Tb927.8.5440	TB-24 flagellar calcium-binding protein TB-24	1 & 2	24	198	88	3.5×10^{-8}	18
Tb927.11.1740	TbIFT88 intraflagellar transport protein IFT88, putative	1 & 2	89	57	42	0.001	19
Tb927.4.4380	PPase1 vacuolar-type proton translocating pyrophosphatase 1, putative	1 & 2	86	163	78	4.8×10^{-7}	9
Tb927.11.15910	iron superoxide dismutase	1 & 2	22	161	101	2.0×10^{-9}	12
Tb927.5.1810	lysosomal/endosomal membrane protein p67; lysosomal membrane glycoprotein	1 & 2	72	156	53	0.00013	15
Tb927.3.3760	TRYP1 tryparedoxin	1 & 2	15	44	35	0.01	7
Tb927.8.1990	TRYP2 tryparedoxin peroxidase	1 & 2	25	154	93	1.6×10^{-8}	6
Tb927.4.5010	calreticulin, putative	1 & 2	45	142	72	1.1×10^{-6}	11
Tb927.10.16120	inosine-5'-monophosphate dehydrogenase; IMP dehydrogenase	1 & 2	48	168	82	1.2×10^{-7}	15
Tb927.3.2960	IAGNH inosine-adenosine-guanosine-nucleosidehydrolase	1 & 2	35	123	74	6.3×10^{-7}	14
Tb927.7.4420	proteasome alpha 3 subunit, putative	1 & 2	32	56	56	5.6×10^{-6}	13
Tb927.10.15720	RPN9 proteasome regulatory non-ATP-ase subunit 9; 19S proteasome regulatory subunit	1 & 2	45	122	74	9.7×10^{-7}	14

Gene ID	Annotation and Product	Found in	Size (kDa)	Protein score	Peptide score	Expect	Sequence Coverage (%)
Tb927.11.13020	calmodulin	1 & 2	16	93	59	2.7×10^{-5}	11
Tb927.1.2430	histone H3, putative	1 & 2	15	109	78	1.8×10^{-7}	19
Tb927.8.1870	tGLP1 Golgi/lysosome glycoprotein 1	1 & 2	67	109	79	3.3×10^{-7}	11
Tb927.2.4210	glycosomal phosphoenolpyruvate carboxykinase	1 & 2	58	103	93	9.1×10^{-7}	18
Tb927.11.4610	PKA-R protein kinase A regulatory subunit	1 & 2	56	89	89	3.1×10^{-8}	15
Tb927.11.7380	glycerol-3-phosphate dehydrogenase, putative	1 & 2	67	83	83	1.4×10^{-7}	11
Tb927.10.6050	CHC clathrin heavy chain	1 & 2	190	69	52	0.00018	9
Tb927.5.4170	histone H4, putative	1 & 2	11	67	55	0.0001	13
Tb927.10.3210	delta-1-pyrroline-5-carboxylate dehydrogenase, putative	1 & 2	62	66	37	0.0054	6
Tb927.1.3950	alanine aminotransferase, putative	1 & 2	63	64	44	0.0012	11
Tb927.10.14170	aquaporin 9, putative	1 & 2	33	97	69	3.8×10^{-6}	4
Tb927.6.1520	AQP3 aquaporin 3, putative	1 & 2	35	62	41	0.0031	11
Tb927.8.7610	AATP1 amino acid transporter 1, putative	1 & 2	50	60	60	1.9×10^{-5}	19
Tb927.10.5770	VCP valosin-containing protein homolog; Transitional endoplasmic reticulum ATPase, putative	1 & 2	85	50	50	0.0001	4
Tb927.10.2440	MCA4 metacaspase MCA4; cysteine peptidase, Clan CD, family C13, putative	1 & 2	39	50	43	0.00078	11
Tb927.11.3250	dynein heavy chain, putative	1 & 2	53	49	49	0.00041	9
Tb927.1.3830	PGI glucose-6-phosphate isomerase, glycosomal	1 & 2	67	47	34	0.01	9
Tb927.3.290	expression site-associated gene (ESAG, pseudogene), putative	1 & 2	36	33	35	0.0076	18
Tb927.11.1090	calpain-like protein, putative; cytoskeleton assocociated protein, putative	1 & 2	658	47	39	0.0022	2
Tb927.11.1100	calpain, putative; cysteine peptidase, Clan CA, family C2, putative	1 & 2	158	47	39	0.0022	7
Tb927.10.1390	hypoxanthine-guanine phosphoribosyltransferase, putative	1 & 2	26	45	35	0.0098	23
Tb927.4.1080	V-type ATPase, A subunit, putative	1 & 2	67	45	37	0.007	10

	Annotation and Product	Found in	Size (kDa)	Protein	Peptide		Sequence Coverage (%)

Gene ID				score	score	Expect	
Tb927.11.1710	GBP21 mitochondrial RNA binding protein 1; gBP21, MRP1	1 & 2	23	41	41	0.0023	9
Tb927.11.9590	S-adenosylhomocysteine hydrolase, putative	1 & 2	48	39	39	0.0047	3
Tb927.5.2140	regulator of nonsense transcripts 1, putative	1 & 2	93	38	34	0.013	6
Tb927.10.14710	RPS2 40S ribosomal protein S2, putative	1 & 2	28	37	37	0.0076	21
Tb927.8.3770	mitogen-activated protein kinase, putative	1 & 2	47	33	33	0.017	14
Tb927.11.11520	PEX11 glycosomal membrane protein, putative	1 & 2	24	32	32	0.035	12
Tb927.1.2100	calpain-like cysteine peptidase, putative; cysteine peptidase, Clan CA, family C2, putative	1 & 2	126	29	29	0.032	2
Tb927.10.12510	P-type H+-ATPase, putative	1 & 2	100	28	28	0.036	2
Tb927.9.12550	glk1 glycerol kinase, glycosomal	1 & 2	56	502	101	2.1×10^{-9}	19
Tb927.11.8060	hypothetical protein, conserved	1 & 2	63	107	67	5.0×10^{-6}	8
Tb927.3.3000	hypothetical protein, conserved	1 & 2	65	81	50	0.00023	6
Tb927.10.12820	hypothetical protein, conserved	1 & 2	110	76	76	6.7×10^{-6}	6
Tb927.3.3560	hypothetical protein, conserved	1 & 2	69	72	48	0.00025	9
Tb927.7.4500	hypothetical protein, conserved	1 & 2	58	44	30	0.047	3
Tb927.7.3550	hypothetical protein, conserved	1 & 2	138	154	58	4.5×10^{-5}	11
Tb927.3.5490	hypothetical protein, conserved	1 & 2	77	207	87	4.4×10^{-8}	18
Tb927.11.13520	hypothetical protein, conserved	1 & 2	105	64	64	9.6×10^{-6}	11
Tb927.9.2470	hypothetical protein, conserved	1 & 2	85	491	80	2.5×10^{-7}	24
Tb927.7.6090	hypothetical protein, conserved	1 & 2	88	40	32	0.018	14
Tb927.3.4070	hypothetical protein, conserved	1 & 2	64	39	39	0.001	7
Tb927.10.13790	hypothetical protein, conserved	1 & 2	74	35	27	0.047	8
Tb927.3.4110	hypothetical protein, conserved	1 & 2	65	39	39	0.001	11

Appendix 4: Log2 fold differentials (±0.05) of RNA-Seq of overexpressing CARP3 and WT s427

Table 4.1: +0.5 log2 fold differential of overexpressing CARP3 against WT s427

Gene ID	Gene Name	s427	OE-CARP3	log2 (fold-change)	p-value
Tb927.9.16700	ESAG3	0.343901	1.2715	1.88646	0.0037
Tb927.7.5340	CARP3	29.7763	88.9473	1.57879	0.00005
Tb927.5.5530	VSG	0.40614	1.18043	1.53927	0.0004
Tb927.4.220	RHS, Pseudogene	5.22031	13.1233	1.32992	0.00005
Tb927.6.5170	RHS, Pseudogene	0.619013	1.4864	1.26378	0.001
Tb927.2.960	hypothetical protein	31.8733	65.7177	1.04393	0.00125
Tb927.8.2861	SRP RNA, 7SL	26.2085	51.3994	0.971715	0.00005
Tb927.2.6220	TbNT4	5.0098	9.61724	0.94087	0.00005
Tb927.1.340	hypothetical protein, unlikely	6.10631	11.6435	0.931155	0.00065
Tb927.6.210	LRRP, Pseudogene	1.93026	3.58458	0.893007	0.00005
Tb927.9.7400	ESAG11	6.4085	11.8263	0.883938	0.00005
Tb927.1.280	hypothetical protein, conserved	9.64932	17.7809	0.881826	0.00005
Tb927.9.11580	gim5A	27.5732	50.1524	0.863054	0.00005
Tb927.1.80	hypothetical protein, unlikely	16.9237	30.6398	0.856361	0.00075
Tb927.10.110	RHS2, Pseudogene	3.89419	6.95334	0.836383	0.00005
Tb927.5.160	VSG pseugogene	2.47355	4.39907	0.830612	0.00225
Tb927.3.3420	hypothetical protein, pseudogene	2.06463	3.549	0.781526	0.00125
Tb927.2.200	ESAG	332.242	566.152	0.768955	0.00005
Tb927.4.190	RHS, Pseudogene	2.76645	4.70199	0.765235	0.0029
Tb927.9.15980	nucleoside transporter 1, putative	3.59757	6.08911	0.759207	0.00005
Tb927.2.1130	RHS, Pseudogene	2.32881	3.91355	0.748885	0.00245
Tb927.2.6320	TbNT6	11.8535	19.8695	0.745238	0.00005
Tb927.9.5910	hypothetical protein, unlikely	241.798	404.398	0.741973	0.00005
Tb927.4.300	RHS3, Pseudogene	0.915806	1.50728	0.718831	0.001
Tb927.2.1120	ESAG	18.7378	30.1322	0.685354	0.00005
Tb927.11.20150	ESAG	11.2034	17.9423	0.67943	0.00005
Tb927.10.5700	hypothetical protein, conserved	7.72748	12.3655	0.678245	0.00005
Tb927.2.1050	RHS, Pseudogene	51.5513	82.1089	0.671529	0.00005
Tb927.4.240	RHS, Pseudogene	1.35628	2.14634	0.662219	0.0001
Tb927.3.1490	LRRP, putative	4.59357	7.22206	0.652796	0.00005
Tb927.5.3990	VSG, atypical	1.28877	2.00508	0.637668	0.00155
Tb927.1.4560	CFB1B	1.79656	2.79366	0.636918	0.00045
Tb927.2.3340	hypothetical protein	26.729	40.9477	0.615381	0.00005
Tb927.1.360	hypothetical protein, unlikely	56.6585	86.6425	0.612783	0.00005
Tb927.1.60	RNA polymerase (pseudogene), putative	26.322	40.2484	0.612664	0.00005
Tb927.11.15960	amino acid transporter, putative	46.7084	71.3685	0.611604	0.00005
Tb927.9.10460	hypothetical protein, unlikely	23.7993	36.2961	0.608897	0.00005

Gene ID	Gene Name	s427	OE-CARP3	log2 (fold-change)	p-value
Tb927.11.18700	hypothetical protein, conserved	19.5244	29.6746	0.60395	0.00005
Tb927.3.1510	VSG-related	2.6023	3.95193	0.602772	0.00075
Tb927.2.490	RNA polymerase (pseudogene), putative	17.7934	26.9248	0.597595	0.00005
Tb927.2.1110	DNA-directed RNA polymerase III subunit 2,	16.2711	24.5716	0.594674	0.00005
Tb927.4.230	DNA-directed RNA polymerase, pseudogene, putative	19.3689	29.2276	0.593589	0.00005
Tb11.v5.0295	RHS, protein	30.5424	45.9625	0.589642	0.00005
Tb927.11.18650	ESAG1	4.23939	6.37474	0.588509	0.0002
Tb927.1.70	RHS, protein	12.8655	19.3172	0.586376	0.00005
Tb927.6.4110	hypothetical protein	13.1428	19.6785	0.582351	0.0005
Tb927.9.15940	ESAG	22.0071	32.7919	0.575369	0.00005
Tb927.1.5200	ESAG1	11.9938	17.774	0.567477	0.00005
Tb927.6.150	RHS4, putative	5.447	8.05795	0.564949	0.00005
Tb927.2.6150	TbNT2/927	20.0136	29.5518	0.562269	0.00005
Tb927.3.700	hypothetical protein, conserved	26.6346	39.0503	0.55203	0.00005
Tb927.10.100	ESAG, pseudogene	3.39762	4.97662	0.550642	0.0003
Tb927.9.7410	ESAG2	2.58216	3.77491	0.547863	0.0006
Tb927.1.4130	hypothetical protein, unlikely	20.1061	29.2134	0.538994	0.00305
Tb927.1.490	hypothetical protein	53.6021	77.5351	0.532561	0.00005
Tb927.2.6180	iron/ascorbate oxidoreductase family protein, putative	21.558	31.1431	0.530689	0.00005
Tb11.v5.0559	oligosaccharyl transferase subunit, putative	12.7276	18.3433	0.527292	0.00005
Tb927.1.5340	ESAG, pseudogene	23.8772	34.3639	0.525258	0.00005
Tb927.6.5490	ESAG, pseudogene	44.1351	63.3958	0.522461	0.00005
Tb927.4.210	RHS, Pseudogene	22.3444	32.0327	0.519635	0.00005
Tb927.8.5470	Tb-17	38.8959	55.1547	0.503865	0.00005

Table 4.2: -0.5 log2 fold differential of overexpressing CARP3 against WT s427

Gene ID	Gene Name	s427	OE-CARP3	log2 (fold- change)	p-value
Tb927.11.1920	hypothetical protein	8.66682	5.93331	-0.54667	0.0016
Tb927.11.4440	hypothetical protein	8.66392	5.6805	-0.609	0.0013
Tb927.10.10260	EP1	15.891	10.3839	-0.61386	0.00265
Tb927.11.15950	amino acid transporter, putative	97.4208	59.4573	-0.71238	0.00005
Tb927.11.16180	hypothetical protein	8.65323	4.71196	-0.87691	0.00005
Tb927.7.6500	VSG, putative	2.46698	1.17863	-1.06563	0.00005
Tb927.9.15110	60S ribosomal protein L5, putative	17.939	2.2377	-3.00301	0.00005

Appendix 5: Log2 fold differentials (+0.75) of RNA-Seq of R0.8 and WT s427

Table 5.1: +0.75 log2 fold differential of R0.8 against WT s427

Gene ID	Gene name	s427	R0.8	log2 (fold-change)	p-value
Tb927.9.1050	VSG, putative	0.048476	1.56992	5.01727	0.0197
Tb927.9.16890	VSG, pseudogene	0.054673	1.67525	4.9374	0.01815
Tb927.5.5530	VSG, putative	0.415451	5.74266	3.78897	0.00005
Tb927.7.150	VSG, pseudogene	0.181801	1.74576	3.26343	0.00005
Tb927.7.6500	VSG, putative	2.52418	11.5266	2.19108	0.00005
Tb927.7.6530	VSG, pseudogene	0.467402	2.02578	2.11574	0.00005
Tb11.v5.0693	hypothetical protein, unlikely	0.938157	3.80605	2.02039	0.00005
Tb927_10_v4	term=C/D snoRNA	1019.7	3978.84	1.96421	0.00055
Tb927.7.6520	VSG, pseudogene	0.642037	2.48225	1.95092	0.00005
Tb927.9.18120	VSG, pseudogene	0.467699	1.56721	1.74454	0.00005
Tb927.10.140	hypothetical protein	1.63901	5.29894	1.69288	0.0012
Tb927.7.6510	VSG, degenerate	0.373812	1.06534	1.51093	0.0008
Tb927.10.130	hypothetical protein	1.53737	4.23115	1.46059	0.0114
Tb927.6.5170	RHS, pseudogene	0.633076	1.74229	1.46053	0.00025
Tb11.v5.1024	VSG, atypical, putative	0.24986	0.662572	1.40696	0.00755
Tb927.1.4990	hypothetical protein, unlikely	82.6458	216.325	1.38818	0.00005
Tb11.v5.0638	CBP1	1.23866	3.23741	1.38606	0.00005
Tb927.9.16640	VSG, putative	0.262018	0.674071	1.36323	0.003
Tb927.4.5400	VSG, atypical, putative	0.341849	0.873698	1.35378	0.00045
Tb927.11.17840	RHS, degenerate	2.431	5.93722	1.28824	0.0208
Tb927.9.5940	hypothetical protein, unlikely	368.859	897.534	1.2829	0.00005
Tb11.v5.0719	hypothetical protein, conserved	0.944579	2.29342	1.27976	0.00005
Tb927.2.1350	RHS, pseudogene	13.8481	33.5092	1.27487	0.00005
Tb11.v5.0495	RHS, putative	9.9415	23.7722	1.25774	0.00005
Tb927.8.520	hypothetical protein	1.9615	4.67578	1.25325	0.0003
Tb11.v5.0294	RHS, putative	10.1764	24.2239	1.2512	0.00005
Tb927.1.80	hypothetical protein, unlikely	17.3136	40.9293	1.24123	0.00005
Tb927.6.210	hypothetical protein	1.97477	4.65171	1.23608	0.00005
Tb927.4.5440	hypothetical protein	0.420056	0.986892	1.23231	0.04345
Tb927.4.150	hypothetical protein	1.89431	4.42133	1.22281	0.0053
Tb927.9.1280	VSG, atypical, putative	0.837446	1.94752	1.21757	0.00005
Tb927.6.540	VSG-related, putative	0.746857	1.69513	1.18249	0.0001
Tb927.8.500	hypothetical protein	0.595478	1.34594	1.17649	0.0019
Tb927.4.220	RHS, pseudogene	5.34082	11.9006	1.1559	0.00005
Tb927.1.4120	hypothetical protein, unlikely	1659.45	3659.06	1.14077	0.00005
Tb927.3.2540	VSG-related, putative	0.99338	2.16546	1.12426	0.00005
Tb927.2.1380	LRRP, putative	29.4909	63.9276	1.11617	0.00005
Tb927.1.3320	LRRP, putative	3.32492	7.13982	1.10257	0.00005
Tb11.v5.0778	chaperone protein DNAj, putative	0.587261	1.25476	1.09534	0.00075
Tb927.5.5540	VSG, putative	0.594143	1.26471	1.08992	0.00025
Tb927.5.160	RHS, pseudogene	2.53116	5.37182	1.08561	0.00005
Tb927.9.6760	hypothetical protein, conserved	7.83192	16.5144	1.07629	0.00005
Tb927.3.2510	ESAG2	0.61905	1.29656	1.06656	0.0054
Tb927.1.1040	hypothetical protein, unlikely	1.44096	2.95267	1.03498	0.01475
Tb927.5.5560	VSG, putative	0.573179	1.17291	1.03304	0.00085
Tb927.6.130	LRRP, putative	4.56388	9.26546	1.0216	0.00005

Gene ID	Gene name	s427	R0.8	log2 (fold-change)	p-value
Tb927.1.2760	hypothetical protein	1032.42	2087.8	1.01595	0.00005
Tb927.9.7290	VSG-related, putative	4.13381	8.3255	1.01007	0.00005
Tb927.10.110	RHS2, pseudogene	3.98447	7.97086	1.00035	0.00005
Tb927.1.70	RHS4, pseudogene	13.1622	26.138	0.989752	0.00005
Tb927.11.1500	LRRP, pseudogene	2.48759	4.88224	0.972795	0.00005
Tb11.v5.0551	LRRP, putative	6.78665	13.2031	0.960102	0.00005
Tb927.6.150	RHS4, putative	5.57164	10.8177	0.95722	0.00005
Tb927.4.240	RHS, pseudogene	1.38761	2.68864	0.954279	0.00005
Tb927.1.3380	hypothetical protein, unlikely	2.20352	4.21291	0.935008	0.0104
Tb927.2.6350	VSG pseudogene, putative	1.66711	3.16501	0.924862	0.00005
Tb11.v5.0886	hypothetical protein, conserved	0.624996	1.18364	0.921314	0.00015
Tb927.9.4730	hypothetical protein, unlikely	5425.06	10137.8	0.902027	0.00005
Tb11.v5.0448	LRRP, putative	5.42209	10.1072	0.898458	0.00005
Tb927.1.280	hypothetical protein, conserved	9.86678	18.3012	0.891287	0.00005
Tb927.11.1510	LRRP, putative	0.68728	1.2617	0.876395	0.0001
Tb927.11.12710	VSG-related, putative	12.6667	23.0622	0.864485	0.00005
Tb927.9.3150	hypothetical protein, unlikely	50.1277	91.1697	0.862946	0.01805
Tb927.9.9490	hypothetical protein, unlikely	53.4073	96.6069	0.85509	0.00005
Tb927.6.5180	RHS, pseudogene	1.05016	1.89704	0.853134	0.0004
Tb927.11.4060	LRRP, putative	9.04306	16.2723	0.847531	0.00005
Tb927.5.170	hypothetical protein, conserved	6.07009	10.8667	0.840121	0.00005
Tb927.9.16000	hypothetical protein, unlikely	20.3637	36.3842	0.837313	0.0085
Tb927.11.8680	DNA polymerase kappa, putative	0.478067	0.853718	0.836548	0.0049
Tb927.3.570	ESAG2, putative	10.6121	18.9365	0.83546	0.00005
Tb11.v5.0470	GRESAG4	1.37722	2.45491	0.833915	0.00005
Tb927.3.5670	hypothetical protein	7.4402	13.2442	0.831953	0.00005
Tb927.3.2590	hypothetical protein	7.08592	12.6003	0.830432	0.00005
Tb927.8.530	LRRP, putative	5.2968	9.41799	0.830297	0.00005
Tb927.8.510	hypothetical protein	1.93839	3.41989	0.819093	0.00015
Tb927.6.240	hypothetical protein, conserved	13.0102	22.9478	0.818716	0.00005
Tb927.11.19030	ESAG1	1.09264	1.91245	0.807603	0.02745
Tb927.7.4770	PPIase	1.33156	2.31599	0.798513	0.02845
Tb927.9.7530	hypothetical protein, unlikely	4.27885	7.42405	0.794984	0.0019
Tb927.9.7410	ESAG2, putative	2.6414	4.57494	0.792446	0.00005
Tb927.4.300	RHS3, putative	0.936807	1.60912	0.780445	0.0003
Tb927.9.7370	ESAG9, putative	8.73607	14.9635	0.776387	0.00005
Tb927.5.5500	VSG, putative	0.395005	0.675697	0.774507	0.0325
Tb927.6.350	hypothetical protein, conserved	23.8299	40.362	0.760222	0.00005
Tb927.7.6080	receptor-type adenylate cyclase GRESAG 4, putative	5.74798	9.71703	0.757459	0.00005
Tb927.3.5690	hypothetical protein, conserved	9.95538	16.814	0.756112	0.00005
Tb927.7.4840	hypothetical protein, conserved	0.850276	1.43069	0.750704	0.0184

Table 5.2: -0.75 log2 fold differential of R0.8 against WT s427

Gene ID	Gene name	s427	R0.8	log2 (fold-change)	p-value
Tb927.9.2820	hypothetical protein, unlikely	184.187	109.003	-0.7568	0.00005
Tb927.1.4020	hypothetical protein	21.1541	12.4736	-0.76206	0.00005
Tb927.10.1640	hypothetical protein	32.8647	19.3234	-0.76619	0.00005
Tb927.1.1460	hypothetical protein, unlikely	3.08374	1.77217	-0.79916	0.04045
Tb927.8.2861	SRP RNA, 7SL	26.8248	14.9675	-0.84174	0.00095
Tb927.2.6320	TbNT6	12.1216	6.45919	-0.90815	0.00005
Tb927.1.2950	hypothetical protein, unlikely	17.147	8.50618	-1.01137	0.0012
Tb11.v5.0869	cystathione gamma lyase, putative	1.69441	0.834595	-1.02164	0.0244
Tb927.11.7980	hypothetical protein	5.82784	2.85976	-1.02707	0.0118
Tb927.8.2864	small nuclear RNA	224.871	106.254	-1.08157	0.00065
Tb927.1.3590	hypothetical protein, unlikely	13.4306	6.24659	-1.10438	0.0035
Tb927.4.3630	serine threonine-protein phosphatase PP1, putative (Inferred from Sequence Alignment)	24.2375	10.9643	-1.14442	0.00005
Tb927.9.7340	ESAG9, putative	1.96185	0.852413	-1.20259	0.0023
Tb927.9.5140	hypothetical protein, unlikely	15.3513	4.51661	-1.76505	0.01565
Tb927.1.2620	hypothetical protein, unlikely	2.73468	0.614812	-2.15316	0.0124

References:

Acestor, N., Panigrahi, A.K., Ogata, Y., Anupama, A., Stuart, K.D., 2009. Protein composition of Trypanosoma brucei mitochondrial membranes. Proteomics 9, 5497-5508.

Adung'a, V.O., Gadelha, C., Field, M.C., 2013. Proteomic analysis of clathrin interactions in trypanosomes reveals dynamic evolution of endocytosis. Traffic 14, 440-457.

Ahlstrom, M., Lamberg-Allardt, C., 1999. Regulation of adenosine 3',5'-cyclic monophosphate (cAMP) accumulation in UMR-106 osteoblast-like cells: role of cAMP-phosphodiesterase and cAMP efflux. Biochem Pharmacol 58, 1335-1340.

Albisetti, A., Wiese, S., Schneider, A., Niemann, M., 2015. A component of the mitochondrial outer membrane proteome of T. brucei probably contains covalent bound fatty acids. Experimental Parasitology 155, 49-57.

Ali, J.A., Tagoe, D.N., Munday, J.C., Donachie, A., Morrison, L.J., de Koning, H.P., 2013. Pyrimidine biosynthesis is not an essential function for Trypanosoma brucei bloodstream forms. PLoS One 8, e58034.

Alonso, G.D., Schoijet, A.C., Torres, H.N., Flawia, M.M., 2006. TcPDE4, a novel membrane-associated cAMP-specific phosphodiesterase from Trypanosoma cruzi. Mol Biochem Parasitol 145, 40-49.

Alonso, G.D., Schoijet, A.C., Torres, H.N., Flawia, M.M., 2007. TcrPDEA1, a cAMP-specific phosphodiesterase with atypical pharmacological properties from Trypanosoma cruzi. Mol Biochem Parasitol 152, 72-79.

Alsford, S., Eckert, S., Baker, N., Glover, L., Sanchez-Flores, A., Leung, K.F., Turner, D.J., Field, M.C., Berriman, M., Horn, D., 2012a. High-throughput decoding of antitrypanosomal drug efficacy and resistance. Nature 482, 232-236.

Alsford, S., Eckert, S., Baker, N., Glover, L., Sanchez-Flores, A., Leung, K.F., Turner, D.J., Field, M.C., Berriman, M., Horn, D., 2012b. High-throughput decoding of antitrypanosomal drug efficacy and resistance. Nature 482, 232-236.

Alsford, S., Kawahara, T., Glover, L., Horn, D., 2005. Tagging a T. brucei RRNA locus improves stable transfection efficiency and circumvents inducible expression position effects. Mol Biochem Parasitol 144, 142-148.

Alsford, S., Turner, D.J., Obado, S.O., Sanchez-Flores, A., Glover, L., Berriman, M., Hertz-Fowler, C., Horn, D., 2011a. High-throughput phenotyping using parallel sequencing of RNA interference targets in the African trypanosome. Genome Research 21, 915-924.

Alsford, S., Turner, D.J., Obado, S.O., Sanchez-Flores, A., Glover, L., Berriman, M., Hertz-Fowler, C., Horn, D., 2011b. High-throughput phenotyping using parallel sequencing of RNA interference targets in the African trypanosome. Genome Res 21, 915-924.

Amata, E., Bland, N.D., Campbell, R.K., Pollastri, M.P., 2015. Evaluation of pyrrolidine and pyrazolone derivatives as inhibitors of trypanosomal phosphodiesterase B1 (TbrPDEB1). Tetrahedron Lett 56, 2832-2835.

Amata, E., Bland, N.D., Hoyt, C.T., Settimo, L., Campbell, R.K., Pollastri, M.P., 2014. Repurposing human PDE4 inhibitors for neglected tropical diseases: Design, synthesis and evaluation of cilomilast analogues as Trypanosoma brucei PDEB1 inhibitors. Bioorganic & Medicinal Chemistry Letters 24, 4084-4089.

Ang, K.-L., Antoni, F.A., 2002. Reciprocal regulation of calcium dependent and calcium independent cyclic AMP hydrolysis by protein phosphorylation. Journal of Neurochemistry 81, 422-433.

Aravind, L., Ponting, C.P., 1997. The GAF domain: an evolutionary link between diverse phototransducing proteins. Trends Biochem Sci 22, 458-459.

Archer, S.K., Inchaustegui, D., Queiroz, R., Clayton, C., 2011. The cell cycle regulated transcriptome of Trypanosoma brucei. PLoS One 6, e18425.

Azam, M.A., Tripuraneni, N.S., 2014. Selective Phosphodiesterase 4B Inhibitors: A Review. Sci Pharm 82, 453-481.

Baker, D.A., 2010. Malaria gametocytogenesis. Mol Biochem Parasitol 172, 57-65.

Baker, N., Alsford, S., Horn, D., 2011. Genome-wide RNAi screens in African trypanosomes identify the nifurtimox activator NTR and the eflornithine transporter AAT6. Mol Biochem Parasitol 176, 55-57.

Baker, N., de Koning, H.P., Maser, P., Horn, D., 2013. Drug resistance in African trypanosomiasis: the melarsoprol and pentamidine story. Trends Parasitol 29, 110-118.

Baldauf, S.L., 2003. The deep roots of eukaryotes. Science 300, 1703-1706.

Banerjee, C., Sarkar, D., 1992. Isolation and characterization of a cyclic nucleotide-independent protein kinase from Leishmania donovani. Mol Biochem Parasitol 52, 195-205.

Bao, Y., Weiss, L.M., Braunstein, V.L., Huang, H., 2008. Role of protein kinase A in Trypanosoma cruzi. Infect Immun 76, 4757-4763.

Bao, Y., Weiss, L.M., Hashimoto, M., Nara, T., Huang, H., 2009. Protein kinase A regulatory subunit interacts with P-Type ATPases in Trypanosoma cruzi. Am J Trop Med Hyg 80, 941-943.

Bao, Y., Weiss, L.M., Ma, Y.F., Kahn, S., Huang, H., 2010. Protein kinase A catalytic subunit interacts and phosphorylates members of trans-sialidase super-family in Trypanosoma cruzi. Microbes Infect 12, 716-726.

Barrett, M.P., 2010. Potential new drugs for human African trypanosomiasis: some progress at last. Curr Opin Infect Dis 23, 603-608.

Barrett, M.P., Boykin, D.W., Brun, R., Tidwell, R.R., 2007. Human African trypanosomiasis: pharmacological re-engagement with a neglected disease. British Journal of Pharmacology 152, 1155-1171.

Barrett, M.P., Croft, S.L., 2012. Management of trypanosomiasis and leishmaniasis. Br Med Bull 104, 175-196.

Barry, J.D., McCulloch, R., 2001. Antigenic variation in trypanosomes: enhanced phenotypic variation in a eukaryotic parasite. Adv Parasitol 49, 1-70.

Beavo, J.A., 1995. Cyclic nucleotide phosphodiesterases: functional implications of multiple isoforms. Physiol Rev 75, 725-748.

Bender, A.T., Beavo, J.A., 2006. Cyclic nucleotide phosphodiesterases: molecular regulation to clinical use. Pharmacol Rev 58, 488-520.

Benz, C., Clayton, C.E., 2007. The F-box protein CFB2 is required for cytokinesis of bloodstream-form Trypanosoma brucei. Molecular and Biochemical Parasitology 156, 217-224.

Berriman, M., Ghedin, E., Hertz-Fowler, C., Blandin, G., Renauld, H., Bartholomeu, D.C., Lennard, N.J., Caler, E., Hamlin, N.E., Haas, B., Bohme, U., Hannick, L., Aslett, M.A., Shallom, J., Marcello, L., Hou, L., Wickstead, B., Alsmark, U.C., Arrowsmith, C., Atkin, R.J., Barron, A.J., Bringaud, F., Brooks, K., Carrington, M., Cherevach, I., Chillingworth, T.J., Churcher, C., Clark, L.N., Corton, C.H., Cronin, A., Davies, R.M., Doggett, J., Djikeng, A., Feldblyum, T., Field, M.C., Fraser, A., Goodhead, I., Hance, Z., Harper, D., Harris, B.R., Hauser, H., Hostetler, J., Ivens, A., Jagels, K., Johnson, D., Johnson, J., Jones, K., Kerhornou, A.X., Koo, H., Larke, N., Landfear, S., Larkin, C., Leech, V., Line, A., Lord, A., Macleod, A., Mooney, P.J., Moule, S., Martin, D.M., Morgan, G.W., Mungall, K., Norbertczak, H., Ormond, D., Pai, G., Peacock, C.S., Peterson, J., Quail, M.A., Rabbinowitsch, E., Rajandream, M.A., Reitter, C., Salzberg, S.L., Sanders, M., Schobel, S., Sharp, S., Simmonds, M., Simpson, A.J., Tallon, L., Turner, C.M., Tait, A., Tivey, A.R., Van Aken, S., Walker, D., Wanless, D., Wang, S., White, B., White, O., Whitehead, S., Woodward, J., Wortman, J., Adams, M.D., Embley, T.M., Gull, K., Ullu, E., Barry, J.D., Fairlamb, A.H., Opperdoes, F., Barrell, B.G., Donelson, J.E., Hall, N., Fraser, C.M., Melville, S.E., El-Sayed, N.M., 2005. The genome of the African trypanosome Trypanosoma brucei. Science 309, 416-422.

Bhattacharya, A., Biswas, A., Das, P.K., 2009. Role of a differentially expressed cAMP phosphodiesterase in regulating the induction of resistance against oxidative damage in Leishmania donovani. Free Radic Biol Med 47, 1494-1506.

Biasini, M., Bienert, S., Waterhouse, A., Arnold, K., Studer, G., Schmidt, T., Kiefer, F., Cassarino, T.G., Bertoni, M., Bordoli, L., Schwede, T., 2014.

SWISS-MODEL: modelling protein tertiary and quaternary structure using evolutionary information. Nucleic Acids Res 42, W252-258.

Biebinger, S., Wirtz, L.E., Lorenz, P., Clayton, C., 1997. Vectors for inducible expression of toxic gene products in bloodstream and procyclic Trypanosoma brucei. Mol Biochem Parasitol 85, 99-112.

Bieger, B., Essen, L.O., 2001. Structural analysis of adenylate cyclases from Trypanosoma brucei in their monomeric state, Vol 20, 433-445 pp.

Bland, N.D., Wang, C., Tallman, C., Gustafson, A.E., Wang, Z., Ashton, T.D., Ochiana, S.O., McAllister, G., Cotter, K., Fang, A.P., Gechijian, L., Garceau, N., Gangurde, R., Ortenberg, R., Ondrechen, M.J., Campbell, R.K., Pollastri, M.P., 2011. Pharmacological validation of Trypanosoma brucei phosphodiesterases B1 and B2 as druggable targets for African sleeping sickness. J Med Chem 54, 8188-8194.

Blazer, L.L., Roman, D.L., Chung, A., Larsen, M.J., Greedy, B.M., Husbands, S.M., Neubig, R.R., 2010. Reversible, Allosteric Small-Molecule Inhibitors of Regulator of G. Mol Pharmacol 78, 524-533.

Blum, J.A., Neumayr, A.L., Hatz, C.F., 2012. Human African trypanosomiasis in endemic populations and travellers. Eur J Clin Microbiol Infect Dis 31, 905-913.

Borland, G., Bird, R.J., Palmer, T.M., Yarwood, S.J., 2009. Activation of protein kinase Calpha by EPAC1 is required for the ERK- and CCAAT/enhancer-binding protein beta-dependent induction of the SOCS-3 gene by cyclic AMP in COS1 cells. J Biol Chem 284, 17391-17403.

Bos, J.L., 2006. Epac proteins: multi-purpose cAMP targets. Trends Biochem Sci 31, 680-686.

Bradley, P., Misura, K.M.S., Baker, D., 2005. Toward High-Resolution de Novo Structure Prediction for Small Proteins. Science 309, 1868-1871.

Bray, P.G., Barrett, M.P., Ward, S.A., de Koning, H.P., 2003. Pentamidine uptake and resistance in pathogenic protozoa: past, present and future. Trends in Parasitology 19, 232-239.

Breidbach, T., Ngazoa, E., Steverding, D., 2002. Trypanosoma brucei: in vitro slender-to-stumpy differentiation of culture-adapted, monomorphic bloodstream forms. Exp Parasitol 101, 223-230.

Bridges, D.J., Pitt, A.R., Hanrahan, O., Brennan, K., Voorheis, H.P., Herzyk, P., de Koning, H.P., Burchmore, R.J., 2008. Characterisation of the plasma membrane subproteome of bloodstream form Trypanosoma brucei. Proteomics 8, 83-99.

Broadhead, R., Dawe, H.R., Farr, H., Griffiths, S., Hart, S.R., Portman, N., Shaw, M.K., Ginger, M.L., Gaskell, S.J., McKean, P.G., Gull, K., 2006. Flagellar motility is required for the viability of the bloodstream trypanosome. Nature 440, 224-227.

Brun, R., Blum, J., Chappuis, F., Burri, C., 2010. Human African trypanosomiasis. Lancet 375, 148-159.

Brun, R., Don, R., Jacobs, R.T., Wang, M.Z., Barrett, M.P., 2011. Development of novel drugs for human African trypanosomiasis. Future Microbiol 6, 677-691.

Burgin, A.B., Magnusson, O.T., Singh, J., Witte, P., Staker, B.L., Bjornsson, J.M., Thorsteinsdottir, M., Hrafnsdottir, S., Hagen, T., Kiselyov, A.S., Stewart, L.J., Gurney, M.E., 2010. Design of phosphodiesterase 4D (PDE4D) allosteric modulators for enhancing cognition with improved safety. Nat Biotechnol 28, 63-70.

Burri, C., 2010. Chemotherapy against human African trypanosomiasis: is there a road to success? Parasitology 137, 1987-1994.

Burri, C., Brun, R., 2003. Eflornithine for the treatment of human African trypanosomiasis. Parasitol Res 90 Supp 1, S49-52.

Chappuis, F., Loutan, L., Simarro, P., Lejon, V., Buscher, P., 2005. Options for field diagnosis of human african trypanosomiasis. Clin Microbiol Rev 18, 133-146.

Chatelain, E., Ioset, J.R., 2011. Drug discovery and development for neglected diseases: the DNDi model. Drug Des Devel Ther 5, 175-181.

Chen, L., Staubli, S.E.L., Schneider, M.P., Kessels, A.G., Ivic, S., Bachmann, L.M., Kessler, T.M., Phosphodiesterase 5 Inhibitors for the Treatment of Erectile Dysfunction: A Trade-off Network Meta-analysis. European Urology.

Clayton, C.E., 2002. Life without transcriptional control? From fly to man and back again. EMBO J 21, 1881-1888.

Cliff, M.J., Williams, M.A., Brooke-Smith, J., Barford, D., Ladbury, J.E., 2005. Molecular recognition via coupled folding and binding in a TPR domain. J Mol Biol 346, 717-732.

Conti, M., Beavo, J., 2007. Biochemistry and physiology of cyclic nucleotide phosphodiesterases: essential components in cyclic nucleotide signaling. Annu Rev Biochem 76, 481-511.

D'Andrea, L.D., Regan, L., 2003. TPR proteins: the versatile helix. Trends Biochem Sci 28, 655-662.

D'Angelo, M.A., Montagna, A.E., Sanguineti, S., Torres, H.N., Flawia, M.M., 2002. A novel calcium-stimulated adenylyl cyclase from Trypanosoma cruzi, which interacts with the structural flagellar protein paraflagellar rod. J Biol Chem 277, 35025-35034.

D'Angelo, M.A., Sanguineti, S., Reece, J.M., Birnbaumer, L., Torres, H.N., Flawia, M.M., 2004. Identification, characterization and subcellular

localization of TcPDE1, a novel cAMP-specific phosphodiesterase from Trypanosoma cruzi. Biochem J 378, 63-72.

Das, A., Gale, M., Carter, V., Parsons, M., 1994. The protein phosphatase inhibitor okadaic acid induces defects in cytokinesis and organellar genome segregation in Trypanosoma brucei. Journal of Cell Science 107, 3477-3483.

Das, R., Esposito, V., Abu-Abed, M., Anand, G.S., Taylor, S.S., Melacini, G., 2007. cAMP activation of PKA defines an ancient signaling mechanism. Proceedings of the National Academy of Sciences 104, 93-98.

de Koning, H.P., Gould, M.K., Sterk, G.J., Tenor, H., Kunz, S., Luginbuehl, E., Seebeck, T., 2012. Pharmacological validation of Trypanosoma brucei phosphodiesterases as novel drug targets. J Infect Dis 206, 229-237.

de Koning, H.P., Jarvis, S.M., 1999. Adenosine Transporters in Bloodstream Forms of Trypanosoma brucei brucei: Substrate Recognition Motifs and Affinity for Trypanocidal Drugs. Molecular Pharmacology 56, 1162-1170.

de Rooij, J., Rehmann, H., van Triest, M., Cool, R.H., Wittinghofer, A., Bos, J.L., 2000. Mechanism of Regulation of the Epac Family of cAMP-dependent RapGEFs. Journal of Biological Chemistry 275, 20829-20836.

Delbridge, L.M., O'Riordan, M.X., 2007. Innate recognition of intracellular bacteria. Curr Opin Immunol 19, 10-16.

Delespaux, V., de Koning, H.P., 2007. Drugs and drug resistance in African trypanosomiasis. Drug Resist Updat 10, 30-50.

Demonchy, R., Blisnick, T., Deprez, C., Toutirais, G., Loussert, C., Marande, W., Grellier, P., Bastin, P., Kohl, L., 2009. Kinesin 9 family members perform separate functions in the trypanosome flagellum. The Journal of Cell Biology 187, 615-622.

Dessauer, C.W., 2009. Adenylyl Cyclase–A-kinase Anchoring Protein Complexes: The Next Dimension in cAMP Signaling. Molecular Pharmacology 76, 935-941.

Dhalia, R., Reis, C.R.S., Freire, E.R., Rocha, P.O., Katz, R., Muniz, J.R.C., Standart, N., de Melo Neto, O.P., 2005. Translation initiation in Leishmania major: characterisation of multiple eIF4F subunit homologues. Molecular and Biochemical Parasitology 140, 23-41.

Diaz-Benjumea, R., Laxman, S., Hinds, T.R., Beavo, J.A., Rascon, A., 2006. Characterization of a novel cAMP-binding, cAMP-specific cyclic nucleotide phosphodiesterase (TcrPDEB1) from Trypanosoma cruzi. Biochem J 399, 305-314.

Dorsey, P., Keel, C., Klavens, M., Hellstrom, W.J., 2010. Phosphodiesterase type 5 (PDE5) inhibitors for the treatment of erectile dysfunction. Expert Opin Pharmacother 11, 1109-1122.

Dougherty, M.K., Morrison, D.K., 2004. Unlocking the code of 14-3-3. Journal of Cell Science 117, 1875-1884.

Duncan, R., Alvarez, R., Jaffe, C.L., Wiese, M., Klutch, M., Shakarian, A., Dwyer, D., Nakhasi, H.L., 2001. Early response gene expression during differentiation of cultured Leishmania donovani. Parasitol Res 87, 897-906.

Dunphy, J.T., Linder, M.E., 1998. Signalling functions of protein palmitoylation. Biochimica et Biophysica Acta (BBA) - Molecular and Cell Biology of Lipids 1436, 245-261.

Emes, R.D., Yang, Z., 2008. Duplicated paralogous genes subject to positive selection in the genome of Trypanosoma brucei. PLoS One 3, e2295.

Emmer, B.T., Nakayasu, E.S., Souther, C., Choi, H., Sobreira, T.J., Epting, C.L., Nesvizhskii, A.I., Almeida, I.C., Engman, D.M., 2011a. Global analysis of protein palmitoylation in African trypanosomes. Eukaryot Cell 10, 455-463.

Emmer, B.T., Nakayasu, E.S., Souther, C., Choi, H., Sobreira, T.J.P., Epting, C.L., Nesvizhskii, A.I., Almeida, I.C., Engman, D.M., 2011b. Global Analysis of Protein Palmitoylation in African Trypanosomes. Eukaryotic Cell 10, 455-463.

Engstler, M., Thilo, L., Weise, F., Grunfelder, C.G., Schwarz, H., Boshart, M., Overath, P., 2004. Kinetics of endocytosis and recycling of the GPI-anchored variant surface glycoprotein in Trypanosoma brucei. J Cell Sci 117, 1105-1115.

Eperon, G., Balasegaram, M., Potet, J., Mowbray, C., Valverde, O., Chappuis, F., 2014. Treatment options for second-stage gambiense human African trypanosomiasis. Expert Review of Anti-infective Therapy 12, 1407-1417.

Ersfeld, K., Barraclough, H., Gull, K., 2005. Evolutionary relationships and protein domain architecture in an expanded calpain superfamily in kinetoplastid parasites. J Mol Evol 61, 742-757.

Fairlamb, A.H., 2003. Chemotherapy of human African trypanosomiasis: current and future prospects. Trends Parasitol 19, 488-494.

Fairlamb, A.H., Henderson, G.B., Cerami, A., 1989. Trypanothione is the primary target for arsenical drugs against African trypanosomes. Proc Natl Acad Sci U S A 86, 2607-2611.

Fallah, F., 2015. Recent strategies in treatment of pulmonary arterial hypertension, a review. Glob J Health Sci 7, 40643.

Farber, D.B., Danciger, M., 1997. Identification of genes causing photoreceptor degenerations leading to blindness. Curr Opin Neurobiol 7, 666-673.

Fevre, E.M., Coleman, P.G., Odiit, M., Magona, J.W., Welburn, S.C., Woolhouse, M.E., 2001. The origins of a new Trypanosoma brucei rhodesiense sleeping sickness outbreak in eastern Uganda. Lancet 358, 625-628.

Fevre, E.M., Picozzi, K., Jannin, J., Welburn, S.C., Maudlin, I., 2006. Human African trypanosomiasis: Epidemiology and control. Adv Parasitol 61, 167-221.

Firtel, R.A., Meili, R., 2000. Dictyostelium: a model for regulated cell movement during morphogenesis. Curr Opin Genet Dev 10, 421-427.

Flawia, M.M., Tellez-Inon, M.T., Torres, H.N., 1997. Signal transduction mechanisms in Trypanosoma cruzi. Parasitol Today 13, 30-33.

Forman, H.J., 2009. Signal transduction and reactive species. Free Radic Biol Med 47, 1237-1238.

Francis, S., Houslay, M., Conti, M. 2011a. Phosphodiesterase Inhibitors: Factors That Influence Potency, Selectivity, and Action, In: Francis, S.H., Conti, M., Houslay, M.D. (Eds.) Phosphodiesterases as Drug Targets. Springer Berlin Heidelberg, 47-84.

Francis, S.H., Blount, M.A., Corbin, J.D., 2011b. Mammalian Cyclic Nucleotide Phosphodiesterases: Molecular Mechanisms and Physiological Functions, Vol 91, 651-690 pp.

Francis, S.H., Houslay, M.D., Conti, M., 2011c. Phosphodiesterase inhibitors: factors that influence potency, selectivity, and action. Handb Exp Pharmacol, 47-84.

Gadelha, C., Rothery, S., Morphew, M., McIntosh, J.R., Severs, N.J., Gull, K., 2009. Membrane domains and flagellar pocket boundaries are influenced by the cytoskeleton in African trypanosomes. Proc Natl Acad Sci U S A 106, 17425-17430.

Galie, N., Rubin, L.J., Simonneau, G., 2010. Phosphodiesterase inhibitors for pulmonary hypertension. N Engl J Med 362, 559-560; author reply 560.

Garbers, D.L., Chrisman, T.D., Wiegn, P., Katafuchi, T., Albanesi, J.P., Bielinski, V., Barylko, B., Redfield, M.M., Burnett, J.C., Jr., 2006. Membrane guanylyl cyclase receptors: an update. Trends Endocrinol Metab 17, 251-258.

Garcia, E.S., Gonzalez, M.S., de Azambuja, P., Baralle, F.E., Fraidenraich, D., Torres, H.N., Flawia, M.M., 1995. Induction of Trypanosoma cruzi metacyclogenesis in the gut of the hematophagous insect vector, Rhodnius prolixus, by hemoglobin and peptides carrying alpha D-globin sequences. Exp Parasitol 81, 255-261.

Garland, S.L., 2013. Are GPCRs Still a Source of New Targets? Journal of Biomolecular Screening 18, 947-966.

Genestra, M., Cysne-Finkelstein, L., Leon, L., 2004. Protein kinase A activity is associated with metacyclogenesis in Leishmania amazonensis. Cell Biochem Funct 22, 315-320.

Germain, P., Chambon, P., Eichele, G., Evans, R.M., Lazar, M.A., Leid, M., De Lera, A.R., Lotan, R., Mangelsdorf, D.J., Gronemeyer, H., 2006. International Union of Pharmacology. LX. Retinoic acid receptors. Pharmacol Rev 58, 712-725.

Geslain, R., Aeby, E., Guitart, T., Jones, T.E., de Moura, M.C., Charrière, F., Schneider, A., de Pouplana, L.R., 2006. Trypanosoma Seryl-tRNA Synthetase Is a Metazoan-like Enzyme with High Affinity for tRNASec. Journal of Biological Chemistry 281, 38217-38225.

Ghofrani, H.A., Osterloh, I.H., Grimminger, F., 2006. Sildenafil: from angina to erectile dysfunction to pulmonary hypertension and beyond. Nat Rev Drug Discov 5, 689-702.

Gong, K.W., Kunz, S., Zoraghi, R., Kunz Renggli, C., Brun, R., Seebeck, T., 2001. cAMP-specific phosphodiesterase TbPDE1 is not essential in Trypanosoma brucei in culture or during midgut infection of tsetse flies. Mol Biochem Parasitol 116, 229-232.

Goodacre, N.F., Gerloff, D.L., Uetz, P., 2014. Protein Domains of Unknown Function Are Essential in Bacteria. mBio 5.

Gould, M.K., Bachmaier, S., Ali, J.A., Alsford, S., Tagoe, D.N., Munday, J.C., Schnaufer, A.C., Horn, D., Boshart, M., de Koning, H.P., 2013. Cyclic AMP effectors in African trypanosomes revealed by genome-scale RNA interference library screening for resistance to the phosphodiesterase inhibitor CpdA. Antimicrob Agents Chemother 57, 4882-4893.

Gould, M.K., de Koning, H.P., 2011. Cyclic-nucleotide signalling in protozoa. FEMS Microbiol Rev 35, 515-541.

Grab, D.J., Nikolskaia, O.V., Inoue, N., Thekisoe, O.M., Morrison, L.J., Gibson, W., Dumler, J.S., 2011. Using detergent to enhance detection sensitivity of African trypanosomes in human CSF and blood by loop-mediated isothermal amplification (LAMP). PLoS Negl Trop Dis 5, e1249.

Gross-Langenhoff, M., Hofbauer, K., Weber, J., Schultz, A., Schultz, J.E., 2006. cAMP is a ligand for the tandem GAF domain of human phosphodiesterase 10 and cGMP for the tandem GAF domain of phosphodiesterase 11. J Biol Chem 281, 2841-2846.

Grunfelder, C.G., Engstler, M., Weise, F., Schwarz, H., Stierhof, Y.D., Boshart, M., Overath, P., 2002. Accumulation of a GPI-anchored protein at the cell surface requires sorting at multiple intracellular levels. Traffic 3, 547-559.

Gu, Z.C., Enenkel, C., 2014. Proteasome assembly. Cell Mol Life Sci 71, 4729-4745.

Gull, K., 2003. Host-parasite interactions and trypanosome morphogenesis: a flagellar pocketful of goodies. Curr Opin Microbiol 6, 365-370.

Haimeur, A., Ouellette, M., 1998. Gene amplification in Leishmania tarentolae selected for resistance to sodium stibogluconate. Antimicrob Agents Chemother 42, 1689-1694.

Hainard, A., Tiberti, N., Robin, X., Lejon, V., Ngoyi, D.M., Matovu, E., Enyaru, J.C., Fouda, C., Ndung'u, J.M., Lisacek, F., Muller, M., Turck, N., Sanchez, J.C., 2009. A combined CXCL10, CXCL8 and H-FABP panel for the staging of human African trypanosomiasis patients. PLoS Negl Trop Dis 3, e459.

Hall, N., Berriman, M., Lennard, N.J., Harris, B.R., Hertz-Fowler, C., Bart-Delabesse, E.N., Gerrard, C.S., Atkin, R.J., Barron, A.J., Bowman, S., Bray-Allen, S.P., Bringaud, F., Clark, L.N., Corton, C.H., Cronin, A., Davies, R., Doggett, J., Fraser, A., Gruter, E., Hall, S., Harper, A.D., Kay, M.P., Leech, V., Mayes, R., Price, C., Quail, M.A., Rabbinowitsch, E., Reitter, C., Rutherford, K., Sasse, J., Sharp, S., Shownkeen, R., MacLeod, A., Taylor, S., Tweedie, A., Turner, C.M., Tait, A., Gull, K., Barrell, B., Melville, S.E., 2003. The DNA sequence of chromosome I of an African trypanosome: gene content, chromosome organisation, recombination and polymorphism. Nucleic Acids Res 31, 4864-4873.

Hamedi, A., Botelho, L., Britto, C., Fragoso, S.P., Umaki, A.C., Goldenberg, S., Bottu, G., Salmon, D., 2015. In vitro metacyclogenesis of Trypanosoma cruzi induced by starvation correlates with a transient adenylyl cyclase stimulation as well as with a constitutive upregulation of adenylyl cyclase expression. Mol Biochem Parasitol.

Hamet, P., Pang, S.C., Tremblay, J., 1989. Atrial natriuretic factor-induced egression of cyclic guanosine 3':5'-monophosphate in cultured vascular smooth muscle and endothelial cells. J Biol Chem 264, 12364-12369.

Hammarton, T.C., Clark, J., Douglas, F., Boshart, M., Mottram, J.C., 2003. Stage-specific differences in cell cycle control in Trypanosoma brucei revealed by RNA interference of a mitotic cyclin. J Biol Chem 278, 22877-22886.

Handa, N., Mizohata, E., Kishishita, S., Toyama, M., Morita, S., Uchikubo-Kamo, T., Akasaka, R., Omori, K., Kotera, J., Terada, T., Shirouzu, M., Yokoyama, S., 2008. Crystal structure of the GAF-B domain from human phosphodiesterase 10A complexed with its ligand, cAMP. J Biol Chem 283, 19657-19664.

Hanna, M.H., Nowicki, J.J., Fatone, M.A., 1984. Extracellular cyclic AMP during development of the cellular slime mold Polysphondylium violaceum: comparison of accumulation in the wild type and an aggregation-defective mutant. J Bacteriol 157, 345-349.

Hayakawa, A., Hayes, S., Leonard, D., Lambright, D., Corvera, S., 2007. Evolutionarily conserved structural and functional roles of the FYVE domain. Biochem Soc Symp, 95-105.

Hotez, P.J., Fenwick, A., Savioli, L., Molyneux, D.H., 2009. Rescuing the bottom billion through control of neglected tropical diseases. Lancet 373, 1570-1575.

Hotez, P.J., Molyneux, D.H., Fenwick, A., Kumaresan, J., Sachs, S.E., Sachs, J.D., Savioli, L., 2007. Control of neglected tropical diseases. N Engl J Med 357, 1018-1027.

Hotez, P.J., Molyneux, D.H., Fenwick, A., Ottesen, E., Ehrlich Sachs, S., Sachs, J.D., 2006. Incorporating a rapid-impact package for neglected tropical diseases with programs for HIV/AIDS, tuberculosis, and malaria. PLoS Med 3, e102.

Houslay, M.D., Baillie, G.S., Maurice, D.H., 2007. cAMP-Specific phosphodiesterase-4 enzymes in the cardiovascular system: a molecular toolbox for generating compartmentalized cAMP signaling. Circ Res 100, 950-966.

Huang, H., 2011. Signal transduction in Trypanosoma cruzi. Adv Parasitol 75, 325-344.

Huang, H., Weiss, L.M., Nagajyothi, F., Tanowitz, H.B., Wittner, M., Orr, G.A., Bao, Y., 2006. Molecular cloning and characterization of the protein kinase A regulatory subunit of Trypanosoma cruzi. Mol Biochem Parasitol 149, 242-245.

Huang, H., Werner, C., Weiss, L.M., Wittner, M., Orr, G.A., 2002. Molecular cloning and expression of the catalytic subunit of protein kinase A from Trypanosoma cruzi. Int J Parasitol 32, 1107-1115.

Huang, R., Martinez-Ferrando, I., Cole, P.A., 2010. Enhanced interrogation: emerging strategies for cell signaling inhibition. Nat Struct Mol Biol 17, 646-649.

Huang, Z., Myers, K., Khatra, B., Vijayaraghavan, S., 2004. Protein 14-3-3ζ Binds to Protein Phosphatase PP1γ2 in Bovine Epididymal Spermatozoa. Biology of Reproduction 71, 177-184.

Inoue, M., Nakamura, Y., Yasuda, K., Yasaka, N., Hara, T., Schnaufer, A., Stuart, K., Fukuma, T., 2005. The 14-3-3 Proteins of Trypanosoma brucei Function in Motility, Cytokinesis, and Cell Cycle. Journal of Biological Chemistry 280, 14085-14096.

Jacobs, R.T., Nare, B., Phillips, M.A., 2011a. State of the art in African trypanosome drug discovery. Curr Top Med Chem 11, 1255-1274.

Jacobs, R.T., Nare, B., Wring, S.A., Orr, M.D., Chen, D., Sligar, J.M., Jenks, M.X., Noe, R.A., Bowling, T.S., Mercer, L.T., Rewerts, C., Gaukel, E., Owens, J., Parham, R., Randolph, R., Beaudet, B., Bacchi, C.J., Yarlett, N., Plattner, J.J., Freund, Y., Ding, C., Akama, T., Zhang, Y.K., Brun, R., Kaiser, M., Scandale, I., Don, R., 2011b. SCYX-7158, an Orally-Active Benzoxaborole for the Treatment of Stage 2 Human African Trypanosomiasis. PLoS Negl Trop Dis 5, e1151.

Jäger, A.V., De Gaudenzi, J.G., Mild, J.G., Cormack, B.M., Pantano, S., Altschuler, D.L., Edreira, M.M., 2014. Identification of novel cyclic nucleotide binding proteins in Trypanosoma cruzi. Molecular and Biochemical Parasitology 198, 104-112.

Jansen, C., Wang, H., Kooistra, A.J., de Graaf, C., Orrling, K.M., Tenor, H., Seebeck, T., Bailey, D., de Esch, I.J., Ke, H., Leurs, R., 2013. Discovery of novel Trypanosoma brucei phosphodiesterase B1 inhibitors by virtual screening against the unliganded TbrPDEB1 crystal structure. J Med Chem 56, 2087-2096.

Jaski, B.E., Fifer, M.A., Wright, R.F., Braunwald, E., Colucci, W.S., 1985. Positive inotropic and vasodilator actions of milrinone in patients with severe congestive heart failure. Dose-response relationships and comparison to nitroprusside. J Clin Invest 75, 643-649.

Jin, S.L., Bushnik, T., Lan, L., Conti, M., 1998. Subcellular localization of rolipram-sensitive, cAMP-specific phosphodiesterases. Differential targeting and activation of the splicing variants derived from the PDE4D gene. J Biol Chem 273, 19672-19678.

Johner, A., Kunz, S., Linder, M., Shakur, Y., Seebeck, T., 2006. Cyclic nucleotide specific phosphodiesterases of Leishmania major. BMC Microbiol 6, 25.

Kabani, S., Fenn, K., Ross, A., Ivens, A., Smith, T.K., Ghazal, P., Matthews, K., 2009. Genome-wide expression profiling of in vivo-derived bloodstream parasite stages and dynamic analysis of mRNA alterations during synchronous differentiation in Trypanosoma brucei. BMC Genomics 10, 427.

Kaiser, M., Bray, M.A., Cal, M., Bourdin Trunz, B., Torreele, E., Brun, R., 2011. Antitrypanosomal Activity of Fexinidazole, a New Oral Nitroimidazole Drug Candidate for Treatment of Sleeping Sickness. Antimicrobial Agents and Chemotherapy 55, 5602-5608.

Kaneko, T., Hamazaki, J., Iemura, S., Sasaki, K., Furuyama, K., Natsume, T., Tanaka, K., Murata, S., 2009. Assembly pathway of the Mammalian proteasome base subcomplex is mediated by multiple specific chaperones. Cell 137, 914-925.

Kaur, K.J., Ruben, L., 1994. Protein translation elongation factor-1 alpha from Trypanosoma brucei binds calmodulin. Journal of Biological Chemistry 269, 23045-23050.

Ke, H., Wang, H., 2007. Crystal structures of phosphodiesterases and implications on substrate specificity and inhibitor selectivity. Curr Top Med Chem 7, 391-403.

Kelley, L.A., Sternberg, M.J., 2009. Protein structure prediction on the Web: a case study using the Phyre server. Nat Protoc 4, 363-371.

Kennedy, P.G., 2004. Human African trypanosomiasis of the CNS: current issues and challenges. J Clin Invest 113, 496-504.

Kennedy, P.G., 2006. Diagnostic and neuropathogenesis issues in human African trypanosomiasis. Int J Parasitol 36, 505-512.

Kennedy, P.G., 2008a. The continuing problem of human African trypanosomiasis (sleeping sickness). Ann Neurol 64, 116-126.

Kennedy, P.G., 2008b. Diagnosing central nervous system trypanosomiasis: two stage or not to stage? Trans R Soc Trop Med Hyg 102, 306-307.

Kennedy, P.G., 2012. An alternative form of melarsoprol in sleeping sickness. Trends Parasitol 28, 307-310.

Keravis, T., Lugnier, C., 2010. Cyclic nucleotide phosphodiesterases (PDE) and peptide motifs. Curr Pharm Des 16, 1114-1125.

Keravis, T., Lugnier, C., 2012. Cyclic nucleotide phosphodiesterase (PDE) isozymes as targets of the intracellular signalling network: benefits of PDE inhibitors in various diseases and perspectives for future therapeutic developments. British Journal of Pharmacology 165, 1288-1305.

Kolev, N.G., Franklin, J.B., Carmi, S., Shi, H., Michaeli, S., Tschudi, C., 2010. The Transcriptome of the Human PathogenTrypanosoma brucei at Single-Nucleotide Resolution. PLoS Pathog 6, e1001090.

Kramer, S., 2012. Developmental regulation of gene expression in the absence of transcriptional control: The case of kinetoplastids. Molecular and Biochemical Parasitology 181, 61-72.

Krishnamurthy, S., Moorthy, B.S., Xin Xiang, L., Xin Shan, L., Bharatham, K., Tulsian, N.K., Mihalek, I., Anand, G.S., 2014. Active site coupling in PDE:PKA complexes promotes resetting of mammalian cAMP signaling. Biophys J 107, 1426-1440.

Kuboki, N., Inoue, N., Sakurai, T., Di Cello, F., Grab, D.J., Suzuki, H., Sugimoto, C., Igarashi, I., 2003. Loop-mediated isothermal amplification for detection of African trypanosomes. J Clin Microbiol 41, 5517-5524.

Kuepfer, I., Hhary, E.P., Allan, M., Edielu, A., Burri, C., Blum, J.A., 2011. Clinical presentation of T.b. rhodesiense sleeping sickness in second stage patients from Tanzania and Uganda. PLoS Negl Trop Dis 5, e968.

Kumari, B., Kumar, R., Kumar, M., 2014. PalmPred: An SVM Based Palmitoylation Prediction Method Using Sequence Profile Information. PLoS ONE 9, e89246.

Kunz, S., Beavo, J.A., D'Angelo, M.A., Flawia, M.M., Francis, S.H., Johner, A., Laxman, S., Oberholzer, M., Rascon, A., Shakur, Y., Wentzinger, L., Zoraghi, R., Seebeck, T., 2006. Cyclic nucleotide specific phosphodiesterases of the kinetoplastida: a unified nomenclature. Mol Biochem Parasitol 145, 133-135.

Kunz, S., Oberholzer, M., Seebeck, T., 2005. A FYVE-containing unusual cyclic nucleotide phosphodiesterase from Trypanosoma cruzi. FEBS J 272, 6412-6422.

la Cour, T., Gupta, R., Rapacki, K., Skriver, K., Poulsen, F.M., Brunak, S., 2003. NESbase version 1.0: a database of nuclear export signals. Nucleic Acids Research 31, 393-396.

Langmead, B., Trapnell, C., Pop, M., Salzberg, S.L., 2009. Ultrafast and memory-efficient alignment of short DNA sequences to the human genome. Genome Biol 10, R25.

Langousis, G., Hill, K.L., 2014. Motility and more: the flagellum of Trypanosoma brucei. Nat Rev Microbiol 12, 505-518.

Laxman, S., Beavo, J.A., 2007. Cyclic nucleotide signaling mechanisms in trypanosomes: possible targets for therapeutic agents. Mol Interv 7, 203-215.

Laxman, S., Rascon, A., Beavo, J.A., 2005. Trypanosome cyclic nucleotide phosphodiesterase 2B binds cAMP through its GAF-A domain. J Biol Chem 280, 3771-3779.

Laxman, S., Riechers, A., Sadilek, M., Schwede, F., Beavo, J.A., 2006. Hydrolysis products of cAMP analogs cause transformation of Trypanosoma brucei from slender to stumpy-like forms. Proc Natl Acad Sci U S A 103, 19194-19199.

Lejon, V., Buscher, P., Sema, N.H., Magnus, E., Van Meirvenne, N., 1998. Human African trypanosomiasis: a latex agglutination field test for quantifying IgM in cerebrospinal fluid. Bull World Health Organ 76, 553-558.

Lejon, V., Legros, D., Richer, M., Ruiz, J.A., Jamonneau, V., Truc, P., Doua, F., Dje, N., N'Siesi, F.X., Bisser, S., Magnus, E., Wouters, I., Konings, J., Vervoort, T., Sultan, F., Buscher, P., 2002. IgM quantification in the cerebrospinal fluid of sleeping sickness patients by a latex card agglutination test. Trop Med Int Health 7, 685-692.

Lejon, V., Reiber, H., Legros, D., Dje, N., Magnus, E., Wouters, I., Sindic, C.J., Buscher, P., 2003. Intrathecal immune response pattern for improved diagnosis of central nervous system involvement in trypanosomiasis. J Infect Dis 187, 1475-1483.

Li, E., Hristova, K., 2006. Role of receptor tyrosine kinase transmembrane domains in cell signaling and human pathologies. Biochemistry 45, 6241-6251.

Li, J.B., Gerdes, J.M., Haycraft, C.J., Fan, Y., Teslovich, T.M., May-Simera, H., Li, H., Blacque, O.E., Li, L., Leitch, C.C., Lewis, R.A., Green, J.S., Parfrey, P.S., Leroux, M.R., Davidson, W.S., Beales, P.L., Guay-Woodford, L.M., Yoder, B.K., Stormo, G.D., Katsanis, N., Dutcher, S.K., 2004. Comparative genomics identifies a flagellar and basal body proteome that includes the BBS5 human disease gene. Cell 117, 541-552.

Li, Z., Wang, C.C., 2003. A PHO80-like cyclin and a B-type cyclin control the cell cycle of the procyclic form of Trypanosoma brucei. J Biol Chem 278, 20652-20658.

Liu, W., Apagyi, K., McLeavy, L., Ersfeld, K., 2010. Expression and cellular localisation of calpain-like proteins in Trypanosoma brucei. Molecular and Biochemical Parasitology 169, 20-26.

Lopez, M.A., Saada, E.A., Hill, K.L., 2015. Insect stage-specific adenylate cyclases regulate social motility in African trypanosomes. Eukaryot Cell 14, 104-112.

Luttrell, L.M., Maudsley, S., Bohn, L.M., 2015. Fulfilling the Promise of 'Biased' GPCR Agonism. Molecular Pharmacology.

MacGregor, P., Szoor, B., Savill, N.J., Matthews, K.R., 2012. Trypanosomal immune evasion, chronicity and transmission: an elegant balancing act. Nat Rev Microbiol 10, 431-438.

MacLean, L., Chisi, J.E., Odiit, M., Gibson, W.C., Ferris, V., Picozzi, K., Sternberg, J.M., 2004. Severity of human african trypanosomiasis in East Africa is associated with geographic location, parasite genotype, and host inflammatory cytokine response profile. Infect Immun 72, 7040-7044.

MacLean, L.M., Odiit, M., Chisi, J.E., Kennedy, P.G., Sternberg, J.M., 2010. Focus-specific clinical profiles in human African Trypanosomiasis caused by Trypanosoma brucei rhodesiense. PLoS Negl Trop Dis 4, e906.

MacLeod, E.T., Maudlin, I., Welburn, S.C., 2008. Effects of cyclic nucleotides on midgut infections and maturation of T. b. brucei in G. m. morsitans. Parasit Vectors 1, 5.

Magnus, E., Vervoort, T., Van Meirvenne, N., 1978. A card-agglutination test with stained trypanosomes (C.A.T.T.) for the serological diagnosis of T. B. gambiense trypanosomiasis. Ann Soc Belg Med Trop 58, 169-176.

Malki-Feldman, L., Jaffe, C.L., 2009. Leishmania major: effect of protein kinase A and phosphodiesterase activity on infectivity and proliferation of promastigotes. Exp Parasitol 123, 39-44.

Mancini, P.E., Patton, C.L., 1981. Cyclic 3',5'-adenosine monophosphate levels during the developmental cycle of Trypanosoma brucei brucei in the rat. Mol Biochem Parasitol 3, 19-31.

Martinez, S.E., Heikaus, C.C., Klevit, R.E., Beavo, J.A., 2008. The structure of the GAF A domain from phosphodiesterase 6C reveals determinants of cGMP binding, a conserved binding surface, and a large cGMP-dependent conformational change. J Biol Chem 283, 25913-25919.

Matthews, K.R., 2005. The developmental cell biology of Trypanosoma brucei. J Cell Sci 118, 283-290.

Maurer-Stroh, S., Eisenhaber, B., Eisenhaber, F., 2002. N-terminal N-myristoylation of proteins: prediction of substrate proteins from amino acid sequence1. Journal of Molecular Biology 317, 541-557.

Maurice, D.H., Ke, H., Ahmad, F., Wang, Y., Chung, J., Manganiello, V.C., 2014. Advances in targeting cyclic nucleotide phosphodiesterases. Nat Rev Drug Discov 13, 290-314.

Merchant, S.S., Prochnik, S.E., Vallon, O., Harris, E.H., Karpowicz, S.J., Witman, G.B., Terry, A., Salamov, A., Fritz-Laylin, L.K., Marechal-Drouard, L., Marshall, W.F., Qu, L.H., Nelson, D.R., Sanderfoot, A.A., Spalding, M.H., Kapitonov, V.V., Ren, Q., Ferris, P., Lindquist, E., Shapiro, H., Lucas, S.M., Grimwood, J., Schmutz, J., Cardol, P., Cerutti, H., Chanfreau, G., Chen, C.L., Cognat, V., Croft, M.T., Dent, R., Dutcher, S., Fernandez, E., Fukuzawa, H., Gonzalez-Ballester, D., Gonzalez-Halphen, D., Hallmann, A., Hanikenne, M., Hippler, M., Inwood, W., Jabbari, K., Kalanon, M., Kuras, R., Lefebvre, P.A., Lemaire, S.D., Lobanov, A.V., Lohr, M., Manuell, A., Meier, I., Mets, L., Mittag, M., Mittelmeier, T., Moroney, J.V., Moseley, J., Napoli, C., Nedelcu, A.M., Niyogi, K., Novoselov, S.V., Paulsen, I.T., Pazour, G., Purton, S., Ral, J.P., Riano-Pachon, D.M., Riekhof, W., Rymarquis, L., Schroda, M., Stern, D., Umen, J., Willows, R., Wilson, N., Zimmer, S.L., Allmer, J., Balk, J., Bisova, K., Chen, C.J., Elias, M., Gendler, K., Hauser, C., Lamb, M.R., Ledford, H., Long, J.C., Minagawa, J., Page, M.D., Pan, J., Pootakham, W., Roje, S., Rose, A., Stahlberg, E., Terauchi, A.M., Yang, P., Ball, S., Bowler, C., Dieckmann, C.L., Gladyshev, V.N., Green, P., Jorgensen, R., Mayfield, S., Mueller-Roeber, B., Rajamani, S., Sayre, R.T., Brokstein, P., Dubchak, I., Goodstein, D., Hornick, L., Huang, Y.W., Jhaveri, J., Luo, Y., Martinez, D., Ngau, W.C., Otillar, B., Poliakov, A., Porter, A., Szajkowski, L., Werner, G., Zhou, K., Grigoriev, I.V., Rokhsar, D.S., Grossman, A.R., 2007. The Chlamydomonas genome reveals the evolution of key animal and plant functions. Science 318, 245-250.

Molyneux, D.H., Hotez, P.J., Fenwick, A., 2005. "Rapid-impact interventions": how a policy of integrated control for Africa's neglected tropical diseases could benefit the poor. PLoS Med 2, e336.

Mony, B.M., MacGregor, P., Ivens, A., Rojas, F., Cowton, A., Young, J., Horn, D., Matthews, K., 2014. Genome-wide dissection of the quorum sensing signalling pathway in Trypanosoma brucei. Nature 505, 681-685.

Moore, D.A., Edwards, M., Escombe, R., Agranoff, D., Bailey, J.W., Squire, S.B., Chiodini, P.L., 2002. African trypanosomiasis in travelers returning to the United Kingdom. Emerg Infect Dis 8, 74-76.

Mugasa, C.M., Adams, E.R., Boer, K.R., Dyserinck, H.C., Buscher, P., Schallig, H.D., Leeflang, M.M., 2012. Diagnostic accuracy of molecular amplification tests for human African trypanosomiasis--systematic review. PLoS Negl Trop Dis 6, e1438.

Mumba, D., Bohorquez, E., Messina, J., Kande, V., Taylor, S.M., Tshefu, A.K., Muwonga, J., Kashamuka, M.M., Emch, M., Tidwell, R., Buscher, P., Meshnick, S.R., 2011. Prevalence of human African trypanosomiasis in the Democratic Republic of the Congo. PLoS Negl Trop Dis 5, e1246.

Munday, J.C., Rojas López, K.E., Eze, A.A., Delespaux, V., Van Den Abbeele, J., Rowan, T., Barrett, M.P., Morrison, L.J., de Koning, H.P., 2013.

Functional expression of TcoAT1 reveals it to be a P1-type nucleoside transporter with no capacity for diminazene uptake. International Journal for Parasitology: Drugs and Drug Resistance 3, 69-76.

Munday, J.C., Tagoe, D.N.A., Eze, A.A., Krezdorn, J.A.M., Rojas López, K.E., Alkhaldi, A.A.M., McDonald, F., Still, J., Alzahrani, K.J., Settimo, L., De Koning, H.P., 2015. Functional analysis of drug resistance-associated mutations in the Trypanosoma brucei adenosine transporter 1 (TbAT1) and the proposal of a structural model for the protein. Molecular Microbiology, n/a-n/a.

Naula, C., Schaub, R., Leech, V., Melville, S., Seebeck, T., 2001. Spontaneous dimerization and leucine-zipper induced activation of the recombinant catalytic domain of a new adenylyl cyclase of Trypanosoma brucei, GRESAG4.4B. Mol Biochem Parasitol 112, 19-28.

Naula, C., Seebeck, T., 2000. Cyclic AMP signaling in trypanosomatids. Parasitol Today 16, 35-38.

Nett, I.R., Martin, D.M., Miranda-Saavedra, D., Lamont, D., Barber, J.D., Mehlert, A., Ferguson, M.A., 2009. The phosphoproteome of bloodstream form Trypanosoma brucei, causative agent of African sleeping sickness. Mol Cell Proteomics 8, 1527-1538.

Niemann, M., Wiese, S., Mani, J., Chanfon, A., Jackson, C., Meisinger, C., Warscheid, B., Schneider, A., 2013. Mitochondrial Outer Membrane Proteome of Trypanosoma brucei Reveals Novel Factors Required to Maintain Mitochondrial Morphology. Molecular & Cellular Proteomics 12, 515-528.

Nikawa, J., Cameron, S., Toda, T., Ferguson, K.M., Wigler, M., 1987. Rigorous feedback control of cAMP levels in Saccharomyces cerevisiae. Genes Dev 1, 931-937.

Njiru, Z.K., 2012. Loop-mediated isothermal amplification technology: towards point of care diagnostics. PLoS Negl Trop Dis 6, e1572.

Norrander, J.M., deCathelineau, A.M., Brown, J.A., Porter, M.E., Linck, R.W., 2000. The Rib43a protein is associated with forming the specialized protofilament ribbons of flagellar microtubules in Chlamydomonas. Molecular biology of the cell 11, 201-215.

O'Hara, B.P., Wilson, S.A., Lee, A.W., Roe, S.M., Siligardi, G., Drew, R.E., Pearl, L.H., 2000. Structural adaptation to selective pressure for altered ligand specificity in the Pseudomonas aeruginosa amide receptor, amiC. Protein Eng 13, 129-132.

Oberholzer, M., Langousis, G., Nguyen, H.T., Saada, E.A., Shimogawa, M.M., Jonsson, Z.O., Nguyen, S.M., Wohlschlegel, J.A., Hill, K.L., 2011. Independent analysis of the flagellum surface and matrix proteomes provides insight into flagellum signaling in mammalian-infectious Trypanosoma brucei. Mol Cell Proteomics 10, M111 010538.

Oberholzer, M., Marti, G., Baresic, M., Kunz, S., Hemphill, A., Seebeck, T., 2007. The Trypanosoma brucei cAMP phosphodiesterases TbrPDEB1 and TbrPDEB2: flagellar enzymes that are essential for parasite virulence. FASEB J 21, 720-731.

Oberholzer, M., Saada, E.A., Hill, K.L., 2015. Cyclic AMP Regulates Social Behavior in African Trypanosomes. MBio 6.

Ochatt, C.M., Ulloa, R.M., Torres, H.N., Tellez-Inon, M.T., 1993. Characterization of the catalytic subunit of Trypanosoma cruzi cyclic AMP-dependent protein kinase. Mol Biochem Parasitol 57, 73-81.

Ochiana, S.O., Gustafson, A., Bland, N.D., Wang, C., Russo, M.J., Campbell, R.K., Pollastri, M.P., 2012. Synthesis and evaluation of human phosphodiesterases (PDE) 5 inhibitor analogs as trypanosomal PDE inhibitors. Part 2. Tadalafil analogs. Bioorganic & Medicinal Chemistry Letters 22, 2582-2584.

Odiit, M., Coleman, P.G., Liu, W.C., McDermott, J.J., Fevre, E.M., Welburn, S.C., Woolhouse, M.E., 2005. Quantifying the level of under-detection of Trypanosoma brucei rhodesiense sleeping sickness cases. Trop Med Int Health 10, 840-849.

Ogbadoyi, E.O., Robinson, D.R., Gull, K., 2003. A high-order trans-membrane structural linkage is responsible for mitochondrial genome positioning and segregation by flagellar basal bodies in trypanosomes. Mol Biol Cell 14, 1769-1779.

Olefsky, J.M., 2001. Nuclear receptor minireview series. J Biol Chem 276, 36863-36864.

Omori, K., Kotera, J., 2007a. Overview of PDEs and Their Regulation. Circulation Research 100, 309-327.

Omori, K., Kotera, J., 2007b. Overview of PDEs and their regulation. Circ Res 100, 309-327.

Orr, G.A., Werner, C., Xu, J., Bennett, M., Weiss, L.M., Takvorkan, P., Tanowitz, H.B., Wittner, M., 2000. Identification of Novel Serine/Threonine Protein Phosphatases inTrypanosoma cruzi: a Potential Role in Control of Cytokinesis and Morphology. Infection and Immunity 68, 1350-1358.

Orrling, K.M., Jansen, C., Vu, X.L., Balmer, V., Bregy, P., Shanmugham, A., England, P., Bailey, D., Cos, P., Maes, L., Adams, E., van den Bogaart, E., Chatelain, E., Ioset, J.-R., van de Stolpe, A., Zorg, S., Veerman, J., Seebeck, T., Sterk, G.J., de Esch, I.J.P., Leurs, R., 2012. Catechol Pyrazolinones as Trypanocidals: Fragment-Based Design, Synthesis, and Pharmacological Evaluation of Nanomolar Inhibitors of Trypanosomal Phosphodiesterase B1. Journal of Medicinal Chemistry 55, 8745-8756.

Ortiz, D., Sanchez, M.A., Quecke, P., Landfear, S.M., 2009. Two novel nucleobase/pentamidine transporters from Trypanosoma brucei. Molecular and Biochemical Parasitology 163, 67-76.

Overath, P., Engstler, M., 2004. Endocytosis, membrane recycling and sorting of GPI-anchored proteins: Trypanosoma brucei as a model system. Mol Microbiol 53, 735-744.

Paindavoine, P., Rolin, S., Van Assel, S., Geuskens, M., Jauniaux, J.C., Dinsart, C., Huet, G., Pays, E., 1992. A gene from the variant surface glycoprotein expression site encodes one of several transmembrane adenylate cyclases located on the flagellum of Trypanosoma brucei. Mol Cell Biol 12, 1218-1225.

Pan, J., Snell, W.J., 2000. Signal transduction during fertilization in the unicellular green alga, Chlamydomonas. Curr Opin Microbiol 3, 596-602.

Panigrahi, A.K., Ogata, Y., Zikova, A., Anupama, A., Dalley, R.A., Acestor, N., Myler, P.J., Stuart, K.D., 2009. A comprehensive analysis of Trypanosoma brucei mitochondrial proteome. Proteomics 9, 434-450.

Parnell, E., Palmer, T.M., Yarwood, S.J., 2015. The future of EPAC-targeted therapies: agonism versus antagonism. Trends in Pharmacological Sciences 36, 203-214.

Parsons, M., Ruben, L., 2000. Pathways involved in environmental sensing in trypanosomatids. Parasitol Today 16, 56-62.

Paterou, A., Walrad, P., Craddy, P., Fenn, K., Matthews, K., 2006. Identification and stage-specific association with the translational apparatus of TbZFP3, a CCCH protein that promotes trypanosome life-cycle development. J Biol Chem 281, 39002-39013.

Pays, E., Tebabi, P., Pays, A., Coquelet, H., Revelard, P., Salmon, D., Steinert, M., 1989. The genes and transcripts of an antigen gene expression site from T. brucei. Cell 57, 835-845.

Pepin, J., Milord, F., 1994. The treatment of human African trypanosomiasis. Adv Parasitol 33, 1-47.

Pepin, J., Milord, F., Meurice, F., Ethier, L., Loko, L., Mpia, B., 1992. High-dose nifurtimox for arseno-resistant Trypanosoma brucei gambiense sleeping sickness: an open trial in central Zaire. Trans R Soc Trop Med Hyg 86, 254-256.

Pfaffl, M.W., 2001. A new mathematical model for relative quantification in real-time RT-PCR. Nucleic Acids Res 29, e45.

Picozzi, K., Fevre, E.M., Odiit, M., Carrington, M., Eisler, M.C., Maudlin, I., Welburn, S.C., 2005. Sleeping sickness in Uganda: a thin line between two fatal diseases. BMJ 331, 1238-1241.

Pierre, S., Eschenhagen, T., Geisslinger, G., Scholich, K., 2009. Capturing adenylyl cyclases as potential drug targets. Nat Rev Drug Discov 8, 321-335.

Pollastri, M.P., Campbell, R.K., 2011. Target repurposing for neglected diseases. Future Med Chem 3, 1307-1315.

Potter, L.R., 2011. Regulation and therapeutic targeting of peptide-activated receptor guanylyl cyclases. Pharmacology & Therapeutics 130, 71-82.

Pozuelo Rubio, M., Campbell D , G., Morrice N , A., Mackintosh, C., 2005. Phosphodiesterase 3A binds to 14-3-3 proteins in response to PMA-induced phosphorylation of Ser(428). Biochem J 392, 163-172.

Pozuelo Rubio, M., Geraghty, K.M., Wong, B.H.C., Wood, N.T., Campbell, D.G., Morrice, N., Mackintosh, C., 2004. 14-3-3-affinity purification of over 200 human phosphoproteins reveals new links to regulation of cellular metabolism, proliferation and trafficking. Biochemical Journal 379, 395-408.

Punta, M., Coggill, P.C., Eberhardt, R.Y., Mistry, J., Tate, J., Boursnell, C., Pang, N., Forslund, K., Ceric, G., Clements, J., Heger, A., Holm, L., Sonnhammer, E.L.L., Eddy, S.R., Bateman, A., Finn, R.D., 2012. The Pfam protein families database. Nucleic Acids Research 40, D290-D301.

Radivojac, P., Vacic, V., Haynes, C., Cocklin, R.R., Mohan, A., Heyen, J.W., Goebl, M.G., Iakoucheva, L.M., 2010. Identification, analysis, and prediction of protein ubiquitination sites. Proteins: Structure, Function, and Bioinformatics 78, 365-380.

Radziszewski, W., Chopra, M., Zembowicz, A., Gryglewski, R., Ignarro, L.J., Chaudhuri, G., 1995. Nitric oxide donors induce extrusion of cyclic GMP from isolated human blood platelets by a mechanism which may be modulated by prostaglandins. Int J Cardiol 51, 211-220.

Rascon, A., Soderling, S.H., Schaefer, J.B., Beavo, J.A., 2002. Cloning and characterization of a cAMP-specific phosphodiesterase (TbPDE2B) from Trypanosoma brucei. Proc Natl Acad Sci U S A 99, 4714-4719.

Ren, J., Wen, L., Gao, X., Jin, C., Xue, Y., Yao, X., 2008. CSS-Palm 2.0: an updated software for palmitoylation sites prediction. Protein Engineering Design and Selection 21, 639-644.

Resh, M.D., 1999. Fatty acylation of proteins: new insights into membrane targeting of myristoylated and palmitoylated proteins. Biochim Biophys Acta 1451, 1-16.

Robinson, D.R., Sherwin, T., Ploubidou, A., Byard, E.H., Gull, K., 1995a. Microtubule polarity and dynamics in the control of organelle positioning, segregation, and cytokinesis in the trypanosome cell cycle. J Cell Biol 128, 1163-1172.

Robinson, D.R., Sherwin, T., Ploubidou, A., Byard, E.H., Gull, K., 1995b. Microtubule polarity and dynamics in the control of organelle positioning, segregation, and cytokinesis in the trypanosome cell cycle. The Journal of Cell Biology 128, 1163-1172.

Rodbell, M., 1980. The role of hormone receptors and GTP-regulatory proteins in membrane transduction. Nature 284, 17-22.

Rolin, S., Hanocq-Quertier, J., Paturiaux-Hanocq, F., Nolan, D., Salmon, D., Webb, H., Carrington, M., Voorheis, P., Pays, E., 1996. Simultaneous but independent activation of adenylate cyclase and glycosylphosphatidylinositol-phospholipase C under stress conditions in Trypanosoma brucei. J Biol Chem 271, 10844-10852.

Rolin, S., Paindavoine, P., Hanocq-Quertier, J., Hanocq, F., Claes, Y., Le Ray, D., Overath, P., Pays, E., 1993. Transient adenylate cyclase activation accompanies differentiation of Trypanosoma brucei from bloodstream to procyclic forms. Mol Biochem Parasitol 61, 115-125.

Ross, D.T., Raibaud, A., Florent, I.C., Sather, S., Gross, M.K., Storm, D.R., Eisen, H., 1991. The trypanosome VSG expression site encodes adenylate cyclase and a leucine-rich putative regulatory gene. EMBO J 10, 2047-2053.

Rotureau, B., Morales, M.A., Bastin, P., Spath, G.F., 2009. The flagellum-mitogen-activated protein kinase connection in Trypanosomatids: a key sensory role in parasite signalling and development? Cell Microbiol 11, 710-718.

Rubenstein, L.A., Zauhar, R.J., Lanzara, R.G., 2006. Molecular dynamics of a biophysical model for beta2-adrenergic and G protein-coupled receptor activation. J Mol Graph Model 25, 396-409.

Saada, E.A., Kabututu, Z.P., Lopez, M., Shimogawa, M.M., Langousis, G., Oberholzer, M., Riestra, A., Jonsson, Z.O., Wohlschlegel, J.A., Hill, K.L., 2014. Insect stage-specific receptor adenylate cyclases are localized to distinct subdomains of the Trypanosoma brucei Flagellar membrane. Eukaryot Cell 13, 1064-1076.

Sager, G., Ravna, A.W., 2009. Cellular efflux of cAMP and cGMP - a question about selectivity. Mini Rev Med Chem 9, 1009-1013.

Salmon, D., Bachmaier, S., Krumbholz, C., Kador, M., Gossmann, J.A., Uzureau, P., Pays, E., Boshart, M., 2012a. Cytokinesis of Trypanosoma brucei bloodstream forms depends on expression of adenylyl cyclases of the ESAG4 or ESAG4-like subfamily. Mol Microbiol 84, 225-242.

Salmon, D., Vanwalleghem, G., Morias, Y., Denoeud, J., Krumbholz, C., Lhommé, F., Bachmaier, S., Kador, M., Gossmann, J., Dias, F.B.S., De Muylder, G., Uzureau, P., Magez, S., Moser, M., De Baetselier, P., Van Den Abbeele, J., Beschin, A., Boshart, M., Pays, E., 2012b. Adenylate Cyclases of Trypanosoma brucei Inhibit the Innate Immune Response of the Host. Science 337, 463-466.

Sanchez, M.A., Ullman, B., Landfear, S.M., Carter, N.S., 1999. Cloning and Functional Expression of a Gene Encoding a P1 Type Nucleoside Transporter from Trypanosoma brucei. Journal of Biological Chemistry 274, 30244-30249.

Sanchez, M.A., Zeoli, D., Klamo, E.M., Kavanaugh, M.P., Landfear, S.M., 1995. A family of putative receptor-adenylate cyclases from Leishmania donovani. J Biol Chem 270, 17551-17558.

Sassone-Corsi, P., 2012. The cyclic AMP pathway. Cold Spring Harb Perspect Biol 4.

Schaap, P., 2005. Guanylyl cyclases across the tree of life. Front Biosci 10, 1485-1498.

Schmid, A., Meili, D., Salathe, M., 2014. Soluble adenylyl cyclase in health and disease. Biochimica et Biophysica Acta (BBA) - Molecular Basis of Disease 1842, 2584-2592.

Seebeck, T., Gong, K., Kunz, S., Schaub, R., Shalaby, T., Zoraghi, R., 2001. cAMP signalling in Trypanosoma brucei. Int J Parasitol 31, 491-498.

Seebeck, T., Schaub, R., Johner, A., 2004. cAMP signalling in the kinetoplastid protozoa. Curr Mol Med 4, 585-599.

Seebeck, T., Sterk, G.J., Ke, H., 2011. Phosphodiesterase inhibitors as a new generation of antiprotozoan drugs: exploiting the benefit of enzymes that are highly conserved between host and parasite. Future Med Chem 3, 1289-1306.

Shakur, Y., de Koning, H.P., Ke, H., Kambayashi, J., Seebeck, T., 2011. Therapeutic potential of phosphodiesterase inhibitors in parasitic diseases. Handb Exp Pharmacol, 487-510.

Shalaby, T., Liniger, M., Seebeck, T., 2001. The regulatory subunit of a cGMP-regulated protein kinase A of Trypanosoma brucei. Eur J Biochem 268, 6197-6206.

Sherwin, T., Gull, K., 1989. Visualization of detyrosination along single microtubules reveals novel mechanisms of assembly during cytoskeletal duplication in trypanosomes. Cell 57, 211-221.

Siegel, T.N., Hekstra, D.R., Wang, X., Dewell, S., Cross, G.A., 2010a. Genome-wide analysis of mRNA abundance in two life-cycle stages of Trypanosoma brucei and identification of splicing and polyadenylation sites. Nucleic Acids Res 38, 4946-4957.

Siegel, T.N., Hekstra, D.R., Wang, X., Dewell, S., Cross, G.A.M., 2010b. Genome-wide analysis of mRNA abundance in two life-cycle stages of Trypanosoma brucei and identification of splicing and polyadenylation sites. Nucleic Acids Research 38, 4946-4957.

Siman-Tov, M.M., Aly, R., Shapira, M., Jaffe, C.L., 1996. Cloning from Leishmania major of a developmentally regulated gene, c-lpk2, for the catalytic subunit of the cAMP-dependent protein kinase. Mol Biochem Parasitol 77, 201-215.

Siman-Tov, M.M., Ivens, A.C., Jaffe, C.L., 2002. Molecular cloning and characterization of two new isoforms of the protein kinase A catalytic subunit from the human parasite Leishmania. Gene 288, 65-75.

Simarro, P.P., Diarra, A., Ruiz Postigo, J.A., Franco, J.R., Jannin, J.G., 2011. The human African trypanosomiasis control and surveillance programme of the World Health Organization 2000-2009: the way forward. PLoS Negl Trop Dis 5, e1007.

Simarro, P.P., Franco, J., Diarra, A., Postigo, J.A., Jannin, J., 2012a. Update on field use of the available drugs for the chemotherapy of human African trypanosomiasis. Parasitology 139, 842-846.

Simarro, P.P., Franco, J.R., Cecchi, G., Paone, M., Diarra, A., Ruiz Postigo, J.A., Jannin, J.G., 2012b. Human African trypanosomiasis in non-endemic countries (2000-2010). J Travel Med 19, 44-53.

Sprague, G.F., Jr., 1991. Signal transduction in yeast mating: receptors, transcription factors, and the kinase connection. Trends Genet 7, 393-398.

Stich, A., Abel, P.M., Krishna, S., 2002. Human African trypanosomiasis. BMJ 325, 203-206.

Strickler, J.E., Patton, C.L., 1975. Adenosine 3',5'-monophosphate in reproducing and differentiated trypanosomes. Science 190, 1110-1112.

Subota, I., Julkowska, D., Vincensini, L., Reeg, N., Buisson, J., Blisnick, T., Huet, D., Perrot, S., Santi-Rocca, J., Duchateau, M., Hourdel, V., Rousselle, J.-C., Cayet, N., Namane, A., Chamot-Rooke, J., Bastin, P., 2014. Proteomic Analysis of Intact Flagella of Procyclic Trypanosoma brucei Cells Identifies Novel Flagellar Proteins with Unique Sub-localization and Dynamics. Molecular & Cellular Proteomics 13, 1769-1786.

Svobodova, M., Zidkova, L., Cepicka, I., Obornik, M., Lukes, J., Votypka, J., 2007. Sergeia podlipaevi gen. nov., sp. nov. (Trypanosomatidae, Kinetoplastida), a parasite of biting midges (Ceratopogonidae, Diptera). Int J Syst Evol Microbiol 57, 423-432.

Taelman, H., Schechter, P.J., Marcelis, L., Sonnet, J., Kazyumba, G., Dasnoy, J., Haegele, K.D., Sjoerdsma, A., Wery, M., 1987. Difluoromethylornithine, an effective new treatment of Gambian trypanosomiasis. Results in five patients. Am J Med 82, 607-614.

Tagoe, D.N.A., Kalejaiye, T.D., De Koning, H.P., 2015. The ever unfolding story of cAMP signalling in trypanosomatids: vive la difference! Frontiers in Pharmacology 6.

Tetley, L., Vickerman, K., 1985. Differentiation in Trypanosoma brucei: host-parasite cell junctions and their persistence during acquisition of the variable antigen coat. J Cell Sci 74, 1-19.

Tiberti, N., Hainard, A., Lejon, V., Courtioux, B., Matovu, E., Enyaru, J.C., Robin, X., Turck, N., Kristensson, K., Ngoyi, D.M., Vatunga, G.M., Krishna, S., Buscher, P., Bisser, S., Ndung'u, J.M., Sanchez, J.C., 2012. Cerebrospinal fluid neopterin as marker of the meningo-encephalitic stage of Trypanosoma brucei gambiense sleeping sickness. PLoS One 7, e40909.

Torreele, E., Bourdin Trunz, B., Tweats, D., Kaiser, M., Brun, R., Mazué, G., Bray, M.A., Pécoul, B., 2010. Fexinidazole – A New Oral Nitroimidazole Drug Candidate Entering Clinical Development for the Treatment of Sleeping Sickness. PLoS Negl Trop Dis 4, e923.

Truc, P., Lejon, V., Magnus, E., Jamonneau, V., Nangouma, A., Verloo, D., Penchenier, L., Buscher, P., 2002. Evaluation of the micro-CATT, CATT/Trypanosoma brucei gambiense, and LATEX/T b gambiense methods for serodiagnosis and surveillance of human African trypanosomiasis in West and Central Africa. Bull World Health Organ 80, 882-886.

Ulloa, R.M., Mesri, E., Esteva, M., Torres, H.N., Tellez-Inon, M.T., 1988. Cyclic AMP-dependent protein kinase activity in Trypanosoma cruzi. Biochem J 255, 319-326.

van den Abbeele, J., Rolin, S., Claes, Y., Le Ray, D., Pays, E., Coosemans, M., 1995. Trypanosoma brucei: stimulation of adenylate cyclase by proventriculus and esophagus tissue of the tsetse fly, Glossina morsitans morsitans. Exp Parasitol 81, 618-620.

Van der Mey, M., Hatzelmann, A., Van der Laan, I.J., Sterk, G.J., Thibaut, U., Timmerman, H., 2001a. Novel selective PDE4 inhibitors. 1. Synthesis, structure-activity relationships, and molecular modeling of 4-(3,4-dimethoxyphenyl)-2H-phthalazin-1-ones and analogues. J Med Chem 44, 2511-2522.

Van der Mey, M., Hatzelmann, A., Van Klink, G.P., Van der Laan, I.J., Sterk, G.J., Thibaut, U., Ulrich, W.R., Timmerman, H., 2001b. Novel selective PDE4 inhibitors. 2. Synthesis and structure-activity relationships of 4-aryl-substituted cis-tetra- and cis-hexahydrophthalazinones. J Med Chem 44, 2523-2535.

Vandamme, J., Castermans, D., Thevelein, J.M., 2012. Molecular mechanisms of feedback inhibition of protein kinase A on intracellular cAMP accumulation. Cell Signal 24, 1610-1618.

Vassella, E., Reuner, B., Yutzy, B., Boshart, M., 1997. Differentiation of African trypanosomes is controlled by a density sensing mechanism which signals cell cycle arrest via the cAMP pathway. J Cell Sci 110 (Pt 21), 2661-2671.

Vaughan, S., Gull, K., 2003. The trypanosome flagellum. J Cell Sci 116, 757-759.

Vickerman, K., 1985. Developmental cycles and biology of pathogenic trypanosomes. Br Med Bull 41, 105-114.

Vij, A., Biswas, A., Bhattacharya, A., Das, P.K., 2014. A soluble phosphodiesterase in Leishmania donovani negatively regulates cAMP signaling by inhibiting protein kinase A through a two way process involving catalytic as well as non-catalytic sites. The International Journal of Biochemistry & Cell Biology 57, 197-206.

Vincent, I.M., Creek, D., Watson, D.G., Kamleh, M.A., Woods, D.J., Wong, P.E., Burchmore, R.J., Barrett, M.P., 2010. A molecular mechanism for eflornithine resistance in African trypanosomes. PLoS Pathog 6, e1001204.

Walter, R.D., Buse, E., Ebert, F., 1978. Effect of cyclic AMP on transformation and proliferation of leishmania cells. Tropenmed Parasitol 29, 439-442.

Walter, R.D., Nordmeyer, J.P., Konigk, E., 1974. Adenylate cyclase from Trypanosoma gambiense. Hoppe Seylers Z Physiol Chem 355, 427-430.

Wang, C., Ashton, T.D., Gustafson, A., Bland, N.D., Ochiana, S.O., Campbell, R.K., Pollastri, M.P., 2012. Synthesis and evaluation of human phosphodiesterases (PDE) 5 inhibitor analogs as trypanosomal PDE inhibitors. Part 1. Sildenafil analogs. Bioorganic & Medicinal Chemistry Letters 22, 2579-2581.

Wang, H., Yan, Z., Geng, J., Kunz, S., Seebeck, T., Ke, H., 2007. Crystal structure of the Leishmania major phosphodiesterase LmjPDEB1 and insight into the design of the parasite-selective inhibitors. Mol Microbiol 66, 1029-1038.

Waters, C.M., Bassler, B.L., 2005. Quorum sensing: cell-to-cell communication in bacteria. Annu Rev Cell Dev Biol 21, 319-346.

Welburn, S.C., Picozzi, K., Fevre, E.M., Coleman, P.G., Odiit, M., Carrington, M., Maudlin, I., 2001. Identification of human-infective trypanosomes in animal reservoir of sleeping sickness in Uganda by means of serum-resistance-associated (SRA) gene. Lancet 358, 2017-2019.

Wickware, P., 2002. Resurrecting the resurrection drug. Nat Med 8, 908-909.

Wilson, Z.N., Gilroy, C.A., Boitz, J.M., Ullman, B., Yates, P.A., 2012. Genetic dissection of pyrimidine biosynthesis and salvage in Leishmania donovani. J Biol Chem 287, 12759-12770.

Wu, Y., Deford, J., Benjamin, R., Lee, M.G., Ruben, L., 1994. The gene family of EF-hand calcium-binding proteins from the flagellum of Trypanosoma brucei. Biochemical Journal 304, 833-841.

Xie, Z., Cai, T., 2003. Na+-K+--ATPase-mediated signal transduction: from protein interaction to cellular function. Mol Interv 3, 157-168.

Yang, J., Yan, R., Roy, A., Xu, D., Poisson, J., Zhang, Y., 2015. The I-TASSER Suite: protein structure and function prediction. Nat Methods 12, 7-8.

Zhang, X., Feng, Q., Cote, R.H., 2005. Efficacy and selectivity of phosphodiesterase-targeted drugs in inhibiting photoreceptor

phosphodiesterase (PDE6) in retinal photoreceptors. Invest Ophthalmol Vis Sci 46, 3060-3066.

Zoraghi, R., Corbin, J.D., Francis, S.H., 2004. Properties and functions of GAF domains in cyclic nucleotide phosphodiesterases and other proteins. Mol Pharmacol 65, 267-278.

Zoraghi, R., Seebeck, T., 2002. The cAMP-specific phosphodiesterase TbPDE2C is an essential enzyme in bloodstream form Trypanosoma brucei. Proc Natl Acad Sci U S A 99, 4343-4348.

Review

The ever unfolding story of cAMP signalling in in Trypanosomes: vive la difference!